REPORT DOCUMENTATION PAGE

The public reporting burden for this collection of information is estimated to average 1 hour per response, including the time for reviewing instructions, searching existing data sources, gathering and maintaining the data needed, and completing and reviewing the collection of information. Send comments regarding this burden estimate or any other aspect of this collection of information, including suggestions for reducing the burden, to Department of Defense, Washington Headquarters Services, Directorate for Information Operations and Reports (0704-0188), 1215 Jefferson Davis Highway, Suite 1204, Arlington, VA 22202-4302. Respondents should be aware that notwithstanding any other provision of law, no person shall be subject to any penalty for failing to comply with a collection of information if it does not display a currently valid OMB control number.
PLEASE DO NOT RETURN YOUR FORM TO THE ABOVE ADDRESS.

1. REPORT DATE *(DD-MM-YYYY)*	2. REPORT TYPE	3. DATES COVERED *(From - To)*
19-04-2004	Final Report	01-01-1999 through 30-09-2003

4. TITLE AND SUBTITLE
Right whale habitat and migration in the northwest Atlantic Ocean

5a. CONTRACT NUMBER

5b. GRANT NUMBER
N00014-00-1-0085

5c. PROGRAM ELEMENT NUMBER

6. AUTHOR(S)
Bruce R. Mate

5d. PROJECT NUMBER

5e. TASK NUMBER

5f. WORK UNIT NUMBER

7. PERFORMING ORGANIZATION NAME(S) AND ADDRESS(ES)
Oregon State University
312 Kerr Administration Building
Corvallis OR 97331-2140

8. PERFORMING ORGANIZATION REPORT NUMBER

9. SPONSORING/MONITORING AGENCY NAME(S) AND ADDRESS(ES)
Office of Naval Research
800 N Quincy Street
Arlington VA 22217-5000

10. SPONSOR/MONITOR'S ACRONYM(S)
ONR

11. SPONSOR/MONITOR'S REPORT NUMBER(S)

12. DISTRIBUTION/AVAILABILITY STATEMENT
Distribution unlimited

13. SUPPLEMENTARY NOTES

20040607 031

14. ABSTRACT
This study successfully used OSU-developed Argos implantable satellite-monitored radio tags to collect location data on large endangered whale species. These data were used determine feeding and migratory movements, and characterize critical habitats. Whales studied included Hawaiian humpback whales, Eastern North Pacific blue whales, North Atlantic right whales, Sea of Cortez fin whales, and Gulf of Mexico sperm whales. Oregon State University leads the field worldwide in tag longevity and reliabilty; the longest-running tags to date are on Gulf of Mexico sperm whales and have transmitted for 20 months so far.

15. SUBJECT TERMS
satellite-monitored, radio tags, whale, cetacean, critical habitat, right whale, blue whale, fin whale, sperm whale, humpback whale

16. SECURITY CLASSIFICATION OF:			17. LIMITATION OF ABSTRACT	18. NUMBER OF PAGES	19a. NAME OF RESPONSIBLE PERSON
a. REPORT	**b. ABSTRACT**	**c. THIS PAGE**	UL	4	Bruce R. Mate
Unclass.	Unclass.	Unclass.			**19b. TELEPHONE NUMBER** *(Include area code)* 541-867-0202

FINAL REPORT

GRANT #: N00014-00-1-0085

PRINCIPAL INVESTIGATOR: Bruce R. Mate

INSTITUTION: Oregon State University

GRANT TITLE: Right whale habitat and migration in the
northwest Atlantic Ocean

AWARD PERIOD: 1 Jan 1999 - 30 September 2003

OBJECTIVE: To determine the feeding and migratory
movements of endangered cetaceans and characterize their
critical habitats.

APPROACH: Whales are tagged using OSU-developed Argos
satellite-monitored radio tags (implanted, with a saltwater
switch and transmission antenna protruding). Tag duty
cycles are programmed to: 1)maximize satellite reception,
which depends on the location of the whale and the orbit of
TIROS-N satellites used by Argos; 2) quality of data
(obtaining more frequent transmissions); and 3) extended
operational life (requiring less frequent transmissions).
As whales surface to breathe, tags transmit to an overhead
satellite, which uses Doppler effect to determine the
location of the tag. Location data are then downloaded from
the Argos data collection node to our laboratory, for
analysis and mapping.

ACCOMPLISHMENTS:
In Feb./Dec. 1999 we tagged humpback whales in Hawaii.
Whales had a short stay after tagging (average = 11 days).
This turnover rate suggests 8-10K whales in Hawaii instead
of 2-3K. One tagged humpback stopped mid-migration
(probably to feed) at the Kermit Roosevelt sea mount for 38
days. During migration, whales usually swam day and night
at a consistent speed of 3.5+ miles per hour.

In July/Oct.1999 we tagged blue whales off the California
coast. Three were tracked >5 months (max = 247 days). Five
whales went into the Sea of Cortez by early January, long
before the previously acknowledged period of peak numbers
(March/April). The high percentage of tagged whales using
the area (5 of 7 going south of U.S. waters = 71%) is in

contrast to 5% of the population previously estimated to use this area. One whale was tracked to the Costa Rica Dome upwelling, which we now believe is a likely calving area.

In July-Aug. 2000, we tagged 44 North Atlantic right whales in the Bay of Fundy: 16 with Argos tags and 28 with OSU-designed suction-cup-mounted time/depth recorders (TDRs). Analysis showed the animals dive regularly to the depth of maximum copepod (preferred prey) concentration, usually between 100 and 200 meters, just above the bottom mixed layer. One tag transmitted for 126 days, allowing us to follow the movements of an adult female through the feeding season and her fall migration to Georgia, a known wintering area. Two tagged right whales had not previously been seen and were added to the catalogue. There was evidence of antenna failure in resighted tagged whales; this was corrected in a later tag design. Data from this study was used in a decision to shift international shipping lanes in the Bay of Fundy to reduce whale/ship collisions.

In Oct. 2000, we tagged 13 blue whales near the Farallon Islands off central California. One whale went to a sea mount NW of California and 1,500 miles offshore. Four whales went to the Costa Rica Dome and stayed there for the entire winter; two also transmitted through the spring migration back into U.S. waters.

In March 2001 we tagged 11 fin whales and four blue whales in the Sea of Cortez to determine if fin whales are year-round residents in the Sea of Cortez. We tracked fin whales for five months (11,185 miles), well into the summer feeding season; all stayed in the Sea of Cortez. One blue whale mother (with calf) was tracked for 213 days and 7,305 miles. She left the Sea of Cortez and moved north, but never reached California. Instead, she spent the summer off Punta Eugenia, not previously known as a summer foraging area.

In July 2001, doctoral student Mark Baumgartner deployed TDRs to 35 North Atlantic right whales in the Bay of Fundy. His study also collected oceanographic data, which showed where the greatest densities of copepods could be found.

In August 2001, we tagged a sperm whale during a NOAA pilot project in the Gulf of Mexico (GOM). The tag lasted 137 days (5,116 miles), and showed the sperm whale resident along the 900-meter contour near the Mississippi Delta for

95 days, then traveling in a counter-clockwise path around the GOM to the Gulf of Campeche. The success of this pilot project gave rise to a three-year sperm whale research project funded by MMS and the oil and gas industry.

In March 2002, we tagged two blue whales in the Sea of Cortez, before a mechanical failure of our crossbow tag applicator. One animal was tracked for 198 days (8,214 miles). Like the mother/calf pair from 2001, this whale never crossed into U.S. waters, spending 4.5 months off San Ignacio Lagoon and Punta Eugenia. The second whale was tracked for 98 days (3,688 miles), crossing into California waters for only 4.5 days before heading back into Mexican waters, where it remained for the duration of its tracking period. The crossbow malfunction led us to further develop a safer, more reliable air-powered applicator, which now provides nearly complete tag deployment.

In September 2002, we tagged 15 humpback whales off the coast of Gabon; the first time humpbacks have been tagged in the southern hemisphere. The longest track was 104 days (5,093 miles), and reached the Antarctic ice edge. Breeding season distribution was varied. Some whales traveled north of the equator and west along the African coast as far as Ghana; others went west to the offshore islands of Sao Tome and Principe (proving that whales from these islands are not a separate stock, as previously thought), and some went south offshore.

CONCLUSIONS:
Hawaiian humpback whales may not always fast during migration as previously thought; duration of stay at the Hawaiian Islands indicates this stock may be larger than current estimates. Gabon humpbacks spread north, south and west during their breeding season; afterwards some go as far south as the Antarctic ice shelf. The Costa Rica Dome is very likely a blue whale calving area, and is certainly a wintering area, where feeding probably continues all winter. Not all Eastern North Pacific blue whales summer off California, as previously thought; since population estimates of this stock are made by ship and aerial surveys off the California coast, an underestimation of the calving rates and population could result. Sea of Cortez fin whales are likely year-round residents. North Atlantic right whales move nearshore past every major seaport on the East coast during their southward migration. Changes to tag design and applicator have increased tag longevity and

reliability; as of this writing, tags on sperm whales have lasted 20 months and counting.

SIGNIFICANCE: Our program leads the field worldwide in tag reliability and longevity. Our ONR-sponsored research has dramatically increased knowledge regarding movements and critical habitats of right, sperm, humpback, blue and fin whales, which is useful for mitigation and conservation.

PUBLICATIONS AND ABSTRACTS (for total period of grant):

Etnoyer, P., D. Canny, B.R. Mate, and L. Morgan. 2004. Persistent pelagic habitats in the Baja California to Bering Sea (B2B) Ecoregion. Oceanography, 17(1): 90-101.

Baumgartner, M.F. 2003. Comparisons of *Calanus finmarchius* fifth copepodite abundance estimates from nets and an optical plankton counter. Journal of Plankton Research 25(7): 855-868.

Baumgartner, M.F. and B.R. Mate. 2003. Summertime foraging ecology of North Atlantic right whales. Mar Eco Prog Ser, 264:123-135.

Baumgartner,M.F.; T.V.N. Cole, P.J. Clapham, and B.R. Mate. 2003. North Atlantic right whale habitat in the lower Bay of Fundy and on the Southwestern Scotian Shelf during 1999-2001. Mar Eco Prog Ser, 264:137-154.

Baumgartner, M.F., T.V.N. Cole, R.G. Campbell, G.J. Teegarden, and E.G. Durbin. 2003. Associations between North Atlantic right whales and their prey, Calanus finmarchius, over diel and tidal time scales. Mar Eco Prog Ser, 264:155-166.

Durbin, E., Teegarden, G., Campbell, R. Cembella, A., Baumgartner, M., and B.R. Mate. 2002. North Atlantic right whales, *Eubalaena glacialis*, exposed to paralytic shellfish poisoning (PSP) toxins via a zooplankton vector, *Calanus finmarchicus*. Harmful Algae, 1(2002): 243-251.

Krutzikowsky, G. K. and B. R. Mate. 2000. Dive and surfacing characteristics of bowhead whales *(Balaena mysticetus)* in the Beaufort and Chukchi Seas. Can. J. Zool. 78:1182-1198.

Lagerquist, B. A., K. M. Stafford and B. R. Mate. 2000. Dive characteristics of satellite-monitored blue whales (*Balaenoptera musculus*) off the Central California Coast. Mar. Mammal Sci. 16(2):375-391.

Persistent Pelagic Habitats in the Baja California to Bering Sea (B2B) Ecoregion

Peter Etnoyer, Aquanautix Consulting · Los Angeles, California USA

David Canny, Ecospective · San Francisco, California USA

Bruce Mate, Oregon State University · Newport, Oregon USA

Lance Morgan, Marine Conservation Biology Institute · Glen Ellen, California USA

Abstract

The Baja California to Bering Sea (B2B) Marine Conservation Initiative seeks to establish a network of Marine Protected Areas within the Exclusive Economic Zones of the NAFTA countries- Canada, Mexico, and the United States. This network is designed to capture ecologically significant habitat for marine species of common conservation concern and pelagic regions of high productivity, with due consideration for the inter-annual sea surface temperature fluctuations of the El Niño Southern Oscillation (ENSO). Here, we present analytical methods that define pelagic habitat based upon the density of steep temperature gradients, or fronts, and we quantify their spatial and temporal persistence over a single ENSO cycle (1996-1999) to benefit marine conservation and marine management strategies.

We find that less than 1% of the Northeast Pacific ocean exhibits a persistent (> 8 mo/yr) concentration of temperature fronts (> .2km/km^2) within and between years. The Baja California Frontal System (BCFS) is the largest concentration found within the multinational federal waters, between 0 and 300 km east of Baja California Sur. The BCFS appears more active under La Niña conditions, while the next largest persistent concentration, North Pacific Transition Zone, appears more active under El Niño conditions. We demonstrate habitat functions associated with the BCFS for blue whales (*Balaenoptera musculus*), swordfish (*Xiphias gladius*), and striped marlin (*Tetrapturus audax*). We recommend management and protection for this pelagic "hotspot" to the Mexican government and the tri-national Commission for Environmental Cooperation.

Introduction

Pelagic habitat is an important component of marine management strategies that hope to protect highly migratory species like tuna, turtles, and whales. These species are all known to range over basin scales (Block et al., 2001; Bowen et al., 1995; Calambokides et al., 1990) with little regard for international maritime borders. Their annual migrations are tuned to the logic of comfort and resource abundance, tracking ocean conditions that favor warm winter water and nursing grounds for part of the year, and high productivity spurred in some areas by nutrients in the melting ice of summer flows in the other part of the year. While it was once thought that these migrations were direct, and without sustenance, it has been shown that some distant migrations use "stepping stones." For example, nearly half a million South American shorebirds stop in Delaware Bay to double their weight eating horseshoe crab eggs before continuing to nesting grounds in the Canadian Arctic (Harrington, 1996). In the Northeast Pacific, southward migrating blue whales are known to linger and feed as they migrate south on

California and Baja California coasts (Mate et al., 1999). Marine management strategies that fail to identify pelagic "stepping stones" cannot guarantee full protection to pelagic species (Hyrenbach et al., 2000).

The United Nations Convention on the Law of the Sea granted coastal nations exclusive economic zones (EEZs) and provided exclusive rights to all waters and submerged lands within 200 nautical miles (370 km) of national coastlines (United Nations Convention on the Law of the Sea, 1982). This act doubled some national territories, and created new opportunities that bring contemporary concerns to bear upon marine managers in coastal nations. Benthic and pelagic seafood resources are valuable renewable natural resources, and sustain a major portion of the human diet in developed and developing nations. However, resource abundance can fluctuate on seasonal, interannual, and decadal scales (Kawasaki and Omori, 1988; Lluch-Belda et al., 1989). These resources are finite and exhaustible, a fact recently come to light in commercial fishing, in science, in law, and in the media. Pelagic

resources are shared between the human population and marine populations. There is a compelling need to estimate pelagic resource abundance (e.g., Antarctic krill) to avoid the over-concentration of fishing effort (Hewitt et al., 2002). We must understand spatial and temporal variability in the open ocean if we ever hope to achieve sustainable maritime fisheries.

Pelagic fishery resources (e.g., tuna, anchovy, swordfish, and shark) can be particularly challenging for marine managers because these stocks are highly migratory, the fisheries for them are international and decentralized, and effort and landings are difficult to assess. The need for conservation and management of pelagic regions is growing due to the combined threats of pelagic overfishing (Worm et al., 2003; Pauley et al., 1998) and rapid developments in commercial (Roffer, 1987) and recreational (Roffer, 2000) fisheries technology. Studies of pelagic fish landings in the North Pacific indicate that these fishes stand at 10% of their historical abundance (Myers and Worm, 2003). The UN Fisheries and Agriculture Organization (1999) claims 21% of global fisheries are over fished, depleted, or recovering while 50% are at maximum capacity.

Pelagic fisheries regulation traditionally takes the form of quotas, gear restrictions and time closures. These fisheries have thus far proven immune to spatial management strategies within national waters, because species aggregations and the features that drive them are ephemeral in space and time, and have not been well quantified. Yet, pelagic fisheries do have a spatial component and marine species can benefit from spatial management strategies. Commercial fishermen are known to focus their efforts on sea surface temperature (SST) and chlorophyll maps provided by commercial satellite fishing services (Terrafin, Roffer's, SeaStar) that collect data from the National Oceanic and Atmospheric Administration's (NOAA) Polar Operational Environmental Satellites (POES). Steep gradients in sea surface temperature and chlorophyll are known to provide habitat for some species, and aggregate others (Franks, 1992). High biological productivity is often attributed to these features, due to density-driven aggregation, and increased vertical flux resulting in high primary and secondary production (Olson et al., 1994: Olson and Backus, 1984; Owen, 1981; Fournier, 1979).

Hydrographic fronts mark the boundaries between two dissimilar water masses. These fronts can be detected in satellite imagery derived from passive remote sensing of infrared radiation emitted by the sea surface. SST products consist of a grid of cells (or pixels) with values for temperature. These products are available from NASA's Jet Propulsion Laboratory, and others, at different spatial and temporal scales. SST fronts are derived from edge detection algorithms,

> **Benthic and pelagic seafood resources are valuable renewable natural resources, and sustain a major portion of the human diet in developed and developing nations.**

essentially slope functions that identify the highest rate of change in temperature across a surface, and discern this boundary between adjacent water masses. The density difference between these moving water masses acts to aggregate phytoplankton and zooplankton along the flow boundary, and to generate vertical advection in plankton and nutrients (Bakun, 1996). High concentrations of fish larvae and invertebrate larvae, and high primary productivity, are associated with shelf break and pelagic frontal features (Munk et al., 1995; Roughgarden et al., 1988)

Some species associations for pelagic temperature fronts are well documented. The endangered Loggerhead sea turtle (*Caretta caretta*) migrates along a 17° C isotherm in the Northeast Pacific Transition Zone (NPTZ) thought to aggregate jellyfish and other meroplankton (Polovina et al., 2000). Albacore tuna (*Thunnus alalunga*) landings are also concentrated along a .2 mg/m^3 chlorophyll isopleth north of the Hawaiian islands (Polovina et al., 2001; Kimura, 1997; Laurs et al., 1984). The presence, position, and strength of temperature fronts guide the Hawaiian and the North Atlantic longline fisheries for swordfish (*Xiphias gladius*) (Seki et al., 2002; Podesta et al.,1993). Regionally, bluefin tuna (*Thunnus thynnus*) (Schick et al, in review) in the Gulf of Maine, piscivorous seabirds in the Alaskan Aleutian Islands (Decker and Hunt, 1996; Kinder et al., 1993), neon flying squid in the Northeast Pacific (Gong et al., 1993) and sperm whales (Davis et al., 2002) and butterfish in the Gulf of Mexico (Herron et al., 1989) have also been shown to concentrate along frontal boundaries. These hydrographic features drive fisheries and species, so it seems proper that they drive some form of marine management strategy.

The North American Commission for Environmental Cooperation (CEC), established in 1993 to implement the environmental provisions of the North American Free Trade Agreement (NAFTA), is developing a network of Marine Protected Areas (MPAs) for Baja California to Bering Sea (B2B) region. This program seeks to identify both ecological and institutional linkages within the Exclusive Economic Zones (EEZ) of Canada, Mexico, and the United States, including Alaska. One project of the network is to define priority conservation areas (PCAs) for both benthic and pelagic habitats, using physical, biological, and social data with special consideration for interannual variation, e.g., El Niño Southern Oscillation (ENSO). To accomplish this task, we developed methods of analysis to define persistent pelagic habitat, and to quantify species associations for those pelagic habitats. Here we present spatial analysis methods we used to define pelagic habitats based upon steep temperature gradients, or fronts, in the Northeast Pacific.

Methods

We present a comparison of sea surface temperature frontal density across the Northeast Pacific for the years 1996-1999. These years include one of the most dramatic ENSO regime shifts on record (Chavez et al., 1999). The ENSO year June 1997 to June 1998 represents a strong El Niño and June 1998 to June 1999 represents a strong La Niña. (Patzert, pers. comm.) Using this approach, we capture frontal features in alternate ENSO phases. We map the distribution of large frontal concentrations for the Northeast Pacific, and quantify their persistence within and between years. We use these as proxies for high secondary productivity. We test this assumption qualitatively by comparing the strongest and most persistent frontal concentrations to published fisheries literature, and to residential behavior in tagged blue whales. Blue whales (*Balaenoptera musculus*) are an international transboundary stock recovering from overexploitation (Calambokides, et al., 1990) and they are a species of common conservation concern for Canada, Mexico, and the United States.

Frontal features are ephemeral in space and time, shifting north and south by 10 to 1000 km depending on the season, the year, and the state of ENSO. Some oceanic fronts are more stable, formed by persistent topographically steered convergences (Wolanski and Hamner, 1988) of warm and cold water masses (e.g., the Gulf Stream, the Loop Current, the California Current). These continental features are excluded here using techniques that minimize the search radius within a moving window over the grid surface. Frontal density analysis is one of three investigations designed to discriminate "ecological value" from satellite derived information. SST, altimetry, and primary productivity analyses all informed B2B's Priority Conservation Area (PCA) mapping exercise for Pacific North America. PCAs are defined as continentally unique areas of high biodiversity or ecological value, under anthropogenic threat, with opportunities for conservation. The B2B analysis extent is defined spatially at 12 N to 72 N, 90 E to 180 E and temporally between January 1996 and December 1999 (Etnoyer et al., 2002). Pelagic "ecological value" analyses were restricted to data sets that encompassed the entire B2B extent in space and time (Morgan et al, in press).

NASA's Jet Propulsion Laboratory (JPL) Physical Oceanography Distributed Active Archive Center (PO.DAAC) makes several SST data sets available from their PO.DAAC Ocean ESIP Tool (POET: http://seablade.jpl.nasa.gov/gui/) including daily, weekly, and monthly 9 km resolution Advanced Very High Resolution Radar (AVHRR) available from 1985 through mid-2003 and weekly 18 km Miami Multichannel Sea Surface Temperature (MCSST) available from January of 1981 through January of 2001. NOAA Coastwatch West Coast Regional node offers 2.5 km monthly and bi-weekly composites for the survey time

period, but not for the spatial extent. This information was only used to compare to lower resolution datasets.
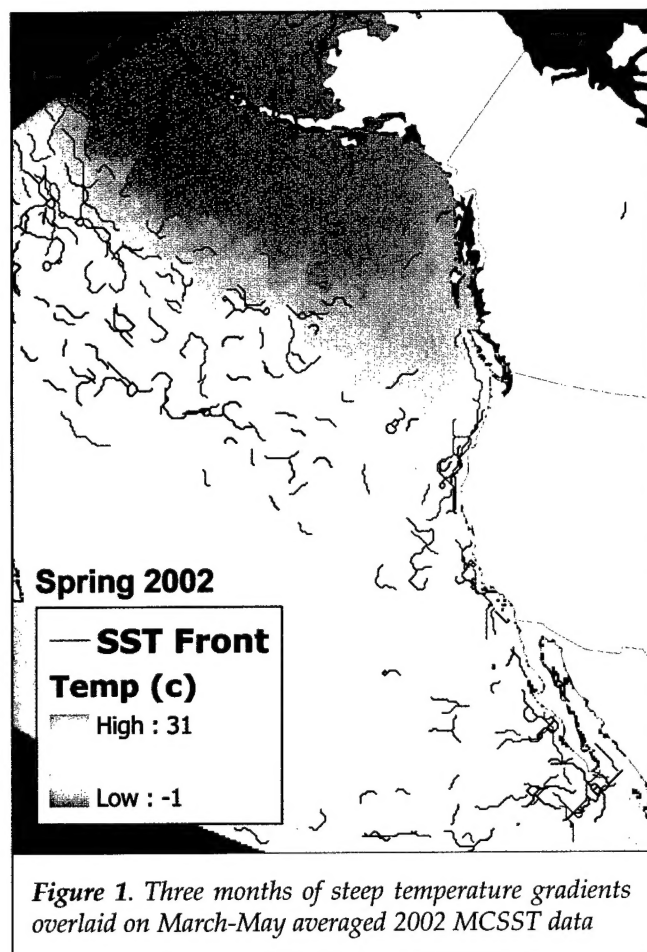
Monthly averages minimize cloudiness (no data values) by averaging cloud-free data values. Clouds still obscure between five and fifteen percent of monthly averaged AVHRR. Large storm systems can hover in the Gulf of Alaska for weeks at a time. Edge detection algorithms run on daily AVHRR would therefore register a false paucity of temperature fronts in the Gulf of Alaska. Therefore, Miami MCSST, an interpolated cloud-free data product, was chosen to better represent the hydrographic regime of North Pacific waters. We tested the effect of temporal scale on edge detection by comparing frontal density persistence (described below) values in weeks per year to the frontal persistence values in months per year, and found temperature fronts derived from monthly 18 km interpolated SST satisfactory for a four year inter-annual study of the strongest most persistent hydrographic temperature fronts in the Northeast Pacific.

Mean monthly probability of front occurrence has precedent in studies of North Atlantic waters by Ullman and Cornillon (1999). Still, monthly averaged SST is not an ideal product for thermal edge detection. Edge detection algorithms run over a monthly averaged grid surface might confound a single front meandering over several weeks into many fronts which are fixed in position over the course of a month's time. This is a potential source of error. Theoretically, these artifacts would be evenly distributed throughout the dynamic regime of the Northeast Pacific, and error distributed evenly across a surface, we believe, should still lead to fairly accurate relative measures.

Temperature gradients are also scale dependent and can be highly fractured, with dozens of steep temperature gradients across a 100 km transect (Ullman and Cornillon, 1999). In an effort to better understand the effects of spatial scale upon edge detection, we compared edge position and line length across all these scales: 18 km MCSST, 9 km AVHRR, and 2 km Coastwatch for NOAA Subregion J, east of Baja California Sur.

We ran a slope function across a 3 pixel x 3 pixel (48 km x 48 km for the 18 km MCSST, 7.5 km x 7.5 km Coastwatch SST, etc.) moving window to identify the rate of change in temperature values, and we set a threshold for the highest rate of change (.02° C/ km), the top 10% in a histogram of flux across the grid surface. We converted those cell value features to lines by connecting the centerpoint of grid cells with greater than .02° C change between pixels. Figure 1 shows three different months of line output over three months averaged SST. We calculated the linelength in kilometers, and density of these lines in km/km², for each month over four years, across the Northeast Pacific.

Differences between the total predicted linelength of 18 km MCSST interpolated data (2800 km) and 9 km AVHRR data (1905 km) for the first week in January

Figure 1. *Three months of steep temperature gradients overlaid on March-May averaged 2002 MCSST data*

Inside the figure:

Spring 2002

— **SST Front**

Temp (c)

High : 31

Low : -1

1998, for example, were small, but differences between 2 km Coastwatch data (10,500 km), MCSST, and AVHRR for this month were large, with MCSST underestimating higher resolution line length by 80%. The frontal features were spatially consistent across all scales, but autocorrelated between coarse and medium scales.

Another moving widow calculation estimated the density of monthly frontal features, in kilometers, of front per pixel, and we set a "high density" threshold for the top 10% (6.5 km per 18 km²) of those cell values. We generate binary monthly grids (1= high density, 0 = not high density), summing them to generate a grid of frontal density persistence values, in months per year. This strategy is akin to one an analyst might use to identify a "windy pass" in the terrestrial environment, rather than demarcate individual gusts and breezes. We use the resulting summed monthly grid to generate annual (June to May) maps of high density persistence. The maps identify only those aggregations that persist for more than three months (in green). A value of twelve (in red) means the region exhibits a high concentration of steep temperature gradients throughout the year (Figure 2). We compare the area of extent for persistent (> 8 mos) concentrations SST fronts between years.

We then compare the location of residential feeding behavior for Mate's tagged whales to the density of frontal features within our study area. Blue whales have been shown to capitalize on oceanographic regions (chlorophyll rich upwelling fronts) characterized by high productivity (Fiedler et al., 1998), and aggregate to feed upon krill within the Channel Islands (Mate et al., 1999). Satellite tagged blue whales in 1995 traveled directly from the Channel Islands down along the coast of Baja California during which time they are presumably either feeding or looking for food (Mate et al., 1999). Residential behavior is defined here as ten or more days within a 200km radius. Residential behavior by several blue whale individuals in a recurrent region, we assume, indicates a key habitat for this Marine Species of Common Conservation Concern at the CEC. Residential behavior at high trophic levels may also point to increased biological productivity, and a pelagic habitat for many other species. Therefore, we broaden the concept of a pelagic habitat with a review of fisheries literature to identify cross-taxa habitat functions for the largest, most persistent concentration of SST fronts in Pacific North American federal waters.

Results

Persistent concentrations of high frontal density are not omnipresent in the Northeast Pacific under either ENSO regime. Less than one percent (.52 %) of the grid cells exhibited a high density of temperature fronts for nine months or more, even under the most active conditions (La Niña, 1998-1999). These cells were all concentrated in a zone 500 km by 250 km, centered about 150 km off the coast of Pacific Baja California Sur, referred to here as the Baja California Frontal System (BCFS). We define the BCFS not as a single persistent front, but as a dynamic region characterized by a persistent high concentration of frontal features generated by the confluence of the cool southbound California Current and warmer northbound Davidson Current (a.k.a. the California Counter-Current) as it intersects the Baja California Peninsula.

The Northeast Pacific as a whole was less active (in terms of concentration and persistence) for SST fronts under El Niño (1997-1998) conditions (.29% of cells in the grid were active nine months and more), but the BCFS system remained the most persistent, and the most active region for temperature fronts in the Northeast Pacific between years (Figure 2). Persistent high-density cells were found outside of Mexico's EEZ in 98-99 in the North Pacific Transition Zone (> 9 mos/yr) and the Channel Islands, as seasonal (3 mos) and subannual concentrations (< 9 mos). Regions exhibiting seasonal (3 mos) activity account for less than 10% of the Northeast Pacific Ocean when summed. La Niña years appear more active for frontal features (9.35% are high-density cells for three months or more) than El Niño years (8.4% are high-density cells three months or more). We identified four small
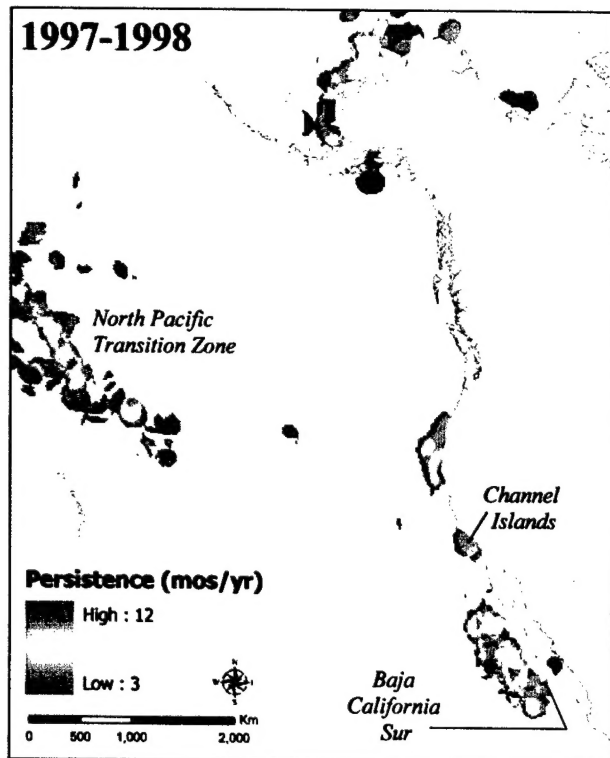
Figure 2. *Persistence, in months per year, for concentrations of sea surface temperature fronts in the Northeast Pacific. Red values indicate exceptional densities of temperature gradients: 12 months per year. Green values indicate seasonal concentrations. The years defined June 1997-1998 (El Niño) and June 1998-1999 (La Niña) vary most in intensity near Baja California Sur and the North Pacific Transition Zone.*

concentrations (averaging ~500 km²) of frequent (6-8 mos) frontal concentration in the Northeast Pacific during the El Niño year of 1998—the North Pacific Transition Zone, Point Conception offshore, the Channel Islands, and BCFS. We also identified many offshore seasonal concentrations dispersed throughout the region.

Satellite telemetry on live pelagics reveals that the four tagged blue whales transiting the BCFS in October and November of 1998 lingered between two weeks and twenty-nine days within a radius of 225 km (Figure 3). Residence time in the BCFS varied from 11 to 25 days before continuing southeast, or losing data transmission. One whale (blu404175) traveled 2250 km in 16 days before taking up residence in the BCFS for 15 days within an 80 km radius. Individual whale movements consistently overlap frontal features, or maintain positions between two frontal features (Figure 4). Only one of two whales from 1995 displayed similar residential behavior in the BCFS. All six whales described in Mate et al. (1999) display similar residential behavior in the Channel Islands, where we find a high subannual concentration of frontal features.

A literature review of BCFS and species associations indicates truly exceptional landings of the sword-fish *(Xiphias gladius)* (Sosa-Nishizaki and Shimizu, 1991) by 35 years of Japanese tuna longliners in the North Pacific, and the highest catch per unit effort (CPUE) over 10 years for striped marlin *(Tetrapturus audax)* in the entire Pacific (Squire and Suzuki, 1991; Figures 5 and 6). The region we refer to here as an "exceptionally persistent high concentration of temperature fronts in Mexico's Pacific EEZ" is referred to in fisheries literature as simply "the waters off Baja California." That vague terminology contrasts markedly with the depth of investigations into monthly catch per unit effort (CPUE) for tuna and billfish fisheries in the Pacific. Sosa-Nishizaki and Shimizu (1991) describe the waters off Baja California in terms of Japanese longline tuna boat concentration, saying "the size of this area begins to diminish from April, stays small in August and September, then expands again from October to reach its maximum in December."

Discussion

The North Pacific Transition Zone, Baja California Frontal System, and Channel Islands pelagic regions are shown here to be rare, spatially explicit, and persistent concentrations of steep temperature gradients in the Northeast Pacific within and between years. The
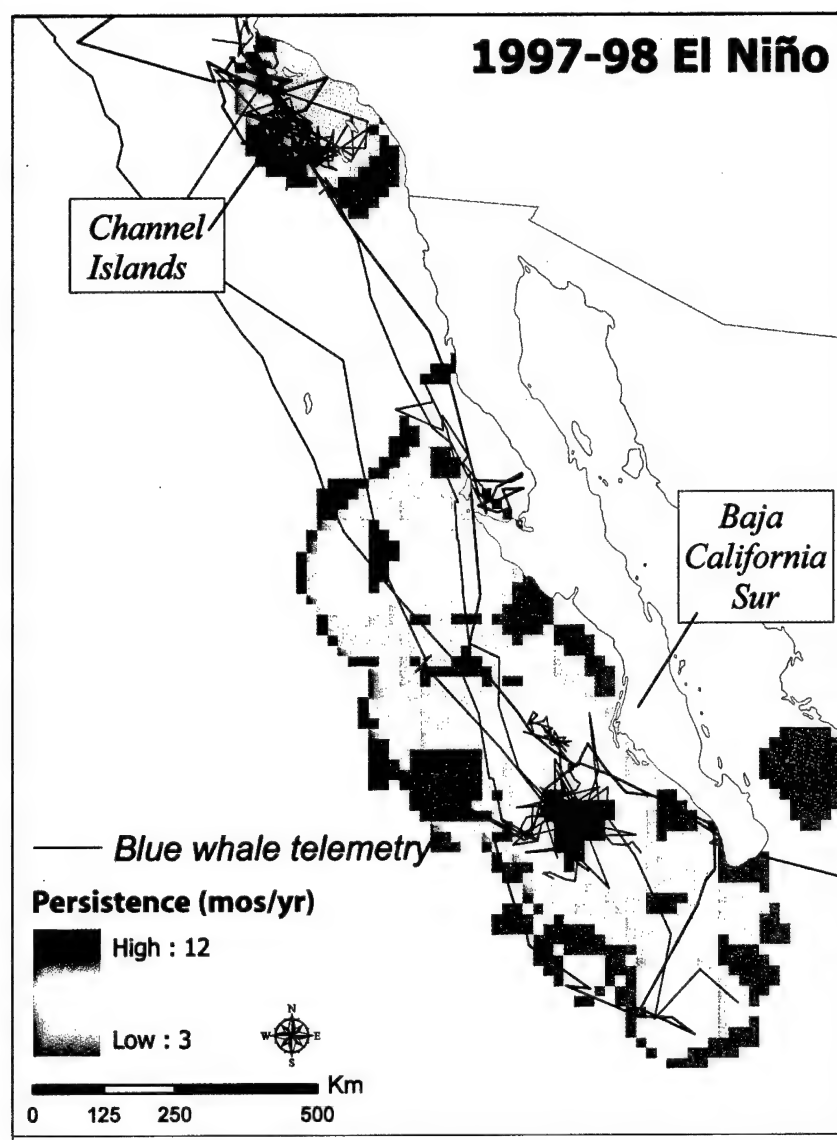
Figure 3. *Blue whale telemetry from Bruce Mate, OSU overlaid on frontal density persistence values.*
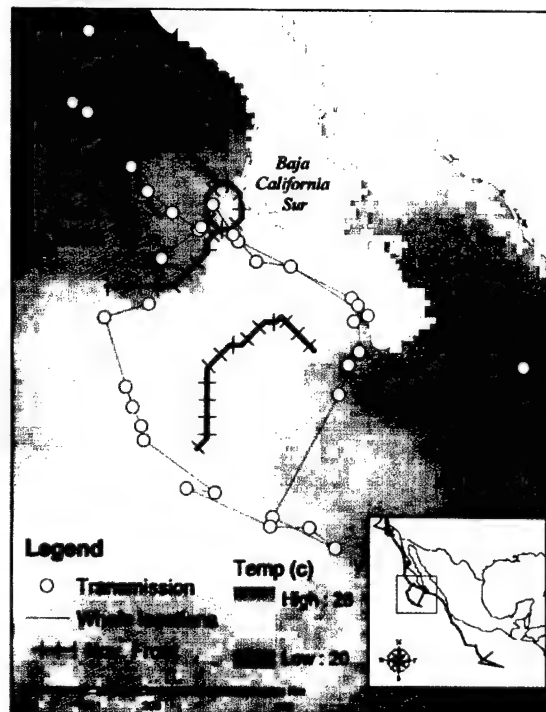
Gulf of California likely advects warm nutrient-laden water into the cooler waters of the BCFS, so it is possible that SST fronts themselves are only a physical part of the greater trophic exchange equation. The fisheries literature describes "expansion" in the BCFS area beginning in October. This coincides with the residence periods of our southward migrating blue whales. These whale migrations are presumably triggered by decreasing day length, increasing moonlight, or dropping September temperatures that may or may not signal resource abundance in the BCFS. Perhaps even the genetic memory of migratory experience imparts a softer departure date for blue whales feeding off Alaska.

It is remarkable that the 35 years of longline CPUE data described earlier does not consider interannual variability. Our analysis suggests that the temperature fronts around Baja are reduced during an El Niño year. El Niño may force warm, homogenous waters northward, or downward where they may be poorly resolved by the MCSST data. It is also possible that the dynamics of mixing are truly repressed under El Niño conditions.
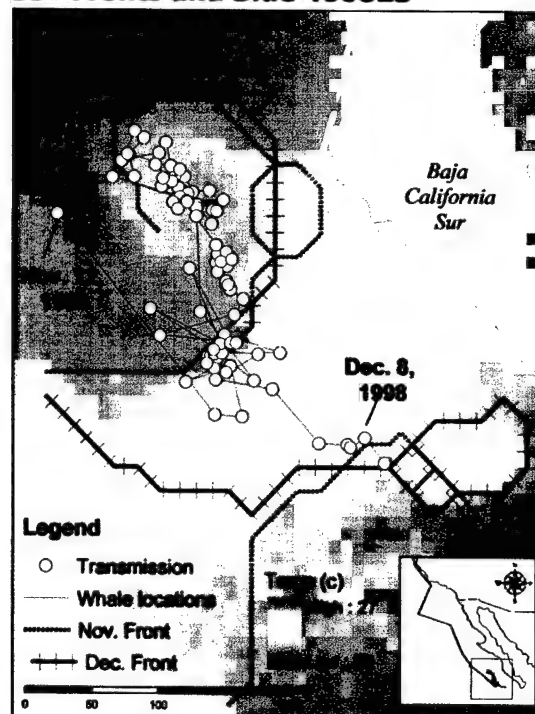
Satellite telemetry from blue whales clearly demonstrates residence times of 15 to 30 days in and around this frontal system. Aerial surveys from Gendron (2002) further support our contention that the BCFS is an explicit pelagic habitat for blue whales. Still, commercial fisheries data proved to be the best quantitative measure of productivity to the highest trophic levels. Those data are coarse (5 degree) but they span the entire ocean basin, providing 50 years of evidence that the BCFS is as unique for fisheries in the Northeast Pacific as it is for temperature gradients. The coincidence of Swordfish, striped marlin, and blue whale populations begs important questions-for example, What are they eating? What other species frequent the area? Swordfish and striped marlin are known to be non-selective, feeding on squid, anchovy, and mackerel. Blue whales are thought to feed exclusively on krill. Therefore, these waters either support separate and abundant prey populations, or one of these pelagics is switching prey.
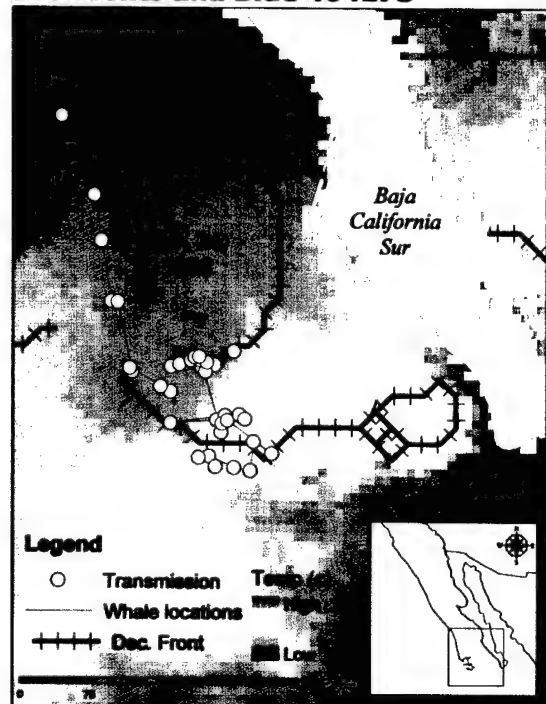
latter regions fall within the boundaries of the Baja to Bering (B2B) Marine Conservation Initiative. We recommended two ecologically valuable pelagic habitats for consideration as Priority Conservation Areas based upon this analysis—the BCFS and the Channel Islands. We have shown that these features are unique within the Northeast Pacific, they are persistent, they fall within an EEZ, and they provide habitat for commercial and endangered species. The Channel Islands satisfy threat and opportunity criteria, but the BCFS does not, so the BCFS was designated an "important oceanographic area" in the B2B PCA mapping exercise.

Temperature fronts near the BCFS are generated by mixing of the cool southbound California Current as it meets the warmer waters of northbound Davidson Current (also the California Counter-Current). The
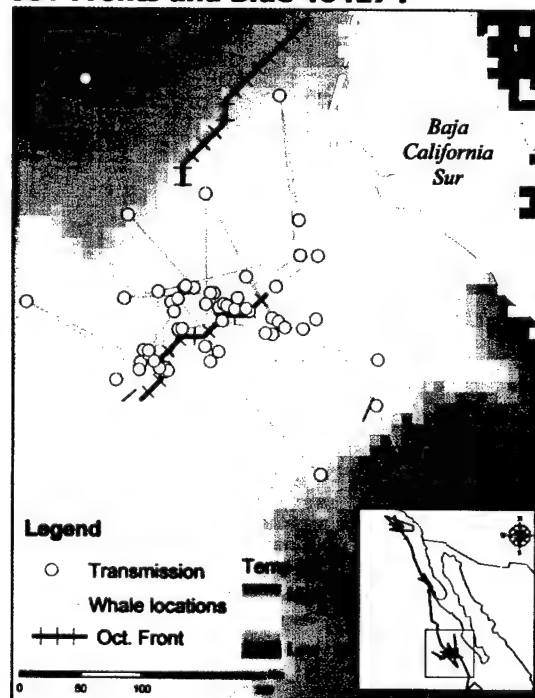
Figure 4. *Individual tracks from satellite-tagged blue whales* (Balaenoptera musculus) *indicate individual affinity for frontal features in and around the Baja California Frontal System. These whales were on a southeastern bearing before circling in the BCFS. A greater extent of their migrations are shown on insets to the lower right of each panel. Lines between locations indicate the chronological order of locations and do not represent the whales' actual tracks between locations.*
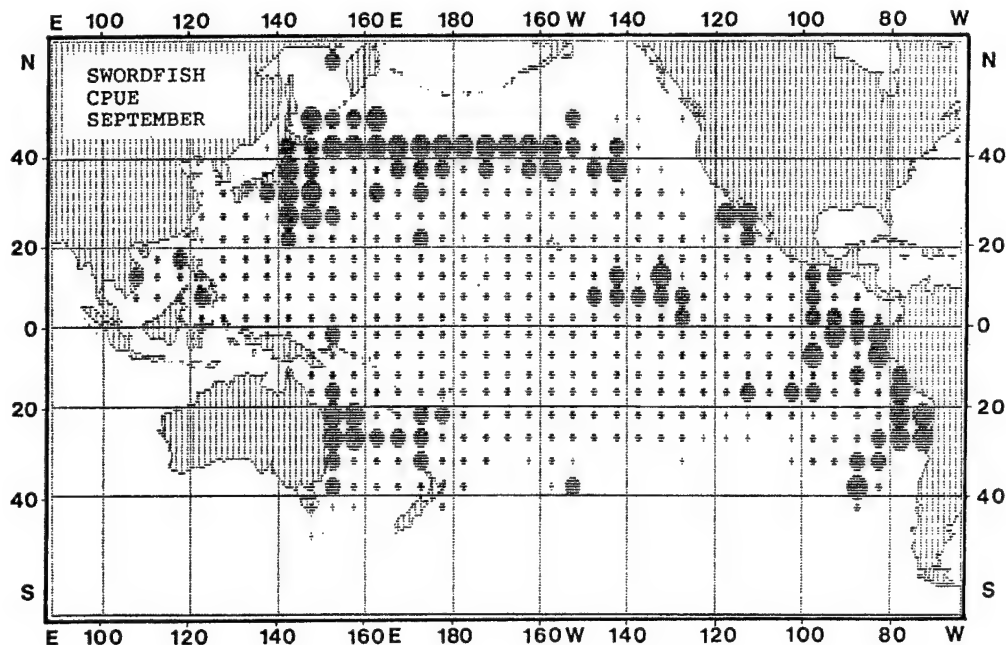
Figure 5. *Reprinted from Sosa-Nishizaki and Shimizu, 1991. Monthly swordfish catch per unit effort (CPUE) from Japanese longliners, averaged over 35 years. Swordfish landings are consistently high off Baja California.*

Something draws species to the BCFS from far away. Squire and Au (1990) observed a rapid rebuilding of striped marlin populations after the cessation of Japanese longlining in the Mexican EEZ in 1979, which they attributed to immigration from other areas of the Pacific into the "major feeding and growth area in the Northeast Pacific." For Loggerhead turtles like J. Nichol's *Adelita,* there is also evidence of distant emigration from this region, in a six-year, trans-Pacific journey from Baja California to Japan (Nichols et al., 2000). The BCFS is clearly known to Mexican researchers as a special place in Mexican waters. This study simply shows that the BCFS is a very special place in the entire North Pacific, and that it lies within the federal waters of the B2B Marine Conservation Initiative. This study also shows that smaller, less persistent frontal systems populate Northeast Pacific federal waters.

Mexico has a history of fisheries research and management, but scientists and managers will need international support and recognition to extend Mexican management capacity into Pacific pelagic waters. Mexico felt the economic sting of "dolphin-safe tuna" standards in 1992. Even now, Mexico is protesting a US embargo of net caught tuna before the World Trade Organization. But these are gear and trade issues. The recreational fishing industry may offer some hope for spatial management in a continentally significant pelagic feature like the BCFS. Sport fishing for billfish has been a permitted activity in Mexico since 1937, with an economic value that rivals commercially fished tuna. Waters within 50 nautical miles of the Baja California coast have been reserved for sport fishing since 1983, with an adjacent "billfish protection zone" in the Pacific (Sosa-Nishikazi, 1998). At the very least, sport fishing puts some boats on-the-water with some limits, some standards, and some accountability. Squire and Au (1990) called for "core area management" in the waters off Baja California more than a decade ago. Fortuitously, that study reached its conclusion based upon fisheries biology, and this one reached the same conclusion based upon satellite oceanography.

These results best distinguish heterogeneous waters from homogenous waters across broad latitudes, and only in two dimensions. Further studies should investigate the most understudied, dynamic, and accessible of these areas, the BCFS, at a high spatial resolution in three dimensions, and seek to further quantify multi-specific species aggregations with an active live sampling program. Also, the general effect of temporal and spatial scale upon edge detection warrants some further investigation. Daily cloud-free interpolated sea surface temperature for the Northeast
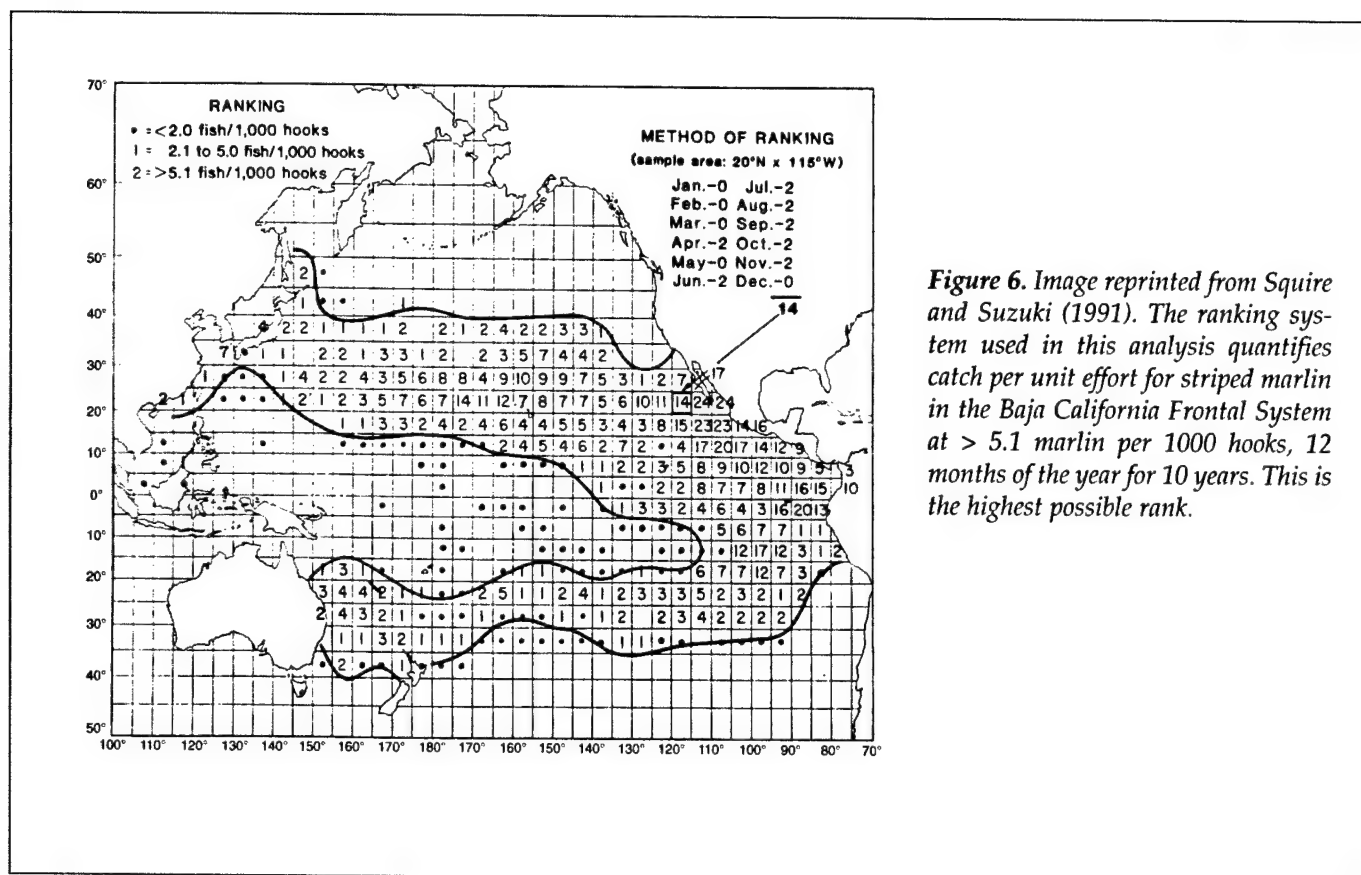
Figure 6. Image reprinted from Squire and Suzuki (1991). The ranking system used in this analysis quantifies catch per unit effort for striped marlin in the Baja California Frontal System at > 5.1 marlin per 1000 hooks, 12 months of the year for 10 years. This is the highest possible rank.

Pacific from the 1/16th degree Navy Layered Ocean Model, for example, may be well suited to this purpose (Rhodes et al., 2002). Ultimately, the finest examinations will pursue daily, high-resolution (< 4km pixel) sea surface temperature available from Coastwatch or from MODIS for small geographic regions, and these examinations will compare those daily SST data to daily blue whale telemetry. Billfishes may not surface enough to transmit daily geoposition.

The efficacy of results from interpolated coarse grain data should also be questioned and further examined. Satellite derived SST data are plagued by clouds, and edge detection algorithms often underestimate the density of temperature fronts (P. Cornillon, pers comm.). Considerable cloud contamination in the 9 km AVHRR monthly SST data seaward of British Colombia suggests that the interpolated 18 km Miami SST data are unlikely to resolve meaningful gradients north of Vancouver, Canada. It is our suspicion that a lack of high-density concentrations may not be indicative of a lack of meaningful convergences, though boreal waters north of Vancouver are dominated by Arctic waters, and more homogenous (in degrees C) than temperate waters.

The first step for conservation of pelagic habitat is to illustrate and describe features like those mentioned here, and to document their functions for species, and then to address the pressures upon them. Enforcement capacity for pelagic features is limited. Our under-standing of these features is weak. Satellite-driven research design has a short history, but offers as much promise to management as it does to fisheries. Management and policy decisions will be made according to each country's needs and realities, but international organizations like the CEC must emphasize the need for pelagic management with similar satellite driven research. The CEC has officially recognized these pelagic features as "important oceanographic areas." We duly encourage the NAFTA countries to extend their management capacity to the frontiers of their EEZ, and to pursue pelagic protected areas for endangered and non-endangered marine species. 🗹

Acknowledgements

Striped marlin 40 miles off Magdelena Bay, Baja California
© Richard Herrmann, Poway, California, http://www.richardherrmann.com

References

Bakun, A., 1996: Patterns in the Ocean: Ocean Processes and Marine Population Dynamics. California Sea Grant/CIB, La Paz, Mexico, 323 pp.

Block, B.A., H. Dewar, S.B. Blackwell, T. Williams, E. Prince, A.M. Boustany, C. Farwell, D.J. Fudge, and A. Seitz, 2001: Migratory movements, depth preferences and thermal biology of Atlantic bluefin tuna. *Science*, 293, 1310-1314.

Bowen B.W., F.A. Abreu-Grobois, G.H. Balazs, Kamezakin., C.J. Limpus, and R.J. Ferl, 1995: Trans-Pacific migrations of the loggerhead turtle (*Caretta caretta*) demonstrated withmitochondrial DNA markers. Pp. 3731-3734 in *Proceedings of the National Academy of Sciences*. The National Academy of Science, Washington, D.C.

Calambokidis, J., G.H. Steiger, J.C. Cubbage, K.C. Balcomb, C. Ewald, S. Kruse, R. Wells, and R. Sears. 1990: Sightings and movements of blue whales off central California 1986-88 from photo-identification of individuals. *Report of the International Whaling Commission*, 12 (Special Issue), 343-348.

Chavez, F.P., P.G. Strutton, G.E. Friederich, R.A. Feely, G.C. Feldman, D. Foley, and M.J. McPhaden, 1999: Biological and chemical response of the equatorial Pacific Ocean to the 1997-98 El Niño, *Science*.

Davis, R.W., J.G. Ortega-Ortiz, C.A. Ribic, W.E. Evans, D.C. Biggs, P.H. Ressler, R.B. Cady, R.R. Leben, K.D. Mullin, and B. Wursig, 2002: Cetacean habitat in the northern oceanic Gulf of Mexico. *Deep-Sea Res.*, 49, 121-142.

Decker, M.B., and G.L. Hunt, Jr., 1996: Murre (*Uria lomvia and U. aalge*) foraging at the frontal system surrounding the Pribilof Islands, Alaska. *Mar. Ecol. Progr. Ser.*, 139, 1-10.

Etnoyer, P.J., D. Canny, and L.E. Morgan, 2002: B2B 1.1 CDROM, Information for Conservation Planning - Baja California to the Bering Sea. Marine Conservation Biology Institute, Redmond, Washington.

Fiedler P.C., S.B. Reilly, R.P. Hewitt, D. Demer, V.A. Philbrick, S. Smith, W. Armstrong, D.A. Crol, B.R. Tershy, and B.R. Mate, 1998: Blue whale habitat and prey in the California Channel Islands. *Deep-Sea Research*, 45, 1781-1801.

Fournier, R.O., M. Van Det, J.S. Wilson, and N.B. Hargreaves, 1979: Influence of the shelf-break off

Nova Scotia on phytoplankton standing stock in winter. *Journal of the Fisheries Board of Canada*, 36, 1228-1237.

Franks, P.J.S., 1992: Swim or sink: accumulation of biomass at fronts. *Marine Ecology Progress Series*, 82, 1-12.

Gendron, D., 2002: Population Ecology of the Blue Whales, *Balaenoptera musculus*, of the Baja California Peninsula. Centro de Investigacion Cientifica y de Educacion Superior de Ensenada (CICESE). Ph.D. Thesis.

Gong, Y., S. Kim, and D.H. An, 1993: Abundance of neon flying squid in relation to oceanographic conditions in the North Pacific. *International North Pacific Fisheries Commission Bulletin*, 53, 191-204.

Harrington, B., and C. Flowers, 1996: *Flight of the Red Knot*, W.W. Norton & Co., New York.

Herron R.C., T. Leming, and J. Li, 1989: Satellite-detected and butterfish aggregations in the northeastern Gulf of Mexico. *Continental Shelf Research*,9(6),569-588

Hewitt R.P., J.L. Watkins, M. Naganobu, P. Tshernyshkov, A.S. Brierley, D.A Demer, S. Kasatkina, Y. Takao, C. Goss, A. Malyshko, M.A. Brandon, S. Kawaguchi, V. Siegel, P.N. Trathan, J.H. Emery, I. Everson, D.G.M. Miller, 2002: Setting a precautionary catch limit for Antarctic krill. *Oceanography* 15 (3), 26-33.

Hyrenbach, D.K., K. Forney, and P. Dayton, 2000: Marine Protected Areas and Ocean Basin Management. *Aquatic Conser : Mar. Freshw. Ecosyst.*, 10, 437-458

Kawasaki, T., and M. Omori, 1988: Fluctuations in the three major sardine stocks in the Pacific and the global trend in mean temperature. In: *Int. Symp. on Long Term Changes in Marine Fish Populations*, Vigo, Spain, T. Wyatt and M.G. Larrañeta, eds., 273-290.

Kimura, S., M. Nakai, and T. Sugimoto, 1997: Migration of albacore, *Thunnus alalunga*, in the North Pacific Ocean in relation to large oceanic phenomena. *Fisheries Oceanography*, 6, 51-57.

Kinder T.H., G.L. Hunt, Jr., D. Schneider., and J.D. Schumacher, 1983: Oceanic fronts around the Pribilof Islands, Alaska: Correlations with seabirds. *Estuarine, Coastal and Shelf Science*, 16, 309-319.

Laurs R.M., P.C. Fiedler, and D.R. Montgomery, 1984: Albacore tuna catch distributions relative to environmental features observed from satellites. *Deep-Sea Research*, 31, 1085-1099.

Lluch-Belda, D., R.J.M. Crawford, T. Kawasaki, A.D. MacCall, R.H. Parrish, R.A. Schwartzlose, and P.E. Smith, 1989: World-wide fluctuations of sardine and anchovy stocks: the regime problem. *S. Afr. J. Mar. Sci.*, 8, 195-205.

Mate, B.R., B.A. Lagerquist, and J. Calambokidis, 1999: Movements of North Pacific blue whales during the feeding season off southern California and southern fall migration. *Marine Mammal Science*

15(4), 1246-1257.

Morgan, L., T. Wilkinson, P. Etnoyer, H. Hermann, 2004: Identify Priority Areas for Conservation in the Baja California to Bering Sea Ecoregion. Proceedings of the Fifth International Conference of the Science and Management of Protected Areas Association (SAMPAA).

Munk P., P.O. Larsson, D. Danielsen, and E. Moksness, 1995: Larval and small juvenile cod Gadus morhua concentrated in the highly productive areas of a shelf break front. *Marine Ecological Progress Series*, 125, 21-30.

Myers R.A., and B. Worm, 2003: Rapid worldwide depletion of predatory fish communities. *Nature*, 423,280-283.

Nichols, W.J., A. Resendiz, J.A. Seminoff, and B. Resendiz, 2000: Transpacific migration of a loggerhead turtle monitored by satellite telemetry. *Bulletin of Marine Science*, 67, 937-947.

Olson, D.B., and R.H. Backus, 1985: The concentration of organisms at fronts: a cold-water fish and a warm-core ring. *Journal of Marine Research* 43, 113-137.

Olson, D.B., G.L. Hitchcock, A.J. Mariano, C.J. Ashjan, G. Peng, R.W. Nero, and G.P. Podesta, 1994: Life on the edge: marine life and fronts. *Oceanography*, 7(2), 52-60.

Owen, R.W., 1981: Fronts and eddies in the sea: mechanisms, interactions and biological effects. Pp. 197-231 in *Analysis of MarineEcosystems*, A.R. Longhurst, ed., Academic Press, New York,.

Pauley, D., V. Christensen, J. Dalsgaard, R. Froese, and F. Torres, Jr., 1998: Fishing down marine food webs. *Science*, 279, 860-863.

Podesta G.P., J.A. Browder, and J.J. Hoey, 1993: Exploring the association between swordfish catch rates and thermal fronts on US longline grounds in the western North Atlantic. *Continental Shelf Research*, 13, 253-277.

Polovina, J.J., D.R. Kobayashi, D.M. Parker, M.P. Seki, and G.H. Balazs, 2000: Turtles on the edge: movement of loggerhead turtles (*Caretta caretta*) along oceanic fronts spanning longline fishing grounds in the central North Pacific, 1997-1998. *Fisheries Oceanography*, 9, 1-13.

Polovina, J.J., E. Howell, D.R. Kobayashi, and M.P. Seki, 2001: The transition zone chlorophyll front, a dynamic global feature defining migration and forage habitat for marine resources. *Progress in Oceanography*, 49, 469-483.

Rhodes, R.C., H.E. Hurlburt, A.J. Wallcraft, C.N. Barron, P.J. Martin, O.M. Smedstad, S.L. Cross, E.J. Metzger, J.F. Shriver, A.B. Kara, and D.S. Ko, 2002: *Navy real-time global modeling systems. Oceanography*, 15(1), 29-43.

Roffer, M.A., 1987: Influence of the Environment on the Distribution and Relative Apparent Abundance of Juvenile Atlantic Bluefin Tuna along the United

States East Coast. Ph.D. Dissertation. University of Miami, Miami, Florida, 154pp.

Roffer, M.A., 2000: Using Satellite Images to Locate Marlin. Pp. 78-81 in *The 2000 Official Guide To Billfishing*, Sports USA Group, Inc. Seminole, Florida, 144pp.

Roughgarden, J., S. Gaines, and H. Possingham, 1988: Recruitment dynamics in complex life cycles. *Science*, 241, 1460-1466.

Schick, R.S., J. Goldstein, and M.E. Lutcavage, 2002:. Bluefin tuna (*Thunnus thynnus*) distribution in relation to sea surface temperature fronts in the Gulf of Maine (1993-1996). *Fish. Oceanogr.* (in review).

Seki, M.P., J.L. Polovina, D.R. Kobayashi, R.R. Bidigare, and G.T. Mitchum, 2002: An oceanographic characterization of swordfish (*Xiphias gladius*) longline fishing grounds in the springtime subtropical North Pacific. *Fish. Oceaogr.*, 11(5), 251-266.

Sosa-Nishizaki, O., 1998: Historical review of the billfish management in the Mexican Pacific. *Ciencias Marinas*, 24(1):95-111.

Sosa-Nishizaki, O., and M. Shimizu, 1991: Spatial and temporal CPUE trends and stock unit inferred from them for the Pacific swordfish caught by the Japanese tuna longline fishery. 1991. *National Research Institute for Far Seas Fisheries. Bulletin*, 28 (March).

Squire, J.L., and D. Au, 1990: .Management of striped marlin (*Tetrapturus audax*) resources in the northeast Pacific a case for local depletion and core area management. In: *Proc. Int. Billfish Symp., Part II*, Kailua-Kona, Hawaii, August 1-5, 1988, 199-214.

Squire, J. L., and Z. Suzuki, 1991: Migration trends of Striped Marlin (*Tetrapturus audax*) in the Pacific Ocean. In: *Planning the Future of Billfishes-Research and Management in the 90s and Beyond*, Part 2, R.H. Stroud, ed., Contributed papers.

Ullman, D.S., and P.C. Cornillon, 1999: Satellite-derived sea surface temperature fronts on the continental shelf off the northeast U.S. coast. *Journal of Geophysical Research*, 104, 23,459-23,478.

United Nations Convention on the Law of the Sea. December 1982.

Wolanski E., and W.H. Hamner, 1988: Topographically controlled fronts in the ocean and their biological importance. *Science*, 241, 177-181.

Worm B., H. Lotze, and R. Myers, 2003: Predator diversity hotspots in the blue ocean. In: *Proceedings of the National Academy of Sciences*. The National Academy of Science, Washington, D.C.

Comparisons of *Calanus finmarchicus* fifth copepodite abundance estimates from nets and an optical plankton counter

MARK F. BAUMGARTNER*

COLLEGE OF OCEANIC AND ATMOSPHERIC SCIENCES, OREGON STATE UNIVERSITY, 104 OCEAN ADMINISTRATION BUILDING, CORVALLIS, OR 97331 USA

PRESENT ADDRESS: BIOLOGY DEPARTMENT, WOODS HOLE OCEANOGRAPHIC INSTITUTION, MS #33, WOODS HOLE, MA 02543 USA

*CORRESPONDING AUTHOR: mbaumgartner@whoi.edu

The response of an optical plankton counter (OPC) to concentrations of Calanus finmarchicus fifth copepodites (C5) ranging from 2 to 1621 copepods m^{-3} was examined during the summers of 1999–2001 over the continental shelf of the northwest Atlantic Ocean. Net tows from either a bongo net or a multiple opening/closing net and environmental sensing system (MOCNESS) were collocated with vertical OPC casts to provide comparable data. OPC-derived particle abundance in the 1.5–2.0 mm equivalent circular diameter range was strongly correlated with net-derived abundance of C. finmarchicus C5 ($r^2 = 0.655$ and 0.726 for comparisons in two independent datasets). Particle abundance in this size range increased with increases in the descent speed of the vertically profiled OPC, which indicated avoidance of the small sampling aperture by C. finmarchicus C5. A regression model was developed to relate OPC particle abundance in the 1.5–2.0 mm size range to the abundance of C. finmarchicus C5 and the descent speed of the OPC. The data fitted the model well ($r^2 = 0.684$) and the inverted model was used as a calibration equation to predict C. finmarchicus C5 abundances from OPC measurements in an independent comparison to net abundances. In that case, the calibration equation underestimated net abundance by an average factor of 2. However, anomalously low OPC particle abundances for some casts suggest that spatial heterogeneity (patchiness) can confound such comparisons.

INTRODUCTION

The calanoid copepod *Calanus finmarchicus* plays a pivotal trophic role in North Atlantic ecosystems by concentrating phytoplankton and microzooplankton biomass and making it directly available to higher trophic levels, such as fish, birds and some marine mammals. *Calanus finmarchicus* has garnered much attention in recent years (Tande and Miller, 1996; Wiebe *et al.*, 2001) because its life history and population dynamics have a significant impact on so many other species. One such species is the North Atlantic right whale (*Eubalaena glacialis*). This highly endangered baleen whale feeds primarily on older copepodite stages of *C. finmarchicus* in its summer feeding grounds over the continental shelf of the northwestern Atlantic Ocean (Stone *et al.*, 1988; Murison and Gaskin, 1989; Woodley and Gaskin, 1996). By summer, *C. finmarchicus* has already undertaken its ontogenetic downward migration and the population is primarily in the resting, fifth copepodite (C5) stage at depth (Miller *et al.*, 1991; Hirche, 1996). To understand better important aspects of right whale ecology, particularly its foraging behaviour and habitat, a method was required to rapidly assess the horizontal and vertical distribution and abundance of *C. finmarchicus* C5. The optical plankton counter (OPC) (Herman, 1988, 1992) has been used as just such a rapid assessment tool in several applications (Sameoto and Herman, 1990; Herman *et al.*, 1991; Heath, 1995; Huntley *et al.*, 1995; Stockwell and Sprules, 1995; Checkley *et al.*, 1997; Osgood and Checkley, 1997). The performance of the OPC has been examined in a wide variety of environments (Herman *et al.*, 1993; Sameoto *et al.*, 1993; Wieland *et al.*, 1997; Sprules *et al.*, 1998; Grant *et al.*, 2000; Woodd-Walker *et al.*, 2000; Zhang *et al.*, 2000; Halliday *et al.*, 2001), and it has shown promise in estimating the abundance of older stages of *Calanus* spp. (Osgood and Checkley, 1997; Heath *et al.*, 1999).

The OPC consists of a light source and a detector

housed in the middle of a flow tunnel through which water passes (Herman, 1988, 1992). Particles in the water partially occlude the collimated beam formed by the light source as they pass through the tunnel. The magnitude of the occlusion measured at the detector is related to the illuminated cross-sectional area of the particle. The OPC, therefore, provides an estimate of numbers and sizes of particles passing through the tunnel. The challenges of making sensible measurements with the OPC are similar to those faced by other rapid assessment methods. Both the OPC and video methods [e.g. (Davis *et al.*, 1992, 1996)] sample relatively small volumes. In a patchy environment, significant concentrations of zooplankton may not be sampled by the instrument, so abundance may be underestimated. Statistical power is also reduced when estimating the concentration of less abundant mesozooplankton from small sample volumes. Furthermore, the small aperture through which particles pass to be sampled by these instruments is susceptible to avoidance by zooplankton. Unlike high-quality video, the OPC and acoustic methods (Holliday and Pieper, 1995) are hampered by their lack of taxonomic discrimination. In particular, a major constituent of OPC-observed particles in neritic waters is thought to be detrital material (Herman, 1992), which may impede taxonomic discrimination based on particle size alone. At high particle concentrations, the OPC is also prone to coincident counts, a phenomenon that occurs when two or more particles occlude the light beam simultaneously and are recorded as a single, larger particle (Herman, 1988; Sprules *et al.*, 1998).

Despite these challenges, the zooplankton community near feeding right whales has characteristics ideal for applying the OPC. The average water column abundance of *C. finmarchicus* C5 is typically in the upper hundreds to low thousands of copepods m^{-3} (Murison and Gaskin, 1989; Mayo and Marx, 1990; Wishner *et al.*, 1995; Woodley and Gaskin, 1996) and the abundances at depth, where the whales concentrate their feeding, are probably much higher (Kenney *et al.*, 1986). Statistical power, therefore, should not be a problem. *Calanus finmarchicus* C5 is typically the dominant zooplankter of its size near right whales, so discrimination based on size alone seems possible. Detrital material, however, is ubiquitous over the continental shelves, so size discrimination may be difficult. In fact, Heath and colleagues (Heath *et al.*, 1999) suggest that 'the high incidence of detrital aggregates would seem to preclude the use of the OPC [for measuring late-stage *C. finmarchicus*] in continental shelf waters'. They based this conclusion on poor correlations between OPC-derived particle abundances and net-derived abundances of *C. finmarchicus* C4 and C5 between 0.05 and 500 copepods m^{-3} in the upper 200 m of the Faroe–Shetland Channel.

This paper examines the response of the OPC to *C. finmarchicus* C5 abundances between 2 and 1621 copepods m^{-3} in a neritic environment. OPC particle abundances were compared to net-derived abundance estimates to determine in which particle size range *C. finmarchicus* C5 could be detected. Avoidance of the OPC's small tunnel opening (2 × 25 cm) by *C. finmarchicus* C5 was also investigated by changing the descent speed for some OPC casts that accompanied net tows. A separate dataset consisting of paired OPC casts in which the descent speed was either varied or held constant between two successive casts was also used to examine avoidance by *C. finmarchicus* C5. Finally, a model relating OPC particle abundance and *C. finmarchicus* C5 abundance was developed and tested with independent data for comparison with the results of Heath and colleagues (Heath *et al.*, 1999). The inverted model is intended to be used as a calibration equation to estimate the abundance of *C. finmarchicus* C5 from OPC-derived particle abundance in future studies.

METHOD

A Focal Technologies OPC (model OPC-1T) was mounted in the centre of an open, 0.8 m diameter by 1.0 m height, cylindrical, galvanized steel cage such that the downward-facing tunnel opening was 2–3 cm from the bottom of the cage. Two different instruments were used in this study: serial numbers TOW015 in 1999 and TOW047 in 2000 and 2001. A conductivity–temperature–depth (CTD) instrument was also housed in the cage. Flow into and around the OPC was unobstructed. During 2000 and 2001, depth was measured by a pressure sensor in the OPC. The OPC was not equipped with a flowmeter, so the volume of water passing through the instrument was estimated simply as the product of the tunnel opening area (0.005 m^2) and the depth traversed by the OPC when profiled vertically. When a cast was not exactly vertical, the calculated volume is an underestimate of the true sampled volume and the resulting particle abundance is overestimated. The per cent error in the calculated volume for wire angles (θ) relative to the vertical is $100[\cos(\theta)-1]$ and is less than 10, 20 and 30% for angles as great as 25°, 36° and 45°, respectively. Wire angles during casts were not explicitly measured, but were typically <30°. The OPC was always deployed in a vertical cast and only the data from the downcast were used. Automated post-processing of the casts removed data associated with (i) low descent speeds (<0.3 m s^{-1}), (ii) direction reversals (during periods of high swell), (iii) excessive changes in relative light attenuance, (iv) non-sequential timer values and (v) invalid timer, depth, or relative light attenuance values. The instrument calibration was checked before and after the 2001 field season

by passing 1.59, 2.38 and 3.18 mm diameter nylon beads through the OPC (corresponding to average digital values of 228, 455 and 749, respectively). Measurement errors were within the manufacturer's specifications of 10% accuracy error (Focal Technologies, 1999). Particle sizes are expressed in units of equivalent circular diameter (ECD), which is the diameter of a circle that has the same area as the illuminated cross-section of the particle.

Collocated net and OPC sampling

Zooplankton samples were collected with 61 cm bongos equipped with 333 μm mesh nets. A CTD was affixed to the tow wire ~1 m above the bongo to telemeter the depth of the nets to the ship. The bongo was lowered at 0.50 m s^{-1} to within 5–10 m of the bottom and then hauled in at 0.33 m s^{-1}. The ship steamed at 0.8–1.0 m s^{-1} (1.5–2.0 knots) during tows. A flowmeter was mounted in the centre of each bongo to estimate the volume filtered by the nets. Depth-stratified, 1 m^2 multiple opening/closing net and environmental sensing system (MOCNESS) (Wiebe *et al.*, 1976, 1985) tows were conducted during 2001 in lieu of bongo tows. The MOCNESS was equipped with six, 150 μm mesh nets and the first of these remained open during the entire downcast to within 10 m of the bottom. The remaining five nets were towed through contiguous depth strata from the bottom of the downcast to the surface. The MOCNESS was towed at 0.5–1.0 m s^{-1} (1.0–2.0 knots) and paid out and hauled in at 0.33 m s^{-1}. The volume filtered by the nets was estimated from a flowmeter positioned outside the net mouth. Zooplankton samples were preserved in a 5% borate-buffered formalin and seawater solution and were subsampled in the laboratory with a Hensen stempel pipette. Subsample volumes were obtained such that 100 or more of the most abundant copepod species were counted. *Calanus finmarchicus* copepodite stages C3 and higher were counted separately while all other taxa were identified to species or genus level. More than 100 *C. finmarchicus* C5 were counted in 74% of the samples (52 of 70) and for those cases where fewer than 100 were counted, the *C. finmarchicus* C5 abundance was typically <55 copepods m^{-3} (14 of 18 cases) and always <200 copepods m^{-3}.

Each bongo tow was collocated with a single OPC cast that was usually conducted immediately prior to the net sampling. A total of 26 collocated bongo tows and OPC casts were conducted on the central and southwestern Scotian Shelf ($n = 12$) and in the lower Bay of Fundy ($n = 14$) aboard NOAA Ship *Delaware II* (cruise DE9908) from July 26 to September 3, 1999 (Figure 1; Table I). Fourteen bongo tows with accompanying OPC casts were conducted in the lower Bay of Fundy ($n = 11$) and on the southwestern Scotian Shelf ($n = 3$) from July 7 to August 31, 2000 aboard NOAA Ship *Delaware II* (cruise DE0007).

From July 23 to August 3, 2001, six MOCNESS tows were conducted from NOAA Ship *Albatross IV* (cruise AL0108) in the lower Bay of Fundy (Figure 1; Table I). These tows were conducted at slack tide and collocated with four OPC casts to reduce differences between the net and OPC abundance estimates attributable to advection of *C. finmarchicus* C5 and horizontal variability in copepod distribution. The local time of slack tide was predicted by TIDES & CURRENTS software (version 2.0) (Nautical Software, 1996) based on US National Oceanic and Atmospheric Administration and Canadian Hydrographic Service harmonic constants. The MOCNESS was towed through a station immediately after two OPC casts were completed there. After the tow, two more OPC casts were conducted at the midpoint of the tow. To investigate the effect of copepod avoidance (see below), three of the MOCNESS tows were accompanied by OPC casts conducted at a nominal descent speed of just over 0.5 m s^{-1} (referred to as the 'slow' AL0108 data). The remaining three MOCNESS tows were accompanied by OPC casts conducted at a nominal descent speed of just below 1.0 m s^{-1} (referred to as the 'fast' AL0108 data).

OPC-derived particle abundances were computed only

Table I: Collocated net and OPC deployment information for each cruise

Cruise	Sampling equipment	Tow type	Mesh size (μm)	No. of tows	No. of samples	OPC casts per tow	OPC descent speed range (m s^{-1})
DE9908	Bongo	double oblique	333	26	26	1	0.44–0.56
DE0007	Bongo	double oblique	333	14	14	1	0.60–0.92
AL0108[a]	MOCNESS	depth stratified	150	3	15	4	0.59–0.66
AL0108[b]	MOCNESS	depth stratified	150	3	15	4	0.87–0.98

[a]Referred to in the text as the 'slow' AL0108 data.
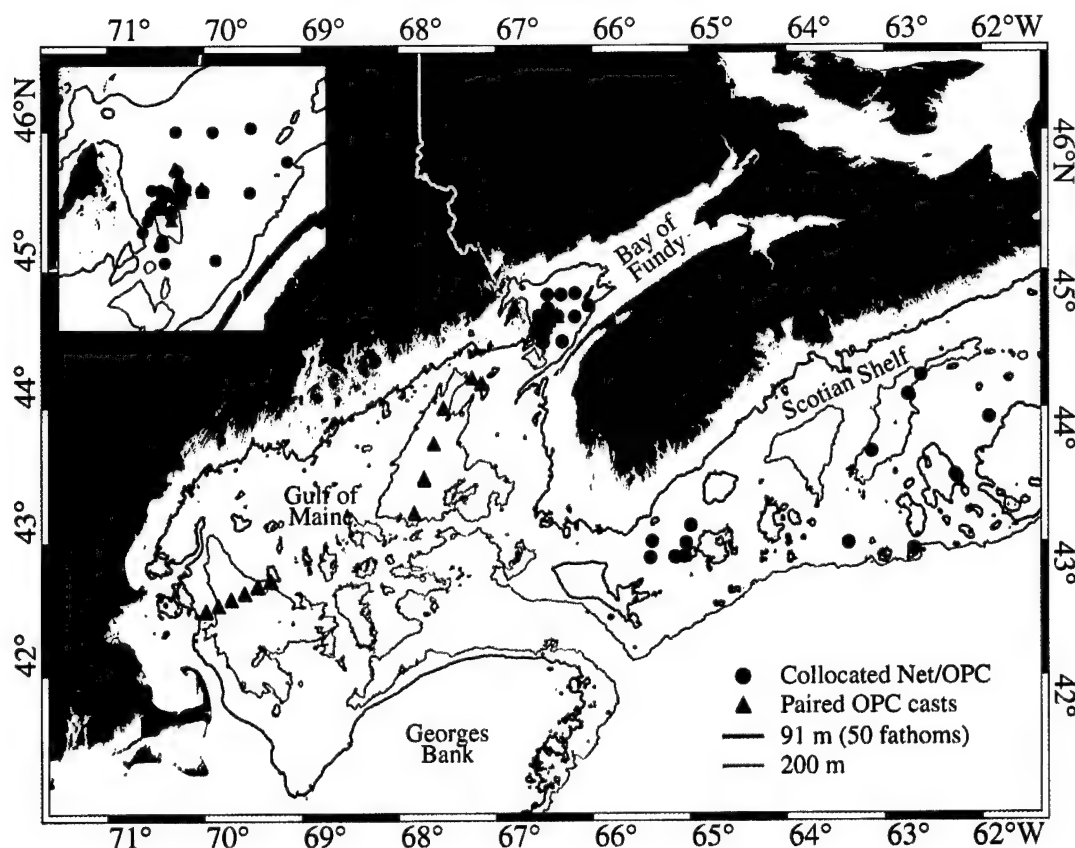[b]Referred to in the text as the 'fast' AL0108 data.

Fig. 1. Study area and locations of collocated OPC casts and net tows (filled circles) and paired OPC casts (filled triangles). Inset shows the study area in the lower Bay of Fundy. The 91 m (50 fathom) and 200 m isobaths are shown.

over the depths that were sampled during the bongo and MOCNESS tows to provide comparable data. The particle abundances from the four OPC casts accompanying each MOCNESS tow were averaged to obtain a single particle abundance estimate for each MOCNESS net sample.

Optimum size range detection

The size range in which *C. finmarchicus* C5 could be best detected was determined using similar methods to those employed by Heath and colleagues (Heath *et al.*, 1999). Particle abundances were computed from the OPC data over a matrix of size ranges systematically defined by the minimum and span of the size range [equivalently, the mid-point and the span of the size range were used in (Heath *et al.*, 1999)]. The minimum of the size range in the matrix varied from 0.25 to 3 mm in 0.05 mm increments and the span of the size range in the matrix varied from 0.20 to 2 mm in 0.05 mm increments. A regression procedure was first used to measure the strength of linear association between the log-transformed, OPC-derived

particle abundances and the collocated, log-transformed, net-derived abundances of *C. finmarchicus* C5 in each of the size ranges of the matrix. The regression coefficients ($a_{i,j}$ and $b_{i,j}$) and the coefficient of determination ($r_{i,j}^2$) were estimated for the following model

$$\log_{10}(OPC) = a_{i,j} + b_{i,j} \log_{10}(NET) \qquad (1)$$

where *OPC* is the particle abundance in the size range indexed by i and j in the matrix (i.e. with a minimum size indexed by i and a span of the size range indexed by j) and *NET* is the net-derived *C. finmarchicus* C5 abundance. Cases where the OPC-derived particle abundance was 0 particles m^{-3} were excluded from the model, and the regression was only performed when 50% or more of the cases had particle abundances >0 particles m^{-3}. The regression procedure was conducted on data from a single cruise only. Data from a second cruise were used in a validation procedure to assess independently the predictive capabilities of the equations obtained in the regression

procedure. Predicted abundances of *C. finmarchicus* C5 were computed from the OPC particle abundances in the validation dataset by inverting equation (1). A root mean square error (RMSE) for the predicted net abundances was computed as follows

$$RMSE_{i,j} = \sqrt{\langle 1/n \sum_{k=1}^{n} \{[\log_{10}(OPC_k) - a_{i,j}/b_{i,j}] - \log_{10}(NET_k)\}^2 \rangle} \quad (2)$$

where $a_{i,j}$ and $b_{i,j}$ are the coefficients obtained in the regression procedure (equation 1), *OPC* and *NET* are the particle and *C. finmarchicus* C5 abundances, respectively, and *n* is the number of cases in the validation dataset. The RMSE was only computed when at least 50% of the validation cases had OPC-derived particle abundances >0 particles m⁻³ (cases with particle abundances of 0 particles m⁻³ were excluded from the validation procedure). *Calanus finmarchicus* C5 was considered to be best detected in those size ranges in which (i) the linear association between the particle abundance and the net-derived C5 abundance was strong (high $r_{i,j}^2$) and (ii) the predictive capability of the detected linear relationship when applied to independent data collected in other years and at different locations was high (low $RMSE_{i,j}$). Based on these criteria, a single size range was selected for further analysis and is referred to as the optimum size range.

The OPC and net data from DE9908 ($n = 26$) were used in the regression procedure, and the OPC data from the 'slow' casts during AL0108 and the corresponding MOCNESS net data ($n = 15$) were used in the validation procedure. Since the assignment of these datasets to the regression or validation procedures is arbitrary, a second analysis of the optimum size range was conducted with the 'slow' AL0108 data and the DE9908 data assigned to the regression and validation procedures, respectively. The DE9908 and 'slow' AL0108 data were chosen for these analyses because the descent speeds of the OPC casts do not vary much within each cruise and are nearly comparable between the two cruises (Table I).

Avoidance: multiple linear regression analysis

To examine avoidance of the OPC by *C. finmarchicus* C5, the effect of descent speed on particle abundance in the optimum size range was tested using multiple linear regression analysis. Avoidance is expected to decrease as descent speed increases because the time for a copepod to react to the oncoming instrument decreases as the descent speed increases (Barkley, 1972). Therefore, measured particle abundance was expected to increase with increasing descent speed if avoidance occurs. The AL0108 MOCNESS tows were accompanied by OPC casts of

different descent speeds to test this hypothesis (Table I) and these data were used in the multiple linear regression analysis. The particle abundance in the optimum size range (*OPC*) was regressed against both the MOCNESS-derived abundance of *C. finmarchicus* C5 (*NET*) and the descent speed (*SPEED*) in the following model

$$\log_{10}(OPC) = \beta_0 + \beta_1 \log_{10}(NET) + \beta_2 SPEED \quad (3)$$

If significant, the back-transformed regression coefficient for the descent speed (10^{β_2}) indicates the multiplicative change in the median particle abundance corresponding to a 1 m s⁻¹ increase in the descent speed after accounting for the effect of the net-derived abundance of *C. finmarchicus* C5 on the particle abundance (Ramsey and Schafer, 1997). The base 10 logarithm of the multiplicative change in the median particle abundance for any increase in descent speed from $SPEED_{slow}$ to $SPEED_{fast}$ can then be expressed as

$$\log_{10}(OPC_{fast}/OPC_{slow}) = \beta_2(SPEED_{fast} - SPEED_{slow}) \quad (4)$$

Avoidance: paired OPC casts

OPC casts were also conducted in rapid succession at the same station (paired OPC casts) to investigate further the effect of descent speed on particle abundance. The descent speeds for the two casts were either held constant (<0.1 m s⁻¹ difference between the two) or deliberately varied (>0.3 m s⁻¹ difference). The average water column particle abundance in the optimum size range was computed for each cast over the common depths sampled in both casts. The log-transformed ratio of these particle abundances was then regressed against the difference in descent speeds between the two casts using the following equation

$$\log_{10}(OPC_{fast}/OPC_{slow}) = \alpha(SPEED_{fast} - SPEED_{slow}) \quad (5)$$

where *OPC* is the particle abundance, *SPEED* is the descent speed, α is the slope of the regression line forced through the origin and the indices 'fast' and 'slow' indicate the cast in the pair with the faster or slower descent speed, respectively. The back-transformed slope of the regression line (10^α) provides an estimate of the multiplicative change in the median particle abundance corresponding to a 1 m s⁻¹ increase in the descent speed and is directly comparable to the coefficient β_2 in equations (3) and (4).

Paired OPC casts with varying descent speeds were conducted in Wilkinson and Jordan Basins in the Gulf of Maine during cruise AL0108 ($n = 9$) and during another cruise conducted aboard NOAA Ship *Delaware II* (cruise DE0108) from August 7 to August 31, 2001 ($n = 10$) (Figure 1). Paired OPC casts with nearly constant descent

speeds were conducted in the Gulf of Maine during DE9908 ($n = 8$) and in the lower Bay of Fundy during AL0108 ($n = 12$). The latter paired OPC casts were the same casts conducted before and after each MOCNESS tow during AL0108.

Final model development

A final regression model of the form in equation (3) was developed as the 'best fit' between the OPC data and the net-derived *C. finmarchicus* C5 abundance. This model was fitted using the DE9908 and all AL0108 data and inverted to produce the following calibration equation

$$\log_{10}(C5) = (1/\beta_1)[\log_{10}(OPC) - \beta_0 - \beta_2 SPEED] \quad (6)$$

where C5 is the abundance of *C. finmarchicus* C5 in copepods m^{-3}. Since the descent speeds of the DE0007 data varied much more than in any of the other datasets (Table I), these data were excluded from the final model development and were used to assess independently the prediction errors in the calibration equation. One case was removed from the DE0007 data prior to this assessment because the OPC-derived particle abundance in the optimum size range was 0 particles m^{-3} (the corresponding net abundance for *C. finmarchicus* C5 was 29.0 copepods m^{-3}).

Caveats

All of the comparisons described above assume that the population of copepods remains the same during collocated sampling so that the performance of the OPC can be directly evaluated. Violations of this assumption are caused by spatial heterogeneity in copepod distribution (patchiness) interacting with advection, ship drift or an incompatibility in the spatial scales over which different methods sample. When the assumption is not met, variability will occur in the comparisons, and serious violations will cause outliers. This variability is independent of the OPC's performance and is the consequence of a genuine feature of copepod distribution in the ocean and the sampling methodology employed here. Truly collocated sampling (e.g. mounting an OPC on a net system) may reduce the effect of copepod patchiness on the comparisons, but the intent of this study was to assess the performance of the OPC under the same deployment conditions that were used in concurrent studies of right whales and *C. finmarchicus* C5 (i.e. a vertical cast with no accompanying net sampler).

RESULTS

Optimum size range detection

The average particle size distribution in regions of high *C. finmarchicus* C5 abundance was characterized by a modal peak at ~1.55 mm (Figure 2a). This mode was absent in regions of lower *C. finmarchicus* C5 abundance. At intermediate abundances, the modal distribution is obscured by smaller particles. Herman and Edvardsen (Herman, 1992; Edvardsen, 2002) measured the response
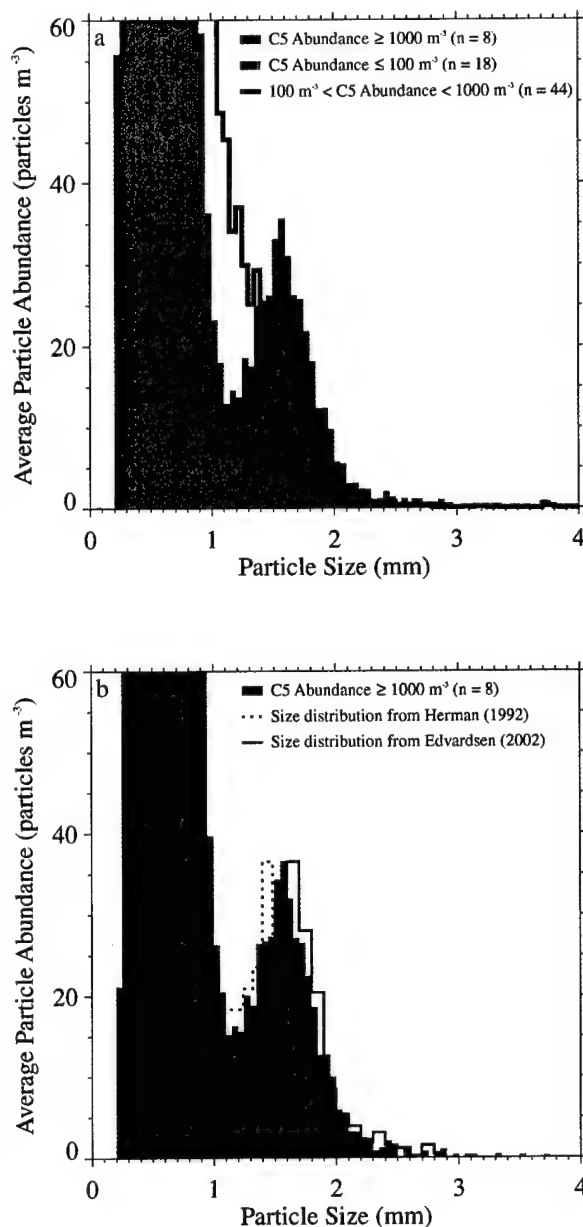

Fig. 2. (a) Average particle size distributions (in units of equivalent circular diameter) for OPC casts associated with tows that yielded *Calanus finmarchicus* C5 abundances in excess of 1000 copepods m^{-3} (dark grey), less than 100 copepods m^{-3} (light grey) and between 100 and 1000 copepods m^{-3} (thick line). **(b)** Comparison of average OPC response at high *C. finmarchicus* C5 abundance (dark grey) with comparably scaled laboratory-derived distributions of preserved (Herman, 1992) (dotted) and live (Edvardsen, 2002) (solid line) *C. finmarchicus* C5.

of the OPC to preserved and live *C. finmarchicus* C5, respectively, in the laboratory (Figure 2b). A similar modal peak to the one observed at high *C. finmarchicus* C5 abundance in the field is apparent in each of these laboratory-derived size distributions. The apparent 0.1–0.2 mm offset in modes is likely to be attributable to calibration differences, preservation effects (e.g. shrinkage, increase in opacity) or true differences in size distributions. Despite these effects, the field- and laboratory-derived distributions are in good agreement.

The regression procedure on the DE9908 data indicated a peak in the coefficient of determination over the size range defined by a minimum of 1.90 mm and a span of 0.95 mm ($r^2 = 0.784$; Figure 3a). A similar result was obtained in the regression procedure on the 'slow' AL0108 data, however the peak in the coefficient of determination occurred at a minimum size of 1.75 mm and a span of 0.40 mm ($r^2 = 0.843$). A local maximum occurred in both analyses at a minimum size of 1.5 mm, although this feature is more pronounced in the DE9908 data (Figure 3a). When the validation procedure was applied to the independent data, a single minimum was observed in the root mean square error for both analyses at a minimum particle size of 1.5 mm (Figure 3b). These
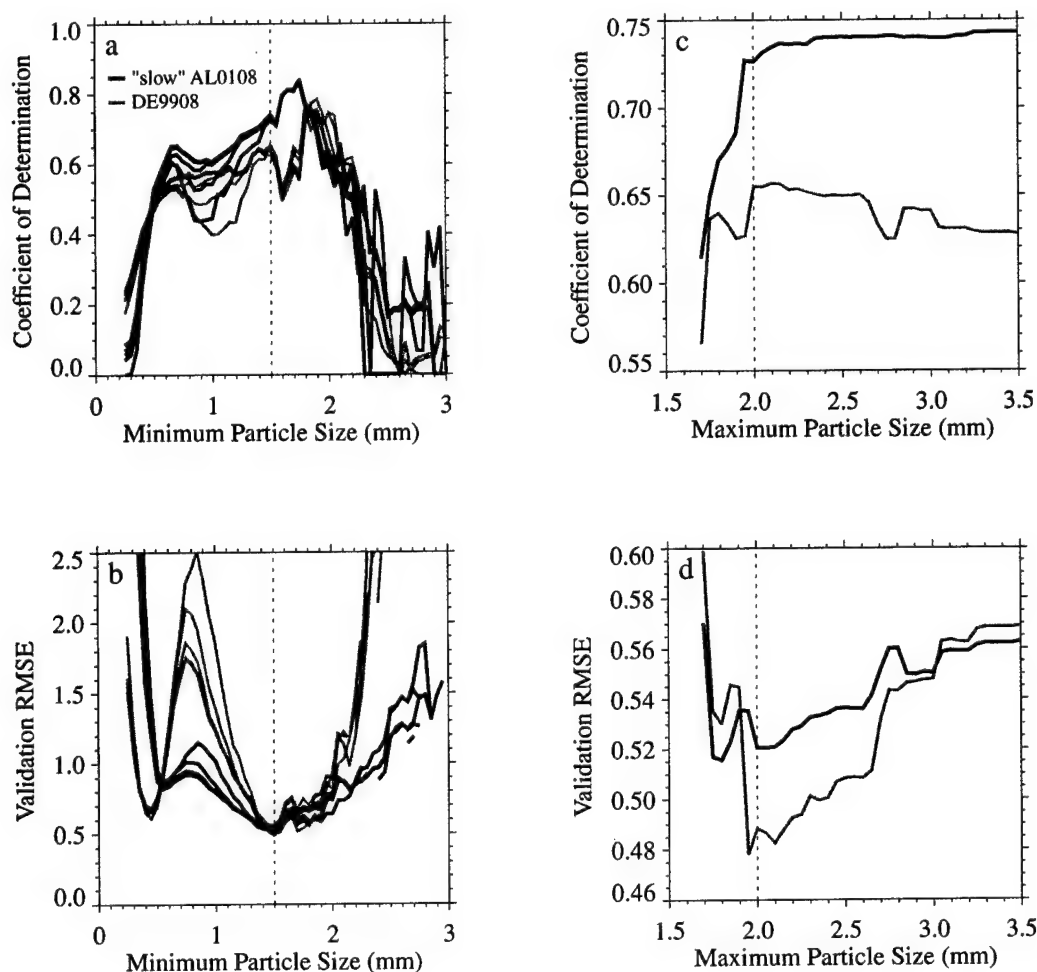

Fig. 3. (a) Coefficients of determination (r^2) obtained in the regression procedure on the DE9908 (grey) and 'slow' AL0108 (black) data for all minimum particle sizes and spans of 0.50, 0.75, 1.00, 1.25 and 1.50 mm. The spans are not differentiated because r^2 is primarily a function of minimum size. (b) Root mean square errors (RMSE) obtained by applying the DE9908 (grey) and 'slow' AL0108 (black) regressions to the validation datasets for all minimum particle sizes and the same spans as in (a). (c) r^2 obtained in the regression procedure on the DE9908 (grey) and 'slow' AL0108 (black) data for all maximum particle sizes associated with a minimum size of 1.5 mm. The maximum size is simply the sum of the minimum size and the span. (d) RMSE obtained by applying the DE9908 (grey) and 'slow' AL0108 (black) regressions to the validation datasets for all maximum particle sizes associated with a minimum size of 1.5 mm. The dotted line indicates the minimum of the optimum particle size range (1.5 mm) in (a) and (b) and the maximum of the optimum particle size range (2.0 mm) in (c) and (d).

results suggest that better correlation can be achieved between OPC particle abundance and net-derived C5 abundance at minimum sizes above 1.5 mm, but the best agreement between the regression equations and the independent data occurs in size ranges with a minimum of 1.5 mm. For both datasets, the coefficient of determination reaches an asymptote for the size range that has a minimum value of 1.5 mm and a maximum value of 2.0 mm (a span of 0.5 mm; Figure 3c) while the RMSE reaches a minimum near this same size range (Figure 3d). An analysis of covariance (Zar, 1999) provided no evidence to suggest that the slopes ($P = 0.26$), elevations ($P = 0.47$) or overall regressions ($P = 0.40$) in the 1.5–2.0 mm size range were different in the two datasets (Figure 4). Based on these results, the 1.5–2.0 mm size range is considered the optimum size range.

Avoidance: multiple linear regression analysis

There was strong evidence that the particle abundance observed by the OPC in the optimum size range during AL0108 increased with increasing descent speed after accounting for the net-derived abundance of *C. finmarchicus* C5 ($P = 0.0009$; Table II). The coefficient for the descent speed in the multiple linear regression model (β_2 in equations 3 and 4) was 1.21 s m^{-1} (95% CI: 0.541–1.88 s m^{-1}).

Avoidance: paired OPC casts

There was also strong evidence that an increase in particle abundance was associated with an increase in the descent speed during the paired OPC casts ($P = 0.0002$; Figure 5). Before fitting the model in equation (5), an intercept was included to test for a change in particle abundance when the descent speed was held constant, but this term was not found to be significant ($P = 0.11$). Note that two sets of paired OPC casts were excluded from the regression analysis because the ratios of the particle abundances were considered outliers (Figure 5). Each of these sets of casts was conducted near a right whale, an area where *C. finmarchicus* C5 abundance is typically patchy (Wishner *et al.*, 1988, 1995; Mayo and Marx, 1990; Beardsley *et al.*, 1996). I suspect that the two casts in each of the sets were not sampling the same population of copepods (i.e. one was in a patch upon which the right whale was probably feeding and the other was outside of the patch). The slope of the regression forced through the origin (α in equation 5) was 0.412 s m^{-1} (95% CI: 0.210–0.615 s m^{-1}), which was significantly lower than the comparable estimate of 1.21 s m^{-1} obtained in the multiple linear regression analysis ($P < 0.0001$).
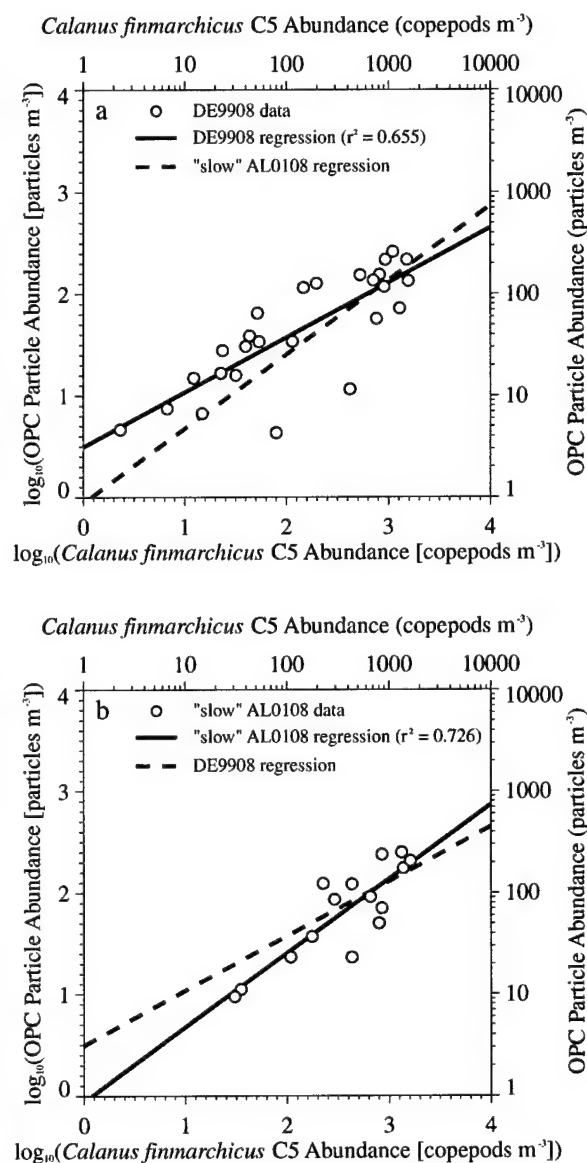

Fig. 4. (a) Scatterplot of log-transformed *C. finmarchicus* C5 abundance and OPC particle abundance in the optimum size range of 1.5 to 2.0 mm for the DE9908 data (circles). The regression line is shown as a solid line and the independent regression of the 'slow' AL0108 data for which the DE9908 data serve as the validation dataset is shown as a dashed line. (b) Similar scatterplot of 'slow' AL0108 data (circles) with regression line (solid line). The independent regression of the DE9908 data for which the 'slow' AL0108 data serve as the validation dataset is shown as a dashed line.

Final model development

The final regression model fitted the DE9908 and AL0108 data well ($r^2 = 0.684$) and was highly significant ($P < 0.0001$) (Table III; Figure 6). When applied to the

Table II: Multiple linear regression analysis to investigate avoidance of the OPC by Calanus finmarchicus C5

Variable	Coefficient	Estimate	Standard error	95% CI	t statistic	P value
Intercept	β_0	−0.5865	0.3749	−1.3558–0.1829	−1.56	0.1294
$\log_{10}$(NET)	β_1	0.6310	0.1193	0.3861–0.8758	5.29	< 0.0001
SPEED	β_2	1.2101	0.3260	0.5412–1.8789	3.71	0.0009

All AL0108 data were fitted to equation (3) to test for the effect of descent speed on OPC-derived particle abundance in the 1.5–2.0 mm size range ($n = 30$, $r^2 = 0.645$, $F = 24.55$, $P < 0.0001$).
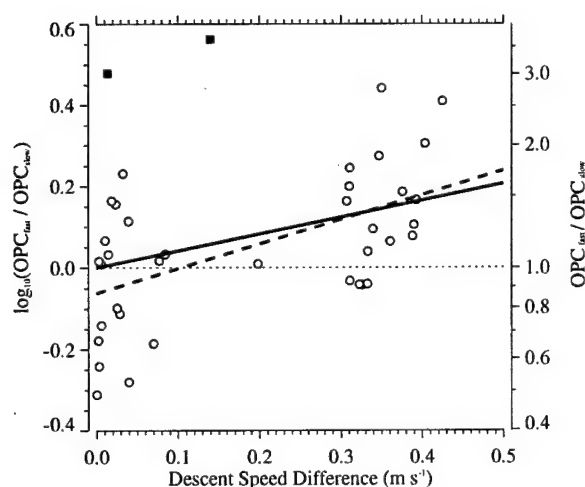

Fig. 5. Scatterplot of descent speed difference and the ratio of OPC particle abundance in the optimum size range for paired OPC casts. The regression line forced through the origin (see equation 5 in the text) is shown as a solid line and the regression line with both a slope and intercept is shown as a dashed line. The regressions excluded the two observations with anomalously high ratios at low descent speed differences (filled squares).

DE0007 data using equation (6) (Figure 7), however, there was suggestive, but inconclusive, evidence that the mean prediction was different from the actual *C. finmarchicus* C5 abundance ($P = 0.060$). The predicted *C. finmarchicus* C5 net abundance was underestimated by an average factor of 1.95 [95% CI: 3.91 (too low) to 1.03 (too high)].

DISCUSSION

The modal peak in the average size distribution at 1.55 mm is unambiguous at high concentrations of *C. finmarchicus* C5, but is absent at lower concentrations (Figure 2a). Furthermore, the regression and validation procedures suggest that the OPC-observed particles in the size range 1.5–2.0 mm are *C. finmarchicus* C5. These results indicate that *in situ C. finmarchicus* C5 is best detected by the OPC in only the larger half of its laboratory-derived size distribution (Herman, 1992; Edvardsen, 2002) where its abundance is not obscured by other, smaller particles. The total abundance of smaller copepods (e.g. *C. finmarchicus* C3 or C4, *Centropages* spp., *Pseudocalanus* spp., *Metridia lucens*, *Temora longicornis* and *Acartia longiremis*) exceeded that of *C. finmarchicus* C5 in nearly 50% of the net samples, whereas the total abundance of larger copepods (e.g. *C. finmarchicus* adults, *Metridia longa*, *C. glacialis*, *C. hyperboreus*)

Table III: Final multiple linear regression model

Variable	Coefficient	Estimate	Standard error	95% CI	t statistic	P value
Intercept	β_0	0.0384	0.1825	−0.3276–0.4044	0.21	0.8341
$\log_{10}$(NET)	β_1	0.5343	0.0626	0.4087–0.6598	8.53	< 0.0001
SPEED	β_2	0.8001	0.2370	0.3248–1.2754	3.38	0.0014

Model fit to all AL0108 and DE9908 data ($n = 56$, $r^2 = 0.684$, $F = 57.32$, $P < 0.0001$).
Coefficients from this model can be used in equation (6) to predict *C. finmarchicus* C5 abundance from OPC-derived particle abundance in the 1.5–2.0 mm size range.
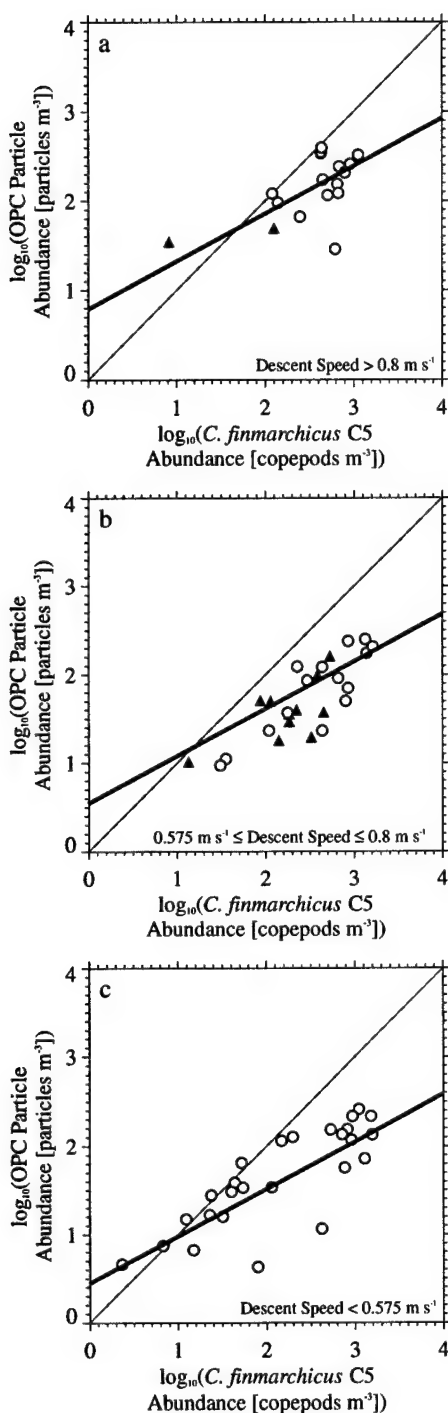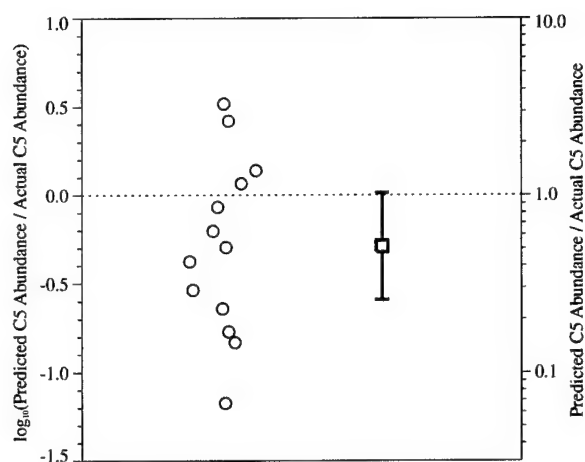
Fig. 7. Ratio of predicted to actual *C. finmarchicus* C5 net abundance for DE0007 data (circles) and the mean of the log-transformed ratio (square) with a 95% confidence interval (error bars).

Fig. 6. Scatterplots of log-transformed *Calanus finmarchicus* C5 abundance and OPC particle abundance in the optimum size range for descent speeds (**a**) >0.8 m s⁻¹ ('fast' AL0108 data), (**b**) between 0.575 and 0.8 m s⁻¹ ('slow' AL0108 data) and (**c**) <0.575 m s⁻¹ (DE9908). Data used to construct the final regression model (Table III) are shown as open circles. Lines indicate the final model corresponding to average descent speeds of (**a**) 0.94 m s⁻¹, (**b**) 0.63 m s⁻¹ and (**c**) 0.51 m s⁻¹. The independent DE0007 data are shown as black triangles.

only exceeded that of *C. finmarchicus* C5 on one occasion. Since smaller particles are more abundant than larger particles in general, the smaller half of the *C. finmarchicus* C5 size distribution is more likely to be obscured by either smaller copepods or detrital particles. In contrast, the larger half of this modal size distribution is infrequently obscured by less abundant, larger copepods or detrital material.

Avoidance of the OPC tunnel opening by *C. finmarchicus* C5 was inferred from the significantly higher particle abundances observed when descent speed was increased. This conclusion is also based on the observations of Miller and colleagues (Miller *et al.*, 1991) that resting *C. finmarchicus* C5 in this region are still responsive and capable of a strong escape reaction. The magnitude of this effect may be substantial. For the 0.30 m s⁻¹ average increase in descent speeds between the 'fast' and 'slow' AL0108 data, median OPC particle abundance increased by a factor of 2.31 (95% CI: 1.45–3.66). For the same 0.30 m s⁻¹ increase in descent speed, the analysis of the paired OPC casts yielded a lower estimate of the factor increase in median OPC particle abundance: 1.33 (95% CI: 1.16–1.53). Avoidance is a function of the size of the sampling aperture and the reaction time and escape velocity of the zooplankton (Barkley, 1964, 1972). The reaction time, in turn, is a function of the distance at which the animal can detect the sampler and the speed of the sampler. Although the sampling aperture and tow speed of an OPC can be held constant across applications, differences in the structure of the vehicle carrying the OPC can alter the pressure wave in front of the sampler and hence, the distance at which zooplankton can detect the oncoming sampler. Therefore, the estimates of the magnitude of avoidance

determined in this study are probably not directly applicable to other vehicles. However, the cage used in the present study was designed to reduce the pressure wave impacting the volume of water immediately in front of the OPC so avoidance was probably minimized. For larger vehicles or vehicles with obstructions near the OPC, the effect of avoidance on OPC particle abundances will probably be worse.

The final model predicted median *C. finmarchicus* C5 abundances from the DE0007 data that were too low by a factor of nearly 2. Most of the predictions (7 of 13) were within a factor of 3, while four of the predictions were gross underestimates between a factor of 4.4 and 14.9 too low. Unreasonably low OPC particle abundances were also observed on two occasions during DE9908 (Figure 4a). Underestimation of this type suggests that the single OPC casts accompanying each of these bongo tows did not sample the same population of *C. finmarchicus* C5 as did the net (i.e. the net sampled a patch of copepods while the OPC missed the patch). In a spatially heterogeneous environment, this would certainly be expected to happen occasionally. In fact, given this confounding by spatial heterogeneity and the differences in sampling methodology between the nets and the OPC, the correlations between the particle abundance and net-derived *C. finmarchicus* C5 abundance were remarkably high. Compared with the OPC, the nets integrated over a much larger horizontal spatial scale (hundreds of meters for towed nets versus discrete OPC vertical profiles), sampled a much larger volume of sea water (average net:OPC ratio of volume sampled was 300:1), probably experienced less avoidance (due to the larger sample aperture) and destroyed detrital particles that were counted by the OPC. Despite these significant differences, the coefficients of determination (r^2) were 0.655, 0.726 and 0.684 for the DE9908 data (Figure 4a), 'slow' AL0108 data (Figure 4b) and the final multiple linear regression model (Figure 6, Table III), respectively. When the two cases with unreasonably low OPC particle abundances are removed from the DE9908 data (Figure 4a), the agreement between the OPC and net abundances becomes much better ($r^2 = 0.840$). These coefficients of determination exceed those obtained by Heath and co-workers (Heath *et al.*, 1999) from samples and measurements collected in the Faroe–Shetland Channel between 500 and 1000 m with a side-by-side mounted plankton net and OPC.

Using a similar regression procedure, Heath and colleagues (Heath *et al.*, 1999) obtained maximum correlations in size ranges that nearly encompass the complete laboratory-derived *C. finmarchicus* C5 size distribution (0.90–1.70 mm in January, 1.02–1.74 mm in March). The abundance of both *C. finmarchicus* C4 and C5 were included in their analysis, but C5 dominated in both

months. Heath and colleagues (Heath *et al.*, 1999) reported that their OPC sampled volumes between 0.25 and 0.5 m^3 during a single 60 s integration interval, which corresponds to tow speeds between 0.83 and 1.67 m s^{-1}. At the average descent speed used during the 'fast' AL0108 casts (0.94 m s^{-1}), the final model determined in this study predicts lower OPC particle abundances than those of Heath and colleagues for similar net abundances of *C. finmarchicus* C5 (Figure 8). Recall, however, that *C. finmarchicus* C5 was best detected in the larger half of its size distribution. Therefore, the final regression equation only models roughly half of the OPC particle abundance contributed by *C. finmarchicus* C5. The contribution of the smaller half of the size distribution can be taken into account simply by doubling the particle abundance obtained from the model. The resulting regression equation is now directly comparable to the Heath regression (Heath *et al.*, 1999) and there is excellent agreement between the two (Figure 8). In fact, no evidence was found to suggest that the regression coefficient for the net abundance of *C. finmarchicus* C5 (Table III) was different from the January (H$_0$: $\beta_1 = 0.492$, $P = 0.50$) or March (H$_0$: $\beta_1 = 0.461$, $P = 0.25$) slopes of the Heath regressions (Heath *et al.*, 1999). Because the results of these two studies are
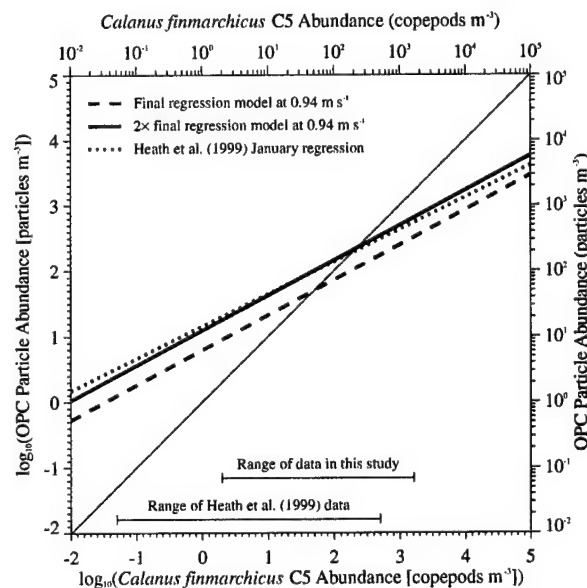

Fig. 8. Final multiple linear regression model (Table III) for a descent speed of 0.94 m s^{-1} (dashed line), the final model at 0.94 m s^{-1} with particle abundances doubled (solid line) and the January regression of Heath and colleagues (Heath *et al.*, 1999) (dotted line). The ranges of net-derived *C. finmarchicus* C5 abundances used in each study are shown. Note that only 4% of the samples from Heath and colleagues (Heath *et al.*, 1999) had combined *C. finmarchicus* C4 and C5 abundances >100 copepods m^{-3} whereas 74% of the samples in the present study had *C. finmarchicus* C5 abundances >100 copepods m^{-3}.

consistent, it seems reasonable to conclude that the regression lines in Figure 8 represent the true response of the OPC to varying abundances of *C. finmarchicus* C5 over nearly five orders of magnitude.

Calanus finmarchicus C5 abundance can be estimated in future studies from the OPC-derived abundance of particles between 1.5 and 2.0 mm using equation (6) and the coefficients in Table III. Since the OPC particle abundances used to determine these coefficients were between 4 and 395 particles m^{-3}, *C. finmarchicus* C5 abundances should only be prudently estimated with equation (6) when OPC particle abundances are in this same range. These particle abundances were determined over very coarse depth strata to be comparable to the *C. finmarchicus* C5 abundances from the corresponding net tows. The OPC, of course, has the capability to provide much finer-scale abundance and distribution information, but calibrating higher particle abundances sometimes found in narrower depth strata is difficult. Near right whales, peak abundances in 5 m depth strata typically exceed 395 particles m^{-3} and can range as high as 1100 particles m^{-3}. Estimating abundances of *C. finmarchicus* C5 using these OPC data requires extrapolation from the calibration equation. The results presented here indicate that the regressions of Heath and colleagues (Heath *et al.*, 1999) could be successfully extrapolated to higher concentrations, which provides some hope, yet no evidence, that these same regressions may apply to *C. finmarchicus* C5 abundances between 1000 and 10 000 copepods m^{-3} or higher.

At higher concentrations, coincidence counts (Herman, 1988) may occur if the concentration of smaller sized particles is also high. Coincidence would reduce the number of particles detected in the 1.5–2.0 mm size range and result in underestimation of the *C. finmarchicus* C5 abundance by the calibration equation. For OPC casts associated with net tows having *C. finmarchicus* C5 abundances >1000 copepods m^{-3}, the total time spent detecting particles (i.e. the total time particles spent traversing the 4 mm wide light beam plus a 4 ms per particle electronics reset time) during each 0.5 s interval of a downcast was rarely >0.25 s. If coincidence counting were frequent, this total processing time would be much closer to 0.5 s. Even near right whales, where discrete layers of particles in the optimum size range can exceed abundances of 1000 particles m^{-3}, total processing time remains below 0.25 s. These results suggest that coincident counting occurs infrequently and it will not affect estimates from the calibration equation for the observed range of OPC particle abundances. Fleminger and Clutter (Fleminger and Clutter, 1965) suggest that avoidance may decrease at higher concentrations, which would result in overestimation of the *C. finmarchicus* C5 abun-

dance by the calibration equation. A test of an additional interaction term [$\log_{10}(NET) \times SPEED$] in the model described by equation (3), however, provided no evidence that the effect of avoidance on the OPC particle abundance varied with *C. finmarchicus* C5 abundance over concentrations between 31 and 1621 copepods m^{-3} ($P = 0.31$). With no evidence of either persistent coincident counting or decreased avoidance at higher concentrations and with appropriate caution, extrapolation of the calibration equation to predict *C. finmarchicus* C5 concentrations from higher OPC particle abundances seems feasible.

Because the calibration equation (equation 6) was developed from comparisons with nets, it is designed to predict *C. finmarchicus* C5 abundances that are equivalent to abundances that could be obtained with nets. None of the issues surrounding net sampling (e.g. net avoidance, extrusion, clogging) have been taken into account in this model, however these problems were not expected to contribute large errors in abundance estimates because the appropriate nets and mesh sizes to sample adequately *C. finmarchicus* C5 were used in this study (Anderson and Warren, 1991; Nichols and Thompson, 1991). Verification of the accuracy of this calibration model in other environments with similar net sampling is therefore possible. In fact, validation of this model with net sampling prior to use is essential, since the model is predicated on *C. finmarchicus* C5 dominance in the 1.5–2.0 mm particle size range. In environments where this is not the case, the model is expected to perform poorly. However, given the dominance of *C. finmarchicus* in many North Atlantic regions and the current questions about the ecology of the fifth copepodite resting stock, I anticipate that the OPC and this calibration equation will serve as useful tools in future *C. finmarchicus* research.

ACKNOWLEDGEMENTS

REFERENCES

Anderson, J. T. and Warren, W. G. (1991) Comparison of catch rates among small and large bongo samplers for *Calanus finmarchicus* copepodite stages. *Can. J. Fish. Aquat. Sci.*, **48**, 303–308.

Barkley, R. A. (1964) The theoretical effectiveness of towed-net samplers as related to sampler size and to swimming speed of organisms. *J. Cons. Perm. Int. Explor. Mer.*, **29**, 146–157.

Barkley, R. A. (1972) Selectivity of towed-net samplers. *Fish. Bull.*, **70**, 799–820.

Beardsley, R. C., Epstein, A. W., Chen, C., Wishner, K. F., Macaulay, M. C. and Kenney, R. D. (1996) Spatial variability in zooplankton abundance near feeding right whales in the Great South Channel. *Deep-Sea Res. II*, **43**, 1601–1625.

Checkley, D. M. Jr., Ortner, P. B., Settle, L. R. and Cummings, S. R. (1997) A continuous, underway fish egg sampler. *Fish. Oceanogr.*, **6**, 58–73.

Davis, C. S., Gallager, S. M., Berman, M. S., Haury, L. R. and Strickler, J. R. (1992) The video plankton recorder (VPR): design and initial results. *Arch. Hydrobiol. Beih. Ergebn. Limnol.*, **36**, 67–81.

Davis, C. S., Gallager, S. M., Marra, M. and Stewart, W. K. (1996) Rapid visualization of plankton abundance and taxonomic composition using the Video Plankton Recorder. *Deep-Sea Res. II*, **43**, 1947–1970.

Edvardsen, A. (2002) Determining zooplankton ESD signatures using an *in situ* OPC in the laboratory. In Zhou, M. and Tande, K. (eds), *Optical Plankton Counter Workshop*. GLOBEC Report 17., GLOBEC International Project Office, Plymouth, UK, pp. 16–21.

Fleminger, A. and Clutter, R. I. (1965) Avoidance of towed nets by zooplankton. *Limnol. Oceanogr.*, **10**, 96–104.

Focal Technologies (1999) *Optical Plankton Counter Users's Guide*. Focal Technologies, Inc., Dartmouth, NS, Canada.

Grant, S., Ward, P., Murphy, E., Bone, D. and Abbott, S. (2000) Field comparison of an LHPR net sampling system and an optical plankton counter (OPC) in the Southern Ocean. *J. Plankton Res.*, **22**, 619–638.

Halliday, N. C., Coombs, S. H. and Smith, C. (2001) A comparison of LHPR and OPC data from vertical distribution sampling of zooplankton in a Norwegian fjord. *Sarsia*, **86**, 87–99.

Heath, M. R. (1995) Size spectrum dynamics and planktonic ecosystem of Loch Linnhe. *ICES J. Mar. Sci.*, **52**, 627–642.

Heath, M. R., Dunn, J., Fraser, J. G., Hay, S. J. and Madden, H. (1999) Field calibration of the optical plankton counter with respect to *Calanus finmarchicus*. *Fish. Oceanogr.*, **8** (suppl. 1), 13–24.

Herman, A. W. (1988) Simultaneous measurement of zooplankton and light attenuance with a new optical plankton counter. *Cont. Shelf Res.*, **8**, 205–221.

Herman, A. W. (1992) Design and calibration of a new optical plankton counter capable of sizing small zooplankton. *Deep-Sea Res.*, **39**, 395–415.

Herman, A. W., Sameoto, D. D., Shunnian, C., Mitchell, M. R., Petrie, B. and Cochrane, N. (1991) Sources of zooplankton on the Nova Scotia Shelf and their aggregations within deep-shelf basins. *Cont. Shelf Res.*, **11**, 211–238.

Herman, A. W., Cochrane, N. A. and Sameoto, D. D. (1993) Detection and abundance estimation of euphausiids using an optical plankton counter. *Mar. Ecol. Prog. Ser.*, **94**, 165–173.

Hirche, H.-J. (1996) Diapause in the marine copepod, *Calanus finmarchicus* – a review. *Ophelia*, **44**, 129–143.

Holliday, D. V. and Pieper, R. E. (1995) Bioacoustical oceanography at high frequencies. *ICES J. Mar. Sci.*, **52**, 279–296.

Huntley, M. E., Zhou, M. and Nordhausen, W. (1995) Mesoscale distribution of zooplankton in the California Current in late spring, observed by Optical Plankton Counter. *J. Mar. Res.*, **53**, 647–674.

Kenney, R. D., Hyman, M. A. M., Owen, R. E., Scott, G. P. and Winn, H. E. (1986) Estimation of prey densities required by western North Atlantic right whales. *Mar. Mamm. Sci.*, **2**, 1–13.

Mayo, C. A. and Marx, M. K. (1990) Surface foraging behavior of the North Atlantic right whale, *Eubalaena glacialis*, and associated zooplankton characteristics. *Can. J. Zool.*, **68**, 2214–2220.

Miller, C. B., Cowles, T. J., Wiebe, P. H., Copley, N. J. and Grigg, H. (1991) Phenology in *Calanus finmarchicus*; hypotheses about control mechanisms. *Mar. Ecol. Prog. Ser.*, **72**, 79–91.

Murison, L. D. and Gaskin, D. E. (1989) The distribution of right whales and zooplankton in the Bay of Fundy, Canada. *Can. J. Zool.*, **67**, 1411–1420.

Nautical Software (1996) *Tides and Currents, version 2.0 Users Guide*, 3rd edn. Nautical Software, Inc., Beaverton, OR, USA.

Nichols, J. H. and Thompson, A. B. (1991) Mesh selection of copepodite and nauplius stages of four calanoid copepod species. *J. Plankton Res.*, **13**, 661–671.

Osgood, K. E. and Checkley, D. M. Jr. (1997) Observations of deep aggregations of *Calanus pacificus* in the Santa Barbara Basin. *Limnol. Oceanogr.*, **42**, 997–1001.

Ramsey, F. L. and Schafer, D. W. (1997) *The Statistical Sleuth: a Course in Methods of Data Analysis*. Duxbury Press, Belmont, CA.

Sameoto, D. D. and Herman, A. W. (1990) Life cycle and distribution of *Calanus finmarchicus* in deep basins on the Nova Scotia shelf and seasonal changes in *Calanus* spp. *Mar. Ecol. Prog. Ser.*, **66**, 225–237.

Sameoto, D., Cochrane, N. and Herman, A. (1993) Convergence of acoustic, optical and net-catch estimates of euphausiid abundance: use of artificial light to reduce net avoidance. *Can. J. Fish. Aquat. Sci.*, **50**, 334–346.

Sprules, W. G., Jin, E. H., Herman, A. W. and Stockwell, J. D. (1998) Calibration of an optical plankton counter for use in fresh water. *Limnol. Oceanogr.*, **43**, 726–733.

Stockwell, J. D. and Sprules, W. G. (1995) Spatial and temporal patterns of zooplankton biomass in Lake Erie. *ICES J. Mar. Sci.*, **52**, 557–564.

Stone, G. S., Kraus, S. D., Prescott, J. H. and Hazard, K. W. (1988) Significant aggregations of the endangered right whale, *Eubalaena glacialis*, on the continental shelf of Nova Scotia. *Can. Field Nat.*, **102**, 471–474.

Tande, K. and Miller, C. B. (1996) Preface to: Trans-Atlantic Study of *Calanus finmarchicus*, Proceedings of a Workshop. *Ophelia*, **44**, i–ii.

Wiebe, P. H., Burt, K. H., Boyd, S. H. and Morton, A. W. (1976) A multiple opening/closing net and environmental sensing system for sampling zooplankton. *J. Mar. Res.*, **34**, 313–325.

Wiebe, P. H., Morton, A. W., Bradley, A. M., Backus, R. H., Craddock, J. E., Barber, V., Cowles, T. J. and Flierl, G. R. (1985) New

developments in the MOCNESS, an apparatus for sampling zooplankton and micronekton. *Mar. Biol.*, **87**, 313–323.

Wiebe, P. H., Beardsley, R. C., Bucklin, A. and Mountain, D. G. (2001) Coupled biological and physical studies of plankton populations in the Georges Bank region and related North Atlantic GLOBEC study sites. *Deep-Sea Res. II*, **48**, 1–2.

Wieland, K., Petersen, D. and Schnack, D. (1997) Estimates of zooplankton abundance and size distribution with the optical plankton counter (OPC). *Arch. Fish. Mar. Res.*, **45**, 271–280.

Wishner, K., Durbin, E., Durbin, A., Macaulay, M., Winn, H. and Kenney, R. (1988) Copepod patches and right whales in the Great South Channel off New England. *Bull. Mar. Sci.*, **43**, 825–844.

Wishner, K. F., Schoenherr, J. R., Beardsley, R. and Chen, C. (1995) Abundance, distribution and population structure of the copepod *Calanus finmarchicus* in a springtime right whale feeding area in the southwestern Gulf of Maine. *Cont. Shelf Res.*, **15**, 475–507.

Woodd-Walker, R. S., Gallienne, C. P. and Robins, D. B. (2000) A test model for optical plankton counter (OPC) coincidence and a comparison of OPC-derived and conventional measures of plankton abundance. *J. Plankton Res.*, **22**, 473–483.

Woodley, T. H. and Gaskin, D. E. (1996) Environmental characteristics of North Atlantic right and fin whale habitat in the lower Bay of Fundy, Canada. *Can. J. Zool.*, **74**, 75–84.

Zar, J. H. (1999) *Biostatistical Analysis*, 4th edn. Prentice Hall, Upper Saddle River, NJ.

Zhang, X., Roman, M., Sanford, A., Adolf, H., Lascara, C. and Burgett, R. (2000) Can an optical plankton counter produce reasonable estimates of zooplankton abundance and biovolume in water with high detritus? *J. Plankton Res.*, **22**, 137–150.

MARINE ECOLOGY
PROGRESS SERIES

Reprint

IR

Summertime foraging ecology of North Atlantic right whales

Mark F. Baumgartner[1,3,*], Bruce R. Mate[2]

[1]College of Oceanic and Atmospheric Sciences, Oregon State University, 104 Ocean Administration Building, Corvallis, Oregon 97331, USA.

[2]Coastal Oregon Marine Experiment Station, Hatfield Marine Science Center, Oregon State University, Newport, Oregon 97365, USA

[3]*Present address:* Biology Department, MS #33, Woods Hole Oceanographic Institution, Woods Hole, Massachusetts 02543, USA

ABSTRACT: North Atlantic right whales were instrumented with suction-cup mounted, time-depth recorders (TDR) during the summers of 2000 and 2001 to examine their diving and foraging behavior. Simultaneous observations of temperature, salinity and the vertical distribution of their principal prey, *Calanus finmarchicus* stage 5 copepodites (C5), were obtained along each whale's track with a conductivity-temperature-depth instrument (CTD) and an optical plankton counter (OPC). Right whale feeding dives were characterized by rapid descent from the surface to a particular depth between 80 and 175 m, remarkable fidelity to that depth for 5 to 14 min and then rapid ascent back to the surface. The average depth of dive was strongly and positively correlated with both the average depth of peak *C. finmarchicus* C5 abundance and the average depth of the bottom mixed layer's upper surface. Significantly longer surface intervals were observed for reproductively active females and their calves when compared to other individuals, indicating that this critical segment of the population may be at increased risk of ship strikes owing to their diving behavior. Ingestion rates calculated from TDR and OPC data exceeded estimated daily metabolic requirements for most of the tagged right whales; however, short deployment durations and uncertainty in metabolic rates make it impossible to judge whether individual right whales were obtaining sufficient energy to meet the metabolic costs of reproduction. Improvements in attachment durations and the development of novel methods to estimate the metabolic rates of large whales *in situ* are required to determine whether right whale reproduction is limited by insufficient food resources.

KEY WORDS: Right whale · *Eubalaena glacialis* · *Calanus finmarchicus* · Diving behavior · Energetics · Aggregation

INTRODUCTION

The foraging behavior of marine mammals is difficult to observe directly, because it often occurs below the sea surface. The miniaturization of sensors and data loggers in recent decades has facilitated the development of time-depth recorders (TDR) to study the diving behavior of marine mammals (Kooyman 1989, Costa 1993), but obtaining information about prey distribution and abundance at the same temporal and spatial scales of the TDR is rarely feasible. The North Atlantic right whale *Eubalaena glacialis* occupies a unique trophic position in the marine ecosystem; it is one of the world's largest predators (up to 17 m), yet it feeds primarily on one of the smallest marine animals, the 2 to 3 mm long calanoid copepod *Calanus finmarchicus*. Assessing the abundance of this copepod at spatial scales that are relevant to a right whale (10s of cm to m in the vertical, 10s to 100s of m in the horizontal) is nearly impossible with conventional net sampling methods. Targeted net sampling is only feasible when right whales are feeding at or very near the surface

and copepod patches can be visually identified (Watkins & Schevill 1976, Wishner et al. 1988, 1995, Mayo & Marx 1990, Beardsley et al. 1996). With the advent of instrumentation to estimate the abundance of zooplankton, however, the distribution of *C. finmarchicus* can now be adequately and rapidly sampled at spatial scales much closer to those utilized by the whales.

North Atlantic right whales are one of the most endangered large whales, and despite international protection from whaling since the 1930s, this species has failed to recover to its pre-exploitation population levels (Clapham et al. 1999). Recent estimates suggest that only around 300 individuals remain (Knowlton et al. 1994, IWC 2001, Kraus et al. 2001), and the current, unacceptably high mortality rates (due, in part, to ship strikes and fishing gear entanglements) are projected to cause extinction within a few centuries (Caswell et al. 1999, Fujiwara & Caswell 2001). Consequently, there is an urgent need for information about the habitat and habitat use of right whales to improve conservation efforts. There is also a need to improve our understanding of food availability and foraging success as determinants of reproductive success. One of the hypotheses to explain the lack of recovery in this population states that centuries of depressed abundance due to whaling has allowed other predators of *Calanus finmarchicus* to flourish (e.g. planktivorous fish, see Payne et al. 1990), so sufficient food resources to support substantial population growth no longer exist (IWC 2001). Recent results linking temporal variability in both crude right whale survival probability (Fujiwara & Caswell 2001) and right whale reproductive success (Kenney et al. 2001) to the North Atlantic Oscillation, which, in turn, affects *C. finmarchicus* abundance (Fromentin & Planque 1996, Greene & Pershing 2000, Conversi et al. 2001), seem consistent with this hypothesis.

Right whales have been observed feeding on older copepodite stages of *Calanus finmarchicus* in Cape Cod Bay (Watkins & Schevill 1976, Mayo & Marx 1990) and in the Great South Channel (Wishner et al. 1988, 1995, Beardsley et al. 1996) in the late winter and spring. Surface feeding occurs occasionally, but subsurface feeding is much more common (Watkins & Schevill 1976, Mayo & Marx 1990, Kenney et al. 1995). During the summer, right whales can be found in the lower Bay of Fundy and on the SW Scotian Shelf, where they continue to feed on older stages of *C. finmarchicus* (Stone et al. 1988, Murison & Gaskin 1989, Woodley & Gaskin 1996). At this time of year, the bulk of the *C. finmarchicus* population consists of stage 5 copepodites (C5) that are in a resting state deep in the water column (Sameoto & Herman 1990, Miller et al. 1991). Net sampling by Murison & Gaskin (1989) in the

lower Bay of Fundy indicated that *C. finmarchicus* C5 was the dominant zooplankter near right whales and that these copepods occurred at depths below 100 m. Both Murison & Gaskin (1989) and Goodyear (1993) observed right whales diving to depths below 100 m in the lower Bay of Fundy.

We report here on a study of right whale diving and foraging behavior in the lower Bay of Fundy and on the southwestern Scotian Shelf. Right whale diving behavior was monitored via suction-cup mounted TDRs, and observations of *Calanus finmarchicus* C5 vertical distribution were obtained near the tagged whales with an optical plankton counter (OPC). These measurements were used to investigate the hypothesis that right whales exploit high abundances of *C. finmarchicus* C5 concentrated in discrete layers. Kenney et al. (1986) suggested that foraging must occur on discrete layers of zooplankton for right whales to satisfy their energetic demands. We used the OPC to sample these discrete layers at temporal and spatial scales similar to those of the foraging whales. Simultaneous observations of temperature and salinity obtained with a conductivity-temperature-depth instrument (CTD) also allowed an investigation of the hydrographic features that promote the formation or persistence of these layers. To address the hypothesis of insufficient food resources, right whale ingestion rates were estimated from the TDR and OPC data and compared to daily metabolic requirements.

MATERIALS AND METHODS

The tag used during the 2000 summer field season consisted of a modified Wildlife Computers model MK7 TDR that recorded pressure (converted to depth at a resolution of 2 m), temperature and relative light intensity every second. The tag needed to be recovered for access to these data. The TDR also included a slot in which a Telonics model CHP-1P, 149 MHz radio transmitter was placed. Syntactic foam floatation was molded around one end of the TDR to make the entire tag positively buoyant. The tag was attached to a whale via a silicone suction cup and detachment was uncontrolled. In 2001, a Vemco model V22P acoustic transmitter was included in the tag to allow tracking while a whale was submerged. The acoustic transmitter emitted 36 kHz pulses at 165 dB (re 1 μPa at 1 m) at intervals proportional to the depth of the tag (e.g. every 1.03 s at 10 m and 0.76 s at 200 m). A corrosive release mechanism was also incorporated in the tag in 2001 that was designed to provide reliable attachment durations of between 1 and 2 h. The suction cup was changed in 2001 to a more robust, rubber material. In both 2000 and 2001, the tag was attached with a 9 m

telescoping pole from an elevated platform in the bow of a 7.5 m rigid-hulled inflatable boat (RHIB).

Visual observations were used to assess the reaction of whales to close boat approaches. However, the value of these observations in gauging the overall effects of tagging is unclear. It is important to consider the effect of tagging on biologically meaningful activities (e.g. feeding, breeding) and to use objective data when doing so. Toward that end, the diving behavior of the tagged whales was also investigated for reactions to close boat approach and tagging. The tagged right whales engaged primarily in feeding behavior (see 'Results'), so only whales tagged for over 1 h with 2 or more feeding dives were examined. The characteristics of the first feeding dive (duration, average dive depth, descent speed, ascent speed) were compared to those of the second, third, fourth and last observed feeding dives to document any significant changes in diving behavior as a result of the tag attachment process. This first feeding dive occurred up to 7.5 min after tag deployment. In addition, the characteristics of the second feeding dive were compared to those of the third, fourth and last dives, and the characteristics of the third feeding dive were compared to those of the fourth and last dives.

Following deployment, the whale was tracked at the surface via the radio transmitter, and in 2001, via the acoustic transmitter when the whale was submerged. Recovery of the tag after detachment was facilitated with these same systems. Right whales were tagged and tracked only during daylight hours. Radio tracking was accomplished with a 4-element Yagi antenna and a receiver. Bearing alone was estimated from the received signal intensity, and the range of the system was over 1 km. Acoustic tracking was accomplished with a directional hydrophone and a receiver. Bearing and horizontal distance to the animal were estimated from the received acoustic signal intensity and, with some experience, these could be judged to within 15° and 50 to 100 m, respectively. The pulse interval was measured, converted to depth and displayed by the acoustic receiver, so an estimate of the depth of the whale was also available in real time. To test the range of the acoustic system, a transmitter was suspended in the lower Bay of Fundy at 75 m and detectability was tested at various distances. The maximum distance tested was 1 km before weather forced an end to the experiment, but the signal was easily detected at this maximum distance.

Upon each resurfacing of a tagged whale after a long dive, the resurfacing position was obtained by parking a RHIB on the exact location and obtaining a global positioning system (GPS) measurement. Shortly thereafter, NOAA Ship 'Delaware II' would occupy this same position and deploy an instrument package consisting of a Seabird model SBE19 CTD and a Focal Technologies model OPC-1T. These instruments were housed in a rosette cage and deployed in a vertical cast at a nominal 0.5 m s^{-1} (2000) or 1.0 m s^{-1} (2001) descent rate. The CTD provided the vertical distribution of temperature and salinity and the OPC provided the vertical distribution of particle abundance in sizes ranging from 0.25 to 20 mm (Herman 1988, 1992). The abundance of *Calanus finmarchicus* C5 was estimated from the OPC data using a calibration equation developed from comparisons between OPC measurements and net samples collected in this same region (Baumgartner 2003). During tracking, behavioral observations and social interactions were noted and when possible photographs were taken for comparison with the New England right whale catalog (Hamilton & Martin 1999) to identify tagged individuals.

Dives were defined as any vertical excursion below 50 m. The period between these dives was typically spent at or just below the surface. Vertical excursions between the surface and 50 m typically occurred during traveling or associations with other right wales. Dives were considered to be initiated when the vertical descent speed exceeded 0.5 m s^{-1} and the descent portion of the dive was terminated when the vertical descent speed dropped below 0.5 m s^{-1} (Fig. 1).

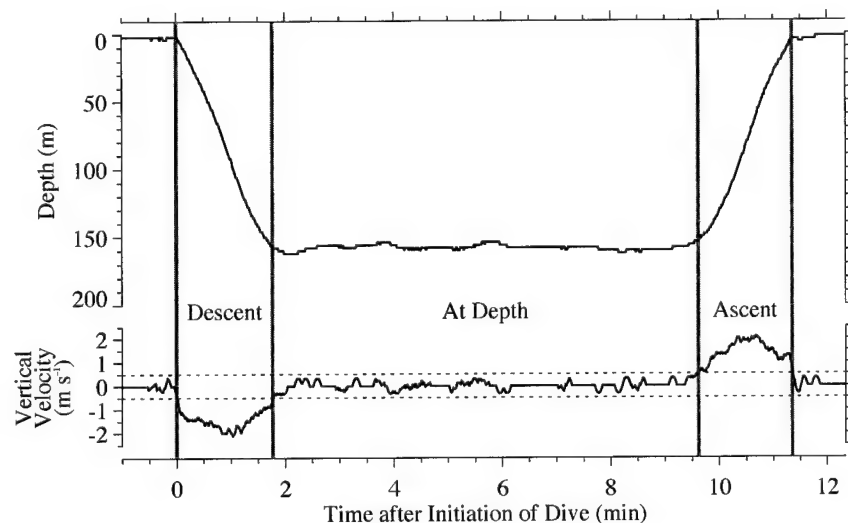Fig. 1. *Eubalaena glacialis*. Typical right whale feeding dive with descent, at depth and ascent portions shown. By convention, the descent portion begins when the downward velocity exceeds 0.5 m s^{-1} and ends when the downward velocity drops below 0.5 m s^{-1}. Likewise, the ascent portion begins when the upward velocity exceeds 0.5 m s^{-1} and ends when the upward velocity drops below 0.5 m s^{-1}

Ascent was initiated when the vertical ascent speed exceeded 0.5 m s^{-1} and the dive was terminated when the vertical ascent speed dropped below 0.5 m s^{-1}. The dive duration was defined as the time between the initiation of the descent and the termination of the ascent. The duration at depth was defined as the time between the termination of the descent and the initiation of the ascent. The mean and SD of the dive depth were computed during the at-depth portion of the dive (i.e. between the termination of the descent and the initiation of the ascent). Classification of dives was facilitated by a Ward's minimum-variance cluster analysis and visualization with multivariate star plots (Johnson 1998). The cluster analysis and visualization were conducted on the dive duration, duration at depth, descent speed, ascent speed and SD of the dive depth. Dives were classified into 3 types: feeding, V-shaped and 'other'. Surface intervals were measured after feeding dives only when the successive dive was also a feeding dive and no social activity was observed. Surface intervals were also expressed as a percentage of the total dive cycle time (PCST: after Dolphin 1987). The total dive cycle time was computed as the sum of the dive duration and the succeeding surface interval.

The vertical distribution of *Calanus finmarchicus* C5 was estimated from the calibrated OPC data in 4 m depth strata below 50 m. The depth of the peak *C. finmarchicus* C5 abundance was chosen as the midpoint of the depth stratum containing the maximum *C. finmarchicus* C5 concentration. The lower Bay of Fundy is characterized by strong tidal flow that interacts with the sea floor to create a turbulent, well-mixed bottom layer. To examine the potential relationships among this bottom mixed layer, the vertical distribution of *C. finmarchicus* C5 and the diving behavior of the tagged right whales, the depth of the top of this layer was determined from the CTD data. The top of this boundary layer was defined as the deepest depth at which the density differed from the bottom density by at least 0.05 kg m^{-3}.

Each tagged whale was considered an independent observation. Therefore, individual dive characteristics (e.g. mean dive depth, dive duration, duration at depth) and associated environmental conditions (peak *Calanus finmarchicus* C5 abundance, depth of peak abundance and bottom mixed layer depth) were averaged to provide a single observation of each variable for each whale. For comparisons between dive characteristics and environmental conditions, only data for dives with accompanying CTD/OPC casts were averaged. Dive characteristics and associated environmental conditions were compared using correlation analysis.

Total ingestion of *Calanus finmarchicus* C5 (I_d) was estimated for each feeding dive as

$$I_d = A_g S T_d E_{C5} C \tag{1}$$

where A_g is the area of the whale's gape (the opening through which water enters the mouth), S is the swimming speed, T_d is the duration at depth, E_{C5} is the energy (calorific) content of a single *C. finmarchicus* C5 and C is the estimated *C. finmarchicus* C5 concentration available to the whale. The total ingestion rate (I') during the period when the whale was tagged was estimated as follows:

$$I' = \frac{T_f \sum I_d}{T_t \sum T_d} \tag{2}$$

where T_f is the total time spent at depth during feeding dives, T_t is the total time the tag was attached to the whale and the summation of I_d and T_d occurred over all dives that had accompanying CTD/OPC casts. The ratio of T_f to T_t is considered the fraction of time spent feeding. The gape area was assumed to be 1.21 m^2 (Mayo et al. 2001) and the energy content of a single *C. finmarchicus* C5 was fixed at 1.62×10^{-3} kcal copepod^{-1} (Comita 1966) or 6.78 J copepod^{-1} (1 kcal = 4186.8 J). In 2001, improved tracking with the acoustic transmitter allowed accurate measurements of both diving and resurfacing locations. The distance between the diving and resurfacing locations divided by the dive duration was used as an estimate of the swimming speed during feeding (S in Eq. 1). These speeds must be considered minimum speeds, however, since we do not know whether the whales foraged along straight-line paths between the diving and resurfacing positions. To account for this, swimming speeds were increased to 1.5 m s^{-1} whenever the observed minimum speed was less than 1.5 m s^{-1}. Speeds were assumed to be 1.5 m s^{-1} for all dives in 2000. In Cape Cod Bay, Mayo et al. (2001) observed average swimming speeds during surface feeding of 1.34 m s^{-1} and Watkins & Shevill (1976) report speeds of 'up to 3 knots' or 1.54 m s^{-1}. Minimum swimming speeds in the present study averaged nearly 1 m s^{-1} (see Table 3 in 'Results'); however, subsurface foraging paths in the Bay of Fundy are not necessarily straight (D. P. Nowacek pers. comm.). Therefore, 1.5 m s^{-1} is assumed to be a reasonable estimate of true speed during feeding.

To investigate whether sufficient food was available to the tagged whales, the rate of ingestion was compared to the estimated rate needed to meet the daily metabolic requirements for maintenance in right whales. For simplicity, a right whale's day was divided into 2 activities: foraging and resting. The metabolic rate during foraging was assumed to be equal to the diving metabolic rate (DMR). Assuming that the

tagged right whales were able to continue to feed at I' for T h each day, the fraction of the daily metabolic requirement met by each whale is

$$\frac{\text{daily assimilation}}{\text{daily requirement}} = \frac{A I' T}{\text{DMR}(T) + \text{RMR}(24 - T)} \quad (3)$$

where A is the assimilation efficiency and RMR is the resting metabolic rate. The time required to meet the daily metabolic requirement (T_{req}) is then

$$T_{\text{req}} = \frac{24 \, \text{RMR}}{A I' + \text{RMR} - \text{DMR}} \quad (4)$$

Both DMR and RMR were assumed to be multiples of the basal metabolic rate (BMR), which was estimated as

$$\text{BMR} = \frac{4186.8}{86400} [70 M^{0.75}] \quad (5)$$

where M is the mass of a right whale in kg. The term in brackets is after Kleiber (1975) and the first term converts Kleiber's expression from kcal d^{-1} to W (or J s^{-1}). The assimilation efficiency and body mass are assumed to be 0.80 (Lockyer 1981) and 40 000 kg (Kenney & Winn 1986), respectively; therefore, BMR = 0.96×10^4 W. The magnitude of DMR is unknown for right whales, but for other species, DMR is $1.5 - 2 \times$ BMR in Weddell seals (Kooyman et al. 1973, Castellini et al. 1992), $2 - 3 \times$ BMR in northern elephant seals (Costa & Williams 1999) and nearly $6 \times$ BMR in the bottlenose dolphin and otariids (sea lions and fur seals) (Costa & Gentry 1986, Costa et al. 1989, Costa & Williams 1999). When compared to other marine mammals, the DMR for right whales is probably low since the energetic costs associated with continuous filter feeding do not appear particularly expensive (relative to lunge feeding in rorquals, for instance; Croll et al. 2001) and their insulating blubber layer is thick. Recent energetic investigations of bowhead whales, a closely related species to the right whale, suggest these whales have very low metabolic rates due, in part, to a very thick blubber layer and a low core temperature (J. C. George pers. comm.). We assume here that DMR = $2 \times$ BMR and RMR = $1 \times$ BMR. For consistency with the literature, we also present ingestion rate as a fraction of the ingestion rate required to meet basal metabolic requirements. This latter rate (I'_{BMR}) is estimated as

$$I'_{\text{BMR}} = \frac{1}{A} \text{BMR} \quad (6)$$

or 1.20×10^4 W.

RESULTS

A total of 28 right whales were tagged in the lower Bay of Fundy between 11 July and 28 August 2000 (Fig. 2). All but 2 of the tags were recovered. The
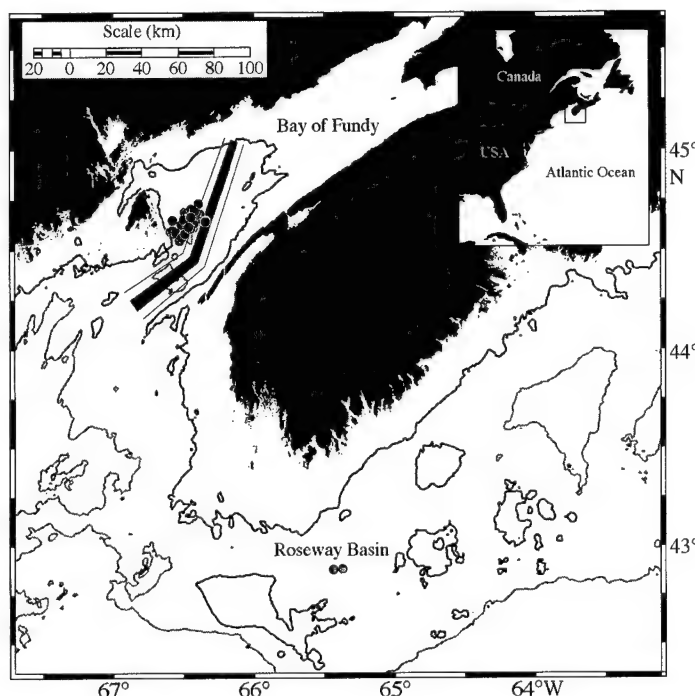

Fig. 2. Map of study area. (◉) Tagging locations in the lower Bay of Fundy and Roseway Basin. Shipping lanes through the lower Bay of Fundy at the time of this study and the 91 m (50 fathom) and 200 m isobaths are also shown

median duration of attachment was 28 min and 23.1% (n = 6) of the tagging events exceeded 1 h. During a single event in 2000, a rubber suction cup was used instead of the silicone cup and the resulting attachment duration was 7 h. A total of 63 complete dives was recorded of which 93.7% (n = 59) were feeding dives, 4.8% (n = 3) were V-shaped and 1.6% (n = 1) were classified as 'other.' From 11 to 29 August 2001, 25 right whales were tagged and all of the tags were recovered. Of these 25 whales, 6 adults (presumably female) with calves, 2 calves and 1 pregnant (R. M. Rolland pers. comm.) female were tagged. Two of the whales were tagged in Roseway Basin on the southwestern Scotian Shelf and the remaining 23 were tagged in the lower Bay of Fundy (Fig. 2). The median duration of attachment was 86 min and 64.0% (n = 16) of the tagging events exceeded 1 h. A total of 86 complete dives was recorded of which 88.4% (n = 76) were feeding dives, 5.8% (n = 5) were V-shaped and 5.8% (n = 5) were classified as 'other.' Of the 149 total dives recorded in both 2000 and 2001, 86.6% (n = 129) had an accompanying CTD/OPC cast which, on average, was conducted 21.5 min after and 158 m away from the whale's resurfacing location.

Strong reaction to tagging or the close approach of the RHIB was uncommon. In 2000, 71% of the 42 whales that were closely approached by the RHIB

(within 10 m) showed no observable reaction (22 of 28 successfully tagged individuals and 8 of 14 unsuccessfully tagged individuals). Of the remaining whales, reactions included lifting the head or flukes, arching the back, rolling to one side, rolling to one side and beating the flukes (on 1 occasion), or performing a head lunge (on 1 occasion). Observations during close boat approaches in 2001 were qualitatively similar to those collected in 2000. The characteristics of the first, second, third, fourth and last feeding dives were compared for the 18 whales that were tagged for over 1 h and had 2 or more feeding dives. The duration of the first feeding dive was, on average, 13% (n = 18, p = 0.0061), 15% (n = 17, p = 0.0039), 17% (n = 16, p = 0.0010) and 14% (n = 12, p = 0.045) shorter than the second, third, fourth and last dives, respectively. In contrast, no significant differences in dive duration (p > 0.05) were detected in comparisons of the second and successive dives or the third and successive dives. Differences in dive duration between the first and successive dives did not depend on the time between tag attachment and the first feeding dive (correlation analysis, p > 0.5). No significant differences in descent speed, ascent speed or dive depth (p > 0.05) were detected in comparisons between the first dive and successive dives.

Based on these results, the effect of the tag attachment process on diving behavior is considered to be small and short-lived; hence, none of the subsequent analyses take this effect into account. Only the duration of the first feeding dive was affected by the tagging process, and the difference between this first dive and successive dives was small (~15% shorter). Reduction in dive duration during the first dive is likely caused by inadequate ventilation during the surfacing interval in which the tag was deployed which, in turn, may be due to evasion of the boat by premature diving, longer submergence times between breaths or increased swim speeds.

Feeding dives were characterized by a rapid descent from the surface to a particular depth, remarkable fidelity to that depth for an average of just over 9 min and then a rapid ascent back to the surface (Fig. 1, Table 1). Ascent speed averaged 0.07 m s⁻¹ (95% CI: 0.01 – 0.13 m s⁻¹) faster than the corresponding descent speed during feeding dives (one-sample t-test, p = 0.026). Excluding the tagged calves, females with calves and the pregnant female, there was no evidence to suggest that PCST was correlated with either depth (r = 0.119, p = 0.73) or dive duration (r = 0.029, p = 0.93). For these indi-

viduals, PCST averaged 21.2% (n = 11, SD = 4.1%, range = 15.8 – 30.1%) whereas for the tagged calves and females with calves, PCST averaged 34.2% (n = 4, SD = 9.2%, range = 24.3 – 44.3%). The PCST for the pregnant female (shown in Fig. 4c) was 51.1%, which was the highest observed. Excluding the pregnant female, dive durations for calves and females with calves were similar to the other whales (2-sample t-test, p = 0.78: however, note low sample size and thus low power of test), but surface intervals were significantly higher (2-sample t-test, p = 0.0011). Surface intervals for calves and females with calves averaged 5.69 min (n = 4, SD = 1.22 min, range = 4.54 – 6.97 min) whereas surface intervals for all other individuals excluding the pregnant female averaged 3.13 min (n = 11, SD = 0.99 min, range = 1.65 – 5.06 min). The pregnant female had the highest average surface interval of 11.08 min.

Traveling (e.g. Fig. 3b) and social activity (e.g. Fig. 3c) were also observed and it was during these times that dives classified as V-shaped and 'other' often occurred. Of the 8 dives classified as V-shaped, 5 were to within 10 m of the bottom mixed layer (e.g. Fig. 4c,d). Of the 6 dives classified as 'other', 2 of the dives were to within 10 m of the bottom mixed layer (Fig. 3b,c) and 4 were to the sea floor (e.g. Fig. 3b). In all, 5 brief excursions to the bottom were observed (e.g. Fig. 3b,d), but none of these individuals remained at or near the bottom. Feeding dives did not occur near the bottom.

We observed increases in dive duration, descent speed and ascent speed with dive depth during feeding dives which contributed to a positive correlation between duration at depth and dive depth (Table 2). These dive characteristics were also strongly and positively correlated with the depth of the peak *Calanus finmarchicus* C5 abundance. There was suggestive, but inconclusive evidence that both dive duration and

Table 1. *Eubalaena glacialis* and *Calanus finmarchicus*. Summary of feeding dive characteristics for whales that engaged in at least 1 feeding dive while tagged. Dive characteristics were initially averaged to provide a single observation for each whale. Distance and minimum speed were computed from the consecutive diving and resurfacing positions obtained in 2001 only. Prey abundance refers to the peak abundance of *C. finmarchicus* C5 in the water column

| Dive characteristics	n	Median	Mean	SD	95% CI	Range
Dive duration (min)	34	12.65	12.17	2.22	11.39–12.94	7.83–16.32
Duration at depth (min)	34	9.50	9.39	2.29	8.59–10.18	4.72–13.55
Descent speed (m s⁻¹)	34	1.38	1.40	0.30	1.29–1.50	0.81–2.00
Ascent speed (m s⁻¹)	34	1.54	1.47	0.26	1.38–1.56	0.93–2.05
Dive depth (m)	34	119.9	121.2	24.2	112.8–129.7	78.7–174.0
Distance (km)	18	0.59	0.59	0.20	0.49–0.70	0.21–0.94
Minimum speed (km h⁻¹)	18	0.85	0.93	0.44	0.71–1.15	0.38–1.94
Prey abundance (copepods m⁻³)	31	6219	7481	4581	5800–9161	2059–20610
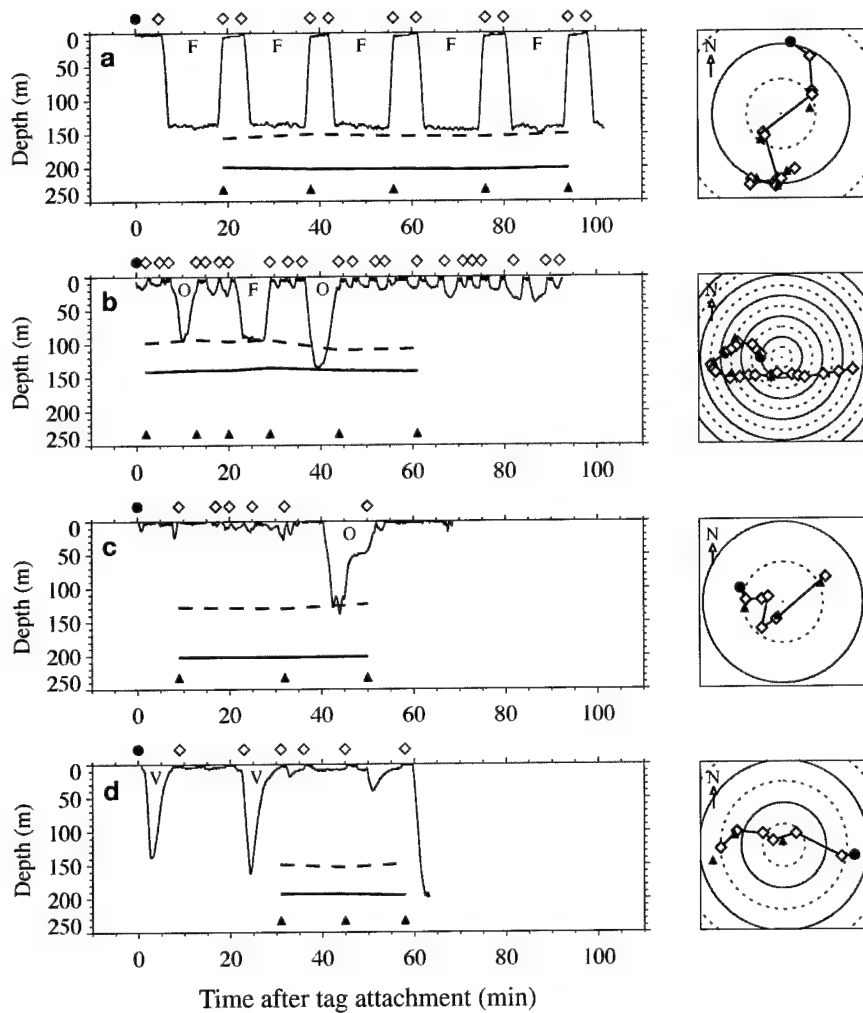
Fig. 3. *Eubalaena glacialis*. Diving and tracking observations illustrating (a) feeding, (b) traveling, (c) socializing and (d) presumed searching behaviors. Individual dives were classified and labeled as feeding (F), V-shaped (V) or 'other' (O). (● ◊) Times (on the time series) and locations (on the accompanying map) of visual contacts. (▲) Times and locations at which a resurfacing occurred and a conductivity-temperature-depth/optical plankton counter (CTD/OPC) cast was conducted. Solid and dashed lines indicate the sea floor and the top of the bottom mixed layer, respectively, measured at the location of each CTD/OPC cast. Concentric lines on the accompanying maps are separated by 0.5 km. Tags detached at depth in (a) and at the bottom in (d)

duration at depth were correlated with peak *C. finmarchicus* C5 abundance (r = 0.339, p = 0.062 for dive duration; r = 0.353, p = 0.051 for duration at depth; Table 2). *C. finmarchicus* C5 were very often aggregated in discrete layers near foraging right whales and the at-depth portion of the whales' dives were spent in or near these layers (Fig. 4). The average depth of dive was strongly correlated with the average depth of peak *C. finmarchicus* C5 abundance (r = 0.902, p < 0.0001, Table 2, Fig. 5a). There was no evidence to suggest that the relationship between the average depth of dive and the average depth of maximum *C. finmarchicus* C5 abundance was different from one-to-one (H_o: intercept = 0, p = 0.93; H_o: slope = 1, p = 0.76). The discrete layers of *C. finmarchicus* C5 upon which the whales presumably fed were often observed near the bottom mixed layer (Fig. 4). Consequently, the whales' average dive depth was strongly correlated with the average depth of the bottom mixed layer (r = 0.865, p < 0.0001, Fig. 5b). Average dive depths were shallower than the bottom mixed layer by an average of 7 m, however, which indicates that *C. finmarchicus* C5 typically aggregated just above the bottom mixed layer.

Since right whales were observed foraging at the depth of maximum *Calanus finmarchicus* C5 abundance, total ingestion (I_d from Eq. 1) was computed for every feeding dive using the estimate of the peak *C. finmarchicus* C5 abundance from the accompanying OPC cast. Ingestion rates (I' from Eq. 2)

Table 2. *Eubalaena glacialis* and *Calanus finmarchicus*. Correlation matrix of feeding dive characteristics for tagged individuals that engaged in at least 1 feeding dive for which an accompanying CTD/OPC cast was conducted. n = 31 for each correlation coefficient. Prey abundance refers to the peak abundance of *C. finmarchicus* C5 in the water column

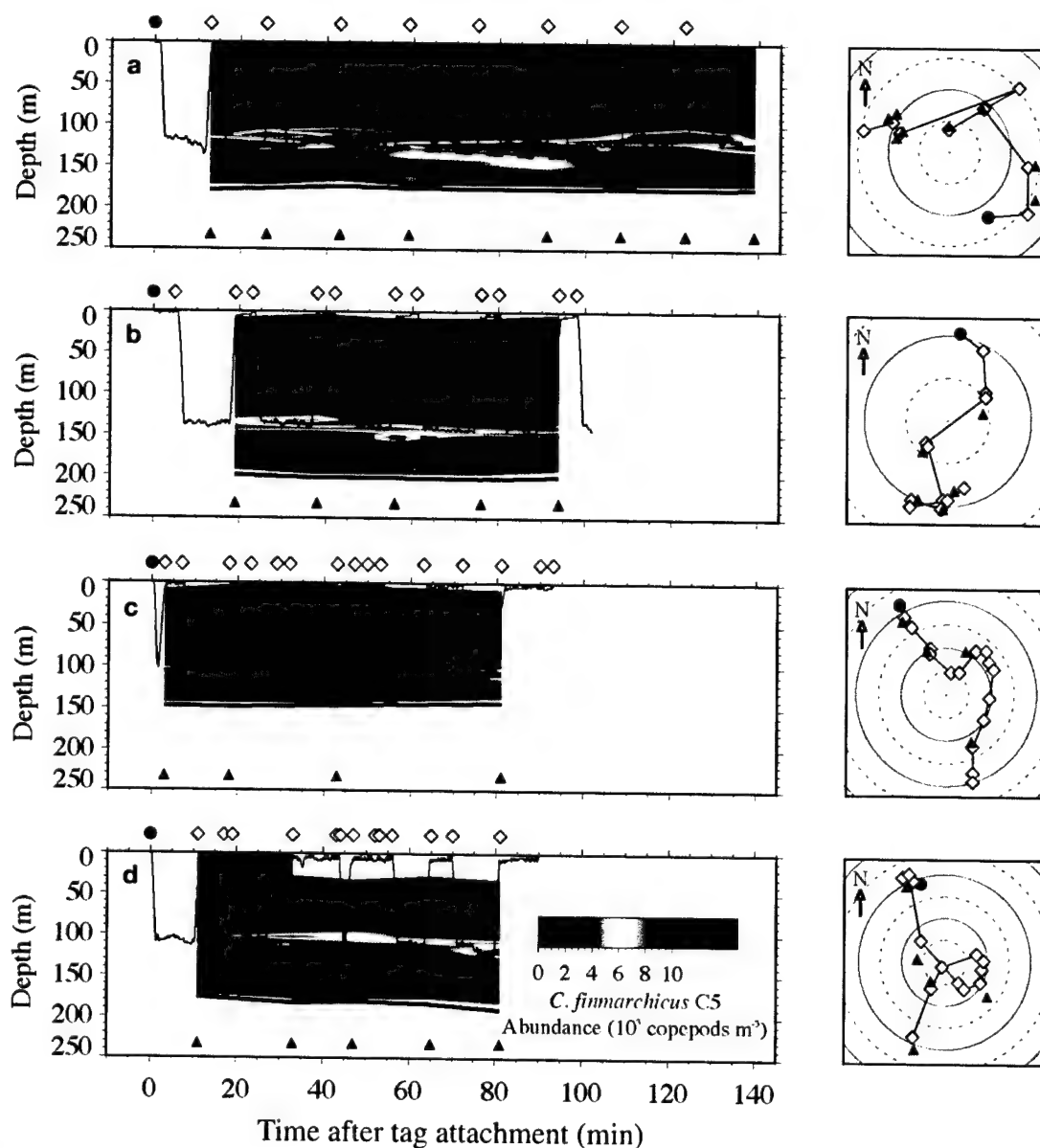|	Dive duration	Duration at depth	Descent speed	Ascent speed	Prey abundance	Depth of peak prey abundance
Dive depth	0.586***	0.447*	0.470**	0.533**	0.093	0.902***
Dive duration		0.974***	0.558**	0.728***	0.339†	0.569***
Duration at depth			0.635***	0.778***	0.353†	0.469**
Descent speed				0.766***	0.234	0.538**
Ascent speed					0.234	0.604***
Prey abundance						0.031
***p < 0.001, **0.001 ≤ p < 0.01, *0.01 ≤ p < 0.05, †0.05 ≤ p < 0.10						

Fig. 4. *Eubalaena glacialis* and *Calanus finmarchicus*. (a–d) Examples of diving and tracking observations during feeding behavior. Contoured *C. finmarchicus* C5 abundance estimated from the OPC casts is shown. Color scale shown in (d) applies to all plots. Symbols and lines are the same as in Fig. 3
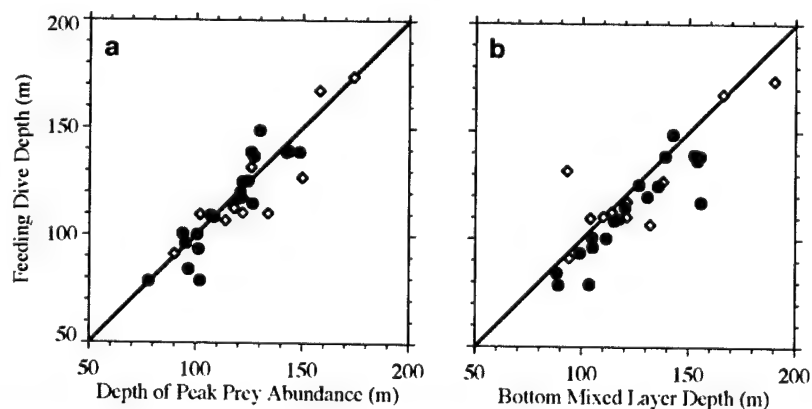

Fig. 5. *Eubalaena glacialis* and *Calanus finmarchicus*. Average depth of feeding dive versus (a) average depth of peak *C. finmarchicus* C5 abundance and (b) average depth of the bottom mixed layer. (●) Tagged whales that had 2 or more feeding dives with accompanying CTD/OPC casts. (◇) Tagged whales that had only 1 feeding dive with an accompanying CTD/OPC cast

Table 3. *Eubalaena glacialis* and *Calanus finmarchicus*. Number of feeding dives, duration of tag attachment, percent time feeding, average minimum speed between diving and resurfacing positions, average peak *C. finmarchicus* C5 abundance below 50 m, ingestion rate (I'), ingestion rate as a fraction of the ingestion rate required to meet estimated basal metabolic requirements (I'_{BMR}), and time required to meet daily metabolic requirement (T_{req}) from Eq. (4). Data are from deployments lasting over 1 h. The first column contains the label used for each whale in Fig. 6. Fig. numbers are also provided for those deployments shown in Figs. 3 and 4. Minimum speeds were not calculated for individuals tagged in 2000 (see 'Materials and methods' for explanation). Missing values for T_{req} indicate $T_{req} > 24$ h

Label in Fig. 6	No. feeding dives	Attachment duration (min)	% time feeding	Speed (m s⁻¹)	Prey abundance (copepods m⁻³)	I' (10⁴ W)	I' (× I'_{BMR})	T_{req} (h)	Fig.
1[a]	0	69	0.0	–	–	0.00	0.00	–	3c
2[a]	0	63	0.0	–	–	0.00	0.00	–	3d
3	0	92	0.0	–	–	0.00	0.00	–	
4[b]	1	93	5.1	1.94	5592	0.45	0.38	–	3b
5	2	102	13.5	0.38	3500	0.53	0.44	–	
6	6	98	48.7	0.75	3124	1.89	1.57	–	
7[b,c]	4	93	30.7	1.01	5124	1.89	1.57	–	4c
8	6	101	63.3	0.95	3020	2.37	1.98	–	
9	4	66	54.5	0.52	3677	2.48	2.07	22.5	
10	7	96	45.9	1.87	3087	2.49	2.08	22.3	
11[a]	9	198	40.6	–	6331	3.23	2.69	14.2	
12	6	112	52.0	0.84	5332	3.31	2.76	13.6	
13	5	87	57.1	0.61	4673	3.39	2.83	13.1	
14	4	82	43.7	0.92	6602	3.53	2.94	12.4	
15	7	118	53.2	0.85	5440	3.55	2.96	12.3	
16[d]	3	66	54.7	0.99	5759	3.73	3.11	11.4	
17[a]	23	422	54.2	–	6233	4.19	3.50	9.6	
18[e]	4	90	33.7	1.54	8672	4.64	3.87	8.4	4d
19	6	86	64.2	0.61	9871	7.69	6.41	4.4	
20[a]	6	68	48.0	–	12867	7.78	6.49	4.4	
21[d]	5	102	57.7	0.68	11893	8.47	7.06	4.0	3a, 4b
22[a]	8	136	68.0	–	14945	12.48	10.41	2.6	4a
Average			40.4	0.96	6618	3.55	2.96		

[a]Whales tagged in 2000. All other whales tagged in 2001; [b]whales tagged in Roseway Basin on southwestern Scotian Shelf. All other whales tagged in Grand Manan Basin of the lower Bay of Fundy; [c]pregnant female; [d]adult (presumably female) with calf; [e]calf

were estimated only for those whales tracked over 1 h (Table 3). Of the 22 tagged individuals examined, 14 had ingestion rates that were high enough to meet estimated daily metabolic requirements. However, 2 of these 14 would have needed to feed for nearly 24 h at the observed ingestion rates to meet this requirement, whereas 4 would have needed less than 5 h. The concentration of *C. finmarchicus* C5 explained 94% of the variation in the estimated ingestion rates when assessed with a regression model forced through the origin (Fig. 6). The resulting regression equation, i.e. $I' = (6.58 \text{ m}^3 \text{ W}) \times C$, suggests that the minimum *C. finmarchicus* C5 concentration required to meet daily metabolic requirements is 3600 copepods m⁻³ (foraging would need to continue for 24 h d⁻¹ to meet this requirement). The minimum peak concentration observed near whales that were tagged for over 1 h and that engaged in feeding dives was ca. 3000 copepods m⁻³ (Table 3), which is in good agreement with the minimum concentration required to meet daily metabolic requirements. One of the tagged whales engaged in behavior that we interpret as searching (Fig. 3d) and peak concentrations of *C. finmarchicus* C5 near this individual averaged ca. 1300 copepods m⁻³. A whale

feeding continuously on this concentration (i.e. 24 h d⁻¹) would ingest only 35% of its daily requirement on average, whereas feeding on a concentration of 3000 copepods m⁻³ would yield 83% of the daily requirement. The evidence from this single individual suggests that right whales may ignore *C. finmarchicus* C5 concentrations as low as 1300 copepods m⁻³ because foraging would not come close to meeting the daily requirement, yet peak concentrations over 3000 copepods m⁻³ that nearly provide the daily requirement may be more acceptable.

DISCUSSION

The stereotypical shape of feeding dives in North Atlantic right whales is optimized for exploiting zooplankton aggregated in discrete layers. Rapid descents and ascents reduce transit time to foraging depths, and these transit times are even further reduced when diving to deeper depths by increasing both descent and ascent rates. Thus, duration at the depth where feeding occurs is maximized. The significantly faster ascents relative to descents are due to the right whale's
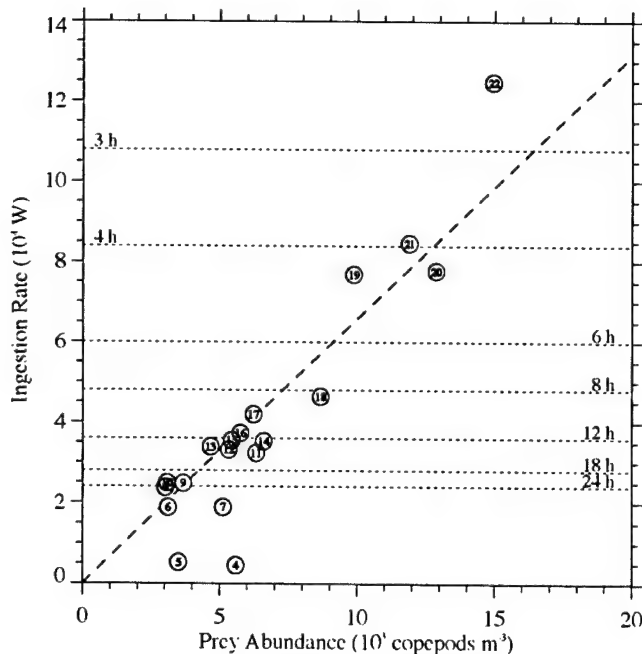
Mar Ecol Prog Ser 264: 123–135, 2003

Fig. 6. *Eubalaena glacialis* and *Calanus finmarchicus*. Estimated ingestion rate versus average peak *C. finmarchicus* C5 abundance. (4) to (22): Labels for whales reference data in Table 3. A linear regression forced through the origin was fitted to the data and is shown as the dashed line. Horizontal, dotted lines indicate the ingestion rates and times spent foraging required to meet daily metabolic needs (e.g. ingestion for 8 h d^{-1} at a rate of 4.8×10^4 W would be sufficient to meet daily metabolic requirements)

positive buoyancy, which the whale must overcome by fluke stroking on descent, but is exploited to reduce energy expenditure by gliding on ascent (Nowacek et al. 2001). The low variability in dive depth during the at-depth portion of the feeding dive is in marked contrast to the high variability in dive depth exhibited by blue and fin whales (Croll et al. 2001). These differences are presumably related to feeding ecology. Right whales feed on zooplankton aggregated in discrete layers by continuously swimming with their mouths agape, but blue and fin whales are gulp feeders that engulf euphausiids or fish along with vast quantities of seawater in a single mouthful. The variability in dive depths during the at-depth portion of these rorquals' dives, therefore, has been interpreted as lunge feeding (Croll et al. 2001). The duration of the tagged right whales' dives (average 12.2 min) were much longer than fin (5.5 min; Croll et al. 2001), blue (6.6 min; Croll et al. 2001) and humpback whales (2.8 min; Dolphin 1987). Croll et al. (2001) have suggested that increased dive durations in the Balaenidae (right and bowhead whales) are a result of lower metabolic costs associated with continuous filter feeding. Conversely, decreased dive durations in rorquals are a consequence of the higher metabolic costs associated with lunge feeding.

When dive durations exceed the capacity for aerobic metabolism, anaerobic metabolism causes lactate to build in the blood which must be cleared during the succeeding surfacing interval. Dives that exceed this aerobic dive limit (ADL), therefore, are associated with disproportionately longer surfacing intervals (Kooyman et al. 1980, 1983). Dolphin (1987) reported increasing PCST for humpback whale dives that exceeded 60 m in depth and suggested that this increased time at the surface was required to repay the oxygen debt incurred during anaerobic metabolism. In the present study, there was no evidence that PCST was correlated with either dive depth or duration for the tagged right whales. We observed average PCST values of 21.2% (excluding calves, females with calves and the pregnant female), which is in good agreement with PCST values for presumed aerobic dives by Weddell seals (21%; Kooyman et al. 1980) and humpback whales (21.4%; Dolphin 1987). These results suggest that the tagged right whales were diving within their ADL. Although the dive durations for calves and females with calves were similar to the other whales, surface intervals were significantly higher, which resulted in a higher PCST for calves and females with calves. The calves were seldom more than a body's length away from their presumed mothers and they often surfaced and dove simultaneously with the adult as well. The extended surface intervals and higher PCST values for the tagged females with calves, then, are interpreted as being governed by the calf's diving capabilities. Theoretical ADL is computed as the total oxygen stores divided by DMR and while total oxygen stores increase linearly with body mass (M), DMR increases with $M^{0.75}$ (Costa & Williams 1999). ADL is therefore proportional to $M^{0.25}$, so a calf's ADL will be lower than that of an adult simply due to its reduced body size. In addition to the effect of body size on ADL, calves must also have higher metabolic rates to fuel growth which will further reduce their ADL. Croll et al. (2001) estimated total O_2 stores for blue and fin whales to be an average 55.6 ml O_2 kg^{-1}. Assuming right whales have similar total O_2 stores and that a calf's DMR = 4 × BMR (i.e. DMR = 4 × [$70M^{0.75}$ kcal d^{-1}] / [4.8 kcal (l O_2)$^{-1}$] / [1440 min d^{-1}]), a 5000 kg calf (New England Aquarium unpubl. data cited in Brown et al. 2001) would have a theoretical ADL of 11.5 min. Observed dive durations for calves and females with calves averaged 11.60 min (n = 5, SD = 2.04 min, range = 8.84 to 14.09 min). The prolonged surface intervals, elevated PCST values and these ADL calculations suggest that right whale calves may dive for durations close to their ADL, but caution is warranted when interpreting these results because of the low sample size and the uncertainty in estimating both total O_2 stores and diving metabolic rate for right whales.

The significantly longer surface intervals observed for calves, females with calves and the pregnant female may indicate that reproductively active females and their calves are at comparatively greater risk for collisions with ships than other animals in the population. Fujiwara & Caswell (2001) estimated that the survivorship of right whale mothers declined from 1980 to 1995, while the survivorship of mature males and (non-calving) females remained unchanged over the same period. Higher rates of mortality among right whale mothers may be due to their use of the calving grounds off the southeast United States, where the volume of shipping traffic is high (Fujiwara & Caswell 2001). However, our results suggest that the diving behavior of reproductively active females and their calves may also place them at greater risk of ship strikes on the feeding grounds as well.

The strong correlation between dive depths and the depth of maximum *Calanus finmarchicus* C5 abundance indicate that right whales are adept at locating and exploiting discrete layers of highly concentrated prey. The accuracy with which they target these layers would seem to rule out the possibility that right whales sample the water column mouthful by mouthful until they reach a suitable prey concentration. Instead, the transition from the descent phase to the at-depth portion of the dive occurs very quickly and the fidelity to the depth initially targeted is often remarkable. These observations suggest that right whales can detect layers of *C. finmarchicus* C5 without opening their mouths. The sensory mechanisms by which the whales accomplish this are unknown, but may include vision or sensory hairs (Kenney et al. 2001). Rowntree (1996) even suggests that the cyamid amphipods that inhabit right whale callosities may aid in locating prey. As is typical for turbid coastal environments, light levels at mid-depth in Grand Manan Basin are probably very low and vision would only be useful during daylight hours. *C. finmarchicus* do not bioluminesce as do some other copepods (e.g. *Metridia* spp.), so direct visual detection of prey in the absence of ambient light is probably not possible. Regardless of the sensory mechanisms employed, right whales may be able to restrict their search for suitable prey concentrations using cues from the physical environment. The tagged right whales rarely ventured into the bottom mixed layer proper and when they did so, it was typically during an excursion to the sea floor that seemed exploratory in nature. There are a variety of cues with which right whales can detect the presence of this mixed layer, including shear at the top of the layer (i.e. rapid velocity changes with depth), turbulence within the layer itself or particular temperature or salinity properties. With foraging experience, right whales may learn that suitable prey concentrations of *C. finmarchicus* are

uncommon in the bottom mixed layer, so only occasional forays into this layer are necessary. Moreover, searching may be further restricted to only a few 10s of m around the top of this boundary layer since *C. finmarchicus* C5 aggregate just above the bottom mixed layer at this time of year.

Our calculations suggest that many of the tagged right whales ingest *Calanus finmarchicus* C5 at rates sufficient to meet daily metabolic requirements. It is very important to bear in mind, however, that the selection of DMR = 2 × BMR, though based on sound reasoning, is truthfully only a guess. Metabolic rates have only been directly measured in species that can be captured and manipulated. Current methods of measuring metabolic rates cannot be applied to adult mysticetes. Croll et al. (2001) observed dive durations in blue and fin whales that were much shorter than calculated ADL values using DMR = 4 × BMR. They inferred from these data that the metabolic costs of lunge feeding were well in excess of 4 × BMR. The number of right whales deemed to be successfully foraging is quite sensitive to the choice of DMR (Fig. 7). If DMR values for right whales also exceed 4 × BMR, then only 4 of the 22 individuals with tag attachments lasting over 1 h would have been ingesting *C. finmarchicus* C5 at a rate sufficient to meet their daily metabolic requirement (Fig. 7). Uncertainties in estimating metabolic rates inhibit our ability to accurately determine whether right whales are able to forage successfully. The development and application of new methods to directly measure either absolute or relative (i.e. diving vs. resting) metabolic rates for large cetaceans is sorely needed.
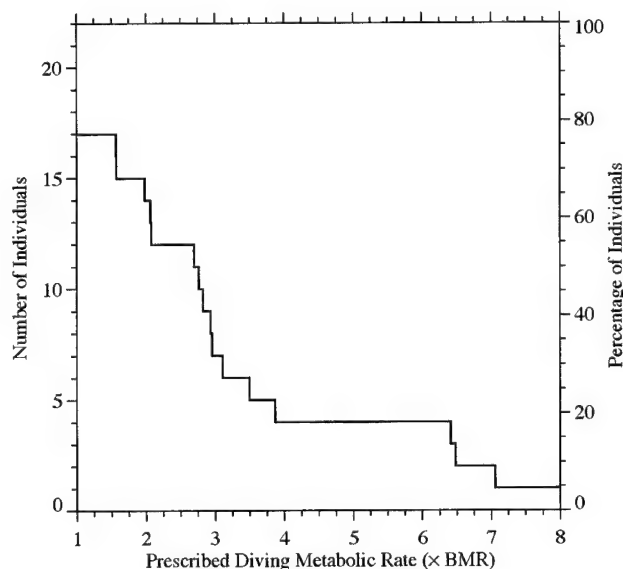

Fig. 7. *Eubalaena glacialis.* Number (and percentage) of whales shown in Table 3 that ingested prey at a rate sufficient to meet daily metabolic requirements for different choices of the diving metabolic rate (DMR). DMR shown as a multiple of the estimated basal metabolic rate (BMR)

Despite the uncertainties in DMR, it is clear that some of the tagged whales were easily ingesting *Calanus finmarchicus* C5 at a rate sufficient to meet their daily metabolic requirements. These whales were able to identify and exploit very dense aggregations of *C. finmarchicus* C5, which indicates that food resources upon which individual right whales can survive seem to exist. Since no emaciated right whales were observed in the field and some tagged whales chose socializing with conspecifics over foraging, this result is in no way surprising. It seems clear that sufficient food resources exist for individual right whales to survive, but the benchmark for successful foraging in a viable population is not simply meeting daily or even annual maintenance requirements. Ingestion must also be sufficient to fuel reproduction, including the metabolic costs of social behavior (a rather energetic activity in right whales), growth of a fetus and support of a newborn calf via lactation. Of the 22 individuals examined, 15 ingested *C. finmarchicus* C5 at rates that would require more than half of the day to be dedicated to foraging just to meet daily metabolic requirements (Table 3). These results might suggest that sufficient food resources do not exist to support the elevated metabolic demands associated with reproduction for most of the population. However, a few caveats must be recalled before such a claim could be made.

The deployment durations during this study were short; most successful deployments were between 0.5 and 2 h. Therefore, the ingestion rates estimated here may not accurately reflect daily ingestion rates. Since we observed a few whales foraging on abundances of *Calanus finmarchicus* C5 in excess of 10 000 copepods m^{-3}, we know that very dense concentrations are occasionally encountered. For those whales that had low ingestion rates during the period they were tagged, it is possible that they might also encounter similarly high abundances after several more hours of foraging effort. Accurate daily ingestion rates can only be obtained with deployments that last at least 24 h. Ingestion rates can further be improved with direct swim speed measurements (relative to the water, not the ground), although we believe the error in the estimated ingestion rates attributable to a fixed swim speed (1.5 m s^{-1}) is relatively small. In light of these considerations, we cannot judge whether sufficient food resources exist to support right whale population growth with our data. However, clear directions for future work are indicated. Day-long deployments with concurrent zooplankton sampling are necessary to obtain accurate daily ingestion rates. Day-long deployments would also yield data on the amount of time devoted to foraging (*T* in Eq. 3), resting and social activities. As mentioned before, innovative methods to measure metabolic rates in large cetaceans are also needed. Finally, it is important to obtain simi-

lar measurements outside the lower Bay of Fundy throughout the spring-summer-fall feeding season. Since right whales are capable of storing fat, it is possible that feeding conditions elsewhere may provide the bulk of the energy required to meet reproductive metabolic costs (e.g. Beardsley et al. 1996). Focusing only on 1 feeding habitat, then, might provide a distorted view of whether sufficient food resources exist to support right whale population growth.

LITERATURE CITED

Baumgartner MF (2003) Comparisons of *Calanus finmarchicus* fifth copepodite abundance estimates from nets and an optical plankton counter. J Plankton Res 25:855–868

Beardsley RC, Epstein AW, Chen C, Wishner KF, Macaulay MC, Kenney RD (1996) Spatial variability in zooplankton abundance near feeding right whales in the Great South Channel. Deep-Sea Res II 43:1601–1625

Brown MW, Brault S, Hamilton PK, Kenney RD and 5 others (2001) Sighting heterogeneity of right whales in the western North Atlantic: 1980–1992. J Cetacean Res Manage Spec Issue 2:245–250

Castellini MA, Kooyman GL, Ponganis, PJ (1992) Metabolic rates of freely diving Weddell seals: correlations with oxygen stores, swim velocity and diving duration. J Exp Biol 165:181–194

Caswell H, Fujiwara M, Brault S (1999) Declining survival probability threatens the North Atlantic right whale. Proc Natl Acad Sci USA 96:3308–3313

Clapham PJ, Young SB, Brownell Jr RL (1999) Baleen whales: conservation issues and the status of the most endangered populations. Mamm Rev 29:35–60

Comita GW, Marshall SM, Orr AP (1966) On the biology of *Calanus finmarchicus*. XIII. Seasonal change in weight, calorific value and organic matter. J Mar Biol Assoc UK 46:1–17

Conversi A, Piontkovski S, Hameed S (2001) Seasonal and interannual dynamics of *Calanus finmarchicus* in the Gulf of Maine (northeastern US shelf) with reference to the North Atlantic Oscillation. Deep-Sea Res II 48:519–530

Costa DP (1993) The secret life of marine mammals: novel

tools for studying their behavior and biology at sea. Oceanography 6:120–128

Costa DP, Gentry RL (1986) Free-ranging energetics of northern fur seals, *Callorhinus ursinus*. In: Gentry RL, Kooyman GL (eds) Fur seals: maternal strategies on land and at sea. Princeton University Press, Princeton, NJ, p 79–101

Costa DP, Williams TM (1999) Marine mammal energetics. In: Reynolds JE III, Rommel SA (eds) Biology of Marine Mammals. Smithsonian Institution Press, Washington, District of Columbia, USA, p 176–217

Costa DP, Croxall JP, Duck C (1989) Foraging energetics of Antarctic fur seals, *Arctocephalus gazella*, in relation to changes in prey availability. Ecology 70:596–606

Croll DA, Acevedo-Gutiérrez A, Tershy BR, Urbán-Ramírez J (2001) The diving behavior of blue and fin whales: is dive duration shorter than expected based on oxygen stores? Comp Biochem Physiol A 129:797–809

Dolphin WF (1987) Dive behavior and estimated energy expenditure of foraging humpback whales in southeast Alaska. Can J Zool 65:354–362

Fromentin J, Planque B (1996) *Calanus* and environment in the eastern North Atlantic. II. Influence of the North Atlantic Oscillation on *C. finmarchicus* and *C. helgolandicus*. Mar Ecol Prog Ser 134:111–118

Fujiwara M, Caswell H (2001) Demography of the endangered North Atlantic right whale. Nature 414:537–541

Greene CH, Pershing AJ (2000) The response of *Calanus finmarchicus* populations to climate variability in the Northwest Atlantic: basin-scale forcing associated with the North Atlantic Oscillation. ICES J Mar Sci 57:1536–1544

Goodyear JD (1993) A sonic/radio tag for monitoring dive depths and underwater movements of whales. J Wildl Manage 57:503–513

Hamilton PK, Martin SM (1999) A catalog of identified right whales from the western North Atlantic: 1935 – 1997. New England Aquarium, Boston, MA

Herman AW (1988) Simultaneous measurement of zooplankton and light attenuance with a new optical plankton counter. Cont Shelf Res 8:205–221

Herman AW (1992) Design and calibration of a new optical plankton counter capable of sizing small zooplankton. Deep-Sea Res 39:395–415

International Whaling Commission (IWC) (2001) Report of the workshop on status and trends of western North Atlantic right whales. J Cetacean Res Manage Spec Issue 2:61–87

Johnson DE (1998) Applied multivariate methods for data analysts. Duxbury Press, Pacific Grove, CA

Kenney RD, Winn HE (1986) Cetacean high-use habitats of the northeast United States continental shelf. Fish Bull 84:345–357

Kenney RD, Hyman MAM, Owen RE, Scott GP, Winn HE (1986) Estimation of prey densities required by western North Atlantic right whales. Mar Mamm Sci 2:1–13

Kenney RD, Winn HE, Macaulay MC (1995) Cetaceans in the Great South Channel, 1979 – 1989: right whale (*Eubalaena glacialis*). Cont Shelf Res 15:385–414

Kenney RD, Mayo CA, Winn HE (2001) Migration and foraging strategies at varying spatial scales in western North Atlantic right whales: a review of hypotheses. J Cetacean Res Manage Spec Issue 2:251–260

Kleiber M (1975) The Fire of Life: an introduction to animal energetics. RE Kreiger Publishing Co, Huntington, NY

Knowlton AR, Kraus SD, Kenney RD (1994) Reproduction in North Atlantic right whales (*Eubalaena glacialis*). Can J Zool 72:1297–1305

Kooyman GL (1989) Diverse divers: physiology and behavior. Springer-Verlag, Berlin

Kooyman GL, Kerem DH, Campbell WB, Wright JJ (1973) Pulmonary gas exchange in freely diving Weddell seals. Respir Physiol 17:283–290

Kooyman GL, Wahrenbrock EA, Castellini MA, Davis RW, Sinnett EE (1980) Aerobic and anaerobic metabolism during voluntary diving in Weddell seals: evidence of preferred pathways from blood chemistry and behavior. J Comp Physiol B 138:335–346

Kooyman GL, Castellini MA, Davis RW, Maue RA (1983) Aerobic diving limits of immature Weddell seals. J Comp Physiol B 151:171–174

Kraus SD, Hamilton PK, Kenney RD, Knowlton AR, Slay CK (2001) Reproductive parameters of the North Atlantic right whale. J Cetacean Res Manage Spec Issue 2: 231–326

Lockyer C (1981) Growth and energy budgets of large baleen whales from the Southern Hemisphere. In: FAO Advisory Committee on Marine Resource Research, Mammals in the sea, Vol III. General papers and large cetaceans. FAO, Rome, p 379–487

Mayo CA, Marx MK (1990) Surface foraging behavior of the North Atlantic right whale, *Eubalaena glacialis*, and associated zooplankton characteristics. Can J Zool 68: 2214–2220

Mayo CA, Letcher BH, Scott S (2001) Zooplankton filtering efficiency of the baleen of a North Atlantic right whale, *Eubalaena glacialis*. J Cetacean Res Manage Spec Issue 2: 225–229

Miller CB, Cowles TJ, Wiebe PH, Copley NJ, Grigg H (1991) Phenology in *Calanus finmarchicus*: hypotheses about control mechanisms. Mar Ecol Prog Ser 72:79–91

Murison LD, Gaskin GE (1989) The distribution of right whales and zooplankton in the Bay of Fundy, Canada. Can J Zool 67:1411–1420

Nowacek DP, Johnson MP, Tyack PL, Shorter KA, McLellan WA, Pabst DA (2001) Buoyant balaenids: the ups and downs of buoyancy in right whales. Proc R Soc Lond B 268: 1811–1816

Payne PM, Wiley DN, Young SB, Pittman S, Clapham PJ, Jossi JW (1990) Recent fluctuations in the abundance of baleen whales in the southern Gulf of Maine in relation to changes in selected prey. Fish Bull 88:687–696

Rowntree VJ (1996) Feeding, distribution, and reproductive behavior of cyamids (Crustacea: Amphipoda) living on humpback and right whales. Can J Zool 74:103–109

Sameoto DD, Herman AW (1990) Life cycle and distribution of *Calanus finmarchicus* in deep basins on the Nova Scotia shelf and seasonal changes in *Calanus* spp. Mar Ecol Prog Ser 66:225–237

Stone GS, Kraus SD, Prescott JH, Hazard KW (1988) Significant aggregations of the endangered right whale, *Eubalaena glacialis*, on the continental shelf of Nova Scotia. Can Field-Nat 102:471–474

Watkins WA, Schevill WE (1976) Right whale feeding and baleen rattle. J Mammal 57:58–66

Wishner K, Durbin E, Durbin A, Macaulay M, Winn H, Kenney R (1988) Copepod patches and right whales in the Great South Channel off New England. Bull Mar Sci 43: 825–844

Wishner KF, Schoenherr JR, Beardsley R, Chen C (1995) Abundance, distribution and population structure of the copepod *Calanus finmarchicus* in a springtime right whale feeding area in the southwestern Gulf of Maine. Cont Shelf Res 15:475–507

Woodley TH, Gaskin DE (1996) Environmental characteristics of North Atlantic right and fin whale habitat in the lower Bay of Fundy, Canada. Can J Zool 74:75–84

MARINE ECOLOGY
PROGRESS SERIES

Reprint

North Atlantic right whale habitat in the lower Bay of Fundy and on the SW Scotian Shelf during 1999–2001

Mark F. Baumgartner[1,4,*], Tim V. N. Cole[2], Phillip J. Clapham[2], Bruce R. Mate[3]

[1]College of Oceanic and Atmospheric Sciences, Oregon State University, 104 Ocean Administration Building, Corvallis, Oregon 97331, USA

[2]National Marine Fisheries Service, Northeast Fisheries Science Center, 166 Water Street, Woods Hole, Massachusetts 02543, USA

[3]Coastal Oregon Marine Experiment Station, Hatfield Marine Science Center, Oregon State University, Newport, Oregon 97365, USA

[4]*Present address:* Biology Department, MS #33, Woods Hole Oceanographic Institution, Woods Hole, Massachusetts 02543, USA

ABSTRACT: Simultaneous visual and oceanographic surveys were conducted in the lower Bay of Fundy and in Roseway Basin of the SW Scotian Shelf during the summers of 1999 to 2001 to investigate the physical and biological oceanographic factors associated with North Atlantic right whale occurrence. Sightings of right whales were recorded along predetermined transects through each region, while both *in situ* and remotely sensed oceanographic measurements were collected. Sampling with plankton nets and an optical plankton counter confirmed that right whales in these regions feed on *Calanus finmarchicus* copepodite stage 5 (C5). Spatial variability in right whale occurrence was associated with water depth and the depth of the bottom mixed layer. *C. finmarchicus* C5 aggregated over the deepest water depths in both regions, and within these areas, right whales occurred where the bottom mixed layer forced discrete layers of *C. finmarchicus* C5 to occur shallower in the water column (allowing more efficient foraging). Annual increases in right whale occurrence appeared to be associated with decreases in sea surface temperature (SST) in both regions; however, this observation merits caution in light of the short duration of the study (3 yr). There was also evidence to suggest that both spatial and interannual variability in right whale occurrence in Roseway Basin may be associated with SST gradient, a proxy for ocean fronts.

KEY WORDS: *Eubalaena glacialis* · Distribution · Habitat · *Calanus finmarchicus* · Fronts · Gulf of Maine · Roseway Basin · AVHRR · SeaWiFS · Optical plankton counter

INTRODUCTION

Despite protection from hunting since the mid 1930s, the North Atlantic right whale *Eubalaena glacialis* remains one of the most endangered species of large whales (Clapham et al. 1999). Mortality from fishing gear entanglement and collisions with ships is of great concern (Kraus 1990, Kenney & Kraus 1993, Knowlton & Kraus 2001) and conservation efforts may be improved with the protection of right whale habitat. However, our understanding of what constitutes right

whale habitat is quite poor. Many studies have indicated that the presence of large aggregations of the right whale's primary prey, older stages of the calanoid copepod *Calanus finmarchicus*, is probably the single most important component of right whale habitat (Watkins & Schevill 1976, Wishner et al. 1988, 1995, Murison & Gaskin 1989, Mayo & Marx 1990, Beardsley et al. 1996, Woodley & Gaskin 1996, Kenney 2001). However, the physical and biological oceanographic features or conditions that promote high abundance and discrete aggregation of this prey over time and space

are not well understood, nor are the means by which right whales locate and exploit these food resources.

North Atlantic right whales occur in Cape Cod and Massachusetts Bays in the late winter and early spring, where they primarily feed on *Calanus finmarchicus*, but have also been observed feeding on *Pseudocalanus* spp., *Centropages* spp., barnacle larvae and euphausiids (Watkins & Schevill 1976, Mayo & Marx 1990). By mid-spring, right whales are typically found in the Great South Channel (Kenney et al. 1995). Here again, they primarily feed on older copepodite stages of *C. finmarchicus* (Wishner et al. 1988, 1995). In the later summer, right whales occupy the lower Bay of Fundy (Kraus et al. 1982) or the southwestern Scotian Shelf (Mitchell et al. 1986). Murison & Gaskin (1989) and Woodley & Gaskin (1996) concluded that the primary prey of right whales in the lower Bay of Fundy was *C. finmarchicus*, and Stone et al. (1988) observed *C. finmarchicus* mandibles in right whale feces collected in Roseway Basin on the southwestern Scotian Shelf. By late fall, right whales abandon the lower Bay of Fundy and, while some animals migrate southward to the only known calving grounds on the coast of the southeastern United States, the whereabouts of the rest of the population in late fall and early winter are currently unknown. Although these seasonal movements between high-use areas have been well documented for some time (CETAP 1982, Winn et al. 1986), recent data acquired from whales outfitted with satellite-monitored radio tags suggest that interregional movements on much shorter time scales are quite common (Mate et al. 1997). Alterations in the seasonal distribution of right whales have also been observed in some years (Payne et al. 1990, Kenney 2001), and there is evidence of other potential high-use areas (Weinrich et al. 2000).

Our study focused on the ecological relationship between right whale occurrence and several biological and physical oceanographic factors in the lower Bay of Fundy and in Roseway Basin on the southwestern Scotian Shelf during the summers of 1999 to 2001. We collected and examined data from visual surveys and from both *in situ* and satellite-borne oceanographic instrumentation to characterize right whale habitat features. We paid particular attention to the occurrence of right whales and the abundance and distribution of the most lipid-rich stage of their prey, *Calanus finmarchicus* copepodite stage 5 (C5), to identify relationships linking the physical environment, *C. finmarchicus* and right whales. These relationships were examined separately over space and time to determine the factors that influence right whale occurrence. Based on these findings, we hope to provide a scientific foundation upon which right whale distribution can be predictively modeled for conservation purposes.

MATERIALS AND METHODS

Data collection and processing. Simultaneous visual and oceanographic surveys were conducted in the lower Bay of Fundy and Roseway Basin during the summers of 1999, 2000 and 2001. North-south (Bay of Fundy) and east-west (Roseway Basin) transects were visually surveyed through a grid of oceanographic stations (Fig. 1). A single survey unit consisted of a 9.3 km (5 nautical miles [n miles]) transect section centered on an oceanographic station. The survey unit length was selected as the approximate scale of horizontal variability in hydrographic properties observed on the Scotian Shelf by Herman et al. (1991). The width of the survey unit was estimated from the maximum distance perpendicular to the trackline at which a right whale was detected during the surveys. This distance was approximately 4.6 km (2.5 n miles), so a single survey unit was defined as a 9.3 × 9.3 km (5 × 5 n miles) area centered on an oceanographic station. Surveys were conducted during cruises designed to accommodate several research objectives, so not all survey units were sampled each year. After 1999 in the lower Bay of Fundy, the present study competed with research objectives that required fair weather conditions and calm seas, so surveys were typically conducted in slightly higher sea states (Beaufort scale 2–5). Each region (lower Bay of Fundy and Roseway Basin) was sampled once per summer except in 2000 when the lower Bay of Fundy was sampled twice (Fig. 2).

Visual surveys were conducted from the flying bridge of NOAA Ship 'Delaware II'. Two observers used mounted, 25×150, 'big eye' binoculars to scan from roughly –90 to +90° relative to the bow while a third observer scanned with hand-held binoculars or with the naked eye. Sightings of marine mammals were recorded by this third observer using a hand-held data-entry system. The date, time, species, number of individuals and the distance and relative bearing to the animal or animals were logged for each encounter. The location of each sighting was later computed along a rhumb line using the observer's bearing and distance estimates and the ship's simultaneous GPS and gyro compass measurement. Sighting conditions, including sea state, glare magnitude and direction, visibility and swell height, were also recorded during the surveys, using either paper forms or the hand-held data-entry system. Visual effort was conducted only while steaming along a transect and not while on station. Ship speed during surveys was nominally 18.5 km h^{-1} (10 knots).

An instrument package, consisting of a Seabird model SBE19 conductivity-temperature-depth instrument (CTD) and a Focal Technologies model OPC-1T optical plankton counter (OPC), was deployed in a
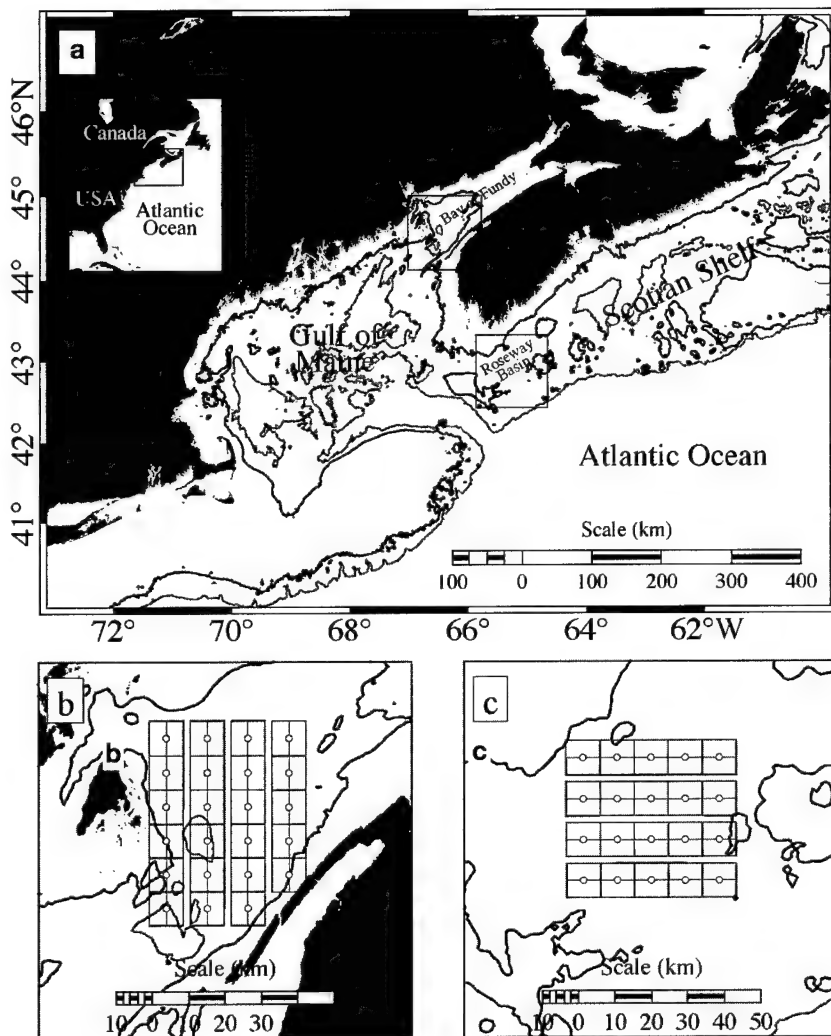
Fig. 1. (a) Location of study areas in the lower Bay of Fundy and Roseway Basin. Survey transects (black lines), oceanographic stations (o) and survey units (gray boxes) in (b) the lower Bay of Fundy and (c) Roseway Basin. 91 m (50 fathom) and 200 m isobaths are shown

vertical cast at each station. The CTD provided vertical profiles of temperature and salinity while the OPC (Herman 1988, 1992) recorded the vertical distribution of particles between 0.25 and 20 mm in size. The vertical distribution of *Calanus finmarchicus* C5 was estimated from the OPC data in 4 m depth strata using the calibration equation developed by Baumgartner (2003) from comparisons between collocated OPC casts and net samples collected during these same cruises.

Concurrent, high resolution, remotely sensed data were also collected from an advanced, very high resolution radiometer (AVHRR) and the sea-viewing, wide field-of-view sensor (SeaWiFS) and processed into sea surface temperature (SST) and surface chlorophyll, respectively. The AVHRR data were processed and archived at the University of Rhode Island (Cornillon et al. 1987) while the SeaWiFS data were processed using the SeaDAS software package (version 4.0). Synoptic images from both sensors were transformed to an equidistant, cylindrical projection (i.e. linear latitude/longitude) at a nominal resolution of 1.1 × 1.1 km and manually co-registered with a digital coastline. Horizontal gradients of both sea surface temperature and surface chlorophyll were computed using a 3 × 3 pixel Sobel gradient operator (Russ 1995). A single, cloud-free, remotely-sensed image within ±3 d of a survey day was selected and the corresponding SST or surface chlorophyll as well as its respec-
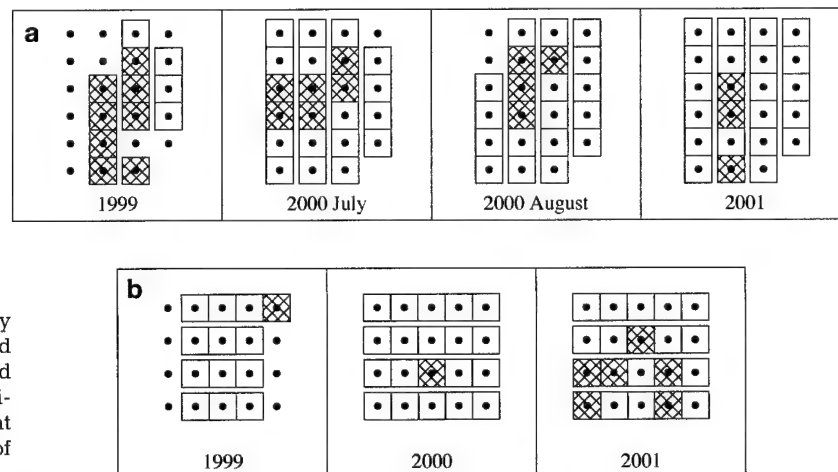

Fig. 2. *Eubalaena glacialis*. Visual survey results for (a) the lower Bay of Fundy and (b) Roseway Basin. Station plan (●) and completed survey units (boxes) are indicated. Survey units with 1 or more right whales sighted are cross-hatched. Dates of surveys are provided in Table 2

tive horizontal gradient magnitude were averaged over each 9.3 × 9.3 km unit surveyed on that day. The median time between midday on a survey day and the corresponding satellite overpass was 0.95 and 1.2 d for AVHRR and SeaWiFS images, respectively. Although higher frequency variability in SST and surface chlorophyll is expected within the ±3 d temporal window (e.g. diurnal warming, tidal excursion of fronts), spatial and interannual variability in these properties at the scales examined here should be much larger in magnitude. Therefore, the ±3 d temporal window is considered appropriate.

Zooplankton samples were obtained periodically in the lower Bay of Fundy and Roseway Basin both in the presence (within a few hundred meters) and absence of right whales. Depth integrated samples were collected with a 61 cm diameter bongo frame equipped with 333 µm mesh nets and 2 General Oceanics digital flowmeters. In the lower Bay of Fundy during 2001, depth-stratified samples were also obtained using a multiple opening-closing net and environmental sensing system (MOCNESS; Wiebe et al. 1976, 1985) equipped with 150 µm mesh nets. Zooplankton sampling was conducted in all years from NOAA Ship 'Delaware II' and additional sampling was conducted from NOAA Ship 'Albatross IV' in 2001. Samples were preserved immediately after collection in a borate-buffered, 5% formalin-seawater solution. Subsamples containing approximately 100 or more of the most abundant species were drawn with a Hensen-stemple pipette and all organisms in each subsample were identified and enumerated to the lowest taxon possible. Abundance estimates of *Calanus finmarchicus* C5 from the nets were compared to OPC-derived

abundances observed in survey units with and without right whales, as well as to OPC-derived abundances observed near right whales (<300 m away) tagged with time-depth recorders (data from Baumgartner & Mate 2003 this issue).

Environmental variables. Right whale occurrence was investigated with respect to 16 environmental variables (Table 1). Water depth was measured at each oceanographic station with a Simrad model EK500 scientific echosounder. A 1.1 × 1.1 km resolution digital bathymetric dataset was compiled from a variety of sounding and gridded bathymetric sources (e.g. National Ocean Service soundings, 2 × 2 min topographic data [Smith & Sandwell 1997], ETOPO5 gridded bathymetry [NGDC 1988]) and depth gradient magnitude was computed from this dataset using the same 3 × 3 pixel Sobel gradient operator used for the AVHRR and SeaWiFS data. Both depth and depth gradient are important habitat descriptors for a variety of cetacean species (Hui 1979, 1985, CETAP 1982, Selzer & Payne 1988, Baumgartner 1997, Baumgartner et al. 2001).

Murison & Gaskin (1989) and Woodley & Gaskin (1996) suggested that right whales in the lower Bay of Fundy occupy waters with high surface stratification. Accordingly, changes in both density and temperature over the upper 50 m of the water column were extracted from the CTD data and analyzed. Baumgartner & Mate (2003) reported that right whales equipped with archival tags foraged just above the bottom mixed layer (BML) in the lower Bay of Fundy and Roseway Basin. Therefore, BML properties were derived from the CTD data and included in the analysis. BML depth was defined as the deepest depth at

Table 1. Environmental variables used in the habitat analyses. BML: bottom mixed layer; SST: sea surface temperature; CTD: conductivity-temperature-depth instrument; OPC: optical plankton counter; AVHRR: advanced, very high resolution radiometer; SeaWiFS: sea-viewing, wide field-of-view sensor

Variable	Source	Units
Depth	Ship echosounder	m
Depth gradient	Digital bathymetry	m km^{-1}
Surface stratification (density)	CTD	kg m^{-3} (50 m)$^{-1}$
Surface stratification (temperature)	CTD	°C (50 m)$^{-1}$
BML temperature	CTD	°C
BML salinity	CTD	PSU
BML density (sigma-t)	CTD	sigma-t units (kg m^{-3})
BML depth	CTD	m
Depth of peak *Calanus finmarchicus* C5 abundance	OPC	m
Peak *C. finmarchicus* C5 abundance	OPC	copepods m^{-3}
Average water column *C. finmarchicus* C5 abundance	OPC	copepods m^{-3}
C. finmarchicus C5 abundance above BML	OPC	copepods m^{-3}
SST	AVHRR	°C
SST gradient	AVHRR	°C km^{-1}
Surface chlorophyll	SeaWiFS	mg m^{-3}
Surface chlorophyll gradient	SeaWiFS	mg m^{-3} km^{-1}

which the density differed from the bottom density by 0.05 kg m^{-3}. Since the BML is uniformly mixed, the temperature, salinity and density measured near the sea floor were considered to be representative of the BML hydrographic properties.

The depth of right whale feeding dives is strongly correlated with the depth of the maximum *Calanus finmarchicus* C5 abundance (Baumgartner & Mate 2003), so this variable was computed from the OPC data and included in the analysis. Several measures of *C. finmarchicus* C5 abundance were also derived from the OPC, including the maximum *C. finmarchicus* C5 abundance observed in the water column, the average water column abundance and the abundance of *C. finmarchicus* C5 above the BML. The latter was computed over a depth stratum spanning 20 m above to 5 m below the BML depth. All abundances of *C. finmarchicus* C5 (x) were transformed as $\log_{10}(x+1)$ prior to analysis.

Remotely sensed SST and surface chlorophyll concentration were examined both for their capacity to represent relevant oceanographic features and for their potential as easily acquired, synoptic datasets upon which predictive models of right whale distribution may be based. High horizontal SST and surface chlorophyll gradients can indicate the presence of ocean fronts, so derived gradient data were included in the analysis to assess whether right whales utilize ocean fronts as habitat, as suggested by Gaskin (1987).

Logistic regression. Since adjacent right whale sightings collected during the systematic surveys were not always expected to be independent of one another, associations between right whale presence and the environmental variables were investigated using logistic regression analysis. The response variable for each survey unit was coded as 1 if one or more right whales were sighted in that unit and 0 if no right whales were sighted (Fig. 2). The log-transformed odds in favor of sighting a right whale in a survey unit (η), also known as the logit of the sighting probability (π), was then modeled as a linear function of the independent variables (V_i) as follows

$$\eta = \text{logit}(\pi) = \ln\left(\frac{\pi}{1-\pi}\right) = \beta_0 + \sum_{i=1}^{p} \beta_i V_i \qquad (1)$$

where β_0 is the intercept, β_i represents the model coefficients and p is the number of independent variables in the model. The significance of model terms were assessed using drop-in-deviance (likelihood ratio) statistics (D) generated from the fitted model and a reduced model that lacked the term or terms of interest. Wald-based z-tests can also be used to assess the significance of individual model terms, but these tests are not considered as accurate as the drop-in-deviance test (Ramsey & Schafer 1997, Hosmer & Lemeshow

2000). However, Wald-based z-tests were conducted when a drop-in-deviance test was inappropriate or to supplement the drop-in-deviance test results. Wald-based 95% confidence intervals (CI) are also reported.

Logistic regression assumes a linear relationship between logits and the independent variables, and this assumption was checked by replacing an environmental variable in a model with a 4-level factor representing 4 levels of the environmental variable's values. The model coefficients for the corresponding dummy variables (including 0 for the reference level) were plotted against the mid-point of the ranges represented by each of the 4 factor levels. There was little evidence of curvature in these plots, and for many variables (including all of the variables found to be significant in the analyses below), the relationship between sighting logits and the environmental variables was clearly linear. Thus, the assumption of linearity for this study was appropriate.

Analysis of sighting conditions. The probability of sighting a right whale is influenced by factors that may prevent a whale from being observed from the survey platform. These factors or sighting conditions include the sea state, atmospheric conditions affecting visibility (e.g. haze, fog) or reflection of the sunshine off the sea surface (i.e. glare). The effect of sighting conditions on sighting probabilities was examined with a logistic regression model that included sea state, visibility and glare fraction as independent variables. Sea state was assessed on the Beaufort scale; visibility was estimated as the maximum distance at which a large object at the sea surface could be seen and the glare fraction was defined as the proportion of the area scanned from −90 to 90° relative to the bow that was obscured by glare.

Analysis of spatial variability. Associations between the spatial distribution of right whales and the environmental variables within each region were examined using logistic regression models that included terms to account for the sighting conditions and regional and annual variability in both sighting probabilities and environmental conditions. To account for regional variability, a single dummy variable representing the region was included in the model to account for regional differences in sighting probabilities, and a regional anomaly of an environmental variable was included to account for regional differences in that variable. In the case of SST, for example, the resulting model would be of the following form:

$$\text{logit}(\pi) = \beta_0 + \beta_1(\text{BOF}) + \beta_2(\text{SST regional anomaly}) \qquad (2)$$

where BOF is a dummy variable with values indicating the lower Bay of Fundy (BOF = 1) or Roseway Basin (BOF = 0) and the SST anomalies for a particular region were computed by subtracting the regional mean SST

from all SST observations in that region. The coefficient β_2 in this model indicates the nature of the relationship between local spatial variability in right whale sighting probability and local spatial variability in SST.

However, interannual variability in both sighting probability and SST can confound the results obtained with the model in Eq. (2). To account for this source of variability, dummy variables representing year were included in the model to account for annual differences in sighting probabilities, and SST anomalies were determined by subtracting the mean SST over a region in a particular year from the observations in that region and year. The resulting model was of the following form:

$$\text{logit}(\pi) = \beta_0 + \beta_1(\text{BOF}) + \beta_2(\text{Y2000}) + \beta_3(\text{Y2001}) + \quad (3)$$
$$\beta_4(\text{BOF} \times \text{Y2000}) + \beta_5(\text{BOF} \times \text{Y2001}) +$$
$$\beta_6(\text{SST regional/annual anomaly})$$

where Y2000 and Y2001 are dummy variables indicating the years 1999 (Y2000 = 0, Y2001 = 0), 2000 (Y2000 = 1, Y2001 = 0) and 2001 (Y2000 = 0, Y2001 = 1). As above, the coefficient β_6 in this model indicates the nature of the relationship between local spatial variability in right whale sighting probability and local spatial variability in SST where 'local' now refers to both space (within region) and time (within year). Models of the form in Eq. (3) were fitted for each of the environmental variables. Additional terms to account for variations in sighting probabilities due to sighting conditions were included when warranted.

Finally, it is possible that the nature of the relationship between local spatial variability in sighting probability and an environmental variable may differ between regions. For example, right whale sighting probability may increase with SST in the lower Bay of Fundy, but may decrease with SST in Roseway Basin. To detect this situation, a model including an interaction term for the region and the environmental variable was fitted. This model is of the form:

$$\text{logit}(\pi) = \beta_0 + \beta_1(\text{BOF}) + \beta_2(\text{Y2000}) + \beta_3(\text{Y2001}) + \quad (4)$$
$$\beta_4(\text{BOF} \times \text{Y2000}) + \beta_5(\text{BOF} \times \text{Y2001}) +$$
$$\beta_6(\text{SST regional/annual anomaly}) +$$
$$\beta_7(\text{BOF} \times \text{SST regional/annual anomaly})$$

A significant drop-in-deviance test of the interaction term (the term involving β_7) provides evidence of an inter-regional difference in the association between sighting probability and SST. The sum of β_6 and β_7 indicates the nature of the relationship between sighting probability and SST in the lower Bay of Fundy (BOF = 1) whereas β_6 alone indicates the nature of this relationship in Roseway Basin (BOF = 0).

Overfitting is a major concern when applying logistic regression models to data containing rare events. Hosmer & Lemeshow (2000) informally suggest that there should be at least 10 events per model parameter (in this study, an event is a survey unit with one or more right whales sighted). The model described in Eq. (3) contains 7 parameters and would therefore require at least 70 survey units with right whale sightings to satisfy these conditions. We observed only 29 units with right whales present. To investigate the effect of this low number of events, the models of the form in equation 3 were refitted without accounting for regional or interannual variability in sighting probabilities. These parsimonious models were of the following form (shown for SST and excluding terms to account for sighting conditions):

$$\text{logit}(\pi) = \beta_0 + \beta_1(\text{SST regional/annual anomaly}) \quad (5)$$

The resulting coefficients and drop-in-deviance tests from these models were compared to the corresponding models of the form in Eq. (3). Substantial differences in these coefficients and test results would indicate overfitting is a concern.

Analysis of interannual variability. Logistic regression was also used to investigate the environmental factors associated with interannual variability in sighting probabilities. However, since this study consists of only 3 yr of data, we consider any such associations to represent tentative trends only. The regression analysis was confined to survey units in which interannual variability actually occurred (i.e. survey units in which no right whales were ever encountered and survey units in which right whales were encountered in every year of the study were excluded). Data from the lower Bay of Fundy for this analysis consisted of surveys in August of 1999, 2000 and 2001 only (i.e. the July 2000 survey was excluded). It is impossible to account for spatial variability in the sighting probabilities in a similar manner as the interannual variability in sighting probabilities was taken into account in the analysis of spatial distribution described above. However, limiting the analysis to only those survey units in which interannual variability occurred reduces the confounding due to this source of variability. Spatial variability in the environmental variables was taken into account by using temporal anomalies as independent variables in the models. These anomalies were determined by subtracting the 3 yr mean of an environmental variable within a single survey unit from each of the observations in that survey unit. The resulting logistic regression model took the following form (excluding terms to account for sighting conditions):

$$\text{logit}(\pi) = \beta_0 + \beta_1(V_\text{T}) \quad (6)$$

where V_T denotes the temporal anomaly of an environmental variable and β_1 indicates the nature of the association between the interannual variability in sighting probabilities and the interannual variability in the environmental variable of interest. Inter-regional differ-

ences in the association between sighting probability and the environmental variables were also investigated using the following model (excluding terms to account for sighting conditions):

$$\text{logit}(\pi) = \beta_0 + \beta_1(V_T) + \beta_2(\text{BOF}) + \beta_3(\text{BOF} \times V_T) \qquad (7)$$

A drop-in-deviance statistic was computed from a reduced model that lacked the last 2 terms in Eq. (7). A significant drop-in-deviance statistic suggested that the association between sighting probability and V_T was different between the lower Bay of Fundy and Roseway Basin.

RESULTS

Zooplankton sampling

Calanus finmarchicus C5 dominated the zooplankton community near right whales. The proportion of *C. finmarchicus* C5 to all copepods was significantly higher in samples collected near right whales than in samples collected in the absence of right whales (333 µm mesh bongo tows only, 2-sample *t*-test after arcsine transformation, $t = 4.21$, p = 0.0003). No other copepod species or copepodite stage of *C. finmarchicus* exhibited a similar dominance. The percent composition of *C. finmarchicus* C5 averaged 67 % near right whales (n = 12) and ranged as high as 92 % in the lower Bay of Fundy, whereas the percent composition of *C. finmarchicus* C5 collected in the absence of right whales averaged only

26 % (n = 14). The abundance of *C. finmarchicus* C5 was also significantly higher in samples collected near right whales than in samples collected in the absence of right whales (333 µm mesh bongo tows only, 2-sample *t*-test, $t = 6.29$, p < 0.0001). Only *C. finmarchicus* adults (p = 0.0034) and *Calanus glacialis* (p = 0.014) exhibited a similar significant trend in abundance, but *C. finmarchicus* C5 was an average 20 and 35 times more abundant than *C. finmarchicus* adults and *C. glacialis*, respectively, in samples collected near right whales.

Zooplankton sampling in the lower Bay of Fundy indicated that *Calanus finmarchicus* C5 average water column abundance near right whales decreased from 1145 copepods m^{-3} in 1999 (n = 7, SD = 322, 95 % CI: 848 – 1443) to 457 copepods m^{-3} in 2000 (n = 3, SD = 74, 95 % CI: 273 – 640) and 505 copepods m^{-3} in 2001 (n = 6, SD = 186, 95 % CI: 311 – 700) (Fig. 3). The respective 2.5- and 2.3-fold decreases in the average *C. finmarchicus* C5 abundance from 1999 to 2000 and from 1999 to 2001 in the lower Bay of Fundy were coincident with estimated 4.8-fold (95 % CI: 1.1 – 20) and 6.8-fold (95 % CI: 1.1 – 42) decreases in the odds of sighting a right whale in a lower Bay of Fundy survey unit over these same time periods. Although only 2 zooplankton samples were collected near right whales in Roseway Basin, the net samples and OPC data suggest that average water column abundance of *C. finmarchicus* C5 either near right whales or in survey units where whales were present increased from 1999 to 2001 (Fig. 3). Interestingly, the OPC-derived average water column abundance of *C. finmarchicus* C5 in survey
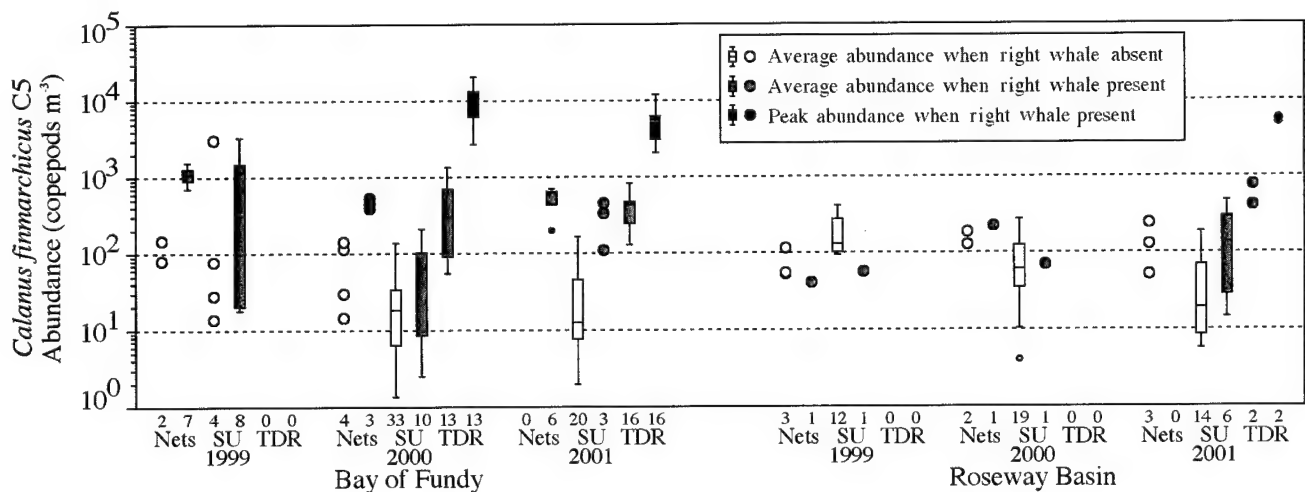

Fig. 3. *Eubalaena glacialis* and *Calanus finmarchicus*. Distribution of *C. finmarchicus* C5 abundance derived from zooplankton samples (Nets), optical plankton counter (OPC) casts conducted in the middle of each survey unit (SU) and OPC casts conducted near whales tagged with time-depth recorders (TDR) for each region and year. Average water column abundances in areas or survey units where right whales were absent or present are indicated as either boxplots (for n > 4) or large circles (for n ≤ 4). The peak water column abundance observed near tagged right whales is indicated as either black histograms or filled black circles (●). Sample sizes for each distribution are shown just below the lower *x* axis. Sample sizes for abundances associated with tagged whales indicate the number of tagged whales for which a single, average *C. finmarchicus* C5 abundance was computed. Data for tagged whales are from Baumgartner & Mate (2003)

units where right whales were absent actually decreased over this same time period (Fig. 3).

A spatial trend in OPC-derived *Calanus finmarchicus* C5 abundance in proximity to right whales is apparent during years when sample sizes were sufficient (2000 and 2001 in the lower Bay of Fundy and during 2001 in Roseway Basin). *C. finmarchicus* C5 abundance increased as the distance to a right whale decreased (i.e. from survey units with right whales absent to survey units with right whales present and finally to within a few hundred meters of a right whale) (Fig. 3). OPC casts conducted along the track of right whales that were tagged with time-depth recorders (Baumgartner & Mate 2003) indicated that average water column abundance of *C. finmarchicus* C5 was roughly an order of magnitude higher near right whales (<300 m away) than in areas where right whales were absent. Baumgartner & Mate (2003) found strong evidence to suggest that right whales feed at the depth of maximum *C. finmarchicus* C5 abundance. The abundance at this depth is at least an order of magnitude higher still than the average water column abundance of *C. finmarchicus* C5 observed near right whales. The net-derived abundances of *C. finmarchicus* C5 obtained near right whales in the lower Bay of Fundy during 2000 and 2001 corroborate the corresponding, but independent OPC-derived average water column abundances obtained near tagged whales (Fig. 3).

Sighting conditions

There was no evidence to suggest that the probability of sighting 1 or more right whales in a survey unit was associated with either visibility ($D = 1.91$, df = 1, p = 0.17) or glare fraction ($D = 0.293$, df = 1, p = 0.59). The potential impacts of both of these factors were largely controlled in the field by halting surveys when visibility was reduced to below 3.7 km (2 n miles) and by running survey transects in a direction opposite the sun when possible (i.e. to the west in the morning and to the east in the afternoon). There was, however, evidence to suggest an effect of sea state on the probability of sighting ($D = 6.166$, df = 1, p = 0.013), and the resulting logistic regression model indicated that the odds of sighting a right whale changed by a factor of 0.628 (95% CI: 0.428 – 0.921) for every unit increase in Beaufort sea state. Due to the significance of this effect, sea state was included in all subsequent logistic regression models.

Regional trends in sighting probabilities

Relative abundance and point estimates of sighting probability declined in the lower Bay of Fundy from 1999 to 2001, while relative abundance in Roseway Basin increased (Table 2). The odds of sighting a right whale decreased significantly from 1999 to 2000 in the lower Bay of Fundy (Wald-based *z*-test, p = 0.033), but there was no evidence of a change from 2000 to 2001 (p = 0.64). There was no evidence of a change in the odds of sighting a right whale from 1999 to 2000 in Roseway Basin (p = 0.31); however, these odds increased significantly from 2000 to 2001 (p = 0.037). There was no evidence that the odds of sighting a right whale were different in the lower Bay of Fundy and Roseway Basin in 1999 (Wald-based *z*-test, p = 0.093) or 2001 (p = 0.54), although the sample size in 1999 was small (Table 2). The odds of sighting a right whale in

Table 2. *Eubalaena glacialis*. Location and dates of surveys. Average sea state during each survey is reported on the Beaufort scale and relative abundance is reported as the number of right whales sighted per 10 km of transect searched. The probability of sighting at least 1 right whale in a survey unit and the corresponding 95% confidence interval (CI) were estimated after accounting for the effect of sea state. Note that the Bay of Fundy survey transects were searched twice during 2000

Location Year	Dates	Average sea state	No. units sampled	No. units with whales	Probability of sighting[a]	Wald's 95% CI[a]	Relative abundance
Bay of Fundy							
1999	19 Aug	2.2	12	8	0.58	0.28–0.83	5.2
2000	20–22 Jul, 20–23 Aug	3.0	43	10	0.22	0.12–0.37	1.9
2001	9–27 Aug	3.9	23	3	0.17	0.05–0.42	0.5
Roseway Basin							
1999	30–31 Aug	4.4	13	1	0.13	0.02–0.57	0.1
2000	23–26 Jul	2.0	20	1	0.03	0.00–0.20	0.5
2001	24–26 Jul	2.6	20	6	0.25	0.11–0.49	1.0

[a]Estimated from logistic regression models with a reference level corresponding to the region and year of interest and a 3.0 Beaufort sea state, e.g. the log-odds of the sighting probability for Roseway Basin in 2000 at a Beaufort sea state of 3.0 was estimated to be β_0 in the following model: $\text{logit}(\pi) = \beta_0 + \beta_1(\text{Sea state} - 3.0) + \beta_2(\text{BOF}) + \beta_3(\text{Y1999}) + \beta_4(\text{Y2001}) + \beta_5(\text{BOF} \times \text{Y1999}) + \beta_6(\text{BOF} \times \text{Y2001})$, where BOF is a dummy variable indicating region (lower Bay of Fundy, BOF = 1; Roseway Basin, BOF = 0), and Y1999 and Y2001 are dummy variables indicating the years 1999 and 2001, respectively

the Bay of Fundy were 9.44 (95% CI: 1.05 – 84.9) times higher than in Roseway Basin in 2000 (p = 0.045). These results support the use of dummy variables in the subsequent spatial models to account for interannual and inter-regional differences in sighting probabilities.

Spatial variability

There was strong evidence that within-region and within-year spatial variability in sighting probability was associated with spatial variability in depth, the depth of maximum *Calanus finmarchicus* C5 abundance, BML density, BML salinity, maximum water column *C. finmarchicus* C5 abundance, average water column abundance of *C. finmarchicus* C5, BML depth and the *C. finmarchicus* C5 abundance above the BML (Table 3). The most significant association detected was between sighting probability and depth (D = 19.54, df = 1, p < 0.0001). All of the other variables with which sighting probability was significantly associated

were correlated with depth (Table 3). There was also evidence of inter-regional differences in the association between sighting probability and BML temperature, SST gradient and surface chlorophyll gradient. Wald-based z-test results suggest right whale sighting probability decreased significantly with increasing BML temperature in the lower Bay of Fundy; however, this variable was also correlated with depth in this region (r = –0.549, p < 0.0001). The model that included depth as an independent variable (without a regional interaction term) indicated that the odds of sighting a right whale increased by a factor of 1.42 (95% CI: 1.19 – 1.69) for every 10 m increase in water depth.

Because of the apparent importance of water depth, a second group of models was investigated with depth as an additional independent variable (Table 4). Of the variables included in these models, only BML depth was found to be significant (D = 5.61, df = 1, p = 0.018). However, these results may be confounded by multi-collinearity owing to the strong correlation between depth and some of the other environmental variables

Table 3. *Eubalaena glacialis*. Test results for each environmental variable in the logistic regression analysis of spatial variability. Drop-in-deviance statistics (D), associated p-values (p) and the model coefficients (Coeff) are reported for models with and without an interaction term to account for inter-regional differences in the association between sighting probability and the environmental variable. Environmental variables were included in the models as anomalies from regional/annual means. Correlation coefficients reported for comparisons between regional/annual anomalies of depth and all other environmental variables. Prey abundance refers to that of *Calanus finmarchicus* C5. All drop-in-deviance statistics have 1 degree of freedom. p = 0.0000 indicates p < 0.00005 and p = 1.00 indicates p ≥ 0.995. Significance: *0.05 > p ≥ 0.01, **0.01 > p ≥ 0.001, ***p < 0.001. Abbreviations as in previous tables

Variable	Correlation with depth	Single variable model[a]			Model allowing inter-regional difference[b]			
		D	p	Coeff	D	p	Fundy Coeff	Roseway Coeff
Depth	–	19.54***	0.0000	0.0351	0.03	0.86		
Depth gradient	–0.280**	0.50	0.48	–0.0452	0.20	0.65		
Surface stratification (density)	–0.072	0.39	0.53	–0.396	0.22	0.64		
Surface stratification (temperature)	0.060	0.01	0.93	–0.0137	0.00	1.00		
BML temperature	–0.222*	1.59	0.21	–0.592	9.55**	0.0020	–4.00*	0.329
BML salinity	0.761***	12.99***	0.0003	3.57	0.37	0.54		
BML density	0.783***	14.96***	0.0001	4.71	0.01	0.93		
BML depth	0.868***	7.26**	0.0070	0.0219	0.01	0.94		
Depth of peak prey abundance	0.749***	15.54***	0.0001	0.0340	2.00	0.16		
Peak prey abundance	0.537***	11.58***	0.0007	1.65	1.37	0.24		
Average water column prey abundance	0.412***	8.01**	0.0047	1.21	0.00	0.97		
Prey abundance above BML	0.388***	3.97*	0.046	0.625	0.05	0.82		
SST	0.055	0.01	0.94	–0.0309	0.37	0.54		
SST gradient	–0.057	0.93	0.34	4.47	5.43*	0.020	–7.24	16.4*
Surface chlorophyll	–0.138	2.22	0.14	–0.660	3.66	0.056		
Surface chlorophyll gradient	–0.113	1.61	0.20	4.34	7.19**	0.0073	–6.16	56.3*

[a]Model (Eq. 3): logit(π) = β_0 + β_1(Sea state) + β_2(BOF) + β_3(Y2000) + β_4(Y2001) + β_5(BOF × Y2000) + β_6(BOF × Y2001) + β_7(Variable). Drop-in-deviance test (D, p) and estimated coefficient (Coeff) reported for the term involving β_7

[b]Model (Eq. 4): logit(π) = β_0 + β_1(Sea state) + β_2(BOF) + β_3(Y2000) + β_4(Y2001) + β_5(BOF × Y2000) + β_6(BOF × Y2001) + β_7(Variable) + β_8(BOF × Variable). Drop-in-deviance test (D, p) reported for the term involving β_8. Estimated coefficients (Coeff) are (β_7 + β_8) and β_7 for the lower Bay of Fundy and Roseway Basin, respectively. Only coefficients for models with a significant interaction term are shown. Wald-based significance of these coefficients indicated with asterisks

Table 4. *Eubalaena glacialis*. Test results for each environmental variable in the logistic regression analysis of spatial variability after accounting for the influence of depth on sighting probabilities. Because multicollinearity may be a problem for these analyses (Table 3), uncorrelated variables (principal components, PCs) were created from a PC analysis of depth and an environmental variable. Results are shown for models that use these PCs as independent variables. PC1 was always significant in these models (p < 0.001), so drop-in-deviance statistics are shown for PC2 only. Abbreviations as in previous tables; significance as in Table 3

Variable	Model including depth[a]			Model with PCs[b]	
	D	p	Coeff	D	p
Depth	–	–	–	–	–
Depth gradient	0.01	0.92	0.00867	0.01	0.91
Surface stratification (density)	0.01	0.94	−0.0575	0.01	0.94
Surface stratification (temperature)	0.00	0.97	0.00750	0.00	0.97
BML temperature	0.07	0.79	−0.162	0.07	0.79
BML salinity	0.01	0.91	0.184	0.01	0.91
BML density	0.08	0.77	0.654	0.08	0.77
BML depth	5.61*	0.018	−0.0413	10.99***	0.0009
Depth of peak prey abundance	1.21	0.27	0.0144	0.25	0.62
Peak prey abundance	1.93	0.16	0.847	1.93	0.16
Average water column prey abundance	0.99	0.32	0.501	0.98	0.32
Prey abundance above BML	0.18	0.67	0.153	0.18	0.67
SST	0.01	0.92	−0.0402	0.01	0.92
SST gradient	2.10	0.15	8.01	2.10	0.15
Surface chlorophyll	1.17	0.28	−0.518	1.17	0.28
Surface chlorophyll gradient	0.83	0.36	−3.51	0.83	0.36

[a]Model: $logit(\pi) = \beta_0 + \beta_1(Sea\ state) + \beta_2(BOF) + \beta_3(Y2000) + \beta_4(Y2001) + \beta_5(BOF \times Y2000) + \beta_6(BOF \times Y2001) + \beta_7(Depth) + \beta_8(Variable)$. Drop-in-deviance test (D, p) and estimated coefficient (Coeff) reported for the term involving β_8
[b]Model: $logit(\pi) = \beta_0 + \beta_1(Sea\ state) + \beta_2(BOF) + \beta_3(Y2000) + \beta_4(Y2001) + \beta_5(BOF \times Y2000) + \beta_6(BOF \times Y2001) + \beta_7(PC1) + \beta_8(PC2)$. Drop-in-deviance test (D, p) reported for the term involving β_8

Table 5. *Eubalaena glacialis*. Logistic regression model of spatial variability with depth and BML depth anomalies (n = 131 survey units, 29 units with right whales present). Residual deviance = 90.39 (df = 122), null deviance = 138.50 (df = 130) and overall drop-in-deviance = 48.11 (df = 8, p < 0.0001). Abbreviations as in previous tables; significance as in Table 3

Term	Coeff	SE	Wald z-statistic	p	Drop in deviance	df	p
Intercept	1.14	1.75	0.65	0.51			
Sea state	−0.871	0.330	−2.64**	0.0083	8.15**	1	0.0043
Region[a]					10.24*	3	0.017
BOF	1.70	1.46	1.17	0.24			
Year[a]					15.42**	4	0.0039
Y2000	−2.80	1.75	−1.60	0.11			
Y2001	−0.00422	1.36	0.00	1.00			
Region × Year					6.52*	2	0.038
BOF × Y2000	0.808	2.03	0.40	0.69			
BOF × Y2001	−2.53	1.89	−1.33	0.18			
Depth	0.0708	0.0193	3.67***	0.0002	17.88***	1	0.0000
BML depth	−0.0413	0.0179	−2.31*	0.021	5.61*	1	0.018

[a]Reduced models for Region and Year drop-in-deviance tests lack both main effects and interaction terms

(Table 3). Therefore, another set of models was examined where the 2 independent variables in a model were the 2 uncorrelated principal components (PC) from a principal components analysis of depth and an environmental variable (Table 4). The first PC was significant (p < 0.001) in all of these models, but the second PC was only significant in the model using principal components constructed from depth and BML depth (D = 10.99, df = 1, p = 0.0009). Since each of these analyses (using the raw environmental variables and using the PCs) yielded similar results (Table 4), we conclude that multi-collinearity was not problematic. The model with depth and BML depth as the independent variables (without the PC analysis) indicated that the odds of sighting a right whale increased by a factor of 1.51 (95% CI: 1.06 – 2.14) for every 10 m decrease in the BML depth after accounting for the effect of water depth (Table 5).

To verify that no other combination of variables produced a more significant model than the one reported in Table 5, models were constructed with sea state, dummy variables for region and year (with interactions) and all possible combinations of 1 or 2 environmental variables (n = 136 models). A reduced model with only sea state and dummy variables for region and year (with interactions) was used to generate drop-in-deviance statistics. The models with depth alone and both depth and BML depth were ranked well above all other models when ordered by the significance of the drop-in-deviance test. Parsimonious versions of the models shown in Tables 3 & 4 were fitted with only sea state and 1 or 2 of the environmental variables to investigate the potential effect of overfitting (see

Eq. 5). The coefficients and drop-in-deviance test results from these models were nearly identical to those shown in Tables 3 & 4. We are therefore confident that overfitting is not a concern in our analysis of spatial variability in right whale occurrence.

Interannual variability

Sighting probability in survey units in which interannual variability occurred was associated with interannual variability in surface density stratification and SST (Table 6). The logistic regression model for SST (Table 7) indicated that the odds of sighting a right whale in a survey unit increased by a factor of 3.19 (95% CI: 1.12 – 9.07) for every 1°C annual decrease in SST within that survey unit. Moreover, a value of 0.918 for this model's area under the receiver operating characteristic (ROC) curve indicated that SST discriminated very well between right whale presence and absence (an area under the ROC curve of 0.9 or greater is considered outstanding discrimination; Hosmer & Lemeshow 2000). Surface density stratification was included as an additional term in the model shown in Table 7, but the drop-in-deviance test for this term was not significant (D = 0.078, df = 1, p = 0.78). There was

no evidence, therefore, of an association between sighting probability and surface density stratification after accounting for SST. The models including regional interaction terms (Eq. 7) provided evidence of an inter-regional difference in the association of sighting probability with annual variation in BML salinity and SST gradient (Table 6). Although the odds of sighting a right whale in a Roseway Basin survey unit increased significantly (Wald-based z-test, p = 0.021) by a factor of 3.78 (95% CI: 1.22 – 11.68) for every 0.1 PSU annual decrease in BML salinity within that survey unit, there was no evidence to suggest that the odds of sighting a right whale in a lower Bay of Fundy survey unit changed with annual variation in BML salinity (p = 0.81). There was only suggestive, but inconclusive evidence of an association between the probability of sighting a right whale in a Roseway Basin survey unit and annual variation in SST gradient (Wald-based z-test, p = 0.068) and no evidence of a similar association in the lower Bay of Fundy (p = 0.56).

DISCUSSION

Our zooplankton and OPC sampling results corroborate the earlier results of Murison & Gaskin (1989),

Table 6. *Eubalaena glacialis*. Test results for each environmental variable in the logistic regression analysis of interannual variability. Drop-in-deviance statistics (D), associated p-values (p) and the model coefficients (Coeff) are reported for models with and without an interaction term to account for inter-regional differences in the association between sighting probability and the environmental variable. Environmental variables were included in the models as anomalies from within-survey-unit 3 yr means. Depth and depth gradient were excluded from this analysis since there is no interannual variability in these variables. Abbreviations as in previous tables; significance as in Table 3

Variable	Single variable model[a]			Model allowing inter-regional difference[b]			
	D	p	Coeff	D	p	Fundy Coeff	Roseway Coeff
Surface stratification (density)	5.53*	0.019	−4.33	1.33	0.51		
Surface stratification (temperature)	1.64	0.20	−0.630	3.69	0.16		
BML temperature	3.67	0.055	−1.02	4.03	0.13		
BML salinity	3.48	0.062	−5.67	6.46*	0.039	1.16	−13.3*
BML density	0.03	0.86	−1.27	4.29	0.12		
BML depth	0.31	0.58	0.0285	1.49	0.47		
Depth of peak prey abundance	0.02	0.89	0.00302	0.48	0.79		
Peak prey abundance	1.75	0.19	1.17	4.36	0.11		
Average water column prey abundance	2.05	0.15	1.06	2.45	0.29		
Prey abundance above BML	1.49	0.22	0.860	3.56	0.17		
SST	7.07**	0.0079	−1.16	3.29	0.19		
SST gradient	1.03	0.31	6.70	8.20*	0.017	−8.48	50.0
Surface chlorophyll	1.58	0.21	−0.866	4.82	0.090		
Surface chlorophyll gradient	1.68	0.20	−8.49	1.07	0.59		

[a]Model (Eq. 6): logit(π) = β_0 + β_1(Sea state) + β_2(Variable). Drop-in-deviance test (D, p) and estimated coefficient (Coeff) reported for the term involving β_2. Drop-in-deviance statistics have 1 df

[b]Model (Eq. 7): logit(π) = β_0 + β_1(Sea state) + β_2(Variable) + β_3(BOF) + β_4(BOF × Variable). Drop-in-deviance test (D, p) reported for terms involving β_3 and β_4. Drop-in-deviance statistics have 2 df. Estimated coefficients (Coeff) are (β_2 + β_4) and β_2 for the lower Bay of Fundy and Roseway Basin, respectively. Only coefficients for models with a significant drop-in-deviance statistic are shown. Wald-based significance of these coefficients indicated with asterisks

Table 7. *Eubalaena glacialis*. Logistic regression model of interannual variability with SST anomaly (n = 27 survey units, 10 units with right whales present). Residual deviance = 18.33 (df = 24), null deviance = 35.59 (df = 26) and overall drop-in-deviance = 17.26 (df = 2, p = 0.0002). Abbreviations as in previous tables; significance as in Table 3

Term	Coeff	SE	Wald z-statistic	p	Drop in deviance	df	p
Intercept	1.68	1.30	1.29	0.20			
Sea state	−0.928	0.508	−1.83	0.068	4.66*	1	0.031
SST	−1.16	0.533	−2.18*	0.030	7.07**	1	0.0079

Woodley & Gaskin (1996) and Stone et al. (1988), indicating that right whales feed on *Calanus finmarchicus* C5 in the lower Bay of Fundy and Roseway Basin. Younger stages of *C. finmarchicus* caught by the bongo nets (C3 and C4) did not exhibit similar trends in dominance or abundance as did *C. finmarchicus* C5 near right whales, and adult *C. finmarchicus* were always much less abundant than *C. finmarchicus* C5. The depth stratified samples, collected with the MOC-NESS in the lower Bay of Fundy during 2001, confirm the existence of deep layers of *C. finmarchicus* C5 observed by Murison & Gaskin (1989) and Baumgart-ner & Mate (2003). These layers are likely composed of animals in diapause because of their deep distribution, stage composition, empty guts, large oil sacs and low activity levels (Baumgartner et al. 2003 this issue). Similar discrete aggregations of *C. finmarchicus* C5 were observed near right whales in Roseway Basin during 2001 (Baumgartner & Mate 2003).

It is interesting, then, that the *Calanus finmarchicus* C5 abundance variables did not emerge as the most important factors in the analyses of either spatial or interannual variability in right whale occurrence. This is likely a consequence of the sampling methodology. The *C. finmarchicus* C5 abundance variables were derived from OPC casts conducted in the center of each survey unit. Since *C. finmarchicus* C5 average water column abundances for these casts were typically lower than those observed near tagged whales (Fig. 3), we infer that *C. finmarchicus* C5 abundance varied on short spatial scales (i.e. copepod patch sizes were small relative to the size of a survey unit). The spatial scales of variation for the physiographic and physical oceanographic variables were expected to be significantly larger. Therefore, the *C. finmarchicus* C5 abundance measured at the station in the center of a survey unit was not always representative of the abundance near right whales in that unit, whereas the corresponding physical observations at the station were probably representative of conditions over most of the survey unit. Since this less ecologically relevant

measurement of *C. finmarchicus* C5 abundance was included in the logistic regression analyses, the strength of the association between right whales and *C. finmarchicus* C5 abundance was probably obscured.

The correlation between average water column abundance of *Calanus finmarchicus* C5 and water depth suggests that the deepest parts of both Roseway Basin and Grand Manan Basin in the lower Bay of Fundy are sites of closed circulation that passively aggregate and retain diapausing *C. finmarchicus* C5. These deep regions thus provide the best foraging grounds within each region, which accounts for the higher probability of sighting right whales in deeper waters. Woodley & Gaskin (1996) also found that right whales utilize the deeper areas of the lower Bay of Fundy and invoked a similar explanation for the accumulation of *C. finmarchicus*. The baroclinic (density-driven) component of the flow in these basins can be estimated from the hydrographic data obtained in this study, but the residual barotropic or depth-independent flow (generated primarily by the tides and an important constituent of the mean currents in these regions) cannot be quantified easily using ship-based methods (Greenberg 1983). Hence, it is difficult to demonstrate that gyres existed in these basins during the study. The existence of a cyclonic gyre in Grand Manan Basin has been inferred, however, from both surface (Fish & Johnson 1937, Hachey & Bailey 1952 cited in Bumpus 1960, Godin 1968 cited in Greenberg 1983) and bottom (Lauzier 1967) observations and corroborated in ocean model studies (Lynch et al. 1996, Xue et al. 2000). Lynch et al. (1996) suggest that tidal rectification produces this gyre. We conducted an unintended drifter experiment in Grand Manan Basin during the summer of 2000 by failing to immediately recover an archival tag that had been attached to a right whale for a foraging ecology study (Baumgartner & Mate 2003). The tag was relocated via radio telemetry 6.5 d later and only 10.5 km away from its last known location (net speed = 1.9 cm s^{-1}). This fortunate recovery suggests that at least the surface circulation in Grand Manan Basin retains particles over weekly time scales. The importance of the barotropic component in the gyre suggests that this particle retention also occurs at depth (Greenberg 1983).

The probability of sighting a right whale was higher in waters with shallow BML depths after accounting for the effect of water depth on sighting probability. One possible explanation for this result is that a shallow BML depth promotes concentration of *Calanus finmarchicus* above it (Fig. 4b), whereas the vertical distribution of *C. finmarchicus* C5 above a deep BML is more uniform (Fig. 4a); these conditions may arise if *C. finmarchicus* C5 actively avoid the upper layers of the water column, perhaps due to increased illumination

Fig. 4. Prey availability scenario depicting (a) a deep bottom mixed layer (BML) depth without a discrete layer of *Calanus finmarchicus* C5 above the BML and (b) a shallow BML depth with a discrete layer above the BML. Horizontal lines indicate the sea surface, BML depth (dashed line), and sea floor (thick line). Vertical distribution of *C. finmarchicus* C5 is represented by dots
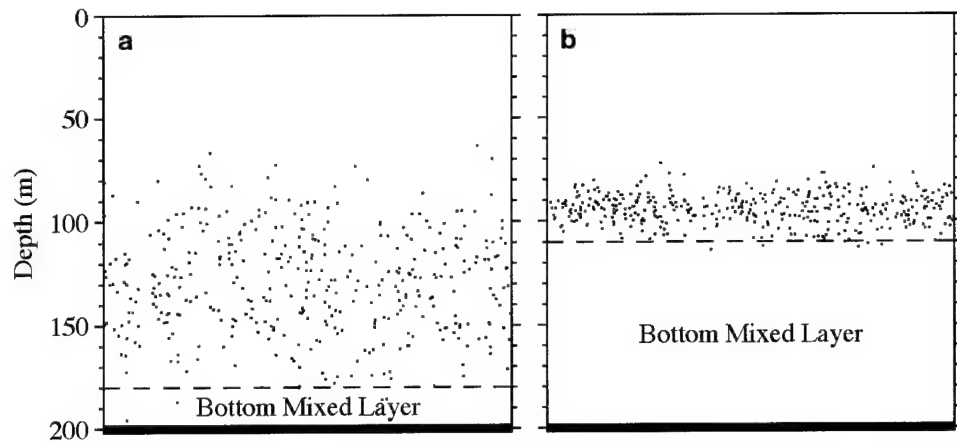
(and hence predation) or warmer temperatures. However, our observations suggest that this scenario does not occur. The abundance of *C. finmarchicus* C5 above the BML was *positively* correlated with BML depth (r = 0.345, p = 0.0001), which implies that *C. finmarchicus* C5 became more abundant or were more discretely concentrated as BML depth increased. A more plausible explanation, then, is that foraging on similar concentrations of *C. finmarchicus* C5 at shallow depths (Fig. 5b) rather than deep depths (Fig. 5a) affords a right whale more feeding time, and thus more energy can be acquired per dive for similar energy expenditure. For a constant total dive time, duration at depth can be extended by reducing transit times between the surface and the depth at which feeding occurs. This can be accomplished by increasing descent and ascent rates and by foraging at shallower depths. Baumgartner & Mate (2003) provide evidence of the former and the present study suggests the latter. Using the average dive duration (12.2 min), descent speed (1.40 m s^{-1}) and ascent speed (1.47 m s^{-1}) from Baumgartner & Mate (2003) and the observed range of BML depths for waters of approximately 200 m depth in this study, we predict that right whales could extend their

feeding time nearly 20% by foraging above a BML depth of 110 m (Fig. 5b) rather than foraging above a BML depth of 180 m (Fig. 5a).

Woodley & Gaskin (1996) reported higher surface temperatures in lower Bay of Fundy areas where right whales were present than in areas without them, but we found no evidence of this. Although Murison & Gaskin (1989) and Woodley & Gaskin (1996) state that right whales in the lower Bay of Fundy tend to frequent waters of high surface stratification, we found no evidence of this when measurements of surface stratification were made and the association was statistically tested.

Gaskin (1987) suggested that the transition zone between tidally mixed and thermally stratified areas is a feature of right whale habitat in the lower Bay of Fundy and on the Scotian Shelf. Despite some supportive anecdotal evidence from Murison & Gaskin (1989), neither they, Woodley & Gaskin (1996) nor we found any quantitative evidence to support an association between right whales and ocean fronts in the lower Bay of Fundy. However, we did find an association between spatial variability in right whale occurrence in Roseway Basin and the 2 proxies for ocean fronts:

Fig. 5. Prey availability scenario depicting (a) a deep BML depth with a discrete layer above the BML and (b) a shallow BML depth with a discrete layer above the BML. Stereotypical right whale dive profiles with a constant dive time are superimposed. Horizontal axis represents time for the dive profiles. Lines and dots as in Fig. 4
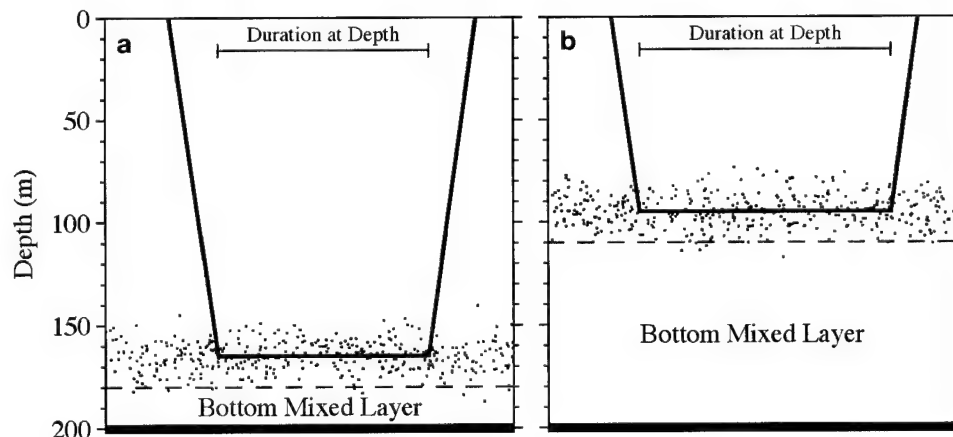
SST gradient and surface chlorophyll gradient. Furthermore, there was some indication that interannual variability in right whale occurrence in Roseway Basin might also be related to SST gradient (Table 6). As SST decreased in Roseway Basin from 1999 to 2001, the regional abundance of fronts increased (Fig. 6). These changes were accompanied by an increase in the occurrence of right whales in the survey region. At the
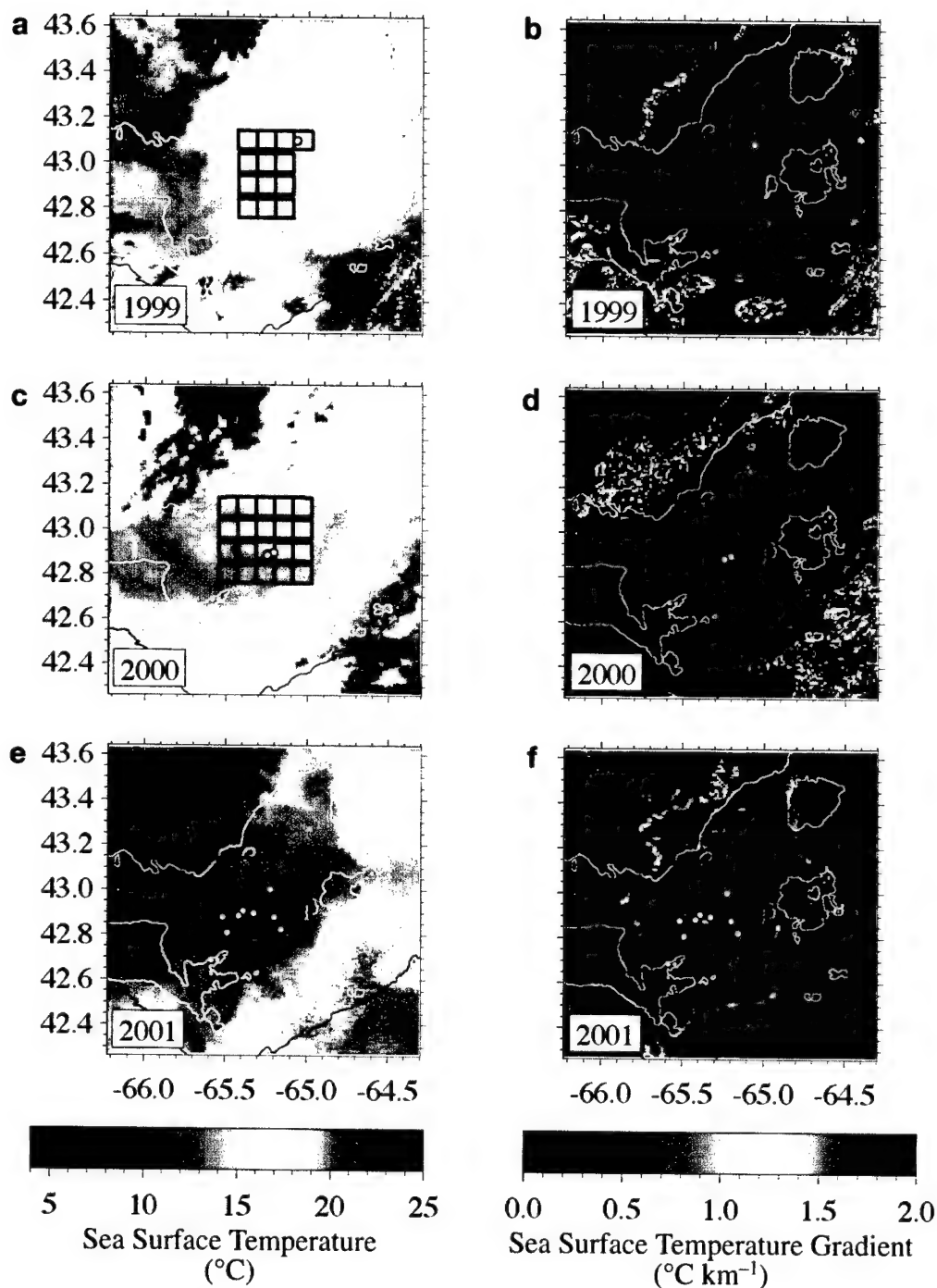

Fig. 6. *Eubalaena glacialis.* (a,c,e) Sea surface temperature and (b,d,f) corresponding SST gradient images associated with the (a,b) 1999, (c,d) 2000 and (e,f) 2001 Roseway Basin surveys. Completed survey units are indicated with boxes and right whale sightings are shown as white circles. Cloud contamination occurs as areas of locally colder temperatures and unrealistically high gradients in the southern and eastern portions of the 1999 images and in the NW (off Cape Sable) and SE portions of the 2000 images. The 2001 images are cloud-free

spatial scales investigated here, ocean fronts on the southwestern Scotian Shelf probably serve a similar aggregative role as closed circulation does in the lower Bay of Fundy. Both physics and animal behavior at a front can promote horizontal and vertical aggregation of *Calanus finmarchicus* (Olson & Backus 1985, Epstein & Beardsley 2001), which produce greater prey concentrations at the comparatively small spatial scales required by filter-feeding right whales.

An association between right whales and ocean fronts in the Great South Channel was reported by Brown & Winn (1989), but surface temperature gradients near the whales were low, and the animals occurred at a median distance of 11.4 km from the persistent front that occurs there in late spring. Brown & Winn (1989) found that right whales remained on the northern, stratified side of this front in a region characterized by warmer surface temperatures. These stratified conditions occur in deep water depths (>100 m) and are associated with cyclonic currents (Chen et al. 1995) that provide closed circulation in the central Great South Channel (the 'SCOPEX' gyre). Miller et al. (1998) suggest that late-stage *Calanus finmarchicus* from 2 separate generations accumulate in this gyre during the spring. The existence of 2 aggregative mechanisms in the Great South Channel, namely a persistent ocean front and closed circulation, may provide profitable foraging grounds for right whales in years of high *C. finmarchicus* productivity and survivorship.

Our analysis of interannual variability in right whale occurrence must be viewed with caution in light of the short duration of the study. Moreover, interannual variation for some environmental observations was not independent in adjacent survey units. For instance, observations of SST in all Roseway Basin survey units simultaneously decreased from 1999 to 2000 and again from 2000 to 2001 (Fig. 6). Nonetheless, the tentative trends identified here (i.e. increasing sighting probability with decreasing SST) seem consistent with conditions that promote increased abundance of *Calanus finmarchicus*. Interannual (Meise-Munns et al. 1990, Conversi et al. 2001) and spatial (Meise & O'Reilly 1996) variability in *C. finmarchicus* C5 abundance are negatively correlated with water temperature in the Gulf of Maine in the summer and fall. These relationships likely reflect more complex variability in factors that affect *C. finmarchicus* productivity at time scales of several years, such as wind mixing, surface stratification and phytoplankton production (Fromentin & Planque 1996, Conversi et al. 2001). Interannual and spatial variability in hydrographic conditions can potentially affect survivorship of *C. finmarchicus* as well. *C. finmarchicus* C5 are not thought to feed while in diapause (Hirche 1983, but see Durbin et al. 1995), but instead rely on their abundant oil reserves to survive throughout the summer and fall. Warmer temperatures increase the rate at which these oil reserves are metabolized and mortality occurs when reserves are depleted (Sameoto & Herman 1990).

Survival of *Calanus finmarchicus* C5 may also decrease in warmer temperatures due to an increase in predatory, warm-water gelatinous zooplankton. Hydrographic conditions in Roseway Basin changed markedly from warm, salty waters in 1999 (n = 13, average SST = 16.10°C, average BML temperature = 6.87°C, average BML salinity = 33.41 PSU) to cool, fresher waters in 2001 (n = 20, average SST = 11.76°C, average BML temperature = 4.64°C, average BML salinity = 33.06 PSU) (Fig. 6). Zooplankton samples from this region in 1999 contained high abundances of gelatinous zooplankton (n = 4), but none of these animals were found in samples collected in 2000 (n = 3) and 2001 (n = 3). Predation by gelatinous zooplankton may have reduced *C. finmarchicus* C5 abundance in Roseway Basin, making this region unsuitable for right whales in 1999. Alternatively, gelatinous animals may be a nuisance to right whales because these zooplankton can clog the whales' baleen. Mayo & Marx (1990) observed right whales 'flushing' their baleen in Cape Cod Bay, which probably functions to remove the viscous organic material and small particulates (including small zooplankton) that are abundant in these waters during spring. In contrast, we observed no flushing behavior in the lower Bay of Fundy, probably because right whales fed on *C. finmarchicus* C5 at depths where the concentration of suspended organic material and smaller zooplankton was very low. If the vertical distributions of *C. finmarchicus* C5 and predatory gelatinous zooplankton coincide in Roseway Basin, then the baleen of feeding right whales would be subject to clogging. The consequent reduction in filtering efficiency or the increase in time required to clear the baleen of debris may make foraging in Roseway Basin unprofitable in years of high gelatinous zooplankton abundance.

Predictive modeling of right whale distribution is a management objective with important conservation implications. Provided the appropriate environmental variables are readily available for input into such a model, one would be able to predict regions where right whales are likely to occur. The present research suggests specific variables that may be useful for predicting the spatial distribution of right whale occurrence in the study areas within a particular year. These include depth and BML depth for both the lower Bay of Fundy and Roseway Basin as well as SST gradient for Roseway Basin. However, prediction within each of these survey areas is presently of limited use. A more useful system would predict right whale occurrence in other areas as well. Extrapolation

of our results to other regions of the spring-summer-fall feeding grounds is unwise, however, since *Calanus finmarchicus* abundance is likely influenced by other factors in other regions and at other times. For instance, *C. finmarchicus* probably do not associate with a BML during the spring since feeding is observed in the upper portion of the water column (Watkins & Schevill 1976, Mayo & Marx 1990, Winn et al. 1995). Also, the importance of depth in this study is related to the aggregation of *C. finmarchicus* C5 in shelf basins; however, a similar relationship would not be expected in Cape Cod Bay, where right whales feed in areas less than 20 m deep (Mayo & Marx 1990). Quantitative examination of right whale occurrence in relation to environmental factors is needed in the other major feeding areas to provide the scientific foundation for a predictive model.

One challenge in these modeling efforts is the availability of relevant environmental variables for inclusion in a predictive model. A hypothetical model for the lower Bay of Fundy and Roseway Basin might require depth, BML depth and SST gradient. Depth is available as a gridded, bathymetric dataset and SST gradient is available as a remotely sensed product from an AVHRR archive (e.g. Cornillon et al. 1987), but BML depth cannot presently be obtained remotely. One attractive solution to this problem is to use the output from an operational ocean model (e.g. Aikman et al. 1996, Kelley et al. 1997). These regional models can provide synoptic forecasts of vertically resolved temperature, salinity and currents and with which right whale distribution may be predicted for several days in advance. While much work remains to be done, including additional right whale ecology research, habitat model development, integration with existing ocean model forecast products and rigorous validation of model predictions, a predictive model with forecast capabilities has compelling promise: improved management of human activities within ephemeral right whale habitats to reduce anthropogenic sources of mortality in this endangered population.

LITERATURE CITED

Aikman F III, Mellor GL, Ezer T, Sheinin D, Chen P, Breaker L, Bosley K, Rao DB (1996) Towards an operational nowcast/forecast system for the U.S. East Coast. In: Malanotte-Rizzoli P (ed) Modern approaches to data assimilation in ocean modeling. Elsevier Oceanography Series, Vol 61. Elsevier Science, New York, NY, p 347–376

Baumgartner MF (1997) The distribution of Risso's dolphin (*Grampus griseus*) with respect to the physiography of the northern Gulf of Mexico. Mar Mamm Sci 13:614–638

Baumgartner MF (2003) Comparisons of *Calanus finmarchicus* fifth copepodite abundance estimates from nets and an optical plankton counter. J Plankton Res 25: 855–868

Baumgartner MF, Mate BR (2003) Summertime foraging ecology of North Atlantic right whales. Mar Ecol Prog Ser 264:123–135

Baumgartner MF, Mullin KD, May LN, Leming TD (2001) Cetacean habitats in the northern Gulf of Mexico. Fish Bull 99:219–239

Baumgartner MF, Cole TVN, Campbell RG, Teegarden GJ, Durbin EG (2003) Associations between North Atlantic right whales and their prey, *Calanus finmarchicus*, over diel and tidal time scales. Mar Ecol Prog Ser 264:155–166

Beardsley RC, Epstein AW, Chen C, Wishner KF, Macaulay MC, Kenney RD (1996) Spatial variability in zooplankton abundance near feeding right whales in the Great South Channel. Deep-Sea Res II 43:1601–1625

Brown CW, Winn HE (1989) Relationship between the distribution pattern of right whales, *Eubalaena glacialis*, and satellite-derived sea surface thermal structure in the Great South Channel. Contin Shelf Res 9:247–260

Bumpus DF (1960) Sources of water contributed to the Bay of Fundy by surface circulation. J Fish Res Board Canada 17:181–197

CETAP (1982) A characterization of marine mammals and turtles in the mid- and north Atlantic areas of the U.S. outer continental shelf. Cetacean and Turtle Assessment Program, Final Report, Bureau of Land Management, Washington, DC

Chen C, Beardsley RC, Limeburner R (1995) Variability of currents in late spring in the northern Great South Channel. Contin Shelf Res 15:451–473

Clapham PJ, Young SB, Brownell RL Jr (1999) Baleen whales: conservation issues and the status of the most endangered populations. Mamm Rev 29:35–60

Conversi A, Piontkovski S, Hameed S (2001) Seasonal and interannual dynamics of *Calanus finmarchicus* in the Gulf of Maine (northeastern US shelf) with reference to the North Atlantic Oscillation. Deep-Sea Res II 48: 519–530

Cornillon P, Gilman C, Stramma L, Brown O, Evans R, Brown J (1987) Processing and analysis of large volumes of

satellite-derived thermal infrared data. J Geophys Res 92: 12 993–13 002

Durbin EG, Campbell RG, Gilman SL, Durbin AG (1995) Abundance, biomass, vertical migration and estimated development rate of the copepod *Calanus finmarchicus* in the southern Gulf of Maine during late spring. Contin Shelf Res 15:571–591

Epstein AW, Beardsley RC (2001) Flow-induced aggregation of plankton at a front: a 2-D Eulerian model study. Deep-Sea Res II 48:395–418

Fish CJ, Johnson MW (1937) The biology of the zooplankton population in the Bay of Fundy and Gulf of Maine with special reference to production and distribution. J Biol Board Can 3:189–322

Fromentin JM, Planque B (1996) *Calanus* and environment in the eastern North Atlantic. II. Influence of the North Atlantic Oscillation on *C. finmarchicus* and *C. helgolandicus*. Mar Ecol Prog Ser 134:111–118

Gaskin DE (1987) Updated status of the right whale, *Eubalaena glacialis*, in Canada. Can Field-Nat 101:295–309

Greenberg DA (1983) Modeling the mean barotropic circulation in the Bay of Fundy and Gulf of Maine. J Phys Oceanogr 13:886–904

Godin G (1968) The 1965 current survey of the Bay of Fundy: a new analysis of the data and an interpretation of results. Mansucript Rep Ser No. 8, Marine Sciences Branch, Energy Mines and Resources, Ottawa

Hachey HB, Bailey WB (1952) The general hydrography of the waters of the Bay of Fundy. Fish Res Board Can Rep Biol Sta No. 455, Ottawa

Herman AW (1988) Simultaneous measurement of zooplankton and light attenuance with a new optical plankton counter. Contin Shelf Res 8:205–221

Herman AW (1992) Design and calibration of a new optical plankton counter capable of sizing small zooplankton. Deep-Sea Res 39:395–415

Herman AW, Sameoto DD, Shunnian C, Mitchell MR, Petrie B, Cochrane N (1991) Sources of zooplankton on the Nova Scotia Shelf and their aggregations within deep-shelf basins. Contin Shelf Res 11:211–238

Hirche HJ (1983) Overwintering *Calanus finmarchicus* and *Calanus helgolandicus*. Mar Ecol Prog Ser 11:281–290

Hosmer DW, Lemeshow S (2000) Applied logistic regression, 2nd edn. John Wiley & Sons, New York, NY

Hui CA (1979) Undersea topography and distribution of dolphins of the genus *Delphinus* in the southern California Bight. J Mammal 60:521–527

Hui CA (1985) Undersea topography and the comparative distributions of 2 pelagic cetaceans. Fish Bull 83: 472–475

Kelley JGW, Aikman F III, Breaker LC, Mellor GL (1997) Coastal ocean forecasts. Sea Technol 38:10–17

Kenney RD (2001) Anomalous 1992 spring and summer right whale (*Eubalaena glacialis*) distributions in the Gulf of Maine. J Cetacean Res Manage Spec Issue 2:209–223

Kenney RD, Kraus SD (1993) Right whale mortality—a correction and an update. Mar Mamm Sci 9:445–446

Kenney RD, Winn HE, Macaulay MC (1995) Cetaceans in the Great South Channel, 1979–1989: right whale (*Eubalaena glacialis*). Contin Shelf Res 15:385–414

Knowlton AR, Kraus SD (2001) Mortality and serious injury of northern right whales (*Eubalaena glacialis*) in the western North Atlantic Ocean. J Cetacean Res Manage Spec Issue 2:193–208

Kraus SD (1990) Rates and potential causes of mortality in North Atlantic right whales (*Eubalaena glacialis*). Mar Mamm Sci 6:278–291

Kraus SD, Prescott JH, Turnbull PV, Reeves RR (1982) Preliminary notes on the occurrence of the North Atlantic right whale (*Eubalaena glacialis*) in the Bay of Fundy. Rep Int Whal Commn 32:407–411

Lauzier LM (1967) Bottom residual drift on the continental shelf area of the Canadian Atlantic coast. J Fish Res Board Can 24:1845–1859

Lynch DR, Ip JTC, Naimie CE, Werner FE (1996) Comprehensive coastal circulation model with application to the Gulf of Maine. Contin Shelf Res 16:875–906

Mate BR, Nieukirk SL, Kraus SD (1997) Satellite-monitored movements of the northern right whale. J Wild Manage 61:1393–1405

Mayo CA, Marx MK (1990) Surface foraging behavior of the North Atlantic right whale, *Eubalaena glacialis*, and associated zooplankton characteristics. Can J Zool 68: 2214–2220

Meise CJ, O'Reilly JE (1996) Spatial and seasonal patterns in abundance and age-composition of *Calanus finmarchicus* in the Gulf of Maine and on Georges Bank: 1977–1987. Deep-Sea Res II 43:1473–1501

Meise-Munns C, Green J, Ingham M, Mountain D (1990) Interannual variability in the copepod populations of Georges Bank and the western Gulf of Maine. Mar Ecol Prog Ser 65:225–232

Miller CB, Lynch DR, Carlotti F, Gentleman W, Lewis CVW (1998) Coupling of an individual-based population dynamic model of *Calanus finmarchicus* to a circulation model for the Georges Bank region. Fish Oceanogr 7: 219–234

Mitchell E, Kozicki VM, Reeves RR (1986) Sightings of right whales, *Eubalaena glacialis*, on the Scotian Shelf, 1966–1972. Rep Int Whal Commn Spec Issue 10:83–107

Murison LD, Gaskin DE (1989) The distribution of right whales and zooplankton in the Bay of Fundy, Canada. Can J Zool 67:1411–1420

NGDC (1988) Digital relief of the surface of the Earth. National Oceanic and Atmospheric Administration Data Announcement 88-MGG-02, National Geophysical Data Center, Boulder, CO

Olson DB, Backus RH (1985) The concentrating of organisms at fronts: a cold-water fish and a warm-core Gulf Stream ring. J Mar Res 43:113–137

Payne PM, Wiley DN, Young SB, Pittman S, Clapham PJ, Jossi JW (1990) Recent fluctuations in the abundance of baleen whales in the southern Gulf of Maine in relation to changes in selected prey. Fish Bull 88:687–696

Ramsey FL, Schafer DW (1997) The statistical sleuth: a course in methods of data analysis. Duxbury Press, Belmont, CA

Russ JC (1995) The image processing handbook, 2nd edn. CRC Press, Boca Raton

Sameoto DD, Herman AW (1990) Life cycle and distribution of *Calanus finmarchicus* in deep basins on the Nova Scotia shelf and seasonal changes in *Calanus* spp. Mar Ecol Prog Ser 66:225–237

Selzer LA, Payne PM (1988) The distribution of white-sided (*Lagenorhynchus acutus*) and common dolphins (*Delphinus delphis*) vs. environmental features of the continental shelf of the northeastern United States. Mar Mamm Sci 4: 141–153

Smith WHF, Sandwell DT (1997) Global seafloor topography from satellite altimetry and ship depth soundings. Science 277:1957–1962

Stone GS, Kraus SD, Prescott JH, Hazard KW (1988) Significant aggregations of the endangered right whale, *Eubalaena glacialis*, on the continental shelf of Nova Scotia. Can Field-Nat 102:471–474

Watkins WA, Schevill WE (1976) Right whale feeding and baleen rattle. J Mammal 57:58–66

Weinrich MT, Kenney RD, Hamilton PK (2000) Right whales (*Eubalaena glacialis*) on Jeffreys Ledge: a habitat of unrecognized importance? Mar Mamm Sci 16:326–337

Wiebe PH, Burt KH, Boyd SH, Morton AW (1976) A multiple opening/closing net and environmental sensing system for sampling zooplankton. J Mar Res 34:313–326

Wiebe PH, Morton AW, Bradley AM, Backus RH, Craddock JE, Barber V, Cowles TJ, Flierl GR (1985) New developments in the MOCNESS, an apparatus for sampling zooplankton and micronekton. Mar Biol 87:313–323

Winn HE, Price CA, Sorensen PW (1986) The distributional biology of the right whale (*Eubalaena glacialis*) in the western North Atlantic. Rep Int Whal Comm Spec Issue 10:129–138

Winn HE, Goodyear JD, Kenney RD, Petricig RO (1995) Dive patterns of tagged right whales in the Great South Channel. Contin Shelf Res 15:593–611

Wishner K, Durbin E, Durbin A, Macaulay M, Winn H, Kenney R (1988) Copepod patches and right whales in the Great South Channel off New England. Bull Mar Sci 43:825–844

Wishner KF, Schoenherr JR, Beardsley R, Chen C (1995) Abundance, distribution and population structure of the copepod *Calanus finmarchicus* in a springtime right whale feeding area in the southwestern Gulf of Maine. Contin Shelf Res 15:475–507

Woodley TH, Gaskin DE (1996) Environmental characteristics of North Atlantic right and fin whale habitat in the lower Bay of Fundy, Canada. Can J Zool 74:75–84

Xue H, Chai F, Pettigrew NR (2000) A model study of the seasonal circulation in the Gulf of Maine. J Phys Oceanogr 30:1111–1135

Associations between North Atlantic right whales and their prey, *Calanus finmarchicus*, over diel and tidal time scales

Mark F. Baumgartner[1,5,*], Tim V. N. Cole[2], Robert G. Campbell[3], Gregory J. Teegarden[4], Edward G. Durbin[3]

[1]College of Oceanic and Atmospheric Sciences, Oregon State University, 104 Ocean Administration Building, Corvallis, Oregon 97331, USA
[2]National Marine Fisheries Service, Northeast Fisheries Science Center, 166 Water Street, Woods Hole, Massachusetts 02543, USA
[3]Graduate School of Oceanography, University of Rhode Island, Narragansett, Rhode Island 02882, USA
[4]Saint Joseph's College, 278 Whites Bridge Road, Standish, Maine 04084, USA

[5]*Present address:* Biology Department, MS #33, Woods Hole Oceanographic Institution, Woods Hole, Massachusetts 02543, USA

ABSTRACT: Temporal variability in the distribution and abundance of North Atlantic right whales *Eubalaena glacialis* and their copepod prey, late-stage *Calanus finmarchicus*, was monitored at an oceanographic station in Grand Manan Basin of the lower Bay of Fundy for 29 h on 2 separate occasions. The vertical distribution of *C. finmarchicus* was measured at $1/2$ h intervals with an optical plankton counter (OPC) and at 6 or 12 h intervals with a MOCNESS. Right whale abundance was estimated from periodic point scans. Late-stage *C. finmarchicus* exhibited diel vertical migration in the upper 100 m of the water column, but the bulk of the population remained at depths below 100 m throughout both the day and night and was likely in diapause. Diel vertical migration is unlikely to be influenced by right whales, but may instead be motivated by abundant, near-surface food resources and avoidance of visual predators. Right whale sighting rate was correlated with OPC-detected *C. finmarchicus* fifth copepodite (C5) abundance at mid-depths (90–140 m); variability in both right whale sighting rate and *C. finmarchicus* C5 abundance in this depth stratum appeared to have similar periodicity to that of the tide. Energetic considerations suggest that right whales continue to feed on deep, diapausing layers of *C. finmarchicus* during the night, but the occasional presence of exploitable near-surface concentrations of *C. finmarchicus* suggests that nighttime near-surface feeding might sometimes occur.

KEY WORDS: Right whale · *Eubalaena glacialis* · *Calanus finmarchicus* · Diel vertical migration · Tides · Gulf of Maine · Bay of Fundy · Optical plankton counter

INTRODUCTION

The North Atlantic right whale *Eubalaena glacialis* feeds primarily upon the calanoid copepod *Calanus finmarchicus*. It accomplishes this by filtering seawater through very fine baleen that can retain large copepods efficiently (Mayo et al. 2001). Because there are only roughly 300 individuals remaining in this endangered population (IWC 2001), right whale predation

probably has a negligible effect on *C. finmarchicus* population dynamics. However, right whale predation on older copepodite stages of *C. finmarchicus* must be intense in some regions where right whales aggregate annually, such as Cape Cod Bay in the late winter (Watkins & Schevill 1976, Mayo & Marx 1990), Great South Channel in the spring (Wishner et al. 1988, 1995, Beardsley et al. 1996) and the lower Bay of Fundy during the summer and early fall (Murison & Gaskin 1989,

Woodley & Gaskin 1996, Baumgartner et al. 2003 this issue). The reliability of both right whale and *C. finmarchicus* aggregations in these regions provides an opportunity to study the unique trophic relationship between this predator and prey.

Studies that have employed net sampling near right whales in the lower Bay of Fundy suggest that right whales feed on *Calanus finmarchicus* fifth copepodites (C5) (Murison & Gaskin 1989, Woodley & Gaskin 1996, Baumgartner et al. 2003). Right whales forage during the day on *C. finmarchicus* C5 that aggregate in discrete layers deep in the water column just above a bottom mixed layer (Baumgartner & Mate 2003 this issue). Nighttime vertical migration to the surface by the copepods in these deep layers would have important implications for right whales. Surface feeding by the whales would be expected to have energetic benefits since transit time to shallower food resources is reduced. For a constant dive duration, reduced transit time increases feeding time, so comparatively more energy can potentially be acquired per dive when feeding near the surface than at depth.

Surface feeding may also be accompanied by costs to the whales, however. Right whale exposure to the natural toxins that cause paralytic shellfish poisoning (PSP) may be enhanced by feeding on near-surface aggregations of *Calanus finmarchicus* that have significantly higher PSP toxin levels than deeper copepods (Durbin et al. 2002). These toxins are produced by the dinoflagellate *Alexandrium fundyense*, which is present in the surface waters of the lower Bay of Fundy during the summer and early fall (Martin & White 1988, Townsend et al. 2001) and is consumed by *C. finmarchicus* (Turriff et al. 1995, Teegarden et al. 2001). Feeding on these contaminated *C. finmarchicus* may have detrimental effects on right whale respiratory capabilities (Geraci 1989). The North Atlantic right whale population also experiences significant mortality due to ship strikes (Kraus 1990, Kenney & Kraus 1993, Knowlton & Kraus 2001), and an increase in the time spent at the surface while feeding there would be expected to increase the risk of collision.

To better understand temporal variability in prey availability for right whales and the potential response of *Calanus finmarchicus* to right whale predation, we occupied oceanographic sta-

tions in the lower Bay of Fundy at which simultaneous diel vertical migration (DVM) studies and periodic point scans of right whales were conducted. The vertical distribution of *C. finmarchicus* C5 was monitored with a vertically profiled optical plankton counter (OPC) deployed every half hour and a multiple opening-closing net and environmental sensing system (MOCNESS) towed every 6 or 12 h. The vertical distributions of other late-stage *C. finmarchicus* (C4 and adults) were also monitored with the MOCNESS. These data were used to investigate vertical migration by *C. finmarchicus* and associated variability in right whale abundance over diel and tidal time scales.

MATERIALS AND METHODS

Two stations were occupied by NOAA ship 'Albatross IV' in Grand Manan Basin of the lower Bay of Fundy during the summer of 2001 (Fig. 1). The first
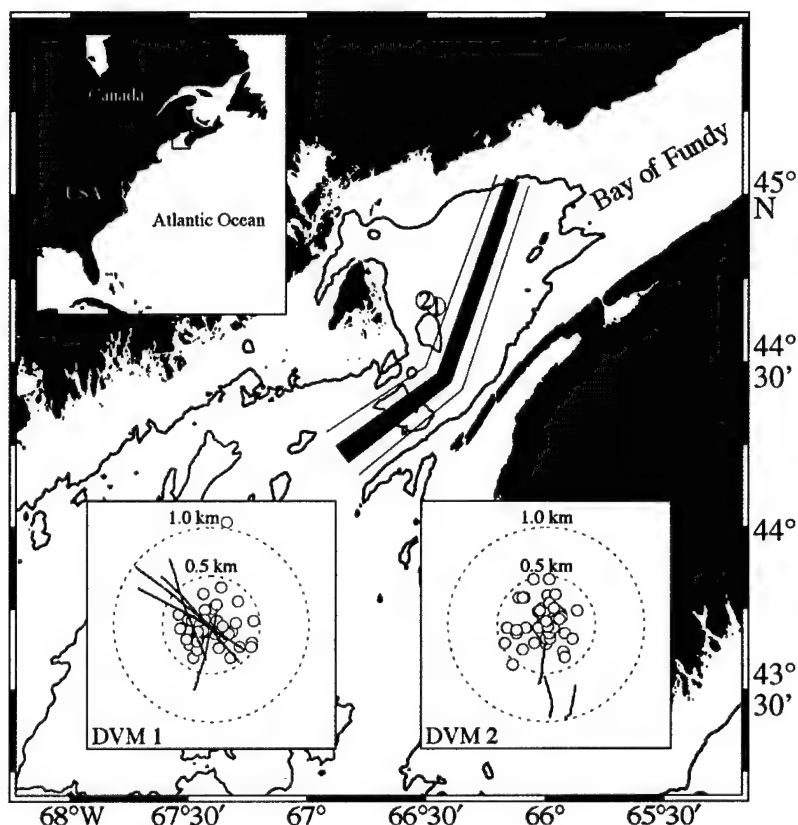

Fig. 1. Map of study area. ①,②: Location of each station in the lower Bay of Fundy. Shipping lanes that passed through this region at the time of the study are also shown (they have since been changed). Location of the study area along the eastern seaboards of the United States and Canada shown in the upper left inset. Optical plankton counter (OPC) cast locations (o) and MOCNESS tow paths (lines) relative to each station (center of plot) shown in the lower insets. DVM: diel vertical migration

study (DVM 1) took place at 44° 40.0' N, 66° 27.5' W on 29 and 30 July. This location was selected because right whales had been consistently sighted there in the 2 previous summers. The second study (DVM 2) was conducted on 31 July and 1 August at a location (44° 41.1' N, 66° 30.3' W) where whales were initially present and abundant. The stations for DVM 1 and 2 were occupied for 29.2 and 28.7 h, respectively. A Focal Technologies model OPC-1T OPC (Herman 1988, 1992) was deployed in a vertical cast at a nominal descent speed of 1.0 m s^{-1} every 30 min during each study. The OPC provided the vertical distribution of particles ranging in size from 0.25 to 20 mm. The abundance of particles between 1.5 and 2.0 mm equivalent circular diameter was computed over 5 m depth strata and converted to *Calanus finmarchicus* C5 abundance using the calibration equation of Baumgartner (2003). Vertical migration rates were determined when coherent changes in the distribution of *C. finmarchicus* C5 were observed in a portion of the water column. The depths of peak abundance during a migration period were regressed against time and the slope of the linear regression is reported as the migration rate. Only depths with peak abundances greater than 100 copepods m^{-3} were used in the regression. Day and night were defined as the periods bracketed by the times of sunset and sunrise as calculated from equations of solar elevation angle for each station (Kirk 1994). The beginning and end of nautical twilight were computed as the times when the solar elevation angle was –12° (i.e. 12° below the horizon) (Bowditch 1995).

At 6 (DVM 1) or 12 (DVM 2) h intervals, a MOCNESS (Wiebe et al. 1976, 1985) equipped with 150 µm mesh nets was towed through the station. The MOCNESS sampled 5 contiguous depth strata from approximately 10 m above the bottom to the surface. These strata were chosen after reviewing OPC data collected prior to the first MOCNESS tow in each DVM study. Samples were preserved in a 10 % formalin-seawater solution and subsampled in the laboratory. All *Calanus finmarchicus* copepodite stages were enumerated in the subsamples, and the abundance of each stage was estimated from these counts, the subsample volume and the volume of seawater filtered by the net. The abundance data from the MOCNESS tows were not used to construct the OPC calibration equation of Baumgartner (2003).

Periodic visual surveys for right whales were conducted during each DVM study from the bow of NOAA Ship 'Albatross IV'. Observers searched for right whales using binoculars and the naked eye during several discrete, daytime survey periods that lasted an average of 34 min (range: 17–50 min). Scans of 3 to 4 min were conducted every 10 to 15 min during a survey period. Sighting rates were computed as the total number of whales sighted within 2000 m of the ship during a survey period divided by the duration of the survey period. Repeat sightings of individual whales were undoubtedly made during successive scans within a survey period, so the sighting rate can only be considered a relative measure of abundance.

The relationship between right whale sighting rates and OPC-derived *Calanus finmarchicus* C5 abundance was examined using correlation analysis. Since *C. finmarchicus* C5 abundance could be computed over multiple depth strata and we had no formal hypothesis addressing in which depth stratum *C. finmarchicus* C5 abundance might influence right whale distribution, we examined correlations between right whale sighting rates and *C. finmarchicus* C5 abundance computed over all possible depth strata. The minimum depth for each depth stratum was systematically varied from 0 to 200 m in 5 m intervals. The maximum depth for each depth stratum was systematically varied from the minimum depth to 200 m in 5 m intervals. For each survey period and depth stratum, *C. finmarchicus* C5 abundance was averaged over the 3 OPC casts spanning the survey period.

Predictions of local tidal currents were acquired from Tides & Currents software (version 2.0) (Nautical Software 1996) based on U.S. National Oceanic and Atmospheric Administration and Canadian Hydrographic Service harmonic constants. The software provided estimates of current speeds and only 2 possible current directions (40° at flood and 235° at ebb) every 30 min at 44° 44' N, 66° 15' W. The tidal currents were integrated over time to estimate the displacement of a passive particle relative to this location. The phase of the tidal predictions was verified by comparing the tidal displacement to the temporal variability in water depth measured continuously by the NOAA Ship 'Albatross IV' scientific echo sounder (Simrad EK-500). The phases of the predictions and observations were in very good agreement such that, for instance, times of maximum tidal displacements coincided with observed periods of high and low water. The predicted times of high tide, low tide, maximum flood currents and maximum ebb currents were therefore considered accurate. The predicted current magnitude (and hence the absolute magnitude of the tidal displacement), however, was not considered accurate, since wind, baroclinic and residual barotropic effects are not included in the predictions.

RESULTS

DVM 1

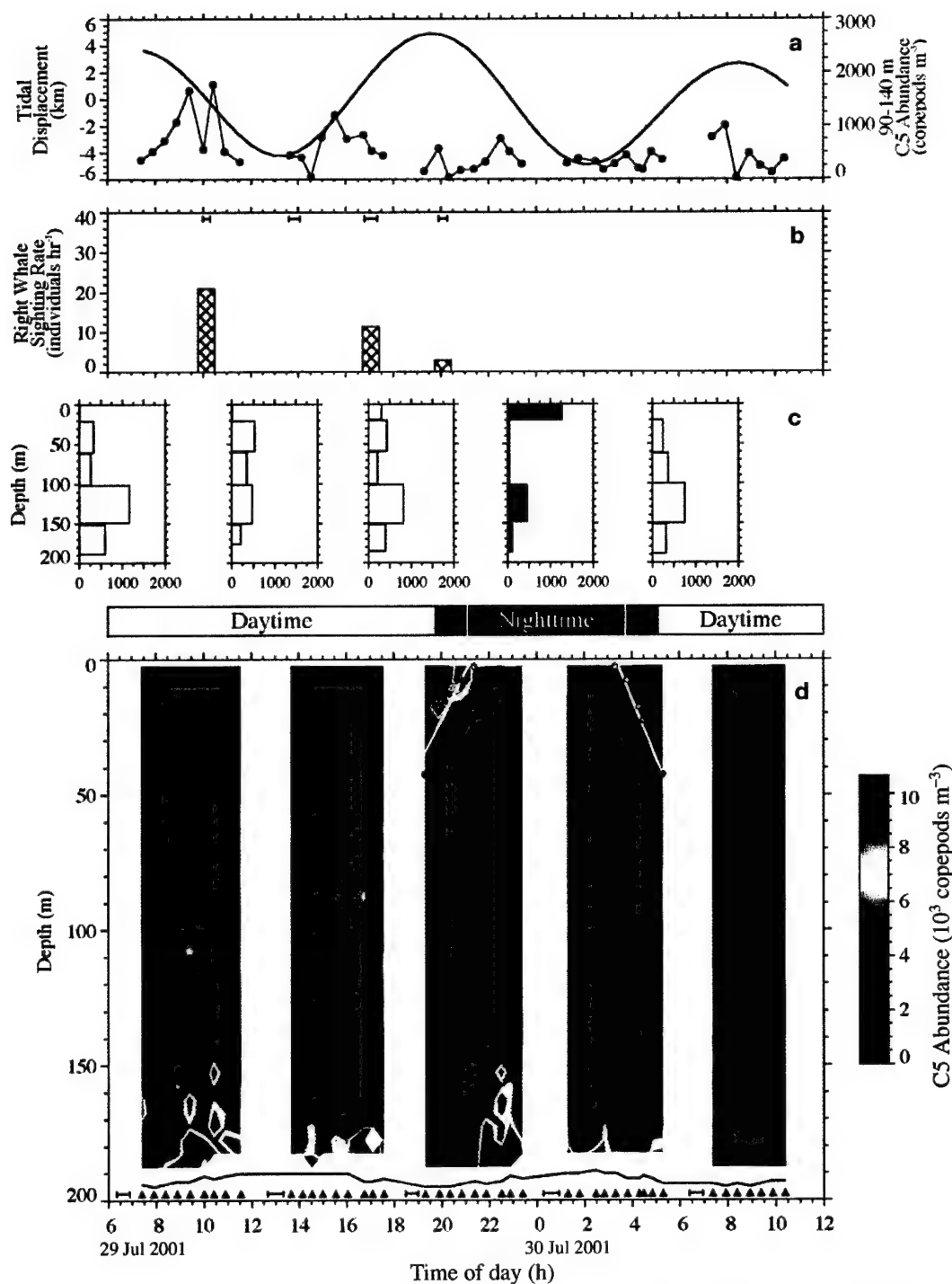The MOCNESS data suggested that the upper 20 m of the water column contained low abundances of

Fig. 2. *Eubalaena glacialis* and *Calanus finmarchicus*. (a) Tidal displacement during DVM 1 showing times of high tide (local maximums) and low tides (local minimums). OPC-detected *C. finmarchicus* C5 abundance between 90 and 140 m shown in red. (b) Right whale sighting rate within 2000 m of the ship. Bars just below top axis indicate survey periods. (c) Vertical distribution of *C. finmarchicus* C5 from the MOCNESS tows (copepods m⁻³). Individual plots are aligned over their respective tow periods in the accompanying plots. (d) Time evolution of OPC-detected *C. finmarchicus* C5 vertical distribution. Thick line at 190 to 195 m represents the bottom; (▲) and (⊢⊣) are times when respective OPC casts and MOCNESS tows were conducted. (●) Peaks in abundance in the upper 60 m at dusk and dawn. Linear regressions from which the migration rates were calculated are also shown (see 'Materials and methods'). Day/night periods and the start/end of nautical twilight (vertical white lines) are indicated above (d). Plots (a), (b) and (d) all have the same time axis (shown in d). Time axes are in Atlantic Standard Time

Calanus finmarchicus C5 for most of the daylight hours; however, the OPC data indicated that *C. finmarchicus* C5 abundance was low over the upper 40 m of the water column during this time (Fig. 2). OPC-detected *C. finmarchicus* C5 inhabiting depths of 40 to 100 m began migrating toward the surface within the half-hour prior to sunset at a rate of 0.50 cm s^{-1} (n = 5, 95% CI = 0.12 to 0.87). The data from the MOCNESS tow at 18:30 h suggested that some *C. finmarchicus* C5 appeared in the upper 20 m well before sunset (Fig. 2). The OPC-detected migrating layer reached the surface waters (<5 m) at the beginning of nautical twilight. The dusk migration resulted in very low nighttime abundances in the depth stratum between 20 and 70–90 m. Within the half-hour before nautical twilight ended, *C. finmarchicus* C5 left the surface waters, migrated downward at 0.60 cm s^{-1} (n = 6, 95% CI = 0.42 to 0.79) and reoccupied depths at or below 40 m by sunrise. The MOCNESS data indicated that *C. finmarchicus* C4, C5 and adult females (C6F) all vertically migrated into and out of the surface waters: C4, C5 and C6F abundance in the upper 20 m averaged 213, 103 and 2 copepods m^{-3} during the daytime and 467, 1288 and 97 copepods m^{-3} during the nighttime, respectively (Fig. 3). A deeper population of *C. finmarchicus* C5 occupying depths between 100 and 150 m did not vertically migrate. The average OPC-derived observations above 150 m were corroborated by the MOCNESS results (Fig. 3c,d).

OPC-detected particle abundances in the size range overlapping that of *Calanus finmarchicus* C5 were very high at times near the bottom (Fig. 2); however, it is unclear if these particles were in fact *C. finmarchicus* C5. The MOCNESS tows did not indicate that large aggregations of *C. finmarchicus* C5 existed near the bottom (Fig. 3c,d). The particle size distribution near the bottom is also inconsistent with the presence of *C. finmarchicus* C5 (Fig. 4). In waters with high *C. finmarchicus* C5 abundance, the particle size distribution is expected to be modal at approximately 1.55 mm (Baumgartner 2003). This modal peak can be readily observed in the average particle size distributions in the surface at night (Fig. 4a), between 40 and 100 m during the day (Fig. 4b) and between 100 and 130 m at all hours (Fig. 4c). No modal peak is apparent in the waters near the bottom (Fig. 4d). Moreover, the times of high particle abundance coincide with the times of maximum flood and ebb currents, which suggests that the particles detected by the OPC near the bottom may be detritus or sediment that has been resuspended by strong tidal flow.

DVM 2

Diel vertical migration was also observed in the upper water column (<80 m) during DVM 2. The OPC detected an aggregation of *Calanus finmarchicus* C5 residing at approximately 40 m depth during the daytime that migrated to the surface at night (Fig. 5, Fig. 6c,d). As was the case during DVM 1, upward
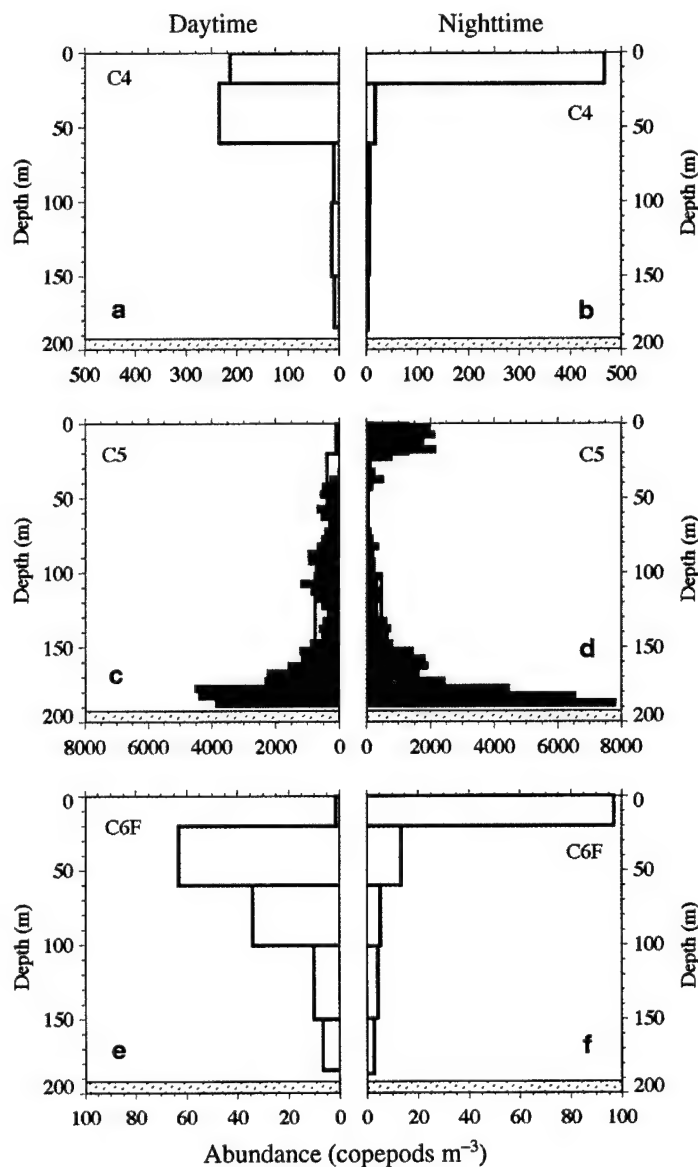

Fig. 3. *Calanus finmarchicus*. Vertical distribution of (a,b) C4, (c,d) C5 and (e,f) adult females (C6F) averaged over all daytime (a,c,e) and nighttime (b,d,f) MOCNESS tows during DVM 1. (c,d) Average OPC-derived, daytime and nighttime vertical distributions of *C. finmarchicus* C5 shown as gray bars. Bottom indicated by the hatched area. Note that the apparent high abundance of *C. finmarchicus* C5 detected near the bottom by the OPC is likely due to resuspended sediments or detritus (see 'Results: DVM 1')
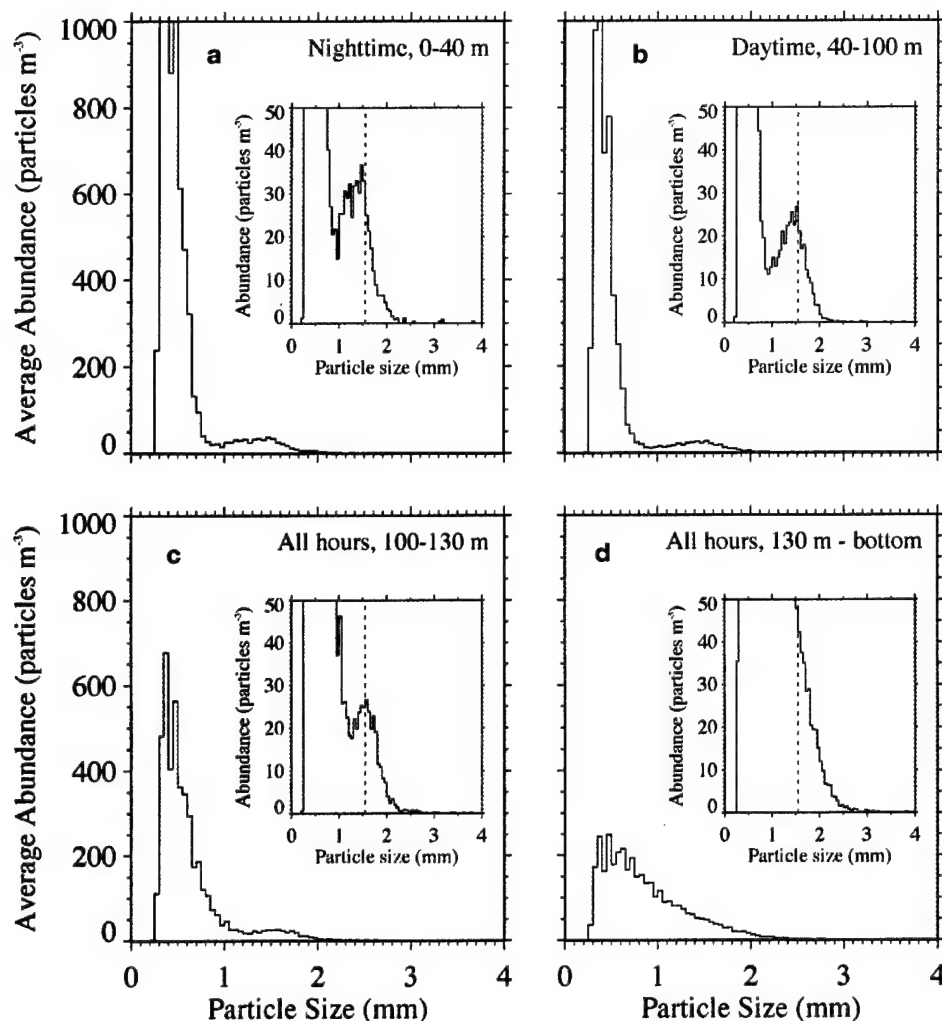
Fig. 4. Average particle size distributions for OPC data collected during DVM 1 (a) between 0 and 40 m at night, (b) between 40 and 100 m during the day, (c) between 100 and 130 m during all hours and (d) between 130 m and the bottom during all hours. Insets show details of average particle distributions between 0 and 50 particles m^{-3}. Dotted line in each inset indicates the expected mode for *Calanus finmarchicus* C5 (1.55 mm) from Baumgartner (2003)

migration began in the half-hour prior to sunset and the migrating layer reached the surface (< 5 m) at the beginning of nautical twilight. The upward migration rate of OPC-detected *C. finmarchicus* C5 (0.67 cm s^{-1}, n = 5, 95% CI = 0.46 to 0.89) was not significantly different from that observed during DVM 1. There were too few resolvable local peaks in abundance to adequately determine the timing or rate of the downward migration at dawn. A substantial portion of the *C. finmarchicus* C5 population resided below 80 m during both the daytime and nighttime. Local peaks in this depth stratum were observed well above the bottom with the exception of a single cast that occurred soon after dawn. The data from this cast had characteristics similar to those observed near the bottom during DVM 1 (e.g. a size distribution similar to Fig. 4d, occurrence at the bottom during maximum tidal currents), so this cast may have also captured a resuspension event. The MOCNESS data corroborated the diel vertical migra-

tion in the upper water column and the presence of the more abundant deep layer of *C. finmarchicus* C5 (Fig. 6c,d). These data also indicated vertical migration into and out of the surface waters by *C. finmarchicus* C4 and C6F as well: C4, C5 and C6F abundance in the upper 20 m averaged 0.3, 1.1 and 0.3 copepods m^{-3} during the daytime and 34, 135 and 28 copepods m^{-3} during the nighttime, respectively (Fig. 6). Agreement between the average OPC-derived *C. finmarchicus* C5 abundance estimates and those of the MOCNESS for all sampled depths was very good (Fig. 6c,d).

Right whale abundance

Significant correlations (p < 0.05) occurred between right whale sighting rates and OPC-derived *Calanus finmarchicus* C5 abundance computed over depth strata having minimum depths of 65 to 110 m and max-

imum depths of 115 to 160 m. The maximum correlation occurred when OPC-derived *C. finmarchicus* C5 abundance was computed between 90 and 140 m (n = 10, r = 0.731, p = 0.016; Fig. 7). There appears to be a single outlier from DVM 2 (survey effort on 31 July,

18:10 to 18:53 h AST) that is characterized by a high sighting rate and a low *C. finmarchicus* C5 abundance (Fig. 7). The *C. finmarchicus* C5 abundance from 90 to 140 m was quite variable around the time of this survey, which may be the result of spatial heterogeneity
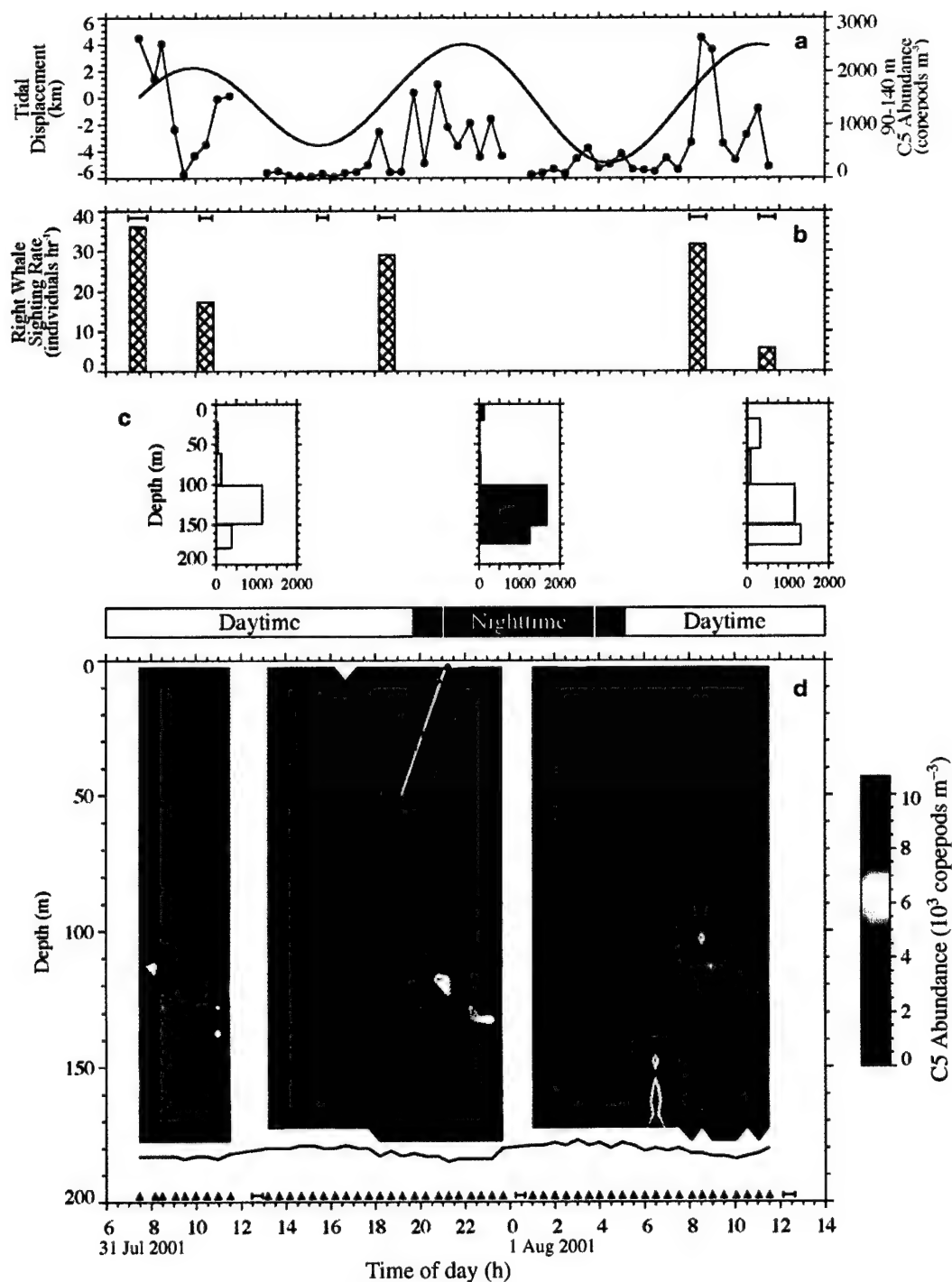

Fig. 5. *Eubalaena glacialis* and *Calanus finmarchicus*. Results from DVM 2. Axes and labels as in Fig. 2. Rate of downward migration at dawn was not estimated (see 'Results: DVM 2')
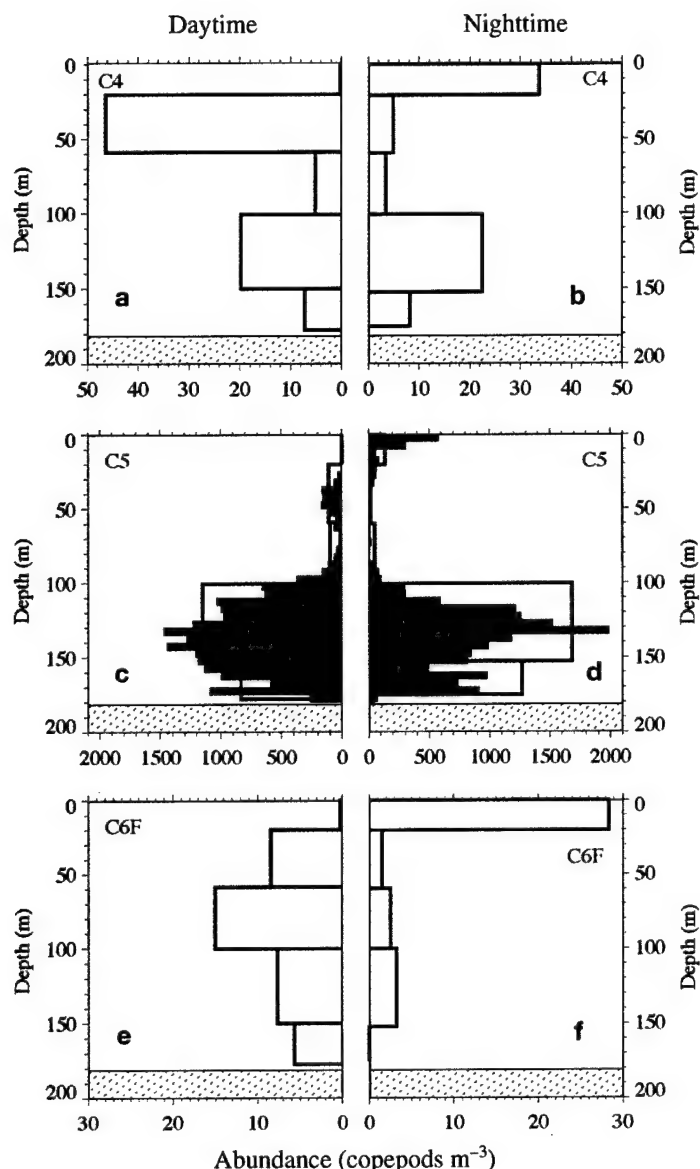
Fig. 6. *Calanus finmarchicus*. Vertical distribution of (a,b) C4, (c,d) C5 and (e,f) adult females (C6F) averaged over all daytime (a,c,e) and nighttime (b,d,f) MOCNESS tows during DVM 2. (c,d) Average OPC-derived, daytime and nighttime vertical distributions of *C. finmarchicus* C5 shown as gray bars. Bottom indicated by the hatched area

(patchiness) in *C. finmarchicus* C5 distribution (Fig. 5). When this outlier is removed, the correlation between right whale sighting rate and 90 to 140 m *C. finmarchicus* C5 abundance becomes remarkably strong and highly significant (n = 9, r = 0.969, p < 0.0001). No significant correlations were detected between right whale sighting rate and *C. finmarchicus* C5 abundance computed in depth strata near the surface, the bottom or spanning the entire water column. Temporal vari-

ability in right whale sighting rates at each fixed oceanographic station appeared to have similar periodicity to that of the tide. This was particularly apparent during DVM 2, when peaks in sighting rates occurred when patches of *C. finmarchicus* C5 at mid-water were advected past the station just before high tide (Fig. 5a,b).

DISCUSSION

A large portion of the *Calanus finmarchicus* C5 population in each DVM study did not migrate, but instead remained below 100 m throughout both day and night. Examination of the MOCNESS samples immediately after collection indicated that these non-migrating copepods had empty guts, well-developed oil sacs and were less active than individuals collected in the migrating layer. These observations indicate that the deep layer was composed of copepods in diapause. Diapause is a resting state employed by *C. finmarchicus* to survive the long period of low food availability during the summer and fall (Hirche 1996). *C. finmarchicus* C5 enter diapause after arresting their development and undertaking an ontogenetic vertical migration to depths where predation may be minimized (Kaartvedt 1996, Dale et al. 1999) and temperatures are low enough to ensure low rates of metabolism and oil reserve depletion (Ingvarsdóttir et al. 1999). In contrast to the diapausing *C. finmarchicus* C5, the copepods that composed the migrating layer had smaller oil sacs (ca. 33% smaller than deep animals) and food in their guts, females had mature oocytes (an indication of active spawning) and surface net and bucket samples revealed the presence of all developmental stages (nauplii, copepodites and adults). These observations indicate an actively feeding and growing population in the upper water column.

The upward vertical migration by copepods at dusk is thought to be motivated by the presence of food in the surface waters (e.g. Dagg et al. 1989, Dagg 1997). DVM may be arrested, however, when surface food resources become depleted (Dagg 1985, Durbin et al. 1995). Campbell et al. (2001) found evidence of food limitation in *Calanus finmarchicus* in surface waters with chlorophyll a concentrations less than 1 µg l⁻¹, whereas *C. finmarchicus* were in much better condition and had higher egg production rates in waters with chlorophyll a concentrations of between
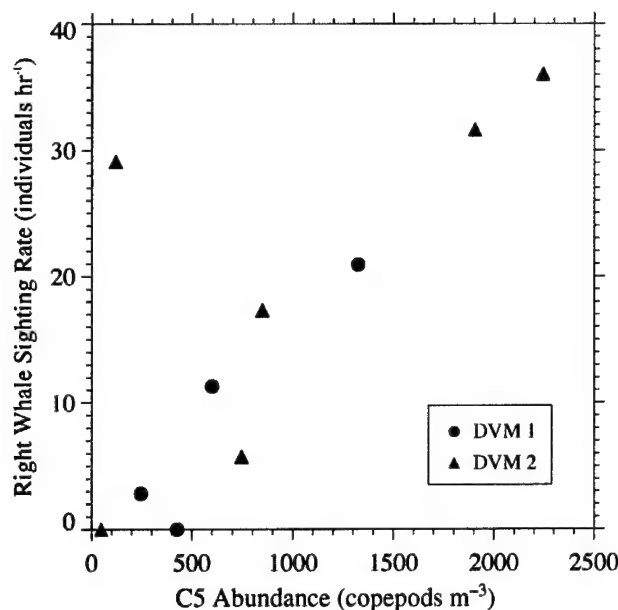
Fig. 7. *Eubalaena glacialis* and *Calanus finmarchicus*. Right whale sighting rate within 2000 m of the ship versus *C. finmarchicus* C5 abundance between 90 and 140 m. (●) Observations from DVM 1; (▲) observations from DVM 2

1.5 and 1.8 µg l^{-1}. During the present study, maximum, *in situ* chlorophyll *a* concentrations in the upper 15 m were greater than 2 µg l^{-1}. Moreover, the presence of all development stages, spawning females and individuals with food in their guts indicate that *C. finmarchicus* in the migrating later were not food limited to any great extent. Migration to the surface layer at dusk by *C. finmarchicus* is therefore likely due to the presence of abundant, exploitable food resources.

Migration out of the surface layers near dawn is widely considered to be a strategy employed by copepods to evade visual predators by seeking refuge below the euphotic zone (e.g. Bollens & Frost 1989, Bollens et al. 1992). Several visual predators of *Calanus finmarchicus* occur in the lower Bay of Fundy, including euphausiids (Kulka et al. 1982), planktivorous fish (Sinclair & Iles 1985) and seabirds (Mercier & Gaskin 1985, Brown & Gaskin 1988). It is possible that right whales could also utilize vision while preying on *C. finmarchicus* in the euphotic zone (Kenney et al. 2001). Despite their high, individual ingestion rates, however, predation pressure from right whales is relatively low and unlikely to influence *C. finmarchicus* DVM behavior. To illustrate this, consider the euphausiid *Meganyctiphanes norvegica* or northern krill, an effective visual predator of copepods (Torgersen 2001). *M. norvegica* is abundant in Grand Manan Basin (Kulka et al. 1982) and has a catholic diet that includes *C. finmarchicus* (McClatchie 1985, Båmstedt & Karlson

1998, Lass et al. 2001, Torgersen 2001). Based on an ingestion rate of 12.5×10^4 W ind.$^{-1}$ (Baumgartner & Mate 2003) or 1.6×10^9 copepods ind.$^{-1}$ d^{-1}, 150 right whales (half of the population) would have an estimated predation rate on *C. finmarchicus* of 0.24×10^{12} copepods d^{-1}. By comparison, *M. norvegica* would have an estimated predation rate 7.5 times that, or 1.8×10^{12} copepods d^{-1}, based on an average abundance of 100 ind. m^{-2} (Kulka et al. 1982), an ingestion rate of 1 copepod ind.$^{-1}$ h^{-1} (Båmstedt & Karlson 1998) and an approximate surface area for Grand Manan Basin of 750 km^2. (The numbers upon which these predation rates are based were chosen from the maximum of their range for right whales and the minimum of their range for *M. norvegica* to provide a conservative estimate of the relative importance of right whale predation relative to that of *M. norvegica*.) Thus, visual predation by more abundant species, such as *M. norvegica* or herring *Clupea harengus*, is expected to have much greater influence over *C. finmarchicus* DVM than predation by right whales.

The selection of daytime depths by the migrating layer of *Calanus finmarchicus* may also be driven by predator avoidance. *C. finmarchicus* C5 and C6F migrated to depths between 40 and 100 m at dawn while *C. finmarchicus* C4 appeared to migrate to shallower depths of between 20 and 60 m. Kulka et al. (1982) and Hurley et al. (1983) described the respective vertical distributions of euphausiids (*Meganyctiphanes norvegica*, *Thysanoessa inermis* and *T. longicaudata*) and chaetognaths (*Sagiita elegans*) during a DVM study in Grand Manan Basin. They reported that nearly all of the euphausiids and chaetognaths occurred below 100 m during net sampling at noon. Although the *in situ* vertical distribution of predators during the present study is unknown (the net sampling was not designed to quantitatively assess invertebrate predator abundance), *C. finmarchicus* may select a daytime depth stratum that is deep and dark enough to minimize visual predation, yet is shallow enough to avoid mortality caused by euphausiids and chaetognaths that are capable of raptorial predation via mechanical detection (Newbury 1972, Torgersen 2001). The daytime vertical distribution of the migrating *C. finmarchicus* also separates them from the deeper diaupausing layers of *C. finmarchicus* C5 upon which right whales feed during the day (Baumgartner & Mate 2003). However, the selection of a daytime depth that minimizes right whale predation is probably only an incidental benefit of avoidance of other, more abundant predators (see above).

Right whale daytime abundance was correlated with OPC-detected *Calanus finmarchicus* C5 abundance at mid-depths (90 to 140 m) and Baumgartner & Mate (2003) demonstrated that tagged right whales in the

lower Bay of Fundy concentrated their foraging effort on deep layers of *C. finmarchicus* C5 below 90 m during the daytime. These results indicate that right whales bypass the migrating layer to feed on the deeper, diapausing *C. finmarchicus* during the day. From the perspective of an optimally foraging whale, feeding in the deeper layer has a higher energetic cost than feeding in the shallower layer because transit time to the depth of feeding is increased and thus feeding time at that depth is decreased. For example, ingestion rates would be reduced by 8 to 19% when feeding on a layer between 90 and 140 m (transit time of 2.1 to 3.3 min) relative to feeding on an identical layer at 50 m (transit time of 1.2 min) based on an average descent speed of 1.40 m s^{-1}, average ascent speed of 1.47 m s^{-1} and average dive duration of 12.2 min (Baumgartner & Mate 2003). However, when compared to the copepods in the migrating layer, the individuals that comprised the deeper diapausing layer were much more abundant, had a higher caloric content (owing to their larger oil sacs) and were less active (i.e. less able to avoid capture). Competition for these deeper *C. finmarchicus* from visual predators would likely be negligible as well. Thus, the energetic benefits of feeding on this deep layer probably far outweigh the relative costs.

During the night, the energetic cost of feeding on the migrating layer would be even further reduced relative to the cost of feeding on the diapausing *Calanus finmarchicus* because near-surface feeding entails almost no transit time at all. The low abundance of migrating animals observed near the surface during the later nighttime hours of DVM 1 and during all of the nighttime hours of DVM 2 suggests that, like during the daytime, feeding on the diapausing *C. finmarchicus* would provide the most energetic benefit. During DVM 1, however, surface concentrations of *C. finmarchicus* C5 in the early nighttime hours exceeded those found in the deeper layer (Figs. 2 & 3d) and were augmented by high *C. finmarchicus* C4 concentrations (Fig. 3b). This high surface abundance may have formed from the concentration of *C. finmarchicus* spread over 40 to 100 m by day into a 10 to 15 m layer at the surface at night. Furthermore, the *C. finmarchicus* C5 abundance in the surface waters at this time exceeded the minimum concentrations upon which right whales have been observed feeding during the day (ca. 3000 copepods m^{-3}; Baumgartner & Mate 2003). Although these surface *C. finmarchicus* were of lower caloric content and were more likely to avoid capture, the decreased energetic cost of foraging at the surface and the relatively high abundance of *C. finmarchicus* suggests that this patch could have provided more energetic benefit than the deep diapausing layer. The right whale sighting rate observed just before this surface patch was encountered, however, was low (Fig. 2), which suggests that the patch may have been ephemeral or too small in size to be readily detected by the whales.

Dolphin movements and abundance have been correlated with tidal currents (e.g. Shane 1980, Parsons 1998, Mendes et al. 2002), but many of these studies document near-shore situations where small-scale tidal fronts can presumably concentrate prey and attract the dolphins (Mendes et al. 2002). In the middle of Grand Manan Basin, the tides do not produce fronts, but should instead advect passive particles in the familiar tidal ellipse (if lower frequency currents are neglected). We therefore had no expectation that temporal variability in right whale abundance around an arbitrary location would be associated with any particular phase of the tide. The observed correlations among right whale sighting rate, mid-water *Calanus finmarchicus* C5 abundance and within-study tidal state are likely the result of (1) advection of both predator and prey by the tides and (2) small scale (100s of m or less) movements by the right whales to keep them within or near prey patches. From our perspective at a fixed geographic location, the tidal currents carried the whales and the patches of *C. finmarchicus* upon which they were feeding near the station, and thus right whale and mid-water *C. finmarchicus* abundance increased. Then, as the tide turned and tidal currents advected both the whales and the patches away from the station, right whale and *C. finmarchicus* abundance decreased. During DVM 2, it appears that the same mid-water patch of *C. finmarchicus* C5 was sampled just before (and possibly just after) each high tide, and right whale abundance was high whenever the patch was present. If this was indeed a single patch observed on 3 separate occasions, then our data suggest that right whales may remain with a patch for up to a day and over spatial scales of several kilometers. Moreover, these data suggest that a patch can persist at these same temporal and spatial scales despite predation by the whales.

LITERATURE CITED

Båmstedt U, Karlson K (1998) Euphausiid predation on copepods in coastal waters of the Northeast Atlantic. Mar Ecol Prog Ser 172:149–168

Baumgartner MF (2003) Comparisons of *Calanus finmarchicus* fifth copepodite abundance estimates from nets and an optical plankton counter. J Plankton Res 25:855–868

Baumgartner MF, Mate BR (2003) Summertime foraging ecology of North Atlantic right whales. Mar Ecol Prog Ser 264:123–135

Baumgartner MF, Cole TVN, Clapham PJ, Mate BR (2003) North Atlantic right whale habitat in the lower Bay of Fundy and on the SW Scotian Shelf during 1999–2001. Mar Ecol Prog Ser 264:137–154

Beardsley RC, Epstein AW, Chen C, Wishner KF, Macaulay MC, Kenney RD (1996) Spatial variability in zooplankton abundance near feeding right whales in the Great South Channel. Deep-Sea Res II 43:1601–1625

Bollens SM, Frost BW (1989) Zooplanktivorous fish and variable diel vertical migration in the marine planktonic copepod *Calanus pacificus*. Limnol Oceanogr 34:1072–1083

Bollens SM, Frost BW, Thoreson DS, Watts SJ (1992) Diel vertical migration in zooplankton: field evidence in support of the predator avoidance hypothesis. Hydrobiologia 234:33–39

Bowditch N (1995) The American practical navigator. Defense Mapping Agency Hydrographic/Topographic Center, Bethesda, MD

Brown RGB, Gaskin DE (1988) The pelagic ecology of the grey and red-necked phalaropes *Phalaropus fulicarius* and *P. lobatus* in the Bay of Fundy, eastern Canada. Ibis 130:234–250

Campbell RG, Runge JA, Durbin EG (2001) Evidence for food limitation of *Calanus finmarchicus* production rates on the southern flank of Georges Bank during April 1997. Deep-Sea Res II 48:531–549

Dagg MJ (1985) The effects of food limitation on diel migratory behavior in marine zooplankton. Arch Hydrobiol Beih Ergebn Limnol 21:247–255

Dagg MJ (1997) Vertical migration and feeding behavior of *Calanus pacificus* females during a phytoplankton bloom in Dabob Bay, U.S. Limnol Oceanogr 42:974–980

Dagg MJ, Frost BW, Walser WE Jr (1989) Copepod diel migration, feeding, and the vertical flux of pheopigments. Limnol Oceanogr 34:1062–1071

Dale T, Bagøien E, Melle W, Kaartvedt S (1999) Can predator avoidance explain varying overwintering depth of *Calanus* in different oceanic water masses? Mar Ecol Prog Ser 179:113–121

Durbin EG, Campbell RG, Gilman SL, Durbin AG (1995) Abundance, biomass, vertical migration and estimated development rate of the copepod *Calanus finmarchicus* in the southern Gulf of Maine during late spring. Contin Shelf Res 15:571–591

Durbin E, Teegarden G, Campbell R, Cembella A, Baumgartner MF, Mate BR (2002) North Atlantic right whales, *Eubalaena glacialis*, exposed to paralytic shellfish poisoning (PSP) toxins via a zooplankton vector, *Calanus finmarchicus*. Harmful Algae 1:243–251

Geraci JR, Anderson DM, Timperi RJ, St Aubin DJ, Early GA, Prescott JH, Mayo CA (1989) Humpback whales (*Megaptera novaeangliae*) fatally poisoned by dinoflagellate toxin. Can J Fish Aquat Sci 46:1895–1898

Herman AW (1988) Simultaneous measurement of zooplankton and light attenuance with a new optical plankton counter. Contin Shelf Res 8:205–221

Herman AW (1992) Design and calibration of a new optical plankton counter capable of sizing small zooplankton. Deep-Sea Res 39:395–415

Hirche HJ (1996) Diapause in the marine copepod, *Calanus finmarchicus*—a review. Ophelia 44:129–143

Hurley PCF, Corey S, Iles TD (1983) Distributional patterns of chaetognaths in the Bay of Fundy. Can J Zool 61:2257–2265

Ingvarsdóttir A, Houlihan DF, Heath MR, Hay SJ (1999) Seasonal changes in respiration rates of copepodite stage V *Calanus finmarchicus* (Gunnerus). Fish Oceanogr 8(Suppl 1):73–83

International Whaling Commission (IWC) (2001) Report of the workshop on status and trends of western North Atlantic right whales. J Cetacean Res Manage Spec Issue 2:61–87

Kaartvedt S (1996) Habitat preference during overwintering and timing of seasonal vertical migration of *Calanus finmarchicus*. Ophelia 44:145–156

Kenney RD, Kraus SD (1993) Right whale mortality—a correction and an update. Mar Mamm Sci 9:445–446

Kenney RD, Mayo CA, Winn HE (2001) Migration and foraging strategies at varying spatial scales in western North Atlantic right whales: a review of hypotheses. J Cetacean Res Manage Spec Issue 2:251–260

Kirk JTO (1994) Light & photosynthesis in aquatic ecosystems, 2nd edn. Cambridge University Press, Cambridge

Knowlton AR, Kraus SD (2001) Mortality and serious injury of northern right whales (*Eubalaena glacialis*) in the western North Atlantic Ocean. J Cetacean Res Manage Spec Issue 2:193–208

Kraus SD (1990) Rates and potential causes of mortality in North Atlantic right whales (*Eubalaena glacialis*). Mar Mamm Sci 6:278–291

Kulka DW, Corey S, Iles TD (1982) Community structure and biomass of euphausiids in the Bay of Fundy. Can J Fish Aquat Sci 39:326–334

Lass S, Tarling GA, Virtue P, Matthews JBL, Mayzaud P, Buchholz F (2001) On the food of northern krill *Meganyctiphanes norvegica* in relation to its vertical distribution. Mar Ecol Prog Ser 214:177–200

Martin JL, White A (1988) Distribution and abundance of the toxic dinoflagellate *Gonyaulax excavata* in the Bay of Fundy. Can J Fish Aquat Sci 45:1968–1975

Mayo CA, Marx MK (1990) Surface foraging behavior of the North Atlantic right whale, *Eubalaena glacialis*, and associated zooplankton characteristics. Can J Zool 68:2214–2220

Mayo CA, Letcher BH, Scott S (2001) Zooplankton filtering efficiency of the baleen of a North Atlantic right whale, *Eubalaena glacialis*. J Cetacean Res Manage Spec Issue 2:225–229

McClatchie S (1985) Feeding behaviour in *Meganyctiphanes norvegica* (M. Sars) (Crustacea: Euphausiacea). J Exp Mar Biol Ecol 86:271–284

Mendes S, Turrell W, Lütkebohle T, Thompson P (2002) Influence of the tidal cycle and a tidal intrusion front on the spatio-temporal distribution of coastal bottlenose dolphins. Mar Ecol Prog Ser 239:221–229

Mercier FM, Gaskin DE (1985) Feeding ecology of migrating red-necked phalaropes (*Phalaropus lobatus*) in the Quoddy region, New Brunswick, Canada. Can J Zool 63:1062–1067

Murison LD, Gaskin DE (1989) The distribution of right whales and zooplankton in the Bay of Fundy, Canada. Can J Zool 67:1411–1420

Nautical Software (1996) Tides & Currents, version 2.0, users guide, 3rd edn. Nautical Software, Beaverton, OR

Newbury TK (1972) Vibration perception by chaetognaths. Nature 236:459–460

Parsons ECM (1998) The behaviour of Hong Kong's resident cetaceans: the Indo-Pacific hump-backed dolphin and the finless porpoise. Aquat Mamm 24:91–110

Shane SH (1980) Occurrence, movements, and distribution of bottlenose dolphin, *Tursiops truncatus*, in southern Texas. Fish Bull 78:593–601

Sinclair M, Iles TD (1985) Atlantic herring (*Clupea harengus*) distributions in the Gulf of Maine-Scotian Shelf area in relation to oceanographic features. Can J Fish Aquat Sci 42:880–887

Teegarden GJ, Campbell RG, Durbin EG (2001) Zooplankton feeding behavior and particle selection in natural assemblages containing toxic *Alexandrium* spp. Mar Ecol Prog Ser 218:213–226

Torgersen T (2001) Visual predation by the euphausiid *Meganyctiphanes norvegica*. Mar Ecol Prog Ser 209: 295–299

Townsend DW, Pettigrew NR, Thomas AC (2001) Offshore blooms of the red tide organism, *Alexandrium* spp., in the Gulf of Maine. Contin Shelf Res 21:347–369

Turriff N, Runge JA, Cembella AD (1995) Toxin accumulation and feeding behaviour of the planktonic copepod *Calanus finmarchicus* exposed to the red-tide dino-

flagellate *Alexandrium excavatum*. Mar Biol 123:55–64

Watkins WA, Schevill WE (1976) Right whale feeding and baleen rattle. J Mammal 57:58–66

Wiebe PH, Burt KH, Boyd SH, Morton AW (1976) A multiple opening/closing net and environmental sensing system for sampling zooplankton. J Mar Res 34:313–326

Wiebe PH, Morton AW, Bradley AM, Backus RH, Craddock JE, Barber V, Cowles TJ, Flierl GR (1985) New developments in the MOCNESS, an apparatus for sampling zooplankton and micronekton. Mar Biol 87:313–323

Winn HE, Goodyear JD, Kenney RD, Petricig RO (1995) Dive patterns of tagged right whales in the Great South Channel. Contin Shelf Res 15:593–611

Wishner K, Durbin E, Durbin A, Macaulay M, Winn H, Kenney R (1988) Copepod patches and right whales in the Great South Channel off New England. Bull Mar Sci 43: 825–844

Wishner KF, Schoenherr JR, Beardsley R, Chen C (1995) Abundance, distribution and population structure of the copepod *Calanus finmarchicus* in a springtime right whale feeding area in the southwestern Gulf of Maine. Cont Shelf Res 15:475–507

Woodley TH, Gaskin DE (1996) Environmental characteristics of North Atlantic right and fin whale habitat in the lower Bay of Fundy, Canada. Can J Zool 74:75–84

North Atlantic right whales, *Eubalaena glacialis*, exposed to paralytic shellfish poisoning (PSP) toxins via a zooplankton vector, *Calanus finmarchicus*

Edward Durbin [a],*, Gregory Teegarden [b], Robert Campbell [a], Allan Cembella [c],
Mark F. Baumgartner [d], Bruce R. Mate [d]

[a] *Graduate School of Oceanography, University of Rhode Island, Narragansett, RI 02882, USA*
[b] *Saint Joseph's College, 278 Whites Bridge Rd, Standish, ME, USA*
[c] *Institute for Marine Biosciences, National Research Council, 1411 Oxford St., Halifax, NS, Canada*
[d] *College of Oceanic and Atmospheric Sciences, Oregon State University, Corvallis, OR, USA*

Abstract

The seriously endangered north Atlantic right whale (*Eubalaena glacialis*) is regularly exposed to the neurotoxins responsible for paralytic shellfish poisoning (PSP) through feeding on contaminated zooplankton acting as a vector of these dinoflagellate toxins. This chronic exposure occurs during several months each summer while the whales are present on their late summer feeding ground in Grand Manan Basin in the lower Bay of Fundy. Based on estimated ingestion rates, we suggest that these toxins could affect respiratory capabilities, feeding behavior, and ultimately the reproductive condition of the whale population. © 2002 Elsevier Science B.V. All rights reserved.

Keywords: Right whale; *Eubalaena*; Dinoflagellate; *Alexandrium*; Zooplankton; *Calanus*; PSP toxin

1. Introduction

The north Atlantic right whale (*Eubalaena glacialis*) is seriously endangered with fewer than 300 individuals remaining (Knowlton et al., 1994). A switch from a slowly recovering population in the 1980s to a declining one in the 1990s appears to be due to recent increased mortality (Fujiwara and Caswell, 2001) from ship collisions and entanglement with fishing gear (Knowlton and Kraus, 2001). However, lower population growth rates and significantly

less blubber thickness of north Atlantic right whales in comparison with south Atlantic right whales off Argentina and South Africa (Best et al., 2001; Cooke et al., 2001; IWC, 2001; Moore et al., 2001) suggest that environmental factors such as toxic chemical exposure and inadequate nutrition may affect survival or reproductive success. One group of toxic chemicals, organochlorines, are not bioaccumulated to levels that are hazardous (Weisbrod et al., 2000) and are thus not likely to be the cause of the poor condition of northern right whales. Another possibility would be through the effects of biotoxins. In New England waters, humpback whales have been killed by eating Atlantic mackerel which contained the potent tetrahydropurine neurotoxins responsible for paralytic shellfish

---

* Corresponding author. Tel.: +1-401-874-6850;
fax: +1-401-874-6853.
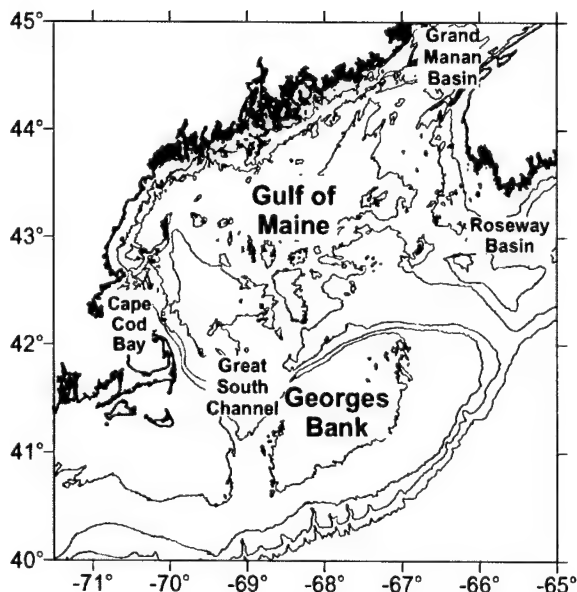*E-mail address:* edurbin@gso.uri.edu. (E. Durbin).

Fig. 1. The continental shelf region off northeastern United States and southeastern Canada showing right whale feeding habitats referred in the text. Isobaths shown are 50, 100, 200 and 1000 m.

poisoning (PSP) (Geraci et al., 1989). In the Gulf of Maine, these toxins are produced by the dinoflagellate *Alexandrium fundyense* and related species, and presumably were obtained by the mackerel through ingestion of contaminated zooplankton. In higher mammals, exposure to PSP toxins, comprising about two dozen naturally occurring derivatives of saxitoxin (STX), can cause neuropathology (including muscle paralysis) by blocking sodium-channel activity associated with neuro-muscular co-ordination. Ingestion of these toxins by right whales could affect respiratory capabilities, feeding behavior, and ultimately the reproductive condition of the whale population.

Right whales can be found in Grand Manan Basin in the lower Bay of Fundy (Fig. 1) during the late summer (Kraus et al., 1982; Winn et al., 1986) where they feed on the lipid rich, older stages of the large copepod *Calanus finmarchicus* (Murison and Gaskin, 1989; Woodley and Gaskin, 1996). This copepod species is known to graze on blooms of *A. fundyense* (Turriff et al., 1995; Teegarden, 1999) which regularly occur in Grand Manan Basin during the summer (Martin and White, 1988; Townsend et al., 2001). Although toxin assimilation in copepods is quite inefficient, high body burdens of PSP toxins may be accumulated during

natural or simulated blooms (Teegarden et al., 1996). Here, we provide evidence for chronic exposure of north Atlantic right whales to PSP toxins from feeding directly on contaminated *C. finmarchicus*. Our results are based on observations of *A. fundyense* abundance, zooplankton toxicity and abundance, and right whale feeding behavior during cruises to Grand Manan Basin in late July 2001 and August 2001.

2. Methods

2.1. Phytoplankton and zooplankton sampling

Sampling was conducted during a NOAA Ship *Albatross IV* cruise (AL0108) from 23 July 2001 to 3 August 2001. *A. fundyense* surface samples were collected with a 20 l bucket, concentrated with a 20 μm mesh net, and counted immediately. Zooplankton were sampled with a 1 m² MOCNESS (0.15 mm mesh nets) at stations near feeding right whales and at two 24-h anchor stations. Prior to each MOCNESS tow, vertical casts were conducted with an optical plankton counter (OPC, Focal Technologies; Herman, 1988, 1992). The OPC, which measured the vertical distribution of particles between 0.25 and 20 mm, provided estimates of *C. finmarchicus* fifth copepodids (C5) using a calibration equation developed from comparisons with net samples (Baumgartner, 2002). Five contiguous depth strata were typically sampled with the MOCNESS and the size of each stratum was selected after examining the results of the preceding OPC casts. At the two anchor stations, MOCNESS samples were collected every 6 or 12 h.

2.2. Toxin analysis

Immediately after the MOCNESS net was retrieved, groups of 100 *C. finmarchicus* C5, the dominant taxon, were placed into vials and frozen (−20 °C) and the remaining sample preserved in 4% buffered formaldehyde for later enumeration. The frozen zooplankton samples were processed and analysed for the complete spectrum of PSP toxins by high-performance liquid chromatography with fluorescence detection (HPLC-FD) (Teegarden et al., 1996; Parkhill and Cembella, 1999). After extraction in 0.1 M acetic acid by ultrasonication (30 s at 25 W;

50% pulse duty cycle) and centrifuge–filtration of the suspension through a 0.45 μm membrane (Millipore Ultrafree-MC, Bedford, MA), duplicate injections of 20 μl of extract were compared with external toxin standards (PSP-1C) provided by the Certified Reference Material Program (CRMP) of the Institute for Marine Biosciences, NRC, Halifax, Canada. Toxin concentrations (μmol/l) were converted by the formula given in Parkhill and Cembella (1999) to toxicity units (in saxitoxin equivalents [STXeq.] per copepod).

The presence of specific PSP toxin analogues was confirmed by subsequent analysis of the copepod filtrate by hydrophilic-interaction liquid chromatography with detection by tandem mass spectrometry (HILIC-MS/MS) (Quilliam et al., 2001). The analyses were performed on an Agilent (Palo Alto, CA) HP1090 LC system with detection by a Perkin-Elmer SCIEX (Concord, Ont., Canada) API-III+ triple quadrupole mass spectrometer equipped with an ion-spray source. Qualitative analyses were carried out in positive ion mode by both full scan and selected reaction monitoring (SRM).

2.3. Right whale ingestion rates

Ingestion rates of copepods by right whales are based on (1) estimated in situ feeding rates from observations during a cruise immediately following AL0108 (Baumgartner, 2002), and (2) an assumption of a fixed weight-specific feeding rate. Weight-specific ingestion rates of PSP toxins were determined from these copepod ingestion rates, observed copepod toxicity and a right whale weight of 40,000 kg (Kenney et al., 1986).

Right whales were tagged with suction-cup mounted, recoverable, time-depth recorders (TDR; Wildlife Computers Inc.) in Grand Manan Basin during a NOAA Ship *Delaware II* cruise (DE0108) from 7–31 August 2001 (Baumgartner, 2002). These tags were attached to right whales from a 7.5 m rigid-hulled inflatable boat (RHIB) using a 9 m telescoping pole. The TDR measured pressure at a port exposed to the seawater and logged the corresponding depth of the tag at a resolution of 2 m once every second. The tagged whales were tracked visually and via radio and acoustic transmitters incorporated in the tag. Precise diving and resurfacing locations were obtained from the RHIB using a global positioning

system (GPS) device. Shortly after obtaining a resurfacing location after a long dive, a vertical cast was conducted with an OPC at this same location from the NOAA Ship *Delaware II*. The abundance of *C. finmarchicus* C5 was estimated from these OPC data in 4 m depth strata. After detachment from the whale, the positively buoyant tag was recovered from the water and the archived data were downloaded. Successful attachment durations were between 1.1 and 2.0 h. Presumed feeding dives were characterized by a rapid descent, remarkable fidelity to a narrow depth strata for 4.7–13.6 min (median = 9.4 min) and a rapid ascent back to the surface.

Ingestion of *C. finmarchicus* C5 for feeding dives was estimated as the product of the filtration efficiency of right whale baleen, the mouth area, the swimming speed, the concentration of *C. finmarchicus* C5 available to the whale and the time at depth (excluding descent and ascent periods). We assumed filtration efficiency for *C. finmarchicus* C5 to be 100% and the mouth area to be 1.21 m^2 (Mayo et al., 2001). Swimming speeds were estimated from the diving and resurfacing positions, but these are likely underestimates of the true swimming speeds since right whales may not always feed along straight paths at depth (Mayo and Marx, 1990; Nowacek, personal communication). Therefore, the swimming speed was assumed to be 1.5 m/s whenever the estimated speed was less than 1.5 m/s (Watkins and Schevill, 1976). Tagged right whales consistently dove to and foraged at the depth of maximum *C. finmarchicus* C5 abundance (Baumgartner, 2002), so the concentration of *C. finmarchicus* C5 available to the whale was assumed to be the maximum concentration in the water column observed by the OPC. Ingestion rates were computed as the total estimated ingestion for all observed feeding dives divided by the duration of the deployment period.

The second approach assumed that right whales eat 4% of their body weight per day (Sergeant, 1969). Assuming that the typical *C. finmarchicus* C5 individual contains 150 μg C (Durbin et al., 1995a), has a carbon content of 55% dry weight (R. Campbell, unpublished), and a water content of 84% (Bamstedt et al., 1986), the estimated wet weight is 1.7 mg. The ingestion rate of *C. finmarchicus* C5 is then estimated to be 9.41×10^8 copepods per day based on a right whale weight of 40,000 kg (Kenney et al., 1986).
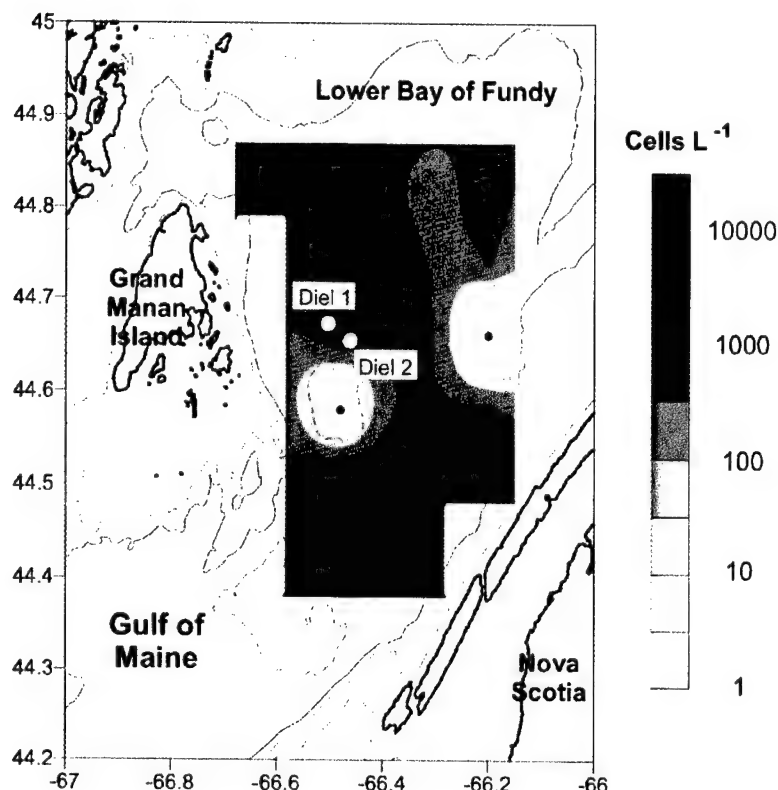
Fig. 2. Surface concentrations of *Alexandrium fundyense* in Grand Manan Basin during 25–26 July 2001. Concentrations are $\log_{10}$ cells/l.

3. Results

A bloom of *A. fundyense* was present in Grand Manan Basin during the cruise (23 July 2001 to 3 August 2001) at cell concentrations of up to 10,400 per liter (Fig. 2). The dominant zooplankter was the copepod *C. finmarchicus*, primarily as stage C5. At two 24-h anchor stations in the right whale feeding area where repeated MOCNESS casts were made, C5 individuals comprised an average of 79 and 94%, respectively, of the *C. finmarchicus* population. At the first anchor station (Diel 1), two *C. finmarchicus* populations were present: (1) an actively feeding and growing surface population comprised of primarily C5, but also containing some C4 and adult females, that was undergoing diel vertical migration, and (2) a deep population of non-migrating C5 individuals between 100 and 180 m, presumably in diapause (Fig. 3). Within the migrating population, C4 and C5 only appeared to be migrating within the upper part of the water column and

did not move down into the diapausing layer during the day, while the adult females were migrating through the whole water column. In contrast, at the second anchor station (Diel 2), most of the population consisted of non-migrating deep dwelling C5. This deep population typically formed a dense layer near the top of a bottom mixed-layer (Fig. 4; Baumgartner, 2002).

Both surface and deep populations of *C. finmarchicus* contained substantial PSP toxin levels when converted to toxicity units (ng STXeq.). Overall mean toxicity of surface (0–60 m) and deep (75–200 m) C5 individuals was 0.87 ng STXeq. per copepod, (100 individuals per sample, $n = 28$, S.D. $= 0.33$, range $= 0.27–1.59$) and 0.41 ng STXeq. per copepod, ($n = 31$, S.D. $= 0.18$, range $= 0.09–0.73$), respectively. There were day–night differences in the mean toxicity of the surface C5 copepodites but not among copepods collected at depth. In the two diel studies, daytime toxicity of surface animals was 0.95 and 0.24 ng STXeq. per copepod while night-time values were 1.51 and
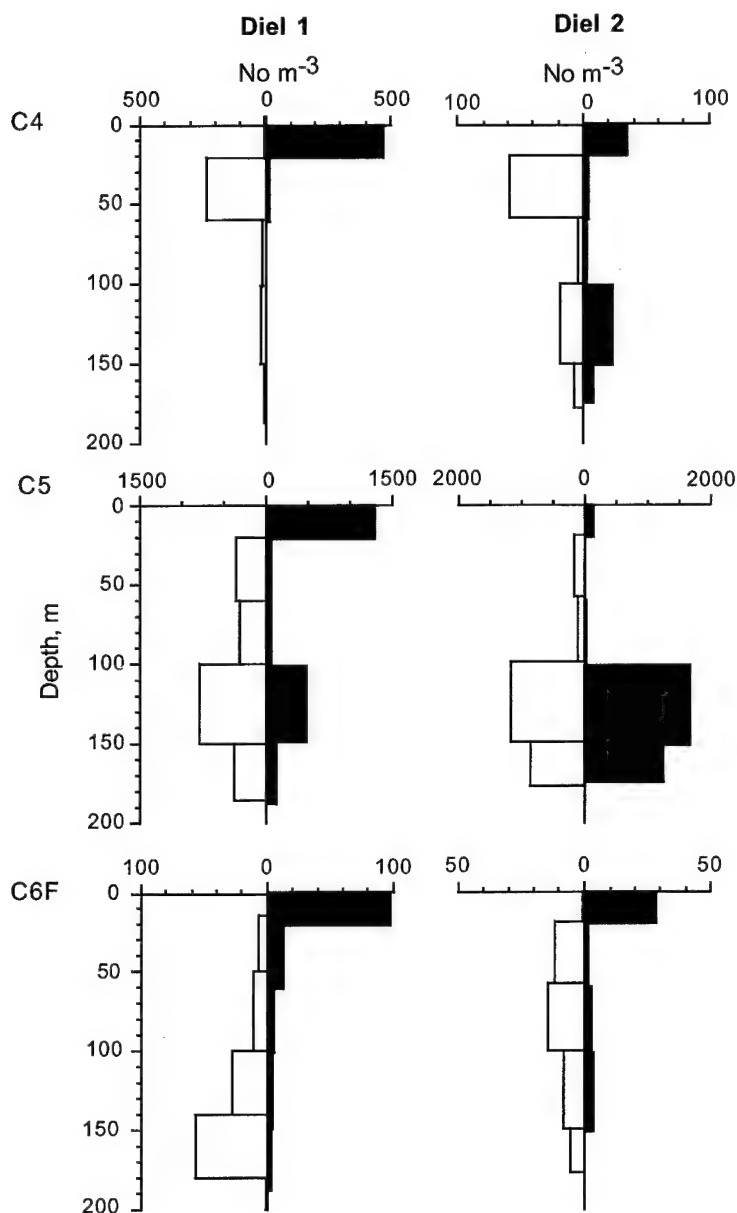
Fig. 3. Day and night *Calanus finmarchicus* C4, C5 and adult female abundance (per m^3) at two anchor stations in Grand Manan Basin during 29–30 July 2001 (Diel 1) and 31 July 2001 to 1 August 2001 (Diel 2). Data are from 1 m^2 MOCNESS samples. At each anchor station, a single night MOCNESS cast was made while the day data are the mean of 3 (Diel 1) and 2 (Diel 2) MOCNESS casts.

0.74 ng STXeq. per copepod, respectively, reflecting higher feeding rates at night. Molar composition profiles indicated a high proportion of potent carbamate derivatives, with neosaxitoxin, saxitoxin, and gonyautoxins contributing 40, 20, and 27%, respectively, to the toxin content of copepod tissues.

Right whales were present in Grand Manan Basin during the period of study and actively feeding at depth on thin dense layers of resting *C. finmarchicus* C5 populations (Fig. 4). The average concentrations of *C. finmarchicus* C5 encountered by tagged, feeding right whales ranged between 3020 and 11,900 copepods/m^3
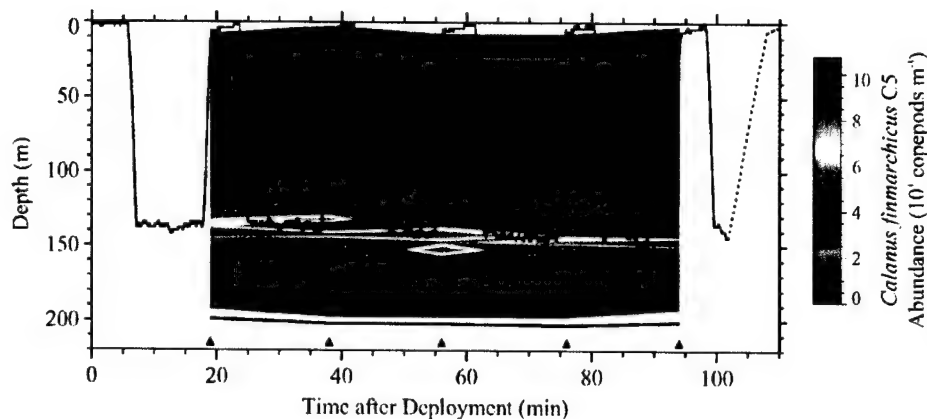
Fig. 4. Foraging behavior of a TDR-tagged right whale in Grand Manan Basin. The whale's dive profile is shown as a solid line and the vertical distribution of *Calanus finmarchicus* C5 along the whale's track is shown shaded in color. The triangles indicate the time at which a resurfacing was observed. A CTD/OPC cast was conducted at the location of each resurfacing shortly after the resurfacing occurred. The dotted line indicates the portion of the TDR record when the tag was detached from the whale. Data from Baumgartner (2002).

($n = 13$, mean = 5742, S.D. = 2832). Estimated ingestion rates for the tagged whales averaged 4.61×10^8 copepods per day ($n = 13$, S.D. = 2.81×10^8, range = 7.4×10^7 to 1.08×10^9). Ingestion rates of PSP toxin by these whales were substantial when expressed in toxicity units. Based on a toxin content of 0.41 ng STXeq. per copepod (the toxicity of the deep copepods), the estimated PSP toxin ingestion rate averaged 4.73 μg STXeq./(kg right whale per day) ($n = 13$, S.D. = 2.88, range = 0.76–11.03). Alternatively, if right whales consume 4% of their body weight per day (Sergeant, 1969), then the PSP toxin ingestion rate would be 9.65 μg STXeq./(kg right whale per day).

4. Discussion and Conclusions

These results clearly demonstrate that right whales are ingesting substantial amounts of PSP toxin while feeding on *C. finmarchicus*, the dominant copepod in their late summer feeding ground in Grand Manan Basin. Because the blooms of *A. fundyense* are a regular occurrence during the summer in this region (Martin and White, 1988; Townsend et al., 2001; the present study) this exposure to PSP toxins is also likely to be a regular occurrence. The actual level of exposure will depend upon the toxin content of the zooplankton in addition to the total ingestion of zooplankton by right whales. In the present study, the

right whales were feeding at depth, therefore their toxin intake was lower than it may have been if they had been feeding on the much more toxic surface copepods.

The differences in toxin content of the migrating and the deep, non-migrating populations of *C. finmarchicus* reflect differences in their physiological status. The migrating copepods were actively feeding at the surface at night and their toxin content will be influenced by their immediate feeding conditions, particularly the proportion as well as the total amount of toxic *A. fundyense* in their diet. The day–night differences in toxin content we observed (with higher toxin levels at night) presumably reflect the higher feeding rates of *C. finmarchicus* at night that have been observed elsewhere in the Gulf of Maine (Durbin et al., 1995b). Decreased daytime toxicity is the result of both evacuation of feces as well as fairly rapid short-term depuration processes (Teegarden, 1999). Laboratory studies show that metabolically active, feeding copepods typically accumulate an "equilibrium maximum" body burden within 48 h of initiating feeding on toxic *Alexandrium* spp., either as sole food or in mixed assemblages of phytoplankton; loss of these toxins is also rapid when ingestion of toxic cells ceases, with usually 90% removed within 48 h (Teegarden, 1999).

The toxin content of these feeding copepods was lower than levels observed in adult female *C. fin-*

marchicus feeding on relatively dense cultures of *A. fundyense* where values of 4 μg STXeq./g wet weight copepod tissue were observed (Turriff et al., 1995). Assuming a copepod wet weight of 1.7 mg, this corresponds to a value of approximately 7 ng STXeq. per copepod which is considerably higher than our night-time values of 1.5 and 0.74 ng STXeq. per copepod. Presumably, the potential exists for much higher values in the field if *A. fundyense* concentrations are sufficiently high.

The presence of significant levels of toxin in the deep non-migrating C5 was surprising. These copepods were observed to have no food in their guts and were presumably in, or entering, diapause when metabolic rates are reduced (Hirche, 1996). In the Gulf of Maine, *C. finmarchicus* undergoes an ontogenetic migration to depth during the summer and enters diapause (Durbin et al., 2000). Most of the population remains in diapause until the following December and January when they mature to the adult stage, return to the surface, and begin feeding and reproducing (Durbin et al., 1997, 2000). It is possible that the non-migrating copepods we observed at depth in Grand Manan Basin had just undergone their ontogenetic migration to depth and were entering diapause. Depuration rates will be lower in these diapausing copepods than actively growing individuals and we might expect toxin content to slowly decline with time. However, there is no information on this, and clearly experiments are needed to investigate retention rates of toxins by these resting copepods.

The presence of toxin in the resting *C. finmarchicus* in Grand Manan Basin may also indicate that these copepods had previously been feeding at the surface in this region before descending rather than being advected in from outside and accumulating in the basin. A potential source region is the westward flowing current along the south of Nova Scotia carrying copepods from the Scotian Shelf. However, surveys in this current have shown *A. fundyense* to be absent (Townsend et al., 2001), which would preclude this option.

The estimated toxin ingestion rates of right whales in Grand Manan Basin are substantial and are similar to the estimated minimum lethal oral dose for humans of 7–16 μg STXeq./kg (Evans, 1972; Schantz et al., 1975). While there is no direct evidence of PSP toxin-related deaths of right whales, we suggest that during their prolonged summer feeding period in this region, they would be experiencing chronic exposure to PSP toxins. Such toxins are potent sodium-channel blockers in muscles and membranes and affect nerve function (Rao, 1993), thus they are likely to have both physiological and behavioral effects. Since PSP toxins are highly water soluble, they are readily absorbed through the gastrointestinal mucosa. They would not be retained in lipophilic tissues such as blubber, but would tend to be transferred from the digestive tract to physiologically active tissues supplied by circulating blood. Initial symptoms of PSP toxicity include parethesia and numbness and a weakening of muscles. In high doses, the PSP toxicity syndrome in mammals is characterized by respiratory difficulties, which may cause death in the absence of ventilatory support (Rao, 1993). These symptoms have led to the suggestion that after ingestion of PSP toxins, whales may lose control over peripheral heat-conserving mechanisms and respiratory capabilities (Geraci et al., 1989).

We suggest that although PSP toxins do not tend to bioaccumulate in most mammalian tissues, chronic effects of repeated PSP toxin exposure will be seen in measures of diving capabilities, including dive times, swimming speeds while at depth, and frequency of dives. Impaired diving capabilities in right whales would lead to reduced ingestion rates and may be a possible explanation for their poorer condition and reduced calving rates despite the high concentrations of *C. finmarchicus* in Grand Manan Basin. Possible evidence of such an effect comes from recent increases in calving intervals for right whales. Right whale occurrence in the lower Bay of Fundy has increased since the abandonment of the summertime Roseway Basin habitat on the Scotian Shelf during 1992–1993 (Kraus et al., 2001). From 1980 to 1993, calving intervals averaged 3.7 years, however, from 1993 to 1998, calving intervals increased significantly to 5.1 years (Kraus et al., 2001). There was no temporal trend in calving intervals prior to 1993 ($n = 87$, $r = 0.168$, $P = 0.12$; Kraus et al., 2001, Table 2), but calving intervals increased significantly at a rate of 4 months per year from 1993 to 1998 ($n = 38$, $r = 0.441$, $P = 0.0056$; Kraus et al., 2001, Table 2). These results suggest that abandonment of Roseway Basin and increased use of the lower Bay of Fundy has been accompanied by increasing calving intervals.

Other effects of toxin ingestion on "whale fitness" may be greater susceptibility to disease, reproductive

failure, disruption of migration and mechanical damage (e.g. by collisions with ships or fouling in nets and other fishing gear). For example, recovery from dives during periods of PSP exposure would likely be longer than normal, and increased time at the surface would increase a whale's chances of being hit by a ship. In fact, Moore et al. (2001) indicate that right whales in Grand Manan Basin do indeed remain at the surface longer and take more breaths per surfacing than whales encountered in Cape Cod Bay. We suggest that these observations are related to PSP toxin exposure. The significance of ingested PSP toxins on the survival of right whales should not be underestimated. Few studies have been conducted on the effects of chronic exposure to PSP toxins or other sodium-channel blocking agents in higher mammals, and no previous data are available on the sub-lethal effects of PSP toxins in cetaceans. Nevertheless, our findings are the first to suggest that physiological impairment via exposure to high dosages of PSP toxins through the food chain may compromise the health of a population.

Acknowledgements

References

Bamstedt, U., 1986. Chemical composition and energy content. In: Corner, E.D.S., O'Hara, S.C.M. (Eds.), The Biological Chemistry of Marine Copepods. Clarendon Press, Oxford, pp. 1–58.

Baumgartner, M.F., 2002. Right whale ecology in the northwest Atlantic Ocean. Ph.D. Thesis. Oregon State University, Corvallis, OR, USA.

Best, P.B., Brandao, A., Butterworth, D.S., 2001. Demographic parameters of southern right whales of South Africa (special issue). J. Cetacean Res. Manage. 2, 161–169.

Cooke, J.G., Rowntree, V.J., Payne, R., 2001. Estimates of demographic parameters for southern right whales (Eubalaena australis) observed of Peninsula Valdes, Argentina (special issue). J. Cetacean Res. Manage. 2, 125–132.

Durbin, E.G., Gilman, S.L., Campbell, R.G., Durbin, A.G., 1995a. Abundance, vertical migration patterns and in situ growth of Calanus finmarchicus in the southern Gulf of Maine during late spring. Cont. Shelf Res. 15, 571–592.

Durbin, E.G., Campbell, R.G., Gilman, S.L., Durbin, A.G., 1995b. In situ feeding of Calanus finmarchicus in the southern Gulf of Maine during late spring. Cont. Shelf Res. 15, 539–570.

Durbin, E.G., Runge, J.A., Campbell, R.G., Garrahan, P.R., Casas, M.C., Plourde, S., 1997. Late fall–early winter recruitment of Calanus finmarchicus on Georges Bank. Mar. Ecol. Progr. Ser. 151, 103–114.

Durbin, E.G., Garrahan, P.R., Casas, M.C., 2000. Abundance and distribution of Calanus finmarchicus on Georges Bank during 1995 and 1996. ICES J. Mar. Sci. 57, 1664–1685.

Evans, M.H., 1972. Tetrodotoxin, saxitoxin, and related substances: their applications in neurobiology. Int. Rev. Neurobiol. 15, 83–176.

Fujiwara, M., Caswell, H., 2001. Demography of the endangered north Atlantic right whale. Nature 414, 537–541.

Geraci, J.R., Anderson, D.M., Timperi, R.J., St. Aubin, D.J., Early, G.A., Prescott, J.H., Mayo, C.A., 1989. Humpback whales (Megatpera novaengliae) fatally poisoned by dinoflagellate toxin. Can. J. Fish. Aquat. Sci. 46, 1895–1898.

Herman, A.W., 1988. Simultaneous measurement of zooplankton and light attenuance with a new optical plankton counter. Cont. Shelf Res. 8, 205–221.

Herman, A.W., 1992. Design and calibration of a new optical plankton counter capable of sizing small zooplankton. Deep Sea Res. 39, 395–415.

Hirche, H.-J., 1996. Diapause in the marine copepod, Calanus finmarchicus: a review. Ophelia 44, 129–143.

International Whaling Commision, Report on the Workshop on Comprehensive Assessment of Right Whales: a world-wide comparison (special issue). J. Cetacean Res. Manage. 2 (2001) 1–60.

Kenney, R.D., Hyman, M.A.M., Owen, R.E., Scott, G.P., Winn, H.E., 1986. Estimation of prey densities required by western north Atlantic right whales. Mar. Mamm. Sci. 2, 1–13.

Knowlton, A.R., Kraus, S.D., 2001. Mortality and serious injury of northern right whales (Eubalaena glacialis) in the western north Atlantic Ocean (special issue). J. Cetacean Res. Manage. 2, 193–208.

Knowlton, A.R., Kraus, S.D., Kenney, R.D., 1994. Reproduction in north Atlantic right whales (Eubalaena glacialis). Can. J. Zool. 72, 1297–1305.

Kraus, S.D., Prescott, J.H., Turnbull, P.V., Reeves, R.R., 1982. Preliminary notes on the occurrence of the north Atlantic right whale (Eubalaena glacialis) in the Bay of Fundy (special issue). Rep. Int. Whale Commun. 32, 407–411.

Kraus, S.D., Hamilton, P.K., Kenney, R.D., Knowlton, A.R., Slay, C.K., 2001. Reproductive parameters of the north Atlantic right whale. J. Cetacean Res. Manage. 2, 321–336.

Martin, J.L., White, A., 1988. Distribution and abundance of the toxic dinoflagellate *Gonyaulax excavata* in the Bay of Fundy. Can. J. Fish. Aquat. Sci. 45, 1968–1975.

Mayo, C.A., Marx, M.K., 1990. Surface foraging behavior of the north Atlantic right whale, *Eubalaena glacialis*, and associated zooplankton characteristics (special issue). Can. J. Zool. 68, 2214–2220.

Mayo, C.A., Letcher, B.H., Scott, S., 2001. Zooplankton filtering efficiency of the baleen of a north Atlantic right whale, *Eubalaena glacialis*. J. Cetacean Res. Manage. 2, 225–229.

Moore, M.J., Miller, C.A., Morss, M.S., Arthur, R., Lange, W.A., Prada, K.G., Marx, M.K., Frey, E.A., 2001. Ultrasonic measurement of blubber thickness in right whales (special issue). J. Cetacan Res. Manage. 2, 301–309.

Murison, L.D., Gaskin, D.E., 1989. The distribution of right whales and zooplankton in the Bay of Fundy, Canada. Can. J. Zool. 67, 1411–1420.

Parkhill, J.P., Cembella, A.D., 1999. Effects of salinity, light, and inorganic nitrogen on growth and toxigenicity of the marine dinoflagellate *Alexandrium tamarense* from northeastern Canada. J. Plank. Res. 21, 939–955.

Quilliam, M.A., Hess, P., Dell'Aversano, C., 2001. Methods of saxitoxin analysis. In: de Koe, W.J., Samson, R.A., van Egmond, H.P., Gilbert, G., Sabino, M. (Eds.), Mycotoxins and Phycotoxins in Perspective at the Turn of the Millennium, AOAC International, Wageningen, Netherlands, pp. 383–391.

Schantz, E.J., Ghazzarossian, V.E., Schnoes, H.K., Strong, F.M., Stringer, J.P., Pezzanite, J.O., Clardy, J., 1975. Paralytic poisons from marine dinoflagellates, In: LoCicero, V.R. (Ed.), Toxic Dinoflagellate Blooms. MA Sci. Technol. Found., Wakefield, MA, pp. 267–274.

Sergeant, D.E., 1969. Feeding rates of cetacea. FiskDir. Skr. Ser. HavUnders. 15, 246–258.

Rao, C.Y., 1993. Paralytic shellfish poisoning. In: Falconer, I.I.R. (Ed.), Algal Toxins in Seafood and Drinking Water. London. Academic Press, pp. 75–86.

Teegarden, G.J., 1999. Mechanisms, Ecology, and Toxicology of Zooplankton Feeding Processes in the Presence of Harmful Algae (*Alexandrium* spp.). Ph.D. Thesis. University of Rhode Island, Kingston, RI, USA.

Teegarden, G.J., Cembella, A.D., 1996. Grazing of toxic dinoflagellates (*Alexandrium* spp.) by estuarine copepods: particle selection and PSP toxins in marine food webs. In: Yasumoto, T., Oshima, Y., Fukuyo, Y. (Eds.), Harmful and Toxic Algal Blooms. Intergovernmental Oceanographic Commission of UNESCO, pp. 393–396.

Townsend, D.W., Pettigrew, N.R., Thomas, A.C., 2001. *Alexandrium* sp. in the Gulf of Maine. Cont. Shelf Res. 21, 347–369.

Turriff, N., Runge, J.A., Cembella, A.D., 1995. Toxin accumulation and feeding behaviour of the planktonic copepod *Calanus finmarchicus* exposed to the red-tide dinoflagellate *Alexandrium excavatum*. Mar. Biol. 123, 55–64.

Watkins, W.A., Schevill, W.E., 1976. Right whale feeding and baleen rattle. J. Mamm. 57, 58–66.

Weisbrod, A.V., Shea, D., Moore, M.J., Stegeman, J.J., 2000. Organochlorine exposure and bioaccumulation in the endangered northwest Atlantic right whale (*Eubalaena glacialis*) population. Environ. Toxicol. Chem. 19, 654–666.

Winn, H.E., Price, C.A., Sorensen, P.W., 1986. Distributional biology of the right whale in the western north Atlantic (special issue). Rept. Int. Whal. Commun. 10, 129–138.

Woodley, T.H., Gaskin, D.E., 1996. Environmental characteristics of north Atlantic right and fin whale habitat in the lower Bay of Fundy. Canada. Can. J. Zool. 74, 75–84.

Dive and surfacing characteristics of bowhead whales (*Balaena mysticetus*) in the Beaufort and Chukchi seas

Gregory K. Krutzikowsky and Bruce R. Mate

Abstract: We received data from eight bowhead whales (*Balaena mysticetus*) equipped with satellite-monitored radio tags for 3–33 days. Of 42 306 dives made by the eight whales during 1695 h, 9573 were sounding dives (>1 min duration). The mean duration of sounding dives for individuals varied from 6.9 to 14.1 min (mean = 10.4 ± 2.4 min, n = 8). Five whales made dives ≥61 min; the longest dives for the other three lasted 56, 45, and 32 min. Five tags measured maximum depths of 29 499 dives during 1220 h and time at depth during 1228 h. All five whales dived >100 m; the deepest dive was 352 m. Whales spent most of their time at depths ≤16 m, but three whales spent most of their time at depths >48 m during some sampling periods. Mean surfacing rates ranged from 18.2 to 47.0/h (mean = 26.2 ± 9.0/h, n = 8). Tags were exposed to air for 4.0–7.3% of the time (mean = 5.5 ± 0.95%, n = 8), and whales were potentially visible from aircraft for 8.5–16.4% of the time (mean = 11.1 ± 2.4%, n = 8). Three whales made longer sounding dives and had lower surfacing rates when in ≥90% ice cover. No consistent diel patterns were found.

Résumé : Nous avons reçu des données sur huit Baleines boréales (*Balaena mysticetus*) munies d'émetteurs-radio contrôlés par satellite durant une période de 3 à 33 jours. De 42 306 plongées faites par huit baleines au cours de 1695 h, 9573 étaient des plongées d'exploration (>1 min). La durée moyenne des plongées d'exploration allait de 6,9 à 14,1 min (la moyenne = 10,4 ± 2,4 min, n = 8). Cinq des baleines ont fait des plongées de ≥61 min et les plongées les plus longues enregistrées chez les trois autres ont duré 56, 45 et 32 min. Cinq marqueurs ont mesuré les profondeurs maximales de 29 499 plongées au cours d'une période de 1220 h et mesuré le temps passé aux différentes profondeurs durant 1228 h. Les cinq baleines ont plongé à plus de 100 m; la plus grande profondeur atteinte au cours d'une plongée a été de 352 m. Les baleines ont passé la plus grande partie de leur temps à des profondeurs de ≤16 m, mais trois d'entre elles sont restées à plus de 48 m au cours de certaines périodes. Les taux moyens de retour en surface allaient de 18,2 à 47,0/h (la moyenne = 26,2 ± 9,0/h, n = 8). Les marqueurs ont été exposés à l'air de 4,0 à 7,3 % du temps (la moyenne = 5,5 ± 0,95 %, n = 8) et les baleines pouvaient être vues d'un aéronef de 8,5 à 16,4 % du temps (la moyenne = 11,1 ± 2,4 %, n = 8). Trois baleines ont fait des plongées exploratoires plus longues et elles avaient des taux de retour en surface moins importants lorsque la couverture de glace était de ≥90 %. Nous n'avons pas trouvé de patterns quotidiens bien définis.

[Traduit par la Rédaction]

Introduction

Until recently, researchers were unable to investigate the dive and surfacing behavior of cetaceans in the wild unless individual animals were readily visible and identifiable. The advent of microprocessor-controlled data loggers linked with miniature satellite radiotelemetry equipment has helped to change this situation. Data can now be gathered around the clock on free-ranging cetaceans worldwide (e.g., Martin and Smith 1992; Mate et al. 1994, 1995; Martin et al. 1994; Heide-Jørgensen and Dietz 1995; Davis et al. 1996). Here we present the first satellite-monitored radiotelemetry data on the dive and surfacing characteristics of bowhead whales (*Balaena mysticetus*) in waters that seasonally host (Moore and Reeves 1993) the largest remaining population of this species (Zeh et al. 1993).

Although this endangered species (Klinowska 1991) is no longer hunted commercially, subsistence hunting of the Bering Sea stock continues (Stoker and Krupnik 1993). Concern about whether other human activities such as mineral exploitation, shipping, and pollution threaten this population have led to numerous studies of bowhead whales in the Beaufort and Chukchi seas (Montague 1993). Studies of the surfacing and diving habits of bowhead whales provide information that is useful to management agencies, as well as clues for interpreting whale behavior. Dive, surfacing, and respiration patterns are used to calculate detection probabilities, to estimate the proportion of time whales are visible from the air (Carroll and Smithhisler 1980; Würsig et al. 1984; Dorsey et al. 1989; Zeh et al. 1993), and to adjust abundance estimates from survey data (Davis et al. 1982;

G.K. Krutzikowsky.[1] Oregon State University, College of Oceanic and Atmospheric Sciences, Hatfield Marine Science Center, Newport, OR 97365, U.S.A.
B.R. Mate. Oregon State University, Department of Fisheries and Wildlife, Coastal Oregon Marine Experiment Station, Hatfield Marine Science Center, Newport, OR 97365, U.S.A.

[1]Author to whom all correspondence should be sent at the following address: Oregon State University, Cooperative Institute for Marine Resource Studies, Hatfield Marine Science Center, Newport, OR 97365, U.S.A. (e-mail: greg.krutz@hmsc.orst.edu).

Table 1. Data collected by satellite-monitored radio tags deployed on bowhead whales in 1992.

Tag No.	Date tagged	Date first data received	Date last data received	No. of sampling periods			
				Duration[a]	Depth[b]	TAD[c]	Locations
D-1	6 Sept.	5–6 Sept.	5–29 Sept.	33	—	—	9
D-2	6 Sept.	3–6 Sept.	5–22 Sept.	49	—	—	13
DZ-1	2 Sept.	1–3 Sept.	2–5 Oct.	222	220	223	136
DZ-2	2 Sept.	3–3 Sept.	7–10 Sept.	42	44	46	18
DZ-3	5 Sept.	8–5 Sept.	6–8 Sept.	19	12	15	5
DZ-4	3 Sept.	8–3 Sept.	6–14 Sept.	78	76	78	52
DZ-5	3 Sept.	1–4 Sept.	7–12 Sept.	59	55[d]	53[d]	28
DZ-6	4 Sept.	1–5 Sept.	6–14 Sept.	63	58	54	30

[a]D tags reported the number of dives in eight duration categories: 0–1 ($\pm$3.5), 1–4, 4–7, 7–10, 10–13, 13–16, 16–19, and >19 min; the longest dive (13–71 $\pm$ 1 min); the longest surfacing (1.5–30.5 $\pm$ 0.5 min); and total time spent under water (68.4–180.0 $\pm$ 0.9 min). DZ tags reported the number of dives in nine duration categories: 0–1 ($\pm$4), 1–4, 4–7, 7–10, 10–13, 13–16, 16–19, 19–25, and >25 min; the longest dive (0–60 $\pm$ 1 min); and the duration of the first dive to the maximum depth (0–60 $\pm$ 1 min).

[b]DZ tags reported the number of dives in eight depth categories: 0–16 ($\pm$1), 17–32 ($\pm$1), 33–48, 49–96, 96–200, 200–400, 400–800, and >800 m; and the deepest dive (0–1024 $\pm$ 8 m).

[c]Time at depth. DZ tags reported time spent in eight depth categories ($\pm$1.8 min): 0–16, 16–32, 32–48, 48–96, 96–200, 200–400, 400–800, and >800 m; the longest surfacing (0–62 $\pm$ 0.5 min); and total time spent at the surface (0–126 $\pm$ 0.5 min).

[d]The depth sensor for this tag was faulty. Only the total numbers of dives and surface times were used from the depth and TAD packets.

Hiby and Hammond 1989). Respiration rates are used to estimate energetic budgets (Thomson 1987). Factors that may affect the diving and surfacing behavior of undisturbed bowhead whales have been investigated (Würsig et al. 1984; Dorsey et al. 1989), and changes in these behaviors are used as a measure of disturbance by vessel, industrial, and seismic activity (Richardson et al. 1985, 1986; Ljungblad et al. 1988). Despite study of their dive durations and surfacing behavior, little is known about the depths to which bowhead whales dive, where in the water column they spend their time, or their nighttime activity.

Methods

We equipped 12 bowhead whales with satellite-monitored radio tags near Shingle Point, Northwest Territories, Canada (68°59′N, 137°26′W), between 30 August and 6 September 1992 (Table 1). Mate et al. (2000) describe the physical details of the tags and deployment methods. We placed tags close to the middorsal line approximately 3 m behind the blowhole, to ensure tag and antenna exposure during surfacings. All whales tagged were of unknown sex and were estimated to be juveniles or subadults (Koski et al. 1993) between 8 and 12 m in length. Two types of tags were deployed: those that recorded depth and duration information (DZ tags, $n = 10$) and those that collected only duration information (D tags, $n = 2$). Data and calculated locations for tags were obtained using the Argos data collection and location system (ADCLS) (Harris et al. 1990). Movements of individual whales and screening of Argos locations are described in the companion paper (Mate et al. 2000). This paper reports dive and surfacing data for eight whales (two D tags and six DZ tags) for which we obtained both location and sensor information.

Each tag collected sensor information during a sampling period and stored 64-bit information "packets" for transmission at a later time. To detect transmission errors, a cyclic redundancy check code was included with each packet (Lin 1970; Wakerly 1978). For each sampling period, D tags collected one packet that included the number of dives in each of eight duration categories or bins, dura-

tion of the longest dive, duration of the longest surfacing, and total time spent under water (Table 1). DZ tags collected three packets for each sampling period (Table 1). The duration packet included the number of dives in each of nine duration bins, duration of the longest dive, and duration of the first dive to the maximum depth. Each dive was assigned to one of eight depth bins, based on its maximum depth. The depth packet included the number of dives in each of eight depth bins and the maximum depth reached. The time-at-depth (TAD) packet included the time spent in each of eight depth bins, total surface time, and duration of the longest surfacing. Maximum and minimum values were established for each transmission field. If data fell outside the range of specified values, they were recorded as underflow or overflow values. For example, D tags reported an underflow if the longest dive in the period lasted <12 min and an overflow if it lasted ≥72 min (Table 1). Data were checked for logical consistency and only valid sensor information was retained.

Times and dates are reported in universal coordinated time (UTC). D tags sampled according to our experimental design: eight 3-h sampling periods beginning at 00:00 UTC each day. The D-tag duty cycle allowed transmissions during the first 100 min of each 12 h. Transmissions rotated through data packets from the previous four sampling periods. A software error in the DZ tags resulted in one 1-h sampling period, six 3-h sampling periods, and one 5-h sampling period, beginning at 02:00 UTC each day. DZ tags could transmit at any time of day. DZ-tag transmissions included four of the six data packets from the two previously completed sampling periods on a rotating basis. All tags were limited to transmitting once every 40 s.

Dive and surface durations were measured by sampling conductivity between the tag housing and a salt-water switch, to determine if the tag was submerged. We defined a dive as a submergence lasting >6 s. A pressure transducer in the DZ tags measured ambient pressure and registered the equivalent depth of seawater in 8-m increments. D tags interrogated the salt-water switch every 0.25 s to determine if the tag was submerged, but tallied time in 2-s intervals. DZ tags tallied time in 6-s intervals but interrogated the salt-water switch and pressure transducer at various intervals: 0.25 s while at depths <8 m, 1 s while at depths of 8–32 m, and 6 s while

at depths >32 m. This was done to conserve battery power during dives, while ensuring that surfacings were detected.

Tags reported short dives (≤1 min) in multiples of either four (DZ tags) or eight (D tags) and shallow dives (≤32 m) in multiples of two (Table 1). If DZ tags returned both duration- and depth-packet data for a sampling period, we compared the minimum and maximum number of dives in each packet to determine the smallest possible range of values. For all tags, the number of dives in the first duration bin was taken to be the mean of the minimum and maximum number of dives possible in that bin during the period. Any uncertainty in the number of dives in the first two depth bins was spread equally between them, resulting in fractional total dive counts. For D tags, the total number of dives in a period was always ±3.5. For DZ tags, the total number of dives was the exact number in 91 sampling periods, ±0.5 in 215 sampling periods, ±1.0 in 177 sampling periods, and ±1.5 in 28 sampling periods. Surfacing rate (surfacings/h) for the sampling period was defined as the total number of dives divided by the period length.

We considered dives >1 min long to be sounding dives. To characterize sounding dives for each period and to make statistical comparisons, we collapsed the duration data for each sampling period into one variable, average duration of sounding dives (SDUR):

[1]   SDUR = Σ (number of dives in the duration bin

$\times$ midpoint of the bin)/(total number of sounding dives)

For dives in the longest bin, the duration of the longest dive (and the first dive to the maximum depth for DZ tags) was known and used in the calculation. Subsequent dives in this bin were multiplied by the midpoint between the longest dive and the bin's minimum value. Sampling periods with overflow values for the longest dive were excluded from these analyses.

We calculated the proportion of each sampling period that tagged animals were potentially visible from the air:

[2]   percentage of time potentially visible = 100 [surface time

+ 10 (dr1)]/period length

where dr1 is the number of dives ≤1 min and both surface time and period length are in seconds. We assumed (*i*) that whales were visible during the surface time tags recorded, (*ii*) that dives ≤1 min were series dives during a surfacing sequence, and (*iii*) that whales were visible during these series dives but not before or after them. The number of dives ≤1 min was multiplied by 10 s, the mean time spent under water between blows measured during three ice-based visual studies of bowhead whale behavior (Carroll and Smithhisler 1980; Rugh and Cubbage 1980; Zeh et al. 1993).

Water depths at Argos locations were determined from National Oceanic and Atmospheric Administration chart No. 16003 or U.S. Defense Mapping Agency chart No. 15026. Ice-cover conditions near whale locations were evaluated from daily ice-analysis charts issued by Environment Canada's Ice Centre in Ottawa and (or) satellite images collected at the Anchorage branch of the U.S. National Weather Service. For each whale, approximate daily sunrise and sunset times (UTC) were determined according to date, Argos locations, and published sunrise and sunset information (U.S. Department of Commerce 1991). Sampling periods were assigned to

one of four classifications to indicate time of day: (1) night, if they began more than 1 h after local sunset and ended more than 1 h before local sunrise; (2) dawn, if sunrise occurred either during the period or within 1 h of the end of the period; (3) day, if they began and ended between sunrise and sunset; and (4) dusk, if sunset occurred either during the period or within 1 h of when the period began. Because so few dawn and dusk periods were recorded for each animal, they were combined into a twilight category for statistical tests.

To determine whether the length of the sampling period affected the data collected by DZ tags, we used multiple linear regression analysis allowing for differences among the whales[2] (Ramsey and Schafer 1996). Because all 1- and 5-h periods occurred during daylight, we included only 3-h periods that occurred during daylight in this analysis. Data for sampling periods when the duration of either the longest dive or the first dive to the maximum depth overflowed were excluded from this analysis.

Sampling-period length did not affect the surfacing rate, the percentage of the period spent at the surface, the percentage of time the whale was potentially visible from the air, SDUR, the duration of the first dive to the maximum depth, or the maximum depth reached for any of the DZ tags. Therefore, sampling periods were treated equally in subsequent statistical comparisons of these variables. However, the longest dive recorded in a sampling period increased when sampling occurred over a longer time. The effects of differences in period length were similar for all tags. Consequently, we compared longest dives for sampling periods of equal length.

Statistical comparisons were accomplished with parametric tests when possible. Data were logarithmically transformed where appropriate and geometric-mean values with 95% confidence intervals (CI) subsequently reported. Visual observation of residual plots and (or) the Kolmogorov–Smirnoff test for normality were used to determine if parametric tests were appropriate. When outliers were present, analyses were done both with and without the outliers, to determine the sensitivity of the analysis to their presence. Between-group differences in means for analysis of variance (ANOVA) tests were accomplished with the Fisher's protected least significant difference (LSD) technique. Nonparametric tests were used to compare medians, if data included underflow–overflow values or data transformations failed to meet the assumptions required for parametric tests. The significance level for all tests was set at 0.05 unless otherwise indicated. The Statgraphics Plus® (Manugistics Inc., Rockville, Md.) statistical software package was used in data analysis.

Results

Dive durations

The distribution of dive durations was highly skewed for every animal, 64–83% of dives lasting ≤1 min (Fig. 1). Overall, 77% of the 42 306 dives made by the eight whales during 1695 h lasted ≤1 min, leaving 9573 sounding dives. Most whales exhibited a general decline in the number of sounding dives of successively longer durations, with notable exceptions from three whales who recorded the highest percentages of sounding dives at 13–19 min (DZ-2) or 10–

---

[2] Dependent variables were substituted into the equation

dependent variable = $\beta_0 + \beta_1$ (period length) + β_2 (DZ-2) + β_3 (DZ-3) + β_4 (DZ-4) + β_5 (DZ-5) + β_6 (DZ-6) + β_7 (period length)(DZ-2)

$+ \beta_8$ (period length)(DZ-3) + β_9 (period length)(DZ-4) + β_{10} (period length)(DZ-5) + β_{11} (period length)(DZ-6)

Period lengths were 1, 3, and 5 h. Tag DZ-1 was used as the standard and other tags (DZ-2 through DZ-6) were put into the equation as indicator variables (1 or 0) to allow for differences among tags. Interaction terms, multiples of period length and tag indicator, tested for differences in the effect of period length by tag. The *t* value and associated *p* value for each coefficient, β_i, in the equation determined the significance of that factor in the model.

Fig. 1. Relative frequency of dives recorded in each duration category by satellite-monitored radio tags deployed on eight bowhead whales in 1992; *n* is the number of dives.
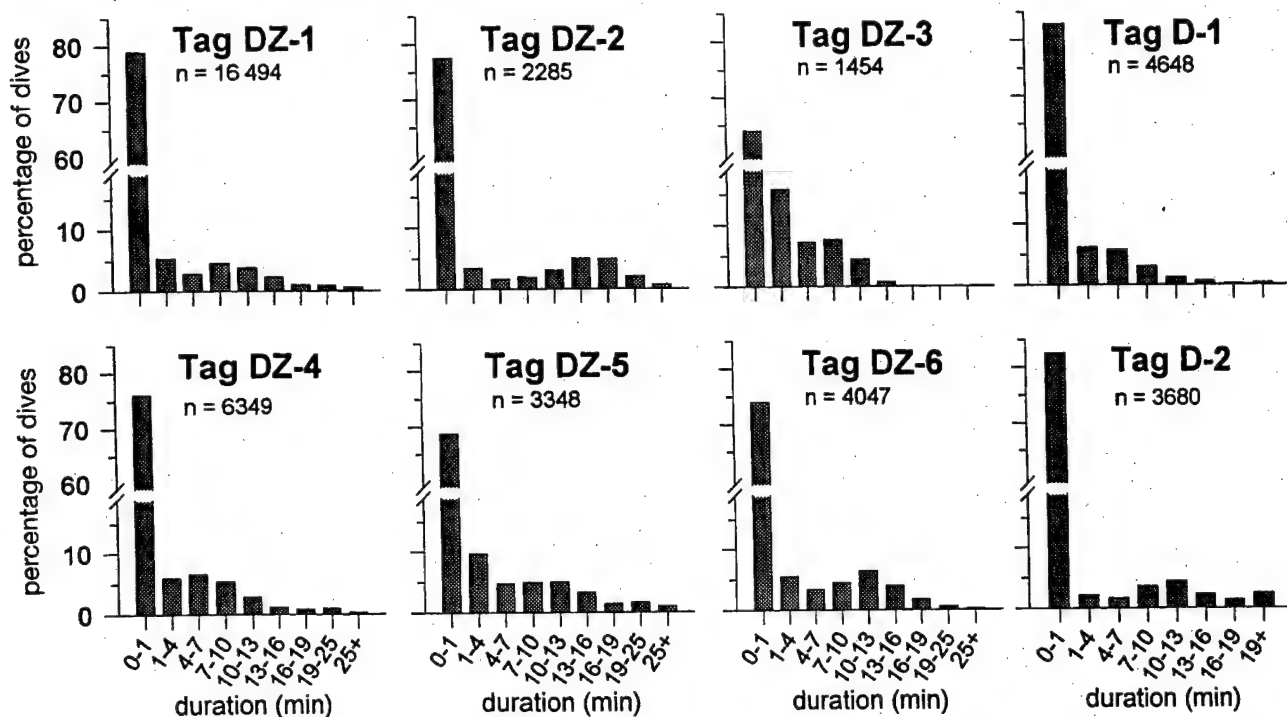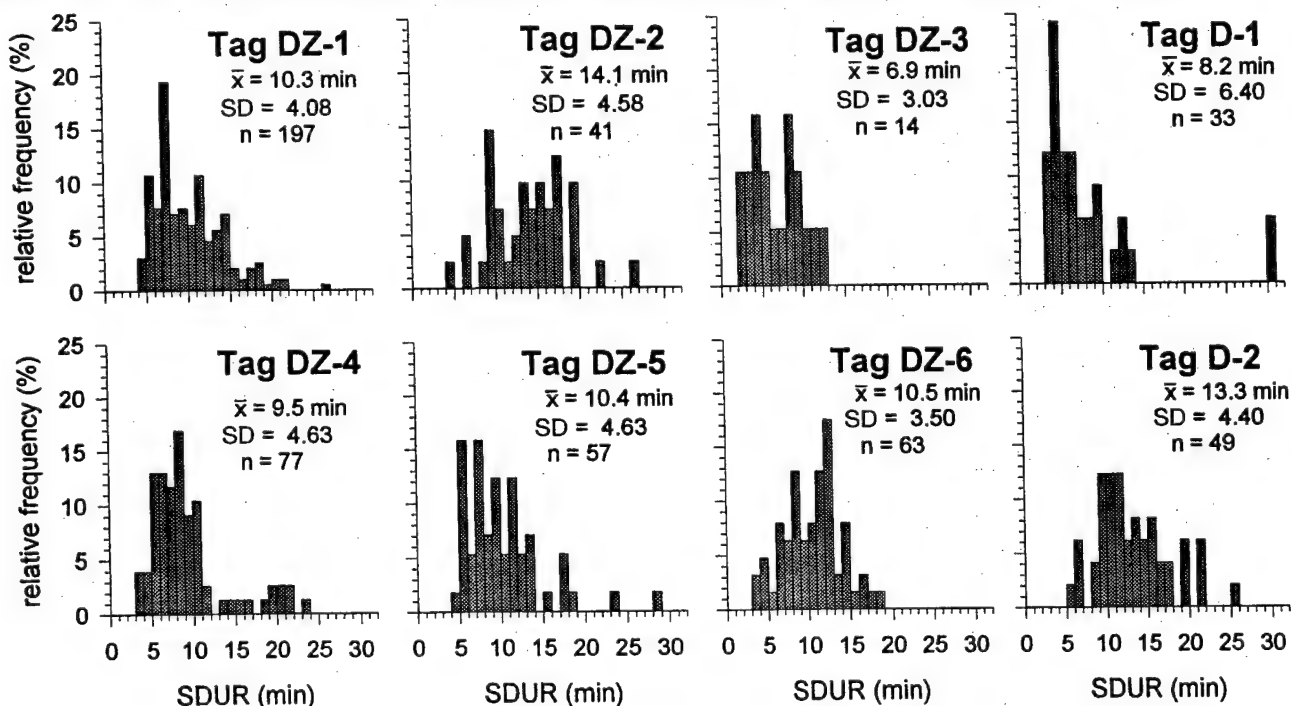

Fig. 2. Relative frequency of average duration of sounding dives (SDUR) during the sampling period for eight bowhead whales equipped with satellite-monitored radio tags; *n* is the number of sampling periods. See the text for calculation of SDUR.

13 min (DZ-6 and D-2) (Fig. 1). SDUR ranged from 2.6 to 30.4 min (*n* = 536). Mean SDUR for individuals varied from 6.9 ± 3.0 to 14.1 ± 4.6 min (mean = 10.4 ± 2.4 min, *n* = 8), and six of the eight whales exhibited a range of 20 min or more across sampling periods (Fig. 2).

Five of the eight tags reported being submerged for at least 61 min, and the longest dives for the other three whales were 56, 45, and 32 min (Fig. 3). The longest dive of known duration, reported by tag D-1, lasted between 62 and 64 min. However, longer dives may have occurred in the 29 sam-

Fig. 3. Relative frequency of the longest dives recorded in a sampling period by eight satellite-monitored radio tags deployed on bowhead whales. Open bars represent underflow or overflow values; *n* is the number of sampling periods.
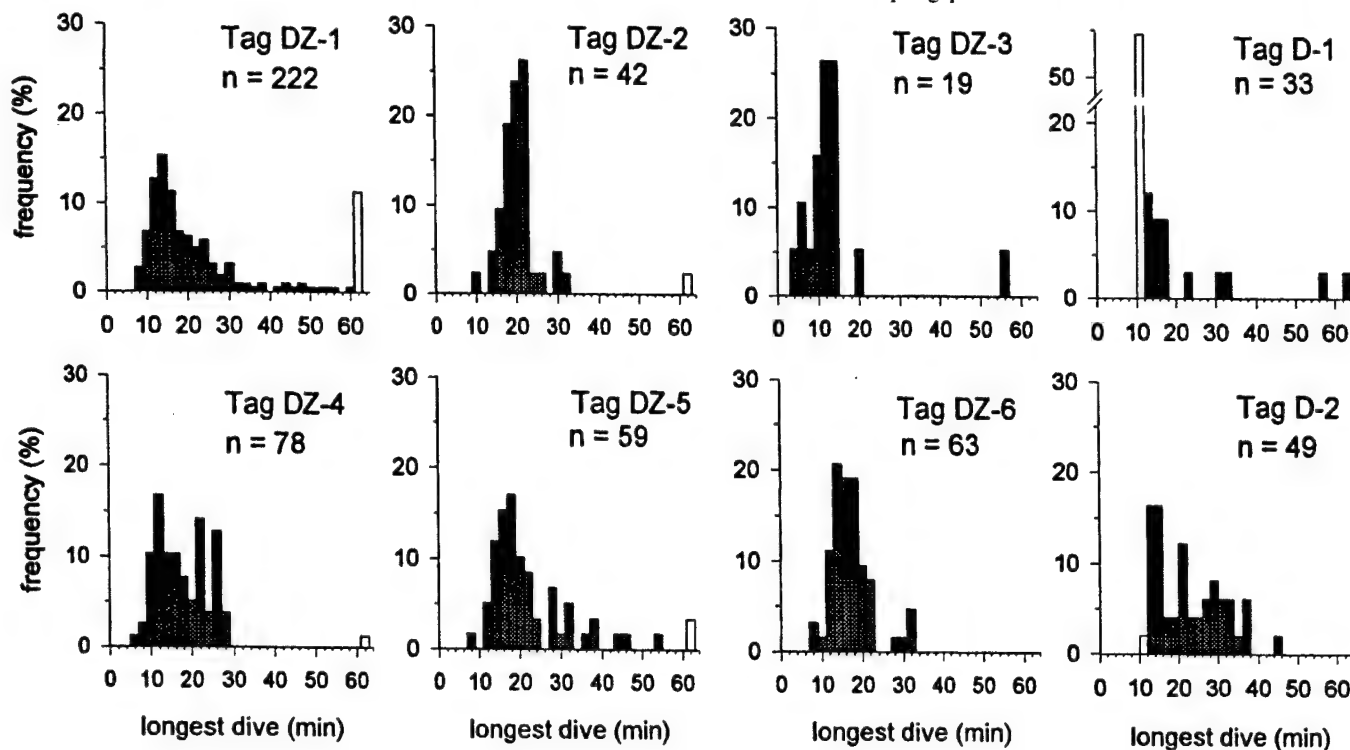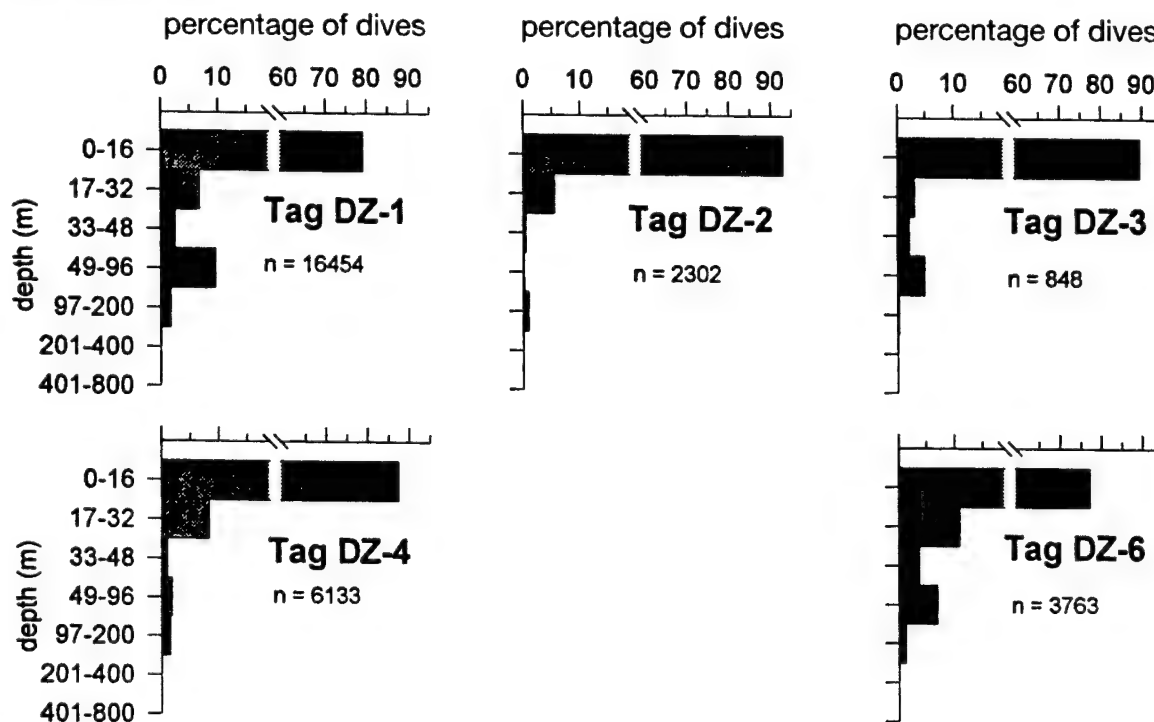

Fig. 4. Relative frequency of the maximum depths of dives recorded by satellite-monitored radio tags deployed on five bowhead whales; *n* is the number of dives.

pling periods during which DZ tags reported dives ≥61 min (overflow value). Most of the dives ≥61 min long occurred in ice cover ≥90%, but tags DZ-1, DZ-2, and DZ-4 recorded dives this long in open water.

Dive depth and TAD

Maximum depths of 29 499 dives made by five whales with DZ tags were measured during 1220 h. Dives ≤16 m accounted for 77–93% of the total number of dives for each

Fig. 5. Percentages of time recorded in each depth category for five bowhead whales equipped with satellite-monitored radio tags; n is the number of hours that TAD was monitored.
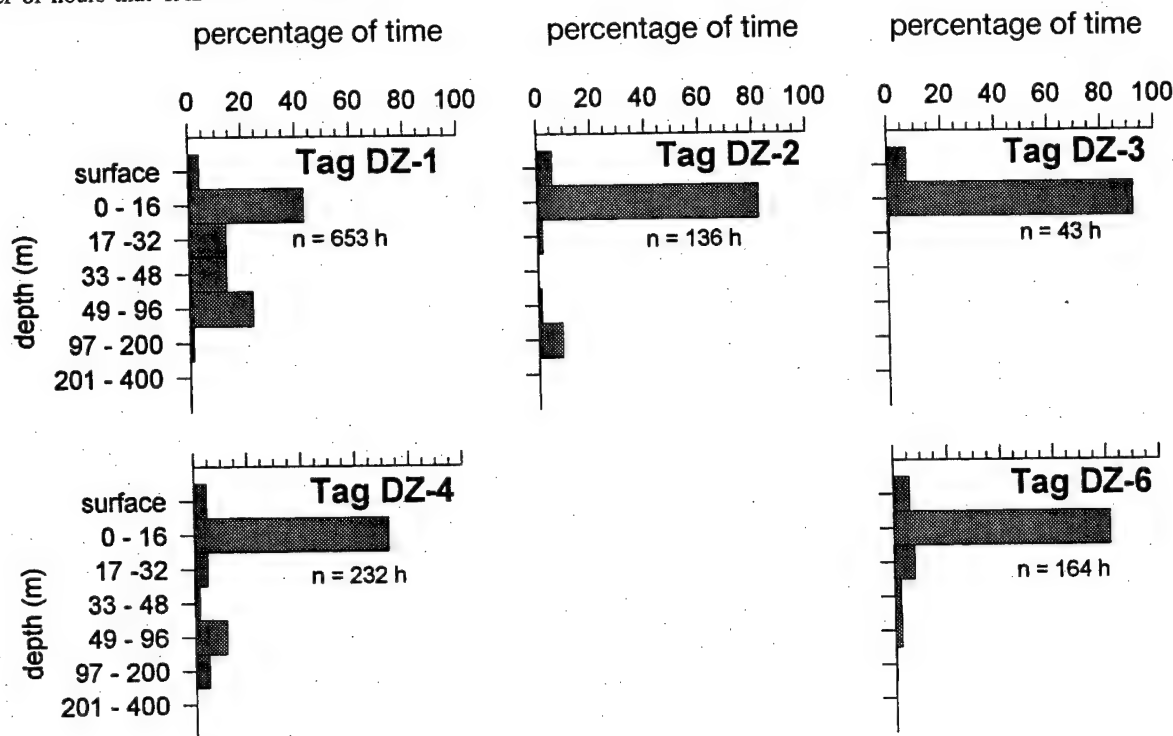

Table 2. Data for the deepest dive during sampling periods recorded by satelite-monitored radio tags on bowhead whales.

| Tag No. | n | Deepest dive (m) | | | | |
		Minimum	Mode	Median	Mean ± SD	Maximum
DZ-1	220	32	96	96	97±41	352
DZ-2	44	<8	32	32	38±34	160
DZ-3	12	<8	<8	56	52±49	128
DZ-4	76	16	32	48	63±43	160
DZ-6	58	16	96	88	84±40	240

whale (Fig. 4). Maximum depth reached during a sampling period ranged from <8 to 352 m and all five whales made dives >100 m deep (Table 2). Several tagged whales exhibited bouts of repeated dives ≥48 m deep.

Overall, during 1228 h, the five whales spent 60% between the surface and 16 m depth, 33% between 17 and 96 m depth, and <3% at depths greater than 96 m, the remainder being spent at the surface. Every whale spent most of its time between the surface and 16 m depth (Fig. 5). However, three individuals (DZ-1, DZ-2, and DZ-4) spent more than half of some periods at depths greater than 48 m.

Relationship between dive depth and duration

The number of short (≤1 min) dives and the number of shallow (≤16 m) dives recorded in a sampling period by DZ tags were positively correlated (r = 0.95–0.97, all p < 0.0001). Thus, the short series dives during a surfacing sequence were probably shallow.

The duration of the first dive to the maximum depth ranged from <1 to ≥61 min (n = 415). Four tags reported the underflow value (<1 min) for this dive in 21 periods. Depth data

were reported in 17 of these 21 periods. The deepest dive was <8 m in five of these periods, 8–16 m in seven periods, and 17–32 m in the other five periods. Considering the close association between short and shallow dives, it seems likely that the first dive to the maximum depth recorded during these periods was one of the short series dives during a surfacing sequence. Three tags reported that the first dive to the maximum depth was ≥61 min long (overflow value) in 15 sampling periods, with dive depths ranging from 16 to 128 m. Of these 15 periods, 12 were recorded by tag DZ-1 in heavy ice conditions. Sampling periods with underflow or overflow values were excluded from further analyses. The first dive to the maximum depth was also the longest dive in 105 of the 367 sampling periods for which the duration of both was known.

To investigate the relationship between duration and depth of the first dive to the maximum depth, a regression analysis was performed on data from each of the five tags. Duration significantly increased with dive depth for four of the five whales, but the linear model explained <36% of the variation around the mean in all cases (Fig. 6). One outlier value

Fig. 6. Results of regression of duration on depth for the first dive in a sampling period to reach the maximum depth recorded in the period for five bowhead whales equipped with satellite-monitored radio tags.
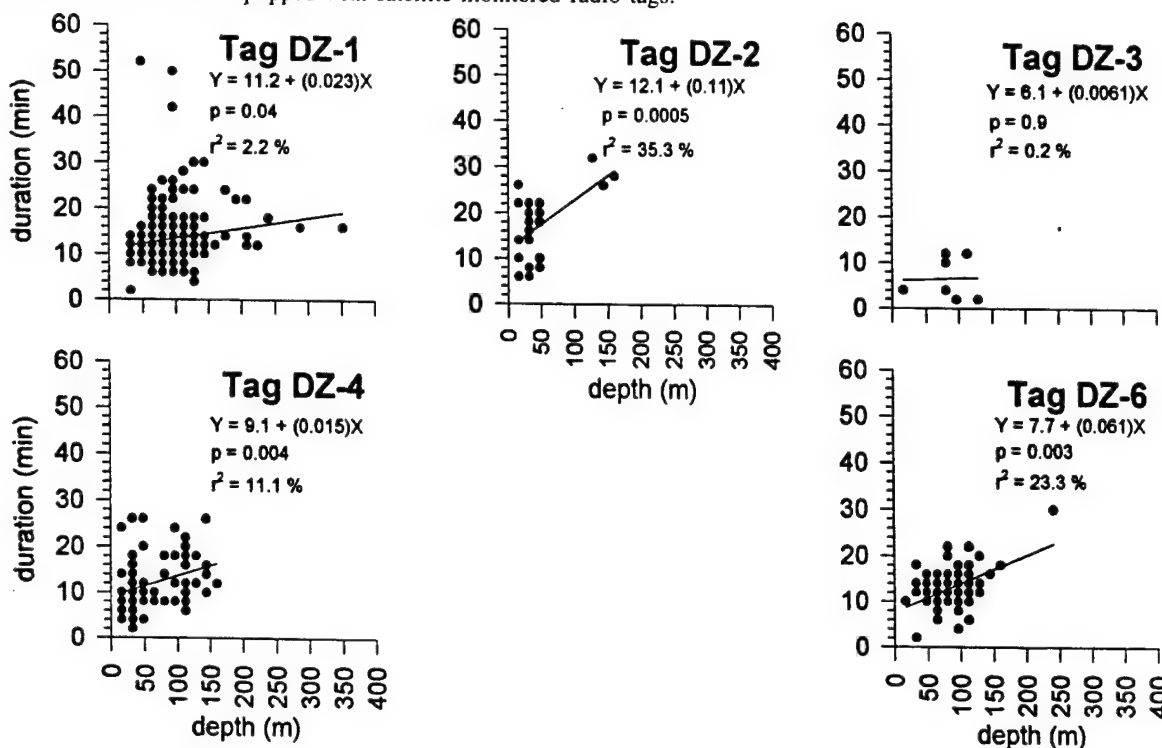

Table 3. Surfacing rate, percentage of time spent at the surface, and percentage of time potentially visible from the air for bowhead whales tagged in 1992.

Tag No.	No. of surfacings/h	Percentage of surface time	Percentage of time potentially visible from the air
DZ-1	25.1±10.8 (229)	4.0±2.04 (223)	9.5±3.0 (214)
DZ-2	18.2±6.5 (45)	5.9±2.02 (46)	10.0±2.3 (40)
DZ-3	25.5±13.3 (19)	7.3±4.32 (16)	12.5±5.8 (15)
DZ-4	26.9±7.3 (79)	4.7±4.36 (78)	10.2±4.4 (78)
DZ-5	18.9±7.9 (63)	4.8±3.27 (54)	8.5±3.6 (51)
DZ-6	22.9±17.5 (68)	6.1±2.67 (61)	10.7±5.2 (59)
D-1	47.0±20.6 (33)	5.7±2.35 (33)	16.4±5.9 (33)
D-2	25.0±12.0 (49)	5.6±1.89 (49)	11.3±2.4 (49)
Mean	26.2±9.0 (8)	5.5±0.95 (8)	11.1±2.4 (8)

Note: Values are given as the mean ± SD, with the sample size in parentheses.

strongly influenced the analysis for tag DZ-6 (Fig. 6), but the positive relationship remained if the outlier was excluded from the analysis ($p = 0.03$).

Surfacings

Both types of tags recorded the longest surfacing duration in each sampling period. Four of the eight whales reported surfacings of longer than 3.5 min. These long surfacings occurred in only 5 of the 560 sampling periods and were approximately 14, 8, 5, 4, and 4 min long.

Individual whales exposed their tags to the air for an average of 4.0–7.3% of the sampling period (Table 3). This translates to exposure at the surface for between 2.4 and 4.4 min/h. Mean rates for individuals ranged from 18.2 to 47.0 surfacings/h (Table 3). Based on the calculations in eq. 2, the mean percentage of the sampling period potentially visible from the air for individuals ranged from 8.5 to 16.4% (Table 3).

Dive and surfacing characteristics in relation to location and environment

Detailed location data for tagged bowhead whales are presented and discussed in the companion paper (Mate et al. 2000). Argos locations were obtained for whales in 291 sampling periods, with individual whales located during 9–136 periods (Table 1). Here we examine aspects of dive and surfacing data in relation to ice cover and time of day. We also

note similarities among three whales that were located in Mackenzie Canyon at about the same time.

Ice cover

Five of the eight whales moved into waters with various degrees of ice cover, but only three were monitored in areas with heavy ice cover ≥90% (Mate et al. 2000). Whale D-1 was surrounded by ≥90% ice cover at its last location just north of the Mackenzie River Delta on 29 September (see Fig. 4 in Mate et al. 2000). Late on 20 September, at its most westerly location (see Fig. 9 in Mate et al. 2000), whale D-2 was surrounded by 90% ice cover. From 20 September until 5 October, when it was last heard from, whale DZ-1 migrated through water with ice cover ≥90% (see Fig. 10 in Mate et al. 2000). These animals exhibited consistent differences in several dive and surfacing variables when they were in heavy (≥90%) versus lighter (<90%) ice cover (Table 4). All three had lower surfacing rates, yet recorded more time at the surface. Although surface time increased, the calculated percentage of time they were potentially visible from the air declined because of the lower surfacing rate. The longest surfacing increased for two of the three whales. Average sounding dive time increased for all three whales, as did the duration of their longest dives. These differences were significant, except for the percentage of time spent at the surface for whales D-1 and D-2, where the power to detect a difference was low, owing to the small sample sizes in heavy ice.

When in heavy ice conditions, whale DZ-1 made longer dives (Fig. 7A), made a higher percentage of dives to depths of >48 m (Fig. 7B), spent more of its time at depths of 49–96 m, and spent less time between 0 and 16 m depth (Fig. 7C). These differences were not simply a function of available water depth. Dive-depth data were received for 56 periods, with locations in water >48 m deep being evenly split between heavy and lighter ice conditions. The percentages of dives ≤16 m deep were nearly identical in the two samples, 77 and 78% in heavy and lighter ice, respectively, but 20% of the dives were to depths of >48 m in heavy ice versus 12% in lighter ice. TAD data were received from 53 sampling periods with locations in water >48 m deep. Although water depths at locations in the 26 periods in light ice ranged up to 1480 m, whale DZ-1 spent 58% of its time in the upper 16 m and 14% of its time at depths of 49–96 m. In contrast, during the 27 periods in heavy ice, water depths ranged only up to 128 m, yet this whale spent most of its time (55%) between 48 and 96 m, with only 22% of its time in the upper 16 m. The tag did not break the surface during four 1-h sampling periods recorded after 19 September. TAD information for these periods hints that surfacing behavior still occurred. Although this whale spent most of its time in these periods at depths of >32 m (mean = 71.8 ± 9.8%), it still spent substantial time in the upper 16 m (mean = 25.8 ± 11.0%); however, it spent very little time in between (mean = 3.0 ± 5.2% at 17–32 m).

Diel variation

To investigate diel patterns of behavior for each whale, we compared data recorded during day, night, and twilight periods for six variables: surfacing rate, percentage of time spent at the surface, duration of the longest dive, logarithmically

Table 4. Comparison of dive and surfacing variables between three bowhead whales in heavy (≥90%) versus lighter (<90%) ice cover.

| | Surfacing rate (no. of surfacings/h) | | Surface time (%) | | Longest surfacing (min) | | Time potentially visible from the air (%) | | SDUR (min) | | Longest dives | | | | | |
| | | | | | | | | | | | 1-h periods | | 3-h periods | | 5-h periods | |
	<90%	≥90%	<90%	≥90%	<90%	≥90%	<90%	≥90%	<90%	≥90%	<90%	≥90%	<90%	≥90%	<90%	≥90%
D-1[a]	47.8	11.8***	4.5	5.5	<1	<1	16.8	8.0***	5.7	30.4***			<12	57***		
	(30)	(3)	(30)	(3)	(30)	(3)	(30)	(3)	(30)	(3)			(30)	(3)		
D-2[a]	27.5	8.5**	5.5	6.5	<1	1–2***	11.5	8.3***	11.7	19.1**			21	28*		
	(45)	(4)	(45)	(4)	(45)	(4)	(45)	(4)	(45)	(4)			(45)	(4)		
DZ-1[b]	32.1±6.8	16.3±8.0***	3.3	4.9***	<0.5	0.5–1.5***	9.1	10.4***	7.7	13.2***	11.1	17.8***	14.7	24.7***	17.2	22.9*
	(128)	(101)	(121)	(102)	(121)	(102)	(117)	(97)	(120)	(77)	(15)	(9)	(91)	(61)	(14)	(7)

Note: Data are from satellite-monitored radio tags. Numbers in parentheses are sample sizes. A significant difference from lighter ice is indicated as follows: *, $p < 0.1$; **, $p < 0.05$; ***, $p < 0.005$. We considered differences to be significant in two cases with $0.1 < p < 0.05$ because of the small sample sizes and subsequent low power to detect differences.
[a]Medians are given for all variables.
[b]Mean and SD are given for surfacing rates. Medians are given for surface time, longest surfacing, time potentially visible from the air, and longest dives. Geometric means are given for SDUR.

Fig. 7. Comparison of dive data recorded by satellite-monitored radio tag DZ-1 on a bowhead whale in light ice (<90%) from 3 to 19 September 1992 and in heavy ice (≥90%) from 20 September to 5 October 1992. (A) Percentage of dives in each duration category; *n* is the number of dives recorded. (B) Percentage of dives in each depth category; *n* is the number of dives recorded. (C) Percentage of time spent in each depth category; *n* is the number of hours of monitoring.
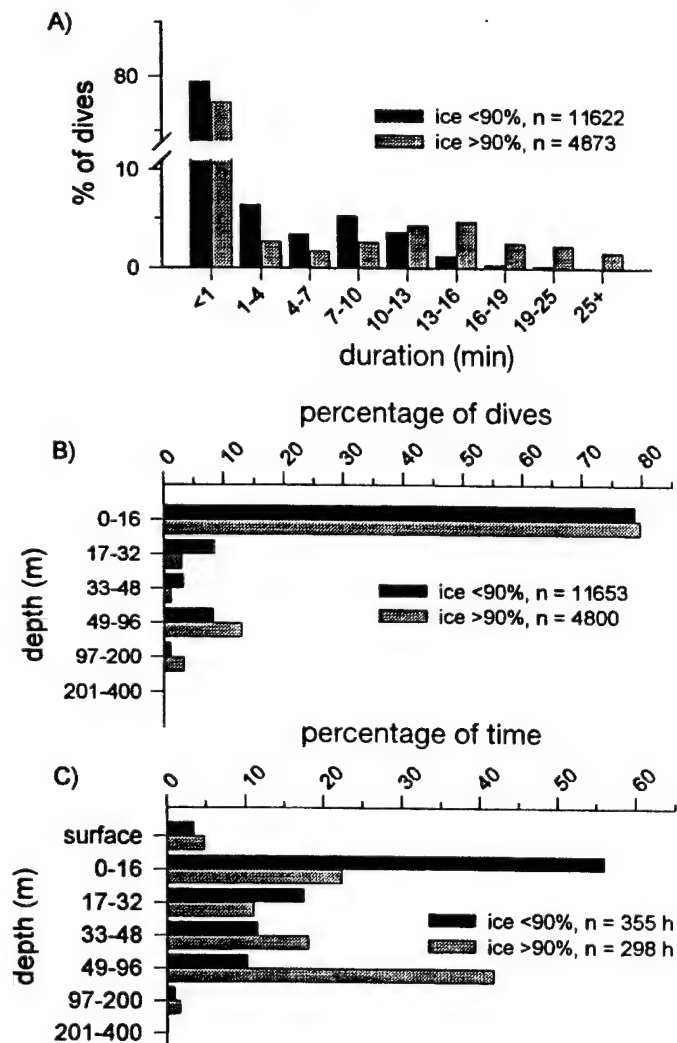
transformed SDUR, deepest dive, and duration of the first dive to the maximum depth. No consistent diel patterns among the whales were found for any of these variables, nor were there any significant differences, except for SDUR, which differed with light level for two tags: D-1 (ANOVA, $F_{[2,30]} = 7.14$, $p = 0.003$) and DZ-6 (ANOVA, $F_{[2,60]} = 4.30$, $p = 0.018$).

Although day and night periods did not differ significantly for tag D-1, the geometric mean SDUR for twilight periods (12.3 min, 95% CI = 9.1–16.8 min, $n = 7$) was about twice as long as those for the day (5.6 min, 95% CI = 4.6–6.9 min, $n = 16$) or night (6.4 min, 95% CI = 4.9–8.3 min, $n = 10$) periods. This difference was influenced by heavy ice cover (≥90%) encountered by this whale on 29 September. Calculated values for SDUR for the two twilight periods that day

(30.4 min) were extreme outliers in the distribution for this whale (Fig. 2). Excluding these two sampling periods from the analysis yielded twilight periods with slightly longer SDURs (geometric mean = 8.6 min, 95% CI = 6.3–8.0 min, $n = 5$) than those of the day or night periods, but not significantly so (ANOVA, $F_{[2,28]} = 2.33$, $p = 0.12$).

For tag DZ-6, the SDUR was 1.5 times longer (95% CI = 1.1–2.0 times longer) for night periods (geometric mean = 11.7 min, 95% CI = 10.1–13.7 min, $n = 16$) than for twilight periods (geometric mean = 8.0 min, 95% CI = 6.8–9.4 min, $n = 14$). Daylight sampling periods had intermediate SDURs (geometric mean = 10.0 min, 95% CI = 9.0–11.1 min, $n = 33$) that did not differ significantly from those of either the night or twilight periods.

Mackenzie Canyon

Whales DZ-4 and DZ-2 made long deep dives and spent most of their time deeper than 48 m in Mackenzie Canyon, and whale D-2 made long dives in this region. These dives were made between 10 and 14 September.

Whale DZ-4 was located 64 times during the almost 11 d we received dive and surfacing data (see Fig. 5 in Mate et al. 2000). It moved into waters 50–200 m deep in Mackenzie Canyon on 10 September, made a short excursion back into Mackenzie Bay late on 12 September, and then returned to the deeper waters of the canyon for the last 2 d of monitoring. During three extended bouts in Mackenzie Canyon, most soundings made by DZ-4 were longer than 16 min, with the longest dives from 18 to 26 min. These bouts occured on 11, 13, and 14 September and lasted for 16, 15, and 13 h, respectively. During these three bouts, whale DZ-4 made repeated deep dives, with maximum dive depths ranging from 80 to 144 m, and spent most of its time at depths greater than 48 m: 34–78% (mean = 69 ± 15.9%, $n = 6$), 58–81% (mean = 66 ± 10.0%, $n = 5$), and 58–80% (mean = 71 ± 9.6%, $n = 6$).

Whale DZ-2 entered water >200 m deep in Mackenzie Canyon on 10 September (see Fig. 7 in Mate et al. 2000). Duration data were received for only 9 h while DZ-2 was in Mackenzie Canyon. Of the 22 sounding dives, 82% were >19 min long, with the longest dive each period being 30–32 min. We received dive-depth data for four sampling periods. Of 31 dives deeper than 16 m, 3 were to depths between 49 and 96 m and 22 were to depths >96 m, the deepest dives being to 112, 128, 160, and 144 m. During the last 17 h it was monitored, whale DZ-2 spent from 61 to 78% of its time (mean = 71% ± 5.6, $n = 5$) between 97 and 200 m deep.

Whale D-2 was located in Mackenzie Canyon waters 100–200 m deep on 12 September (see Fig. 9 in Mate et al. 2000), but data from just one sampling period were obtained. All six sounding dives were >19 min long, the longest dive being 31 min. The SDUR, 26 min, was longer than for any other period. Data received for the periods 24 h before and 24 h afterward also had high percentages of sounding dives >19 min long (67 and 71%), the longest dives being 25 and 29 min, respectively. Unfortunately, the 24-h gaps in data and the lack of locations for 11 and 13 September make it unclear if this whale engaged in extended bouts of long dives in Mackenzie Canyon like DZ-4 and DZ-2.

Discussion

The majority of dives monitored for every whale (64–92%) were short (≤1 min; Fig. 1). For whales with depth-monitoring tags, the majority of dives (68–93%) were also shallow (≤16 m; Fig. 4) and there was an extremely high correlation ($r \geq 0.95$) between the numbers of short and shallow dives. These results agree well with visual studies. Bowhead whales typically make a short dive between breaths during a surfacing sequence and then make a longer sounding dive (Carroll and Smithhisler 1980; Rugh and Cubbage 1980). Aerial observations indicate that they are often visible beneath the water and do not dive deeply during a surfacing sequence (Würsig et al. 1984; Dorsey et al. 1989). Researchers studying bowhead whale surfacing and diving behavior visually count this series of short dives as part of a "surfacing" and measure the interblow interval. The mean interblow intervals for presumably undisturbed non-calf bowhead whales in the Beaufort and Chukchi seas reported in visual studies (Table 5) range from 11.2 to 17.9 s, with an average of 3.2–12.6 blows/surfacing sequence. This translates into 69–92% of all dives being short series dives.

Though bowhead whales must surface to breathe, most of their activities take place under water. The tags we put on bowhead whales were exposed to the air for an average of 4.0–7.3% of a sampling period (Table 3), with the remaining time spent under water. Tagged bowhead whales spent little time resting at the surface. The longest surface duration recorded was 14 min, and surface intervals longer than 3.5 min were recorded in <1% of sampling periods. Ice-based observers can see some exposed body part of bowhead whales migrating past Point Barrow in spring for 3.1% (Carroll and Smithhisler 1980) to 5.2% (Zeh et al. 1993) of the time. Tags would not be exposed to the air the entire time that "some body part was visible," so it might be expected that tags would record less rather than more overall time at the surface. However, animals in the cited studies were actively migrating, whereas tagged whales were monitored during late summer, when bowhead whales are prone to remaining at the surface between blows if they are not actively traveling (Würsig et al. 1984). Bowhead whales have been reported to rest at the surface for over an hour (Carroll and Smithhisler 1980). Either tagged whales did not rest at the surface for that long or their surface resting posture did not constantly expose the tag to the air.

Comparing surfacing rates for tagged bowhead whales with data from visual studies is more problematic. Mean blow rates (blows/min), calculated from the number of blows per surfacing, the duration of surfacings, and the duration of dives, rather than surfacing rates (surfacings/h) have been published for several species of large whales. Mean blow rate describes the respiratory activity of a whale over a longer time period than do any of the constituent variables from which it is calculated (Würsig et al. 1984), but comparisons of mean blow rates between species or even between studies of the same species have been confounded by the use of two different methods of calculation (Dorsey et al. 1989). In method 1, the total number of blows during a series of surfacing-dive cycles is divided by the total duration of these cycles (Sumich 1983; Würsig et al. 1986), while in method 2, a blow rate is calculated for each surfacing–dive cycle and then a mean is computed for the number of surfacing–dive cycles observed (Würsig et al. 1984; Dolphin 1987a, 1987b).

Method 1 gives a better estimate of absolute blow rate and can be approximated by dividing the mean number of blows per surfacing by the sum of the mean durations for surfacings and dives (Dorsey et al. 1989). For comparison, we recalculated mean blow rates (blows/h) for bowhead whales in the Beaufort and Chukchi seas from 16 sets of published values reported in observational studies (Table 5). Assuming one blow for every surfacing recorded, the mean blow rate for tagged whales (Table 5) falls in the lower part of the range of values calculated from visual data. Any or all of the assumptions made in order to convert surfacing rate to blow rate for tagged whales may be violated during a given sampling period. If tags were exposed when no breath (blow) occurred, the blow rate for the period would be overestimated. If the whale took multiple breaths without submerging the tag for 6 s or breathed without exposing the tag, the blow rate for the period would be underestimated.

We did not conduct the extensive follow-up observations of tagged animals necessary to evaluate bias quantitatively, but it seems more likely that our sampling method underestimated rather than overestimated blow rates. Bowhead whales sometimes submerge for less than 6 s or do not submerge at all between blows, and they may expose only their blowholes or break ice to breathe (Carroll and Smithhisler 1980; Rugh and Cubbage 1980; Würsig et al. 1984; Carroll et al. 1987; Richardson et al. 1987; Ljungblad et al. 1988; Dorsey et al. 1989; George et al. 1989; Wartzok et al. 1990[3]; Zeh et al. 1993). Mean blow rates calculated from visual studies are likely to be biased upward because mean dive times (which make up the bulk of the time in the denominator) are biased downward, owing to the difficulty of keeping track of and identifying individual whales after long dives (Würsig et al. 1984; Dorsey et al. 1989; Richardson et al. 1995), but there is no reason to suspect that the other constituent components of the calculation are biased. Indeed, in a study of blue whales (*Balenoptera musculus*) off the California coast in which surfacing–blow rates calculated from boat-based visual observations were compared with those recorded by tags similar to ours, higher rates were found for the visual observations (Lagerquist 1997). Considering the potential biases of each sampling method, true blow rates probably lie between the blow rate values calculated for tagged whales and from observational studies. Mean surfacing rates for bowhead whales in this study (Table 3) were lower than those for either right whales (mean = 42.2 ± 14.8 surfacings/h, $n = 7$, range = 27.3–71.8 surfacings/h; Nieukirk 1992) or blue whales (mean = 40.8 ± 14.4 surfacings/h, $n = 12$, range = 16.8–63.6 surfacings/h; B.A. Lagerquist, personal communication) equipped with similar tags (ANOVA, $p = 0.038$).

The mean percentage of time that tagged bowhead whales were potentially visible from the air was also lower than that

---

[3] D. Wartzok, W.A. Watkins, B. Würsig, J. Guerrero, and J. Schoenherr. 1990. Movements and behavior of bowhead whales. Report from Purdue University, Fort Wayne, Ind., for AMOCO Production Co., P.O.Box 800, Denver, CO 80201, U.S.A.

Table 5. Mean values for respiration and dive variables for bowhead whales in the Beaufort and Chukchi seas, from visual studies and this study of tagged whales.

Source	Mean interblow interval (s)			Mean no. of blows/surfacing	Mean dive time (min)	Mean duration of surfacing (min)	Mean blow rate[a] (blows/h)	Percentage of time visible from the air[b]
	Visible	Under water	Total					
Carroll and Smithhisler 1980	4.7 (31)	10.8 (30)	15.5	6.57 (63)	15.6 (63)	1.52	22.8	8.9
Carroll et al. 1987								
Feeding, 1980–1985			11.9 (361)	12.6 (37)	14.70 (16)	2.32 (39)	44.4	13.6
Migrating, 1980–1985			13.7 (140)	6.5 (78)	11.72 (156)	1.59 (19)	28.8	11.9
Dorsey et al. 1989								
1980			12.9 (915)	4.8 (70)	2.25 (25)	1.25 (99)	82.2	35.7
1981			13.0 (1113)	4.2 (194)	3.80 (80)	1.06 (248)	51.6	21.8
1982			14.9 (795)	7.4 (58)	12.08 (51)	2.05 (70)	31.2	14.5
1983			17.0 (866)	3.2 (299)	1.88 (140)	1.05 (204)	65.4	35.8
1984			11.6 (1472)	5.5 (75)	6.27 (37)	1.10 (94)	45.0	14.9
Ljungblad et al. 1988								
Western Beaufort			13.1 (158)	9.2 (10)	17.93 (10)	1.82 (13)	28.2	9.2
Western Aleutian			13.0 (49)	8.5 (8)	17.80 (4)	1.81 (8)	25.8	9.2
Arctic Star			15.3 (132)	3.8 (19)	14.15 (6)	1.07 (21)	15.0	7.0
Western Polaris			14.8 (246)	8.0 (24)	16.17 (4)	1.97 (25)	26.4	10.9
Rugh and Cubbage 1980	6.1 (112)	11.6 (50)	17.9 (145)	—	7.5 (3)	—	—	—
Richardson et al. 1987								
1985			12.05 (480)	6.18 (17)	7.07 (5)	1.56 (36)	43.2	18.1
1986			11.24 (816)	5.08 (51)	6.32 (23)	0.99 (78)	41.4	13.5
Wartzok et al. 1990, see footnote 3			16.5 (388)	3.6 (52)	4.0 (22)	0.9 (52)	43.8	18.4
Zeh et al. 1993	4.7 (1701)	7.4 (1531)	12.1	7.4 (184)	9.9 (41)	1.3 (184)	39.6	11.6
Unweighted mean ± SD	5.2±0.81 (3)	10.0±2.3 (3)	13.91±2.01 (17)	6.41±2.45 (16)	9.9±5.49 (17)	1.48±0.43 (16)	39.6±16.8 (16)	16.2±8.99 (16)
Unweighted mean ± SD in this study				4.5±1.1 (8)	10.4±2.4 (8)		26.4±9.0 (8)	11.1±2.4 (8)

Note: Values in parentheses are sample sizes.
[a]Calculated as 60 × [mean number of blows per surfacing/(mean duration of surfacing + mean dive time)].
[b]Calculated as 100 × [mean duration of surfacing/(mean duration of surfacing + mean dive time)].

calculated from visual studies (Table 5). Like mean blow rates, methods of calculating percentage of time that bowhead whales are visible from the air in visual studies have varied. We used the method recommended by Dorsey et al. (1989) to recalculate this percentage from observational studies. The potential methodological biases discussed for surfacing–blow rates carry over to calculations here. All the calculations assume that whales are visible from the air between serial dives during a surfacing sequence and, thus, likely yield maximum values. In the field, the depth to which whales dive and environmental conditions, such as water turbidity, sea state, cloud cover, ice cover, and light, are likely to affect the time that animals are actually visible.

Tags recorded 9573 sounding dives in our study. Individual bowhead whales tagged in this study showed highly variable SDUR values (Fig. 2). Tagged whales exhibited bouts of sounding dives of similar duration, both short and long (e.g., 20 h of predominantly short dives and 16-, 15-, and 13-h bouts of predominantly long dives for whale DZ-4). Although Würsig et al. (1984) observed that "bowheads tend to make a series of dives of similar duration rather than alternating long and short dives," the extended time over which this can occur was previously unknown. A qualitative comparison of sounding dives between our study and visual studies is possible. Mean dive times reported in these studies range from 1.88 to 17.93 min (Table 5), with a total of 686 timed "dives." We defined a sounding dive as being >1 min long. In visual studies a "dive" was judged to be a sounding dive on the basis of either (*i*) raising of the flukes or a pronounced body flexion or (*ii*) a submergence greater than some specified period of time (e.g., 75 s in Rugh and Cubbage 1980; 60 s in Würsig et al. 1984; 15 s in Dorsey et al. 1989). Mean SDUR of tagged whales (10.4 ± 2.4 min, $n = 8$ whales) was comparable to the mean of "dive" times from visual studies (9.9 ± 5.49 min, $n = 17$ studies) (Table 5).

Although only about 1% of the sounding dives reported by eight tags could have exceeded 35 min, five of the eight tags were submerged for at least 61 min in one or more sampling periods. For three whales (tags D-1, DZ-2, and DZ-4), these long submergences appear to be extreme outliers, whereas for the other two (tags DZ-1 and DZ-5), they may be viewed as part of the skewed distribution of longest dives (Fig. 3). Were these long submergences real "dives" or artifacts of the sampling method? Bowhead whales have reportedly remained submerged for over an hour. Harpooned bowhead whales have dived for 30, 40, and 60 min in the North Atlantic (Scoresby 1820) and 80 min in the North Pacific (Scammon 1874). Carroll and Smithhisler (1980) refer to an unpublished 1964 manuscript by D.C. Foote which claims that bowhead whales can dive for up to 75 min if they are injured, frightened, or otherwise greatly disturbed.[4] Some of the longest dives recorded for undisturbed bowhead whales include visual observations lasting 26.7 min (Carroll and

Smithhisler 1980) and 30.98 min (Würsig et al. 1984), and time between very high frequency (VHF) radio-tag signals of 32.3 min (Wartzok et al. 1990, see footnote 3) and 41 min (Finley and Goodyear 1993[5]). However, individual whales are difficult to track and identify after long dives (Würsig et al. 1984; Dorsey et al. 1989; Richardson et al. 1995), and the number of dives sampled in these visual studies (Table 5) is an order of magnitude less than those recorded in our study. Dive duration measured as time between received high-frequency (HF)/VHF radio signals may be biased upward, since all signals may not be received during a surfacing sequence, but the bias should be relatively small compared with the dive duration (Wartzok et al. 1990, see footnote 3).

Surfacing behavior that does not expose a tag at the surface could explain some of the very long dives recorded by several animals. To breathe in areas where extensive ice cover exists, bowhead whales may expose just their blowholes in small pools of open water; they regularly break ice up to 20 cm thick and even 60 cm thick (George et al. 1989). Tags would remain under water in these circumstances, registering longer and fewer dives than actually occurred. Three tagged whales had lower surfacing rates and longer sounding dives when they were in ice cover ≥90% (Table 4). The longest dives recorded for D-1, and 92% of the sampling periods with dives ≥61 min long recorded for whale DZ-1, were in areas with ice cover ≥90%. However, not all dives ≥61 min long were made in heavy ice conditions. Tags DZ-1, DZ-2 and DZ-4 each reported one period in which the duration of longest submergence was at least 61 min while they were in open water. It is possible that resting bowhead whales exposing only their blowholes to breathe for over an hour (Carroll and Smithhisler 1980) might not expose their tag to the surface but, for whales DZ-1, DZ-2, and DZ-4, the maximum depth for the period (48, 16, and 16 m respectively) was recorded during the ≥61-min submergence. While it seems likely that some of the long "dives" were artifacts of surfacing behavior that kept tags submerged, some may have been real dives.

This is the first study of bowhead whales to include measuring dive depths, investigating the relationship between dive depth and duration, and examining where in the water column time is spent. All five whales dived to >100 m depth and whales DZ-6 and DZ-1 dived to >200 and >300 m depth, respectively (Table 2). Previous information on depths to which bowhead whales can dive has been anecdotal and indirect. In the western Arctic, bowhead whales surface with mud streaming from their mouths in water up to 40 m deep (Richardson et al. 1995). In the eastern Arctic near Isabella Bay, Baffin Island, bowhead whales feed in troughs 200 m deep, where the highest concentrations of copepods are at depths >100 m (Finley 1987[6], 1990). Although dive depth significantly influenced duration for most tagged bowhead whales, it was not a good predictor of the dive's duration

---

[4] D.C. Foote. 1964. Observations of the bowhead whale at Point Hope, Alaska. Geography Department, McGill University, Montréal, Que., Canada.

[5] K.J. Finley, and J.D. Goodyear. 1993. Dive patterns and feeding habitat of the bowhead whale in Baffin Bay. *In* Abstracts from the Tenth Biennial Conference of The Society for Marine Mammalogy on the Biology of Marine Mammals, held at Galveston, Tex., 11–15 November 1993. p. 48. [Abstr.]

[6] K.J. Finley. 1987. Continuing studies of the eastern stock of bowhead whale at Isabella Bay, Baffin Island, 1986. Report by LGL Ltd., Toronto, for World Wildlife Fund Canada, 60 St. Clair Avenue East, Suite 201, Toronto, ON M4T 1N5, Canada.

(Fig. 6). Theory suggests that deeper dives should be of longer duration for diving animals utilizing a resource at depth (Kramer 1988; Houston and Carbone 1992). There is ample evidence of this for many air-breathing aquatic animals, including sea turtles (Eckert et al. 1986), diving birds (Stonehouse 1967; Kooyman et al. 1992; Williams et al. 1992), pinnipeds (Gentry et al. 1986; Kooyman and Gentry 1986; Feldkamp et al. 1989), odontocetes (Martin and Smith 1992; Martin et al. 1994), and mysticetes (Dolphin 1987a; Lagerquist 1997). Factors other than maximum depth may also strongly influence dive duration. Individual variation, prey depth and abundance, and the activity in which animals engage are factors likely to affect dive time.

Three whales (DZ-2, DZ-4, and D-2) made long dives in the vicinity of Mackenzie Canyon between 10 and 14 September. At least two of these whales were making extended bouts of deep dives in which they spent most of their time at depths $\geq$48 m. We suspect that these animals were feeding in the water column or near the bottom on dense zooplankton patches, probably calanoid copepods. Feeding on zooplankton, primarily copepods and euphausiids (Lowry 1993), is the predominant activity for bowhead whales that summer in the Beaufort Sea (Würsig et al. 1985). Baleen whales must feed where zooplankton is concentrated (Brodie et al. 1978). Zooplankton distribution in the Beaufort Sea is patchy both vertically and horizontally. Patches are usually 5–10 m thick and often extend several kilometres in the horizontal plane, with the thickest layer typically found either midwater or near the bottom (Griffiths et al. 1987). Bowhead whales seem to be able to find and exploit these patches. Zooplankton samples collected near feeding bowhead whales yielded higher prey biomass than samples taken elsewhere in the region (Griffiths and Buchanan 1982; Bradstreet and Fissel 1986; Bradstreet et al. 1987; Griffiths et al. 1987; Wartzok et al. 1990, see footnote 3). Mackenzie Canyon is a productive area in which zooplankton is at times concentrated (Thomson et al. 1986). In late summer, *Calanus hyperboreus* and *Calanus glacialis*, two important copepod prey species for bowhead whales in the Beaufort Sea (Lowry and Burns 1980; Lowry and Frost 1984; Lowry 1993), make a seasonal ontogenetic vertical migration to deeper water (>50 m) to overwinter, although when and to what depths they descend may vary with species, life stage, and geographic location (Maclellan 1967; Prygunkova 1968; Dawson 1978; Geinrikh et al. 1983; Kosobokova 1982; Longhurst et al. 1984; Conover 1988; Hirche 1991). *Calanus hyperboreus* and *C. glacialis* that have descended to deeper water in summer have substantially greater lipid content than those found in the upper 50 m (Head and Harris 1985; Kosobokova 1990) and would be a high-calorie food source for bowhead whales. We recommend that future studies to determine the importance of bowhead whale feeding areas examine zooplankton distribution and abundance to depths of at least 200 m.

When three whales were in heavy ice conditions, their tags recorded fewer and longer dives and more time exposed to the air during fewer surfacings (Table 4). However, calculations suggest that these animals would have been visible from the air for less time (Table 4). Whale DZ-1 also made more dives >48 m deep and spent more time at depths >32 m (Figs. 7B and 7C). These data suggest the whales'

strategy for dealing with areas of heavy ice: long dives to the deeper portion of the water column to avoid deep-keeled ice and longer surface times when open water is found. The four 1-h periods where tag DZ-1 did not break the surface coupled with the 23 very long "dives" ($\geq$61 min) recorded in heavy ice conditions suggest that this animal may have regularly broken ice to breathe.

Most of these findings are consistent with observed behavior of bowhead whales in ice. Würsig et al. (1984) noted longer dive times and more blows per surfacing for whales in ice than for those in open water and that about 75% of the animals observed in ice rested quietly when at the surface. Richardson et al. (1995) reported significantly shorter dive times for bowhead whales migrating through areas with 65–90% ice cover in the fall of 1983 (5.5 min) than for whales migrating through areas with <10% ice cover in the fall of 1985 and 1986 (18.2 min), but noted that the 1983 dive times were probably biased downward by the difficulty of resighting animals in heavy ice conditions after a long dive. Although the number of short series dives in a surfacing sequence decreased slightly, the increased percentage of surface time and the longer duration of longest surface times (at least for two animals) in heavy ice suggest that the whales may have rested at the surface between blows. Thus, the number of blows per surfacing sequence may have increased without a corresponding increase in short-series dives being recorded by the tag.

The directed westward movement of whale DZ-1 during the time it was in heavy ice (Mate et al. 2000) suggests that migration was its dominant activity. Perhaps the most interesting aspect of this whale's behavior during this interval was that it spent much less time near the surface (Fig. 7C). Although submerged swimming offers hydrodynamic advantages over swimming at the surface, animals need only submerge to about three times their body diameter to avoid surface-drag effects (Hertel 1966, p. 227). Bowheads would not have to exceed depths of our shallowest bin (16 m) for hydrodynamic considerations. However, the deep keels of ice floes can reach to 50 m below the surface (LaBelle et al. 1983). Bowhead whales migrating under a frozen lead where the water was 30 m deep avoided an area of deep-keeled multiyear ice and left bottom sediments in and around the hummocks created where they broke newly formed ice 14–18 cm thick to breath (George et al. 1989). Ellison et al. (1987) suggest that bowhead whales may use the differential surface reverberations of their calls (at distances of 1–2 km) to discriminate between areas of rough-bottomed deep-keeled multiyear ice and open water or smooth-bottomed young ice thin enough to break through to breathe. These authors modeled ice keels 10 m deep and a whale producing sound at 15 m, but they noted that the path of propagation of sound might allow bowhead whales in deep Arctic waters to "acoustically image" beyond immediate obstructions if sounds were broadcast below the horizontal. Bowhead whales may travel and vocalize at greater depths, to image ice conditions acoustically at greater distances and move more efficiently through or around areas with deep-keeled multiyear ice.

This is the first study to monitor dive and surfacing characteristics of individual bowhead whales day and night for

up to 33 days. The general lack of diel patterns recorded for tagged bowhead whales suggests that they continue their behavior regardless of light level. For many air-breathing nektonic species, diel changes in diving behavior are linked to diel vertical migration of their prey. In 1988, right whales (*Eubalaena glacialis*) in the Great South Channel made longer dives during the day when copepods migrated to near the bottom and shorter dives at night when copepods were near the surface but, in 1989, when copepods did not vertically migrate, no such difference in dive duration was found (Winn et al. 1995). Other examples include sea turtles (Eckert et al. 1989), penguins (Kooyman et al. 1992; Williams et al. 1992), and pinnipeds (Croxall et al. 1985; Feldkamp et al. 1989). With diel vertical migration absent or weak for most species, vertical distribution of the bowhead whale's zooplankton prey in Arctic waters is tied more to season than to time of day (Bogorov 1946; Kosobokova 1978; Longhurst et al. 1984; Sameoto 1984). Even the two tagged whales that made long deep dives in Mackenzie Canyon did so during day, twilight, and night. Migration also seemed to continue around the clock for whale DZ-1. No discernible time of day was favored for rest.

Studying diving behavior using satellite telemetry requires a thoughtful strategy. From the standpoint of data returns, transmitting information whenever possible throughout the day (DZ tags) rather than for limited periods (D tags) was clearly the superior method. DZ tags returned from 53 to 89% of the possible sampling periods, whereas the two D tags returned only 23 and 37% (Table 1). Tags were positioned well on all eight whales, so the likelihood of a tag being exposed during a surfacing was equal for all whales. Thus the difference reflects transmission schedules. If no transmissions were received during the 100 min that D tags were scheduled to transmit, four sampling periods of data (12 h) were lost. DZ tags, on the other hand, transmitted data for each sampling period during the next two sampling periods (usually 6 h). Unlike archival time–depth recorders (TDRs) that store data and must be retrieved, data recovery from Argos-monitored radio tags is limited to 256-bit transmissions while satellites are overhead. Archival TDRs are suitable only for animals that can be reliably recaptured, such as turtles, birds, and pinnipeds, or for short-term deployment on cetaceans staying in one area (e.g., Croll et al. 1998). Depending on the objectives of the study, one can choose to transmit either compressed summary data for a larger number of dives and surfacings, as we did, or detailed time–depth data at a finer scale for a smaller subset of dives (e.g., Martin and Smith 1992; Martin et al. 1994). Though fine-scale details of individual dives are lost, summary data from satellite-linked tags provide an accurate representation of actual diving behavior that is qualitatively similar to that recorded simultaneously by TDRs, if consideration is given to how tags are programmed (Burns and Castillini 1998).

This study demonstrates the utility of microprocessor-controlled data loggers linked with satellite radiotelemetry for gathering dive and surfacing data on large whales. These methods allow data to be gathered around the clock from several animals simultaneously over a wide geographic range in any weather. Dive data linked to location information provide unique insight into habitat utilization. The first direct measurements of dive depths and time at depth gathered here suggest that assessments of feeding areas must examine potential prey availability to at least 200 m depth. The number of dives and surfacings sampled from these eight whales is an order of magnitude greater than in all previous visual studies of bowhead whales combined, and provides a wealth of information on the variability displayed by individual whales as well as on variability among animals. Understanding this natural variability may ultimately allow us to better measure the effects of human activities on such endangered species.

Acknowledgements

References

Bogorov, B.G. 1946. Peculiarities of diurnal vertical migrations of zooplankton in polar seas. J. Mar. Res. **6**: 25–32.

Bradstreet, M.S.W., and Fissel, D.B. 1986. Zooplankton of a bowhead whale feeding area off the Yukon Coast in August 1985. Report by LGL Ltd., Toronto, to the Canadian Department of Indian Affairs and Northern Development, Ottawa, Ont.

Bradstreet, M.S.W., Thomson, D.H., and Fissel, D.B. 1987. Zooplankton and bowhead feeding in the Canadian Beaufort Sea, 1986. Report by LGL Ltd., Toronto, to the Canadian Department of Indian Affairs and Northern Development, Ottawa, Ont.

Brodie, P.F., Sameoto, D.D., and Sheldon, R.W. 1978. Population densities of euphausiids off Nova Scotia as indicated by net samples, whale stomach contents, and sonar. Limnol. Oceanogr. **23**: 1264–1267.

Burns, J.M., and Castellini, M.A. 1998. Dive data from satellite tags and time–depth recorders: a comparison in Weddell seal pups. Mar. Mamm. Sci. **14**: 750–764.

Carroll, G.M., and Smithhisler, J.R. 1980. Observation of bowhead whales during spring migration. Mar. Fish. Rev. **42**: 80–85.

Carroll, G.M., George, J.C., Lowry, L.F., and Coyle, K.O. 1987. Bowhead whale (*Balaena mysticetus*) feeding near Point Barrow, Alaska, during the 1985 spring migration. Arctic, **40**: 105–110.

Conover, R.J. 1988. Comparative life histories in the genera *Calanus* and *Neocalanus* in high latitudes of the northern hemisphere. Hydrobiologia, **167/168**: 127–142.

Croll, D.A., Tershey, B.R., Hewitt, R.P., Demer, D.A., Fiedler, P.C., Smith, S.E., Armstrong, W., Popp, J.M., Kiekhefer, T., Lopez, V.R., Urban, J., and Gendron, D. 1998. An integrated approach to the foraging ecology of marine birds and mammals. Deep-Sea Res. Part II. Top. Stud. Oceanogr. **45**: 1353–1371.

Croxall, J.P., Everson, I., Kooyman, G.L., Ricketts, C., and Davis, R.W. 1985. Fur seal diving behavior in relation to vertical distribution of krill. J. Anim. Ecol. **54**: 1–8.

Davis, R.A., Koski, W.R., Richardson, W.J., Evans, C.R., and Alliston, W.G. 1982. Distribution, numbers and productivity of the Western Arctic stock of bowhead whales in the eastern Beaufort Sea and Amundson Gulf, summer 1981. Report by LGL Ltd., Toronto, for Sohio Alaska Petroleum Co., Anchorage, and Dome Petroleum Ltd., Calgary. Available from The University of Calgary Library (Arctic Institute of North America Collection), Calgary, AB T2N 1N4, Canada.

Davis, R.W., Worthy, G.A.J., Würsig, B., and Lynn, S.K. 1996. Diving behavior and at-sea movements of an Atlantic spotted dolphin in the Gulf of Mexico. Mar. Mamm. Sci. **12**: 569–581.

Dawson, J.K. 1978. Vertical distribution of *Calanus hyperboreus* in the central Arctic Ocean. Limnol. Oceanogr. **23**: 950–957.

Dolphin, W.F. 1987*a*. Ventilation and dive patterns of humpback whales, *Megaptera noveaeangliae*, on their Alaskan feeding grounds. Can. J. Zool. **65**: 83–90.

Dolphin, W.F. 1987*b*. Dive behavior and estimated energy expenditure of foraging humpback whales in southeast Alaska. Can. J. Zool. **65**: 354–362.

Dorsey, E.M., Richardson, W.J., and Würsig, B. 1989. Factors affecting surfacing, respiration, and dive behaviour of bowhead whales, *Balaena mysticetus*, summering in the Beaufort Sea. Can. J. Zool. **67**: 1801–1815.

Eckert, S.A., Nellis, D.W., Eckert, K.L., and Kooyman, G.L. 1986. Diving patterns of two leatherback sea turtles (*Dermochelys coriacea*) during internesting intervals at Sandy Point, St. Croix, U.S. Virgin Islands. Herpetologica, **42**: 381–388.

Eckert, S.A., Eckert, K.L., Ponganis, P., and Kooyman, G.L. 1989. Diving and foraging behavior of leatherback sea turtles (*Dermochelys coriacea*). Can. J. Zool. **67**: 2834–2840.

Ellison, W.T., Clark, C.W., and Bishop, G.C. 1987. Potential use of surface reverberation by bowhead whales, *Balaena mysticetus*, in under-ice navigation: preliminary considerations. Rep. Int. Whaling Comm. **37**: 329–332.

Feldkamp, S.D., DeLong, R.L., and Antonelis, G.A. 1989. Diving patterns of California sea lions, *Zalophus californianus*. Can. J. Zool. **67**: 872–883.

Finley, K.J. 1990. Isabella Bay, Baffin Island: an important historical and present day concentration area for the endangered bowhead whale (*Balaena mysticetus*) of the eastern Canadian Arctic. Arctic, **43**: 137–152.

Geinrikh, A.K., Kosobokova, K.N., and Rudyakov, Yu.A. 1983. Seasonal variations in the vertical distribution of some prolific copepods of the Arctic basin. Can. Transl. Fish. Aquat. Sci. No. 4925. [Translated from Biologia Tsentral'nogo Arkticheskogo Basseina, 1980, pp. 155–166.]

Gentry, R.L., Kooyman, G.L., and Goebel, M.E. 1986. Feeding and diving behavior of northern fur seals. *In* Fur seals, maternal strategies on land and at sea. *Edited by* R.L. Gentry and G.L. Kooyman. Princeton University Press, Princeton, N.J. pp. 61–78.

George, J.C., Clark, C., Carroll, G.M., and Ellison, W.T. 1989. Observation on the ice-breaking and ice navigation behavior of migrating bowhead whales (*Balaena mysticetus*) near Point Barrow, Alaska, spring 1985. Arctic, **42**: 24–30.

Griffiths, W.B., and Buchanan, R.A. 1982. Characteristics of bowhead feeding areas. *In* Behavior, disturbance responses and feeding of bowhead whales *Balaena mysticetus* in the Beaufort Sea, 1980–81. *Edited by* W.J. Richardson. Report by LGL Ltd., Toronto, for U.S. Bureau of Land Management, Washington, D.C. NTIS No. PB86-152170, National Technical Information Service, Springfield, Va. pp. 347–355.

Griffiths, W.B., Thomson, D.H., and Johnson, G.E. 1987. Zooplankton and hydroaccoustics. *In* Importance of the eastern Alaskan Beaufort Sea to feeding bowhead whales, 1985–86. *Edited by* W.J. Richardson. Report by LGL Ltd., Toronto, to U.S. Minerals Management Service. NTIS No. PB 150271/AS, National Technical Information Service, Springfield, Va. pp. 135–256.

Harris, R.B., Fancy, S.G., Douglas, D.C., Garner, G.W., Amstrup, S.C., McCabe, T.R., and Pank, L.F. 1990. Tracking wildlife by satellite: current systems and performance. U.S. Fish Wildl. Serv. Fish Wildl. Tech. Rep. No. 30.

Head, E.J.H., and Harris, L.R. 1985. Physiological and biochemical changes in *Calanus hyberboreus* from Jones Sound, NWT during the transition from summer feeding to overwintering condition. Polar Biol. **4**: 99–106.

Heide-Jørgensen, M.P., and Dietz, R. 1995. Some characteristics of narwhal, *Monodon monoceros*, diving behaviour in Baffin Bay. Can. J. Zool. **73**: 2120–2132.

Hertel, H. 1966. Structure–form–movement. Reinhold Publishing Corp., New York.

Hiby, A.R., and Hammond, P.S. 1989. Survey techniques for estimating the abundance of cetaceans. Rep. Int. Whaling Comm. Spec. Issue No. 11. pp. 47–80.

Hirche, H.-J. 1991. Distribution of dominant calanoid copepod species in the Greenland Sea during late fall. Polar Biol. **11**: 351–362.

Houston, A.I., and Carbone, C. 1992. The optimal allocation of time during the diving cycle. Behav. Ecol. **3**: 255–265.

Klinowska, M. 1991. Dolphins, porpoises and whales of the world. The IUCN red data book. International Union for Conservation of Nature and Natural Resources (IUCN), Gland, Switzerland, and Cambridge, U.K.

Kooyman, G.L., and Gentry, R.L. 1986. Diving behavior of South African fur seals. *In* Fur seals, maternal strategies on land and at sea. *Edited by* R.L. Gentry and G.L. Kooyman. Princeton University Press, Princeton, N.J. pp. 142–152.

Kooyman, G.L., Cherel, Y., Le Maho, Y., Croxall, J.P., Thorson, P.H., Ridoux, V., and Kooyman, C.A. 1992. Diving behavior and energetics during foraging cycles in king penguins. Ecol. Monogr. **62**: 143–163.

Koski, W.R., Davis, R.A., Miller, G.W., and Withrow, D.E. 1993. Reproduction. *In* The bowhead whale. *Edited by* J.J. Burns, J.J. Montague and C.J. Cowles. Spec. Publ. No. 2., The Society for Marine Mammalogy, Lawrence, Kans. pp. 239–274.

Kosobokova, K.N. 1978. Diurnal vertical distribution of *Calanus hyperboreus* Krøyer and *Calanus glacialis* Jaschnov in the Central Polar Basin. Oceanology, **18**: 476–480.

Kosobokova, K.N. 1982. Composition and distribution of the bio-

mass of zooplankton in the central Arctic basin. Oceanology, **22**: 744–750.

Kosobokova, K.N. 1990. Age-related and seasonal changes in the biochemical makeup of the copepod *Calanus glacialis* as related to the characteristics of its life cycle in the White Sea. Oceanology, **30**: 103–109.

Kramer, D.L. 1988. The behavioral ecology of air breathing by aquatic animals. Can. J. Zool. **66**: 89–94.

LaBelle, J.C., Wise, J.L., Voelker, R.P., Schulze, R.H., and Wohl, G.M. 1983. Alaska ice atlas. Arctic Environmental Information and Data Center, University of Alaska, 707 A Street, Anchorage, AK 99501, U.S.A.

Lagerquist, B.A. 1997. Dive characteristics of northeast Pacific blue whales (*Balaenoptera musculus*) monitored by satellite telemetry. M.S. thesis, Oregon State University, Corvallis.

Lin, S. 1970. An introduction to error-correcting codes. Prentice Hall, Englewood Cliffs, N.J.

Ljungblad, D.K., Würsig, B., Swartz, S.L., and Keene, J.M. 1988. Observations on the behavioral responses of bowhead whales (*Balaena mysticetus*) to active geophysical vessels in the Alaskan Beaufort Sea. Arctic, **41**: 183–194.

Longhurst, A., Sameoto, D., and Herman, A. 1984. Vertical distribution of Arctic zooplankton in summer: eastern Canadian archipelago. J. Plankton Res. **6**: 137–168.

Lowry, L.F. 1993. Foods and feeding ecology. *In* The bowhead whale. *Edited by* J.J. Burns, J.J. Montague, and C.J. Cowles. Spec. Publ. No. 2., The Society for Marine Mammalogy, Lawrence, Kans. pp. 201–238.

Lowry, L.F., and Burns, J.J. 1980. Foods utilized by bowhead whales near Barter Island, Alaska, autumn 1979. Mar. Fish. Rev. **42**: 88–91.

Lowry, L.F., and Frost, K.J. 1984. Foods and feeding of bowhead whales in western and northern Alaska. Sci. Rep. Whales Res. Inst. (Tokyo), **35**: 1–16.

Maclellan, D.C. 1967. The annual cycle of certain calanoid species in west Greenland. Can. J. Zool. **45**: 101–115.

Martin, A.R., and Smith, T.G. 1992. Deep diving in wild, free-ranging beluga whales, *Delphinapterus leucas*. Can. J. Fish. Aquat. Sci. **49**: 462–466.

Martin, A.R., Kingsley, M.C.S., and Ramsay, M.A. 1994. Diving behaviour of narwhals (*Monodon monoceros*) on their summer grounds. Can. J. Zool. **72**: 118–125.

Mate, B.R., Stafford, K.M., Nawojchik, R., and Dunn, J.L. 1994. Movements and dive behavior of a satellite-monitored Atlantic whitesided dolphin (*Lagenorhynchus acutus*) in the Gulf of Maine. Mar. Mamm. Sci. **10**: 116–121.

Mate, B.R., Rossbach, K.A., Nieukirk, S.L., Wells, R.S., Irvine, A.B., Scott, M.D., and Read, A.J. 1995. Satellite-monitored movements and dive behavior of a bottlenose dolphin (*Tursiops truncatus*) in Tampa Bay, Florida. Mar. Mamm. Sci. **11**: 452–463.

Mate, B.R., Krutzikowsky, G.K., and Winsor, M. 2000. Satellite-monitored movements of radio-tagged bowhead whales in the Beaufort and Chukchi seas during the late-summer feeding season and fall migration. Can. J. Zool. **78**: 1168–1181.

Montague, J.J. 1993. Introduction. *In* The bowhead whale. *Edited by* J.J. Burns, J.J. Montague, and C.J. Cowles. Spec. Publ. No. 2., The Society for Marine Mammalogy, Lawrence, Kans. pp. 1–21.

Moore, S.E., and Reeves, R.R. 1993. Distribution and movement. *In* The bowhead whale. *Edited by* J.J. Burns, J.J. Montague, and C.J. Cowles. Spec. Publ. No. 2., The Society for Marine Mammalogy, Lawrence, Kans. pp. 313–386.

Nieukirk, S.L. 1992. Satellite monitored dive characteristics of the northern right whale (*Eubalaena glacialis*). M.S. thesis, Oregon State University, Corvallis, Oreg.

Prygunkova, R.V. 1968. On the growth cycle of *Calanus glacialis* Jaschnov in the White Sea. Dokl. Biol. Sci. **182**: 1447–1450 [Translated from Dokl. Akad. Nauk SSSR, **182**: 1447–1450.]

Ramsey, F.L., and Schafer, D.W. 1996. The statistical sleuth. Duxbury Press, Pacific Grove, Calif.

Richardson, W.J., Fraker, M.A., Würsig, B., and Wells, R.S. 1985. Behavior of bowhead whales, *Balaena mysticetus*, summering in the Beaufort Sea: reactions to industrial activities. Biol. Conserv. **32**: 195–230.

Richardson, W.J., Würsig, B., and Greene, C.R., Jr. 1986. Reactions of bowhead whales, *Balaena mysticetus*, to seismic exploration in the Canadian Beaufort Sea. J. Acoust. Soc. Am. **79**: 1117–1128.

Richardson, W.J., Würsig, B., and Miller, G.W. 1987. Bowhead distribution, numbers, and activities. *In* Importance of the eastern Alaskan Beaufort Sea to feeding bowhead whales, 1985–86. *Edited by* W.J. Richardson. Report by LGL Ltd., Toronto, to U.S. Minerals Management Service. NTIS No. PB 150271/AS, National Technical Information Service, Springfield, Va. pp. 257–366.

Richardson, W.J., Finley, K.J., Miller, G.W., Davis, R.A., and Koski, W.R. 1995. Feeding, social and migration behavior of bowhead whales, *Balaena mysticetus*, in Baffin Bay vs. the Beaufort Sea—regions with different amounts of human activity. Mar. Mamm. Sci. **11**: 1–45.

Rugh, D.J., and Cubbage, J.C. 1980. Migration of bowhead whales past Cape Lisburne, Alaska. Mar. Fish. Rev. **42**: 46–51.

Sameoto, D.D. 1984. Vertical distribution of zooplankton biomass and species in northeastern Baffin Bay related to temperature and salinity. Polar Biol. **2**: 213–224.

Scammon, C.M. 1874. The marine mammals of the northwestern coast of North America together with an account of the American whale fishery. J.H. Carmany, San Francisco. (Reprinted (paperback) 1968, Dover Publications Inc., New York.)

Scoresby, W., Jr. 1820. An account of the Arctic regions, with a history and description of the northern whale-fishery. Archibald Constable, Edinburgh, Scotland. [Reprinted by David and Charles, Newton Abbot, England.]

Stoker, S.W., and Krupnik, I.I. 1993. Subsistence whaling. *In* The bowhead whale. *Edited by* J.J. Burns, J.J. Montague, and C.J. Cowles. Spec. Publ. No. 2., The Society for Marine Mammalogy, Lawrence, Kans. pp.579–629.

Stonehouse, B. 1967. Feeding behaviour and diving rhythms of some New Zealand shags, *Phalacrocoracidae*. Ibis, **109**: 600–605.

Sumich, J.L. 1983. Swimming velocities, breathing patterns, and estimated costs of locomotion in migrating gray whales, *Eschrichtius robustus*. Can. J. Zool. **61**: 647–652.

Thomson, D.H. 1987. Energetics of bowheads. *In* Importance of the eastern Alaskan Beaufort Sea to feeding bowhead whales, 1985–86. *Edited by* W.J. Richardson. Report by LGL Ltd., Toronto, to U.S. Minerals Management Service. NTIS No. PB 150271/AS, National Technical Information Service, Springfield, Va. pp. 417–448.

Thomson, D.H., Fissel, D.B., Marko, J.R., Davis, R.A., and Borstad, G.A. 1986. Distribution of bowhead whales in relation to hydrometerological events in the Beaufort Sea. Environmental Studies Revolving Funds Rep. No. 028, Canadian Department of Indian Affairs and Northern Development, Ottawa.

U.S. Department of Commerce. 1991. Tide tables 1992: high and low water predictions, west coast of North and South America,

including the Hawaiian islands. U.S. Department of Commerce, Rockville, Md.

Wakerly, J. 1978. Error detecting codes, self-checking circuits and applications. North-Holland, New York.

Williams, T.D., Kato, A., Croxall, J.P., Naito, Y., Briggs, D.R., Rodwell, S., and Barton, T.R. 1992. Diving pattern and performance in nonbreeding gentoo penguins (*Pygoscelis papua*) during winter. Auk, **109**: 223–234.

Winn, H.E., Goodyear, J.D., Kenney, R.D., and Petricig, R.O. 1995. Dive patterns of tagged right whales in the Great South Channel. Cont. Shelf Res. **15**: 593–611.

Würsig, B., Dorsey, E.M., Fraker, M.A., Payne, R.S., Richardson, W.J., and Wells, R.S. 1984. Behavior of bowhead whales, *Balaena mysticetus*, summering in the Beaufort Sea: surfacing,

respiration, and dive characteristics. Can. J. Zool. **62**: 1910–1921.

Würsig, B., Dorsey, E.M., Fraker, M.A., Paine, R.S., and Richardson, W.J. 1985. Behavior of bowhead whales, *Balaena mysticetus*, summering in the Beaufort Sea: a description. Fish. Bull. **83**: 357–377.

Würsig, B., Wells, R.S., and Croll, D.A. 1986. Behavior of gray whales summering near St. Lawrence Island, Bering Sea. Can. J. Zool. **64**: 611–621.

Zeh, J.E., Clark, C.W., George, J.C., Withrow, D., Carroll, G.M., and Koski, W.R. 1993. Current population size and dynamics. *In* The bowhead whale. *Edited by* J.J. Burns, J.J. Montague, and C.J. Cowles. Spec. Publ. No. 2., The Society for Marine Mammalogy, Lawrence, Kans. pp. 409–489.

DIVE CHARACTERISTICS OF SATELLITE-MONITORED BLUE WHALES (*BALAENOPTERA MUSCULUS*) OFF THE CENTRAL CALIFORNIA COAST

B. A. LAGERQUIST

Coastal Oregon Marine Experiment Station,
Oregon State University,
Hatfield Marine Science Center,
Newport, Oregon 97365, U.S.A.
E-mail: lagerqub@ucs.orst.edu

K. M. STAFFORD

Cooperative Institute for Marine Resources Studies,
Oregon State University,
Hatfield Marine Science Center,
Newport, Oregon 97365, U.S.A.

B. R. MATE

Coastal Oregon Marine Experiment Station,
Fisheries & Wildlife,
Oregon State University,
Hatfield Marine Science Center,
Newport, Oregon 97365, U.S.A.

ABSTRACT

Dive habits of four Northeast Pacific blue whales (*Balaenoptera musculus*) were studied using satellite-monitored radio tags. Tags summarized dive-duration data into eight 3-h periods daily. One tag additionally summarized dive depth and time-at-depth information for these same periods. Tracking periods ranged from 0.6 to 12.7 d and provided data for 17 three-hour summary periods, representing 2,007 dives (788 of which provided depth information). Total number of dives during a 3-h summary period ranged from 83 to 128. Seventy-two percent of dives were ≤1 min long. All whales spent >94% of their time submerged. Average duration of true dives (dives >1 min) ranged from 4.2 to 7.2 min. Seventy-five percent of depth-monitored dives were to ≤16 m, accounting for 78% of that animal's time. Average depth of dives to >16 m was 105 ± 13 m.

Key words: blue whale, *Balaenoptera musculus,* satellite telemetry, radio-tracking, dive behavior.

Respiration rates and diving patterns are important indices of whale be-
havior and are critical in transforming shipboard and aerial survey counts into
accurate abundance estimates (Doi 1974, CETAP 1982, Hiby and Hammond
1989). Diel variations in activity, which might render whales more visible at
certain times of day, are also significant factors to be taken into account in
assessment techniques (Klinowska 1986). Diving and surfacing behavior has
been examined for bowhead whales (*Balaena mysticetus*; Würsig *et al.* 1984,
Dorsey *et al.* 1989), gray whales (*Eschrichtius robustus*; Würsig *et al.* 1986),
humpback whales (*Megaptera novaeangliae*; Dolphin 1987), minke whales (*Ba-
laenoptera acutorostrata*; Joyce *et al.* 1990, Stern 1992), and fin whales (*Balaen-
optera physalus*; Stone *et al.* 1992, Kopelman and Sadove 1995), but respiration
and diving patterns of blue whales are poorly documented (Leatherwood *et al.*
1982); diel variation in such behavior has not been studied.

In this study we monitored the movements and dive habits of blue whales
in the eastern North Pacific with satellite telemetry. The goals were to re-
motely monitor dive behavior in a large, free-ranging cetacean and examine
possible diel rhythms.

METHODS

Four blue whales were tagged with satellite-monitored radio transmitters
off the coast of central California from 20 August to 30 September 1993. Tags
were deployed 1–4 m behind the blowhole with a 68-kg Barnett compound
crossbow, from a 5.3-m rigid-hulled inflatable boat.

Argos-certified UHF transmitters emitted 400-mW signals to receivers on
two NOAA TIROS-N weather satellites in sun-synchronous polar orbits. To
conserve battery power, transmissions were scheduled to coincide with some
of the times during which satellites were overhead (10–12 times/d for ap-
proximately 6–17 min each). During each transmission cycle, the tags trans-
mitted every 40 sec when at the surface. A saltwater conductivity switch was
used to insure the tag was at the surface before initiating a transmission. The
tags were powered by lithium batteries.

Two types of sensor tags were used: a "duration" type, which collected dive
duration information only, and a "depth" type, which collected information
concerning dive depth as well as duration. We defined a dive as any submer-
gence of the tag for longer than 6 sec. Tag locations were calculated by Service
Argos from Doppler-shift data when two or more messages reached the satellite
during one pass (Fancy *et al.* 1988). Argos provides an estimate of location
accuracy by assigning each of their locations to one of six classes (LC-1, LC-
2, LC-3, LC-0, LC-A, and LC-B). Location classes 0, A, and B have no pre-
dicted accuracy. Distances and speeds were calculated from Argos locations
and then subjected to editing criteria to eliminate unacceptable locations. We
allowed a radius of uncertainty of 11.5 km around each location (representing
a radial error equal to two standard deviations from our testing of locations
<LC-1; Mate *et al.* 1997) and eliminated all locations which resulted in speeds

Table 1. Duration categories for all four tags, and depth and time at depth categories for depth tag only, for blue whales tagged off central California, 1993.

Duration (min)	Depth (m)	Time at depth (%)
0–1	0–16	0–16
1–4	16–32	16–32
4–7	32–48	32–48
7–10	48–96	48–96
10–13	96–152	96–152
13–16	152–200	152–200
16–19	200–248	200–296
19–255	248–296	296–400
	296–400	400–2,040
	400–2,040	

>15 km/h for >1 h, or which were located on land >11.5 km from the nearest shoreline.

Depth Tag

One depth tag (DEP-1) was deployed, consisting of a Telonics (Mesa, AZ) ST-6 Argos transmitter, a Wildlife Computers (Woodinville, WA) controller board, and a pressure transducer. Transmissions were scheduled for four 2-h periods daily. Each 960-msec transmission consisted of a discrete identification code and 256 bits of sensor data, which included a cyclic redundancy check (CRC) code for error detection. Data on every dive were collected and summarized over eight 3-h summary periods daily. The summary information included the number of dives in ten different depth categories, ranging from 0 to 2,040 m; the number of dives in each of eight duration categories, ranging from 6 sec to 255 min; the percentage of time spent in each of nine depth categories, ranging from 0 to 2,040 m (Table 1); duration of the longest dive (2-min resolution), duration of the first dive to the deepest depth (2-min resolution), depth of the deepest dive (16-m resolution), longest surface duration uninterrupted by a submergence of greater than 6 sec (30-sec resolution), and total surface duration (1-min resolution).

The tag housing was a stainless steel cylinder 5 cm in diameter by 19 cm in length and weighing 0.80 kg, with two subdermal attachments. Attachments consisted of stainless steel rods (12.7 cm long, 0.6 cm in diameter) with double-edged blades at the distal end. One pair of folding toggles was mounted behind the blades to prevent outward migration of the tag. The tag was filled with plastic epoxy to reduce air spaces and add structural strength. A flexible 17-cm whip antenna was mounted in one end-cap perpendicular to the tag housing.

Duration Tag

Three duration tags (DUR-1, -2, -3) were deployed. Each consisted of an Oregon State University-designed sampling program loaded in a Telonics ST-6 Argos transmitter. The housings and attachments of these tags were identical to the depth tags with the exception that they lacked a pressure transducer. Duration tags were not filled with plastic epoxy and weighed 0.52 kg.

Duration tags collected data on every dive and summarized the information over eight 3-h summary periods daily. The data collected during each period consisted of the number of dives occurring in each of eight duration categories (Table 1), ranging from 6 sec to 255 min; maximum surface duration (1-min resolution); maximum dive duration greater than 10 min (2-min resolution); and percentage of time submerged (1% resolution).

Transmissions were scheduled for two 100-min periods each day. Each 320-msec transmission consisted of an identification code and 64 bits of data, including a CRC code.

Tag Data

For comparison with other respiration studies in which differentiation was made between blow intervals and dives, we computed average dive duration only for dives >1 min (hereafter referred to as "true dives"). Most blow intervals for blue whales are likely <1 min long, but tag software (1-min resolution in the first duration bin) prevented calculations based on dives of shorter duration.

The average duration of true dives was calculated using the following

$$\bar{x}\mathrm{dur}_i = \sum_{j=2}^{8} \mathrm{mid\text{-}value}_{ij} \cdot \mathrm{dives}_{ij}/\mathrm{tdives}_i$$

where $\bar{x}\mathrm{dur}_i$ = average duration of dives greater than 1 min for period i; mid-value$_{ij}$ = middle value (min) of duration category j in period i; dives$_{ij}$ = number of dives in duration category j for period i. Dives <60 sec were excluded from calculations (duration category 1).

As dives in the upper 16 m of the water column (first depth range) likely represent surface activity associated with breathing, only dives >16 m deep were considered in average depth calculations. The average depth of dives to >16 m during a summary period was calculated using the following

$$\bar{x}\mathrm{dep}_i = \sum_{j=2}^{10} \mathrm{mid\text{-}depth}_{ij} \cdot \mathrm{dives}_{ij}/\mathrm{tdives}_i$$

where $\bar{x}\mathrm{dep}_i$ = average dive depth for period i; mid-depth$_{ij}$ = middle value (m) of depth category j in period i; dives$_{ij}$ = number of dives in depth category j for period i.

Because dives were defined as submergences longer than 6 sec, the depth tag did not begin counting dive duration until 6 sec had elapsed. The first 6 sec of every dive were not included in the duration. For periods with an exact

count of dives, the number of dives was multiplied by 6 sec and the product added to the time spent in the first depth category. For those periods for which there was no exact dive-number information (transmissions in which only time spent at depth information was error-free), the average number of dives from periods with exact dive counts was multiplied by 6 sec to provide a correction factor for the time at depth.

Data were divided into four periods of the day for diel comparisons. For depth tags, summary periods 2, 3, and 4, (2000–0459 PDT) were combined for night, summary periods 6, 7, and 8 (0800–1659 PDT) for day, and summary periods 1 (1700–1959 PDT) and 5 (0500–0759) for dusk and dawn, respectively. For duration tags, summary periods 6, 7, and 8 (2100–0559 PDT) were combined for night, summary periods 2, 3, and 4 (0900–1759 PDT) for day, and summary periods 1 (0600–0859 PDT) and 5 (1800–2059 PDT) for dawn and dusk, respectively. The time periods differed between the two tag types due to their different initialization times.

Visual Observations

Respiration patterns of untagged whales were observed from a 16.6-m vessel (R/V *'Cille*) using the focal animal sampling technique (Altmann 1974). Before beginning an observation, we took general behavioral observations and identification photographs of the whales. If more than one whale was present, the most easily distinguishable animal was chosen for respiration sampling. When it was possible to distinguish both animals in a pair by distinctive coloration or dorsal fin shape, respiration data were collected for both. Observation distances varied from 10 to 150 m.

The desired sampling period was 30 min. Sampling periods were terminated prior to 30 min when the focal animal could no longer be identified. The primary observer called out sightings to a second person who recorded exact times (h:min:sec) of exhalations and behaviors. Four variables similar to those measured in other respiration studies (Würsig *et al*. 1984, 1986; Dolphin 1987; Dorsey *et al*. 1989) were evaluated: true dive time (of dives greater than 1 min, for comparison with our tag data), duration of time at the surface (including time between blows) between successive true dives (surface time), number of blows during the surfacing, and the time between blows (blow interval). As in Dolphin's (1987) humpback study, duration of time at the surface was given the value of 0.1 min when the surface time included only 1 blow. Mean blow interval for each sampling period was calculated by dividing the sum of all blow intervals in a surfacing by the number of blow intervals and then taking the average of that value for all surfacings in the sampling period. Mean blow rate was calculated as described by Dorsey *et al*. (1989), by dividing mean number of blows per surfacing by mean surfacing-dive cycle (mean duration of surfacing plus mean duration of the following true dive). Surface-time proportion (expressed as a percentage) was calculated by dividing mean surface time by mean surfacing-dive cycle.

RESULTS

Tracking periods ranged from 0.6 to 12.7 d and provided error-free information for 2,007 dives (Table 2). Sixty, fifty, and nineteen percent of transmissions contained CRC errors for whales DUR-2, DUR-3, and DEP-1, respectively. Data from these transmissions were not included in analyses. One error-free transmission was received for DUR-1. No statistical comparisons were made due to the small sample sizes.

The total number of dives for a 3-h summary period (all whales) ranged from 83 to 128 ($\bar{x} = 35 \pm 8$/h; $n = 4$; Table 3). Seventy-two percent of these dives were <1 min in duration (range 66.9%–76.0%; $n = 4$; Fig. 1). Dives <4 min in duration accounted for 89.2% of all dives for whale DUR-3. Whales DUR-1 and DUR-2 had their second highest percentage of dives in the 4–7 min range ($\bar{x} = 13.2\% \pm 0\%$ and $12.1\% \pm 10.1\%$, respectively). Only whales DEP-1, DUR-2, and DUR-3 reported dives ≥10 min long. There were not enough data to determine whether the dive distributions followed any diel pattern; however, the dives of whale DUR-3 suggested the possibility of diel variation.

The percentage of time that the animals were submerged during each 3-h summary period ranged from 94.7% to 96.5% ($n = 4$; Table 3).

Dive Duration

Average duration of true dives (per period) for each whale ranged from 4.2 to 7.2 min ($\bar{x} = 5.8 \pm 1.5$ min; $n = 4$; Table 3).

The duration of the longest dive per period for whale DEP-1 ranged from 10 to 18 min ($\bar{x} = 13 \pm 3$ min; $n = 6$). Whale DUR-1 reported 0 for duration of longest dive, meaning no dives >10 min were recorded. Whale DUR-2 also reported 0's for 3 of 4 summary periods. The fourth period reported a maximum dive duration of 15 min. Whale DUR-3 reported 0's for 3 of 6 periods, with an average maximum dive duration of 14 ± 1 min for the remaining 3 periods.

For whale DEP-1, maximum surface duration during a summary period ranged from 7 to 90 sec ($\bar{x} = 48 \pm 28$ sec, $n = 7$). The duration-only tags had a 1-min resolution for this variable, and all reported 0's for maximum surface duration. Thus, there were no surfacings lasting >60 sec in the 11 summary periods reported.

Depth

Whale DEP-1 was the only animal for which depth information was available. Most dives were in the 0–16 m depth range ($\bar{x} = 74.8\% \pm 4.5\%$; $n = 9$; Fig. 2). The second highest percentage of dives ($\bar{x} = 15.4\% \pm 7.4\%$; $n = 9$) were made to 97–152 m. The average depth of dives >16 m was 105 ± 13 m (median = 103 m; range 84–121 m, $n = 9$).

Depth of the deepest dive during a summary period ranged from 112 to

Table 2. Deployment dates, number of days between deployment and date of last message, and number of messages received for four blue whales tagged off central California, 1993. 13 discrete summary periods received for whale DEP-1 contained information for 6 duration histograms, 9 depth histograms, and 7 time-at-depth histograms.

Whale #	Deploy date/time (UTC)	Date/time (UTC) of last message	# Days	# Messages	# Error-free summary periods	# Error-free dives
DUR-1	8/29/93 0001	8/29/93 1332	0.6	1	1	121
DUR-2	8/29/93 0146	9/6/93 0152	8.0	10	4	332
DUR-3	9/17/93 2340	9/30/93 1342	12.7	12	6	768
DEP-1	8/31/93 2105	9/12/93 1516	11.7	16	13	786
TOTAL			32.9	39	24	2,007

Table 3. Means (±SD) and medians of dive data collected during 3-h summary periods for all blue whales tagged off central California in 1993. Means for all whales combined calculated as average of each whale's individual average.

Whale #	% Time submerged	Total number of dives	Duration of true dives (>1 min) (min)	Depth of dives >16 m
All	95.8 ± 0.8 95.9 n = 4	105 ± 23 104 n = 4	5.8 ± 1.5 5.9 n = 4	—
DEP-1	95.9 ± 1.6 96.0 n = 7	88 ± 16 86 n = 6	6.9 ± 1.4 7.2 n = 6	105 ± 13 103 n = 9
DUR-1	96.0 n = 1	121 n = 1	5.0 n = 1	—
DUR-2	96.5 ± 0.6 96.5 n = 4	83 ± 16 79 n = 4	7.2 ± 1.5 7.1 n = 4	—
DUR-3	94.7 ± 2.1 95.0 n = 6	128 ± 42 128 n = 6	4.2 ± 1.8 3.7 n = 6	—

192 m ($\bar{x} = 151 \pm 28$ m; $n = 9$). Duration of the deepest dive during a summary period ranged from 4 to 18 min ($\bar{x} = 9 \pm 5$ min; $n = 6$).

Whale DEP-1 spent most of its time (78.2%) in the 0–16-m depth range, followed by 9.3% of its time at 17–32-m (Fig. 2). Although 15.4% of all dives went to the 97–152-m depth range, whale DEP-1 spent only 1.2% of its time there.

Visual Observation Data

We observed respirations of nine blue whales for a total of 3.3 h (Table 4). Average surface time for all whales was 64.8 ± 15.6 sec ($n = 9$). Average number of blows during these surfacing sequences was 4.0 ± 0.6 ($n = 9$), with mean blow intervals of 21 ± 4.2 sec ($n = 9$). True dive times averaged 3.3 ± 1.4 min ($n = 9$). Submergences <1 min in length accounted for 78.1% $\pm$ 1.7% of all dives. Maximum dive durations for the nine whales ranged from 3.2 to 6.5 min, with an average of 4.7 ± 1.1 min. Mean blow rate was 1.0 ± 0.2 blows per min ($n = 9$). Percentage of time near the surface averaged 25.4% $\pm$ 5.4% ($n = 9$).

Movements

We obtained five locations for whale DEP-1 and two for whale DUR-2. All locations were of location class 0 (LC-0) but fit our editing criteria. The minimum distance travelled from tagging to the last location was 274 km for

whale DEP-1 and 124 km for DUR-2 (Fig. 3). These are straight-line distances and represent minimum distances travelled. As such, estimates of speeds are also minimums.

After tagging, whale DEP-1 travelled 57 km west in 4 h (14.2 km/h), 48 km southeast in 35.9 h (1.3 km/h), east 56 km in 23.7 h (2.4 km/h), south 32 km in 13.0 h (2.5 km/h), and 82 km west in 12.3 h (6.7 km/h). Although the whale was tagged in 280 m of water, all five subsequent locations were in water deeper than 1,000 m.

Following tagging in 90 m of water, whale DUR-2 traveled north-northwest 72 km in 59.6 h (1.2 km/h), then south 52 km in 12.9 h (4.0 km/h). Water depths at the first and second post-tagging locations were 55 m and 370 m, respectively.

Discussion

Dive Duration

Dive-habit studies conducted during whaling operations reported dive durations for blue whales ranging from 10 to 50 min (Laurie 1933, Zenkovich 1936, Tomlin 1967). The longer dives could be due to whales exhibiting avoidance when chased by whaling ships. Doi (1974), Yablokov *et al.* (1974), and Lockyer (1976) also used whaling data but reported much shorter dive durations (5–7, 2–5, and 2–7 min, respectively). These values are much closer to the 5.9-min average true-dive duration from our tagged whales and the 3.3-min average durations from our visual observations. The average duration of dives >1 min for visually observed pygmy blue whales (*B. m. brevicauda*) off Peru was 9.9 min (range = 1.1–26.9 min; Donovan 1984). More recently, Croll *et al.* (1998) reported an average dive duration of 4.3 min for TDR-instrumented blue whales in the Santa Barbara Channel, California. It is unclear, however, what their definition of a dive was.

True-dive durations from this study are in close agreement with recent visual and telemetry studies of other baleen whale species: 2.88 min for summering North Atlantic fin whales (*Balaenoptera physalus*) with boats in the area, and 3.35 min without boats (Stone *et al.* 1992); 2.66 min for surface-feeding and 3.10 min for non-surface-feeding fin whales off eastern Long Island (Kopelman and Sadove 1995); 4.85 min for a fin whale in Iceland (Watkins *et al.* 1984); 3.18 min for summering gray whales (Würsig *et al.* 1986); 3.0 min for humpbacks (*Megaptera novaeangliae*) (Dolphin 1987); 4.42 min for summering bowhead whales (*Balaena mysticetus*) in 1980–1984 (Dorsey *et al.* 1989); 3.43–12.08 min for bowheads (Würsig *et al.* 1984); and 2.12 min for right whales off Cape Cod (Winn *et al.* 1995).

The proportion of the surface-dive cycle spent at the surface (25.4%) for our visually observed blue whales was very similar to reports for other species, with the exception of fin whales (Table 2). This latter difference is likely related to the way in which the data were collected rather than representing a biological difference. Our study defined a true dive to be any submergence
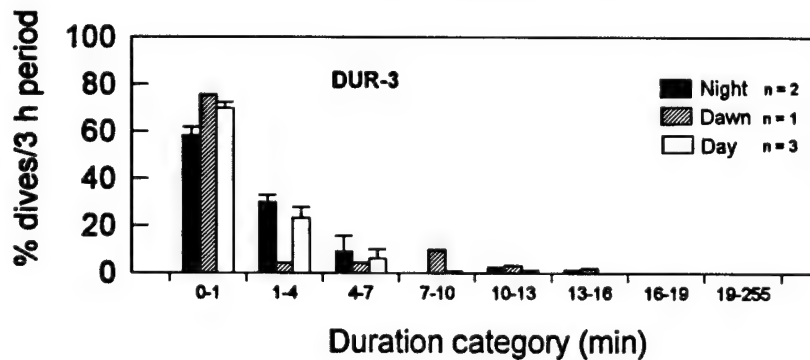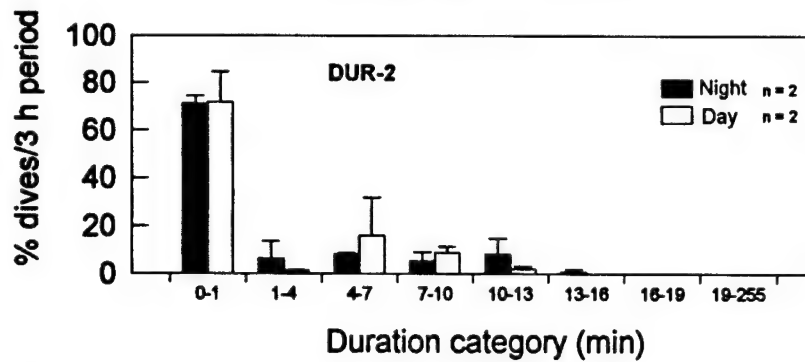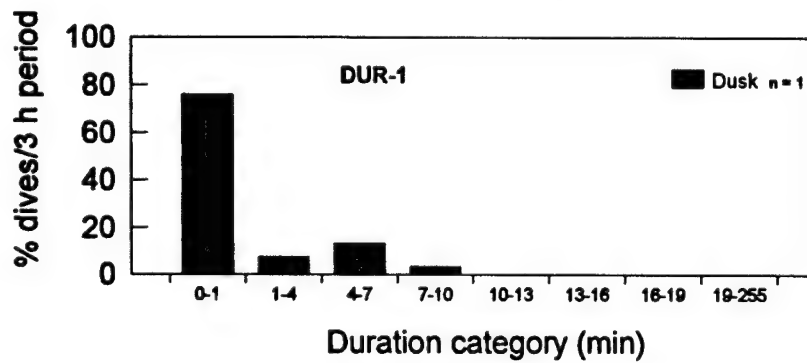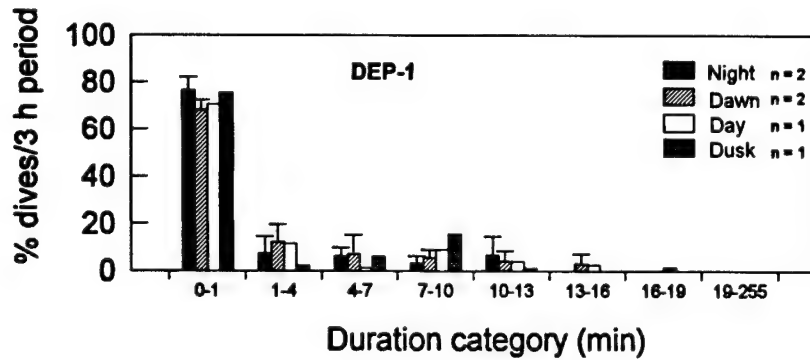
>1 min, while Stone *et al.* (1992) used 25 sec. The latter cutoff would result in shorter surface durations, hence smaller proportions of time spent at the surface, as well as shorter dive durations. This bias is further emphasized when considering proportions of time spent at the surface obtained from our tagged whales. The tags were programmed to record any submergence >6 sec as a dive. Consequently, the average proportion of time submerged for these whales was 95.8%.

Tag Data vs. *Visual Data*

Overall durations of true dives were shorter for the visual observations than those from tagged whales (3.3 *vs.* 5.9 min). The proportion of dives <1 min in length was only slightly higher for whales observed visually than for tagged whales (78% *vs.* 72%). The maximum dive durations reported for the nine visually observed whales were much shorter than those reported for tagged whales. All of these "differences" are likely due to either small sample sizes (total visual observation time being only slightly longer than a single 3-h summary period from tagged whales) or the limitations of observers to reacquire whales which swim out of visual range during long dives (Dorsey *et al.* 1989). Harvey and Mate (1984) discovered similar bias in their analyses of visual *vs.* VHF radio tag data for gray whales (*Esrichtius robustus*).

Dive Depth

The overall distribution of dive depths for whale DEP-1 revealed a bimodal distribution, with most dives between 0–16 m and 97–152 m. Dives in the first 16 m may represent primarily blow intervals during surface time between longer dives. More than 72% of all dives were <1 min in duration and <16 m deep. Surface-feeding may also have contributed to numbers of dives and time in the first 16-m depth range.

Dives to the 97–152-m depth range were the second most frequent (15.2% of all dives) and took place in water >1,000 m deep. Only 1.2% of the whale's total time underwater was spent at that depth range, however. Whale DEP-1 also dove to depths of 200 m, but again, spent very little time there (<1%). Such behavior indicates a pattern of "spike dives" (Martin and Smith 1992) where the whale spends more of its time descending or ascending than swimming along at depth. This may reflect searching the water column for prey or a preference for feeding during descent and/or ascent rather than at the bottom of the dive. A similar pattern was seen in pygmy blue whale dive traces from a depth sounder in the Indian Ocean

←

Figure 1. Average percentage of dives in each of eight duration categories, divided into four times of day, for four blue whales tagged off central California in 1993. Error bars represent one standard deviation.
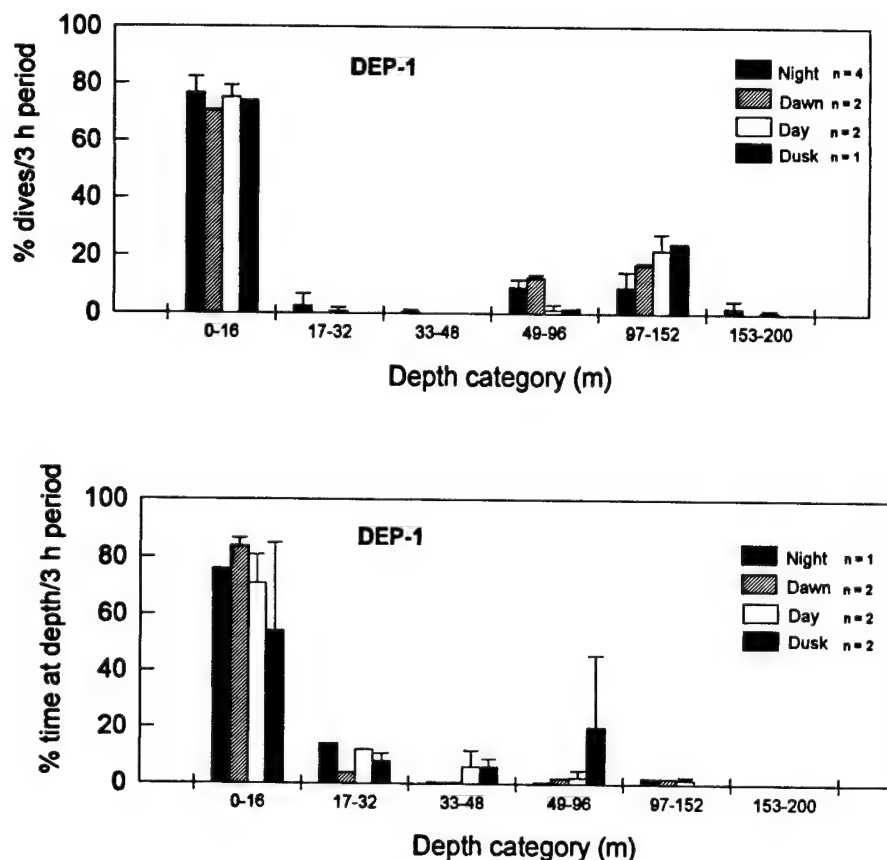
Figure 2. Average percentage of dives reaching their maximum depth in one of six depth categories (n = 9) and average percentage of time spent in each of six depth categories (n = 7) during 3-h summary periods for blue whale DEP-1, tagged off central California in 1993. Histograms divided into four times of day. Error bars represent one standard deviation. Depth categories beyond 200 m not included, as no dives made beyond that depth.

(Alling *et al.* 1991). In several instances the whales appeared to descend below the deep scattering layer and then ascend through it. Right whales east of Cape Cod have been reported occasionally diving deeper than the main prey patch, possibly as a means of detecting changes in depth distribution of prey patches (Winn *et al.* 1995).

Average depth of dives for TDR-instrumented blue whales in the Santa Barbara Channel, California was 68.1 m (Croll *et al.* 1998). This value is almost exactly midway between the average depths reported in this study (average depth of all dives/period = 33 m; average depth of dives >16 m = 105 m). As with duration, it is unclear from Croll *et al.*'s (1998) study what the definition of a dive was.

Table 4. Comparison of visually observed surface/respiration activities for several species of mysticete whales.

| Species	Blow rate (blows/ min)	Blow interval (sec)	Blows per surfacing	Surface time (sec)	% Time near surface	Source
Balaenoptera musculus	1.00	21	4.01	64.8	25.4	This study
Balaenoptera physalus	1.06	13.0	—	—	—	Kopelman and Sadove 1995
	0.84	15	2.8	49.8	13.12	Stone *et al.* 1992 (boat present)
	0.81		3.12	54.6	13.6	(no boat)
Megaptera novaeangliae	1.15	15	3.2	66	25.2	Dolphin 1987
Esrichtius robustus	1.05	13.8	4.2	53.4	22	Würsig *et al.* 1986
Balaena mysticetus	0.77	13.8	4.3	71.4	21	Dorsey *et al.* 1989
	1.28	13.2	4.3	67.2		Würsig *et al.* 1984 (1980–81 data)
	0.70	15	7.4	123		(1982 data)
Eubalaena glacialis	—	11.8	—	—	—	Watkins *et al.* 1996
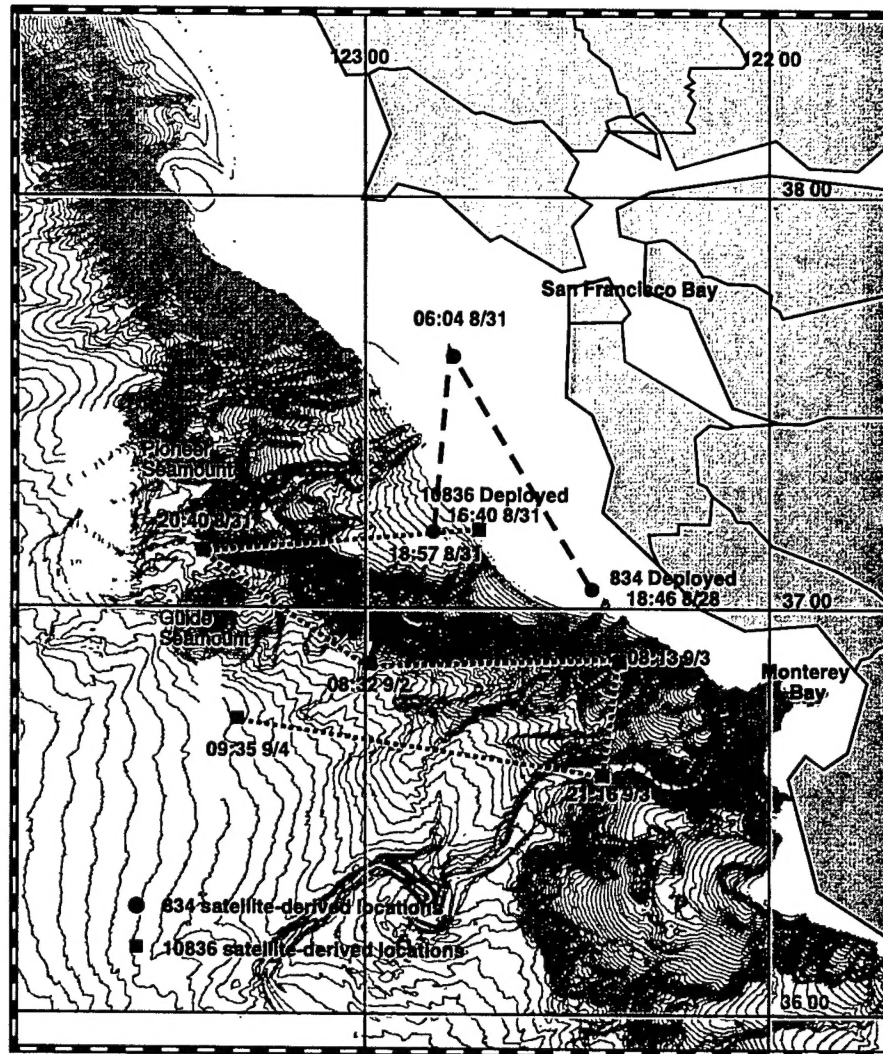
Figure 3. Tagging and satellite-derived locations for whales DEP-1 and DUR-2. Offshore contours begin at depths of 150 m with subsequent contours at 50-m intervals.

Movements

Although only a few locations were received for two whales, they do convey a sense of the range, speed, and variation of movements and depth of water traversed. Neither animal stayed in the area in which it was tagged but ranged widely off the coast of central California. Similar wide-ranging movements were typical of blue whales tagged off Southern California with Argos tags (Mate *et al.* 1999).

The post-tagging locations for whale DUR-2 were both within 40 km of

land over the continental shelf or near the shelf edge (55 m and 370 m water depth, respectively).

After tagging, whale DEP-1 moved to a location 90 km offshore, returned nearshore within 24 km of the coast, and then moved 100 km offshore again in three days. These wide-scale movements may reflect the animal's search for food. The first offshore location was approximately 25 km southeast of Pioneer Seamount (770 m below sea level) and 15 km northwest of Guide Seamount (1,642 m below sea level). Subsequent locations show the animal at the edge of Monterey Canyon and directly over the Canyon itself. Later, the whale was approximately 33 km southeast of Guide Seamount (118 km west of Monterey Bay). As cetacean food is probably most concentrated in regions of high general productivity (Hui 1985), whale locations in these regions may not be coincidental. Regions of irregular bottom topography, such as seamounts and canyons, are often areas of greater upwelling and mixing of nutrients, providing for high densities of plankton (Hui 1979). Pioneer Seamount typically has increased biological productivity (Smith *et al.* 1986). Additionally, great concentrations of zooplankton biomass, particularly *E. pacifica* have been found 185 km west of Monterey Bay (Huntley *et al.* 1995).

For future studies we recommend increasing the transmission repetition rate to 10 or 20 sec to provide more sensor data, as well as more and better-quality locations. We also recommend collecting information on individual dives in addition to summary information, so that direct comparison can be made between the depths and durations of dives and a biologically meaningful differentiation between blow intervals and dives determined. Individual dive information could also allow for examination of the shape of the dives. However, dive-shape information would come at the cost of reporting fewer dives, due to Argos constraints on message length (256 bits/transmission).

This study provides the first telemetered information on the dive habits of free-ranging blue whales. The sample size is small, however. We believe this was due to short-term tag attachment, possibly caused by hydrodynamic drag from the high swimming speeds we observed for blue whales. Additionally, the 40-sec transmission repetition rate combined with blue whales' habit of spending more than 90% of their time underwater limited the number of possible transmissions.

LITERATURE CITED

ALLING, A., E. M. DORSEY AND J. C. D GORDON. 1991. Blue whales (*Balaenoptera musculus*) off the northeast coast of Sri Lanka: Distribution, feeding and individual identification. United Nations Marine Mammal Technical Report 3:247–258.

ALTMANN, J. 1974. Observational study of behavior: Sampling methods. Behaviour 49: 227–267.

CETAP. 1982. Characterization of marine mammals and turtles in the Mid and North Atlantic areas of the U.S. Outer Continental Shelf. Final Report of the Cetacean and Turtle Assessment Program. University of Rhode Island, Graduate School of Oceanography. U.S. Department of the Interior, Bureau of Land Management, Washington, DC. Springfield, VA; NTIS PB83-215855. 570 pp.

CROLL, D. A., B. R. TERSHY, R. P. HEWITT, D. A. DEMER, P. C. FIEDLER, S. E. SMITH, W. ARMSTRONG, J. M. POPP, T. KIEKHEFER, V. R. LOPEZ, J. URBAN AND D. GENDRON. 1998. An integrated approach to the foraging ecology of marine birds and mammals. Deep-Sea Research II 45:1353–1371.

DOI, T. 1974. Further development of whale sighting theory. Pages 359–368 *in* W. E. Schevill, ed. The whale problem; a status report. Harvard University Press, Cambridge, MA.

DOLPHIN, W. F. 1987. Ventilation and dive patterns of humpback whales, *Megaptera novaeangliae,* on their Alaskan feeding grounds. Canadian Journal of Zoology 65: 83–90.

DONOVAN, G. P. 1984. Blue whales off Peru, December 1982, with special reference to pygmy blue whales. Report of the International Whaling Commission 34:473–476.

DORSEY, E. M., W. J. RICHARDSON AND B. WÜRSIG. 1989. Factors affecting surfacing, respiration, and dive behavior of bowhead whales, *Balaena mysticetus,* summering in the Beaufort Sea. Canadian Journal of Zoology 67:1801–1815.

FANCY, S. G., L. F. PANK, D. C. DOUGLAS, C. H. CURBY, G. W. GARNER, S. C. AMSTRUP AND W. L. REGELIN. 1988. Satellite telemetry: a new tool for wildlife research and management. U.S. Department of the Interior, Fish & Wildlife Service, Resource Publication 172. 55 pp.

HARVEY, J. T., AND B. R. MATE. 1984. Dive characteristics and movements of radio-tagged gray whales in San Ignacio Lagoon, Baja California Sur, Mexico. Pages 561–575 *in* M. L. Jones, S. L. Swartz and S. Leatherwood, eds. The gray whale. Academic Press, Orlando, FL.

HIBY, A. R., AND P. S. HAMMOND. 1989. Survey techniques for estimating abundance of Cetaceans. Reports of the International Whaling Commission (Special Issue 11):47–80.

HUI, C. A. 1979. Undersea topography and distribution of dolphins of the genus *Delphinus* in the Southern California Bight. Journal of Mammalogy 60:521–527.

HUI, C. A. 1985. Undersea topography and the comparative distributions of two pelagic cetaceans. Fishery Bulletin, U.S. 83:472–475.

HUNTLEY, M. E., M. ZHOU AND W. NORDHAUSEN. 1995. Mesoscale distribution of zooplankton in the California Current in late spring, observed by optical plankton counter. Journal of Marine Research 53:647–674.

JOYCE, G. G., J. SIGURJÓNSSON AND G. VIKINGSSON. 1990. Radio tracking a minke whale (*Balaenoptera acutorostrata*) in Icelandic waters for the examination of dive-time patterns. Report of the International Whaling Commission 40:357–361.

KLINOWSKA, M. 1986. Diurnal rhythms in Cetacea—a review. Reports of the International Whaling Commission (Special Issue 8):75–88.

KOPELMAN, A. H., AND S. S. SADOVE. 1995. Ventilatory rate differences between surface-feeding and non-surface-feeding fin whales (*Balaenoptera physalus*) in the waters off eastern Long Island, New York, U.S.A., 1981–1987. Marine Mammal Science 11:200–208.

LAURIE, A. 1933. Some aspects of respiration in blue and fin whales. Discovery Reports 7:363–406.

LEATHERWOOD, S., K. GOODRICH, A. L. KINTER AND R. M. TRUPPO. 1982. Respiration patterns and 'sightability' of whales. Report of the International Whaling Commission 32:601–613.

LOCKYER, C. 1976. Growth and energy budgets of large baleen whales from the southern hemisphere. FAO Fisheries Series 5, Mammals in the seas. Volume 3:379–488.

MARTIN, A. R., AND T. G. SMITH. 1992. Deep-diving in wild, free-ranging beluga whales, *Delphinapterus leucas*. Canadian Journal of Fisheries and Aquatic Sciences 49:462–466.

MATE, B. R., S. L. NIEUKIRK AND S. D. KRAUS. 1997. Satellite-monitored movements of the northern right whale. Journal of Wildlife Management 61:1393–1405.

MATE, B. R., B. A. LAGERQUIST AND J. CALAMBOKIDIS. 1999. The movements of North Pacific blue whales during the feeding season of southern California and their southern fall migration. Marine Mammal Science 15:1246–1257.

SMITH, R. C., P. DUSTAN, D. AU, K. S. BAKER AND E. A. DUNLAP. 1986. Distribution of cetaceans and sea-surface chlorophyll concentrations in the California Current. Marine Biology 91:385–402.

STERN, S. J. 1992. Surfacing rates and surfacing patterns of minke whales (*Balaenoptera acutorostrata*) off central California, and the probability of a whale surfacing within visual range. Report of the International Whaling Commission 42:379–385.

STONE, G. S., S. K. KATONA, A. MAINWARING, J. M. ALLEN AND H. D. CORBETT. 1992. Respiration and surfacing rates of fin whales (*Balaenoptera physalus*) observed from a lighthouse tower. Report of the International Whaling Commission 42:739–745.

TOMILIN, A. G. 1967. Mammals of the USSR and adjacent countries. Vol. IX. Cetacea. Jerusalem, Israel Program for Scientific Translations, IPST (1124):76–111.

WATKINS, W. A., K. E. MOORE, J. SIGURJÓNSSON, D. WARTZOK AND G. NOTARBARTOLO DI SCIARA. 1984. Fin whale (*Balaenoptera physalus*) tracked by radio in the Irminger Sea. Rit Fiskideildar 8:1–14.

WATKINS, W. A., J. SIGURJÓNSSON, D. WARTZOK, R. R. MAIEFSKI, P. W. HOWEY AND M. A. DAHER. 1996. Fin whale tracked by satellite off Iceland. Marine Mammal Science 12:569–581.

WINN, H. E., J. D. GOODYEAR, R. D. KENNEY AND R. O. PETRICIG. 1995. Dive patterns of tagged right whales in the Great South Channel. Continental Shelf Research 15(4/5):593–611.

WÜRSIG, B., E. M. DORSEY, M. A. FRAKER, R. S. PAYNE, W. J. RICHARDSON AND R. S. WELLS. 1984. Behavior of bowhead whales, *Balaena mysticetus*, summering in the Beaufort Sea: Surfacing, respiration, and dive characteristics. Canadian Journal of Zoology 62:1910–1921.

WÜRSIG, B., R. S. WELLS AND D. A. CROLL. 1986. Behavior of gray whales summering near St. Lawrence Island, Bering Sea. Canadian Journal of Zoology 64:611–621.

YABLOKOV, A. V., V. M. BEL'KOVICH AND V. I. BORISOV. 1974. Whales and dolphins. Part 1. JPRS-62150-1, Washington, DC (Translation of Russian-language book Kity y Del'finy. 1972. Signal Press 15 Dec. 1971. Nauka, Moscow. 472 pp.).

ZENKOVICH, B. A. 1936. Nablyudeniya nad kitami del' nevostochnykh more i (Observations on the Whales of the Far Eastern Seas). Trudy Dal' nevostochnogo filiala. Akademii Nauk SSSR. Vol. I.